# Identification and characterisation of Mnk inhibitors as potential anti-cancer agents

By

**Sunita K.C. Basnet**

MSc in Integrative Physiology, Bachelor in Pharmaceutical Science

A thesis submitted for the degree of

**Doctor of Philosophy**

Centre for Drug Discovery and Development

Sansom Institute for Health Research

School of Pharmacy and Medical Sciences

Division of Health Sciences



University of
South Australia

December 2017

# Contents

**Declaration**……...v

**Publications**…….……vi

**Statement of authorship**……...viii

**Acknowledgements**…..…….…….…….…….....ix

**Abstract**…….…….……...……xii

**Abbreviations**……...….xvi

**List of figures**…….……..……...…….…xxii

**List of tables**…….....xxv

**1. Introduction** ..... **1**

**1.1 Protein kinases as anticancer targets** ..... **3**

**1.2 Major signalling pathways in cancer** ..... **4**

1.2.1 Ras/Raf/MAPK signalling pathways ..... 4

1.2.2 PI3K/AKT/mTOR signalling pathways ..... 5

1.2.3 Node of convergence of two major signalling pathways ..... 7

**1.3 Eukaryotic initiation factor 4E** ..... **8**

1.3.1 Regulation of eIF4E ..... 9

1.3.2 Role of eIF4E in initiating translation ..... 10

1.3.3 Role of eIF4E in oncogenic translation ..... 12

1.3.4 eIF4E as a target for cancer therapy ..... 13

**1.4 Mnks** ..... **14**

1.4.1 Unique structural features of Mnk protein ..... 16

1.4.2 Mnks as anti-cancer targets ..... 19

1.4.3 Other Mnk substrates ..... 20

1.4.4 Known Mnk inhibitors ..... 22

**1.5 Selectivity of kinase inhibitors** ..... **24**

**1.6 Hypothesis and research aims** ..... **26**

**2. Identification and characterisation of Mnk inhibitors** ..... **28**

**2.1 Introduction** ..... **28**

**2.2 Results** ..... **35**

2.2.1 Developing protocols to measure Mnk1/2 activities with IMAP® and ADP-Glo™ assays....35
2.2.2 Identification of primary hits....41
2.2.3 Dual Mnk1/2 and Mnk2 inhibitors....44
2.2.4 Binding modes of Mnk1/2 inhibitors....45
2.2.5 Selectivity of Mnk inhibitors....51
**2.3 Discussion....53**

**3. Effect of Mnk inhibition in a cellular context....59**

**3.1 Introduction....59**
**3.2 Mnk inhibition in prostate cancer cells....60**
3.2.1 Effect of Mnk inhibitors on the viability of prostate cancer cells....61
3.2.2 eIF4E phosphorylation as a biomarker....65
3.2.3 Mnk inhibition blocks migration of prostate cancer cells....70
**3.3 Inhibition of Mnk in leukaemia cells....74**
3.3.1 Anti-proliferative activity of Mnk inhibitors against leukaemia cell lines .75
3.3.2 Effects of combined inhibition of Mnk and FLT3 in MV4-11 cells....82
3.3.3 Caspase dependent cytotoxicity of Mnk and/or FLT3 inhibition....86
**3.4 Discussion....87**

**4. Isolation and purification of Mnk proteins....91**

**4.1 Introduction....91**
**4.2 Results....92**
4.2.1 Expression systems....92
4.2.2 Protein purification and activation....95
4.2.3 Kinase activity testing with ADP-Glo™ system....100
**4.3 Discussion....102**

**5. Discussion, Future work and Conclusion....104**

**5.1 Discussion....104**
**5.2 Future work....106**
**5.3 Conclusion....108**

**6. Materials and Methods....109**

**6.1 Materials....109**

6.1.1 Compounds ..... 109
6.1.2 Recombinant protein kinases ..... 118
6.1.3 Kinase substrates ..... 118
6.1.4 Assay kits ..... 118
6.1.5 Chemicals and Reagents ..... 119
6.1.6 Antibodies ..... 121
6.1.7 General consumables ..... 122
6.1.8 Instruments ..... 124
6.1.9 Buffers ..... 126
6.1.9.1 Buffers for ADP-Glo™ kinase assays ..... 126
6.1.9.2 Buffers for IMAP® TR-FRET assay ..... 126
6.1.9.3 Buffers for Western blots ..... 127
6.1.9.4 Buffers for protein purification ..... 128
6.1.10 Primers used for DNA sequencing and quantitative reverse transcription-polymerase chain reaction (qRT-PCR) ..... 130
**6.2 Methods ..... 130**
6.2.1 IMAP® TR-FRET kinase assay ..... 130
6.2.2 ADP-Glo™ kinase assay ..... 131
6.2.3 CDK and FLT3 kinase assays ..... 132
6.2.4 Cell culture ..... 132
6.2.5 Cell viability assay ..... 132
6.2.6 HTRF assay ..... 134
6.2.7 Caspase 3/7 activation assay ..... 134
6.2.8 Trypan blue exclusion assay ..... 135
6.2.9 Bio-Rad DC Assay ..... 135
6.2.10 Western blotting ..... 136
6.2.11 Wound healing assays ..... 137
6.2.12 Cell invasion assay ..... 137
6.2.13 Detection of apoptosis ..... 138
6.2.14 Plasmid transformation and cryo stocks ..... 139
6.2.15 Plasmid purification ..... 140
6.2.16 Manual protein purification and buffer exchange ..... 141
6.2.17 Activation of GST-Mnk1a with ERK1 ..... 142
6.2.18 Purity assessment ..... 143

6.2.19 Data analysis ..... 143

**7. References ..... 145**

**8. Appendices ..... 163**

**8.1 Appendix 1 - GST-Mnk2 and His-Mnk2 kinetics ..... 163**

**8.2 Appendix 2 - Interference of inhibitors with ADP-Glo™ system. ..... 165**

**8.3 Appendix 3 - CDK kinase assays ..... 165**

**8.4 Appendix 4 - Profiling data from IMAP® and ADP-Glo™ assays. ..... 168**

**8.5 Appendix 5 - Anti-proliferative and kinase inhibitory activities of Mnk inhibitors ..... 172**

# Declaration

I declare that:

This thesis presents work carried out by me and does not incorporate without acknowledgement any materials previously submitted for a degree or diploma at any university. To the best of my knowledge, it does not contain any materials previously published or written by another person except where due reference is made in the text. All substantive work contributed by others, including jointly authored publications, has been clearly acknowledged.

**Sunita K.C. Basnet**

**Date:** 19 December 2017

1. Diab, S.; Teo, T.; Kumarasiri, M.; Li, P.; Yu, M.; Lam, F.; **K.C. Basnet, S.**; Sykes, M. J.; Albrecht, H.; Milne, R. and Wang, S. Discovery of 5-(2-(Phenylamino)pyrimidin-4-yl)thiazol-2(3*H*)-one Derivatives as Potent Mnk2 Inhibitors: Synthesis, SAR Analysis and Biological Evaluation. *ChemMedChem.* 2014, *9*(5), 962-972.

2. **K.C. Basnet, S.**; Diab, S.; Schmid, R.; Yu, M.; Yang, Y.; Gillam, T.; Teo, T.; Albrecht, H. and Wang, S. Identification of a Highly Conserved Allosteric Binding Site on Mnk1 and Mnk2. *Mol. Pharmacol.* 2015, *88*(5), 935-948.

3. Teo, T.; Yang, Y.; Yu, M.; **K.C. Basnet, S.**; Gillam, T.; Hou, J.; Schmid, R.; Kumarasiri, M.; Diab, S.; Albrecht, H.; Sykes, M. J. and Wang, S. An Integrated Approach for Discovery of Highly Selective Mnk Inhibitors: Screening, Synthesis, SAR Analysis and Biological Evaluations. *Eur. J. Med. Chem.* 2015, *103*, 539-550.

4. Teo, T.; Lam, F.; Yu, M.; Yang, Y.; **K.C. Basnet, S.**; Albrecht, H.; Sykes, M. J. and Wang, S. Pharmacologic Inhibition of Mnks in Acute Myeloid Leukaemia. *Mol. Pharmacol.* 2015, *88*(2), 380-389.

5. Yu, M.; Li, P.; **K.C. Basnet, S.**; Kumarasiri, M.; Diab, S.; Teo, T.; Albrecht, H. and Wang, S. Discovery of 4-(Dihydropyridinon-3-yl)amino-5-methylthieno[2,3-*d*]pyrimidine Derivatives as Potent Mnk Inhibitors: Synthesis, Structure-Activity Relationship Analysis and Biological Evaluation. *Eur. J. Med. Chem.* 2015, *95*, 116-126.

6. Diab, S.; Li, P.; **K.C. Basnet, S.**; Lu, J.; Yu, M.; Albrecht, H.; Milne, R. and Wang, S. Unveiling New Chemical Scaffolds as Mnk Inhibitors. *Future Med. Chem.* 2016, *8*(3), 271-285.

7. Li, P.; Diab, S.; Yu, M.; Adams, J.; Islam, S.; **K.C. Basnet, S.**; Albrecht, H.; Milne, R. and Wang, S. Inhibition of Mnk Induces Apoptosis and Enhances the Anti-Leukaemic Activity of Cytarabine. *Oncotarget* 2016, *7*(35), 56811-56825.

8. Kumarasiri, M.; Teo, T.; Yu, M.; Philip, S.; **K.C. Basnet, S.**; Albrecht, H.; Sykes, M. J. and Wang, S. In Search of Novel CDK8 Inhibitors by Virtual Screening. *J. Chem. Inf. Model*, 2017, 57, 413-416.

9. Zeleke, S.; Yu, M.; Mekonnen, L.; Lam, F.; Islam, S.; Tomusange, K.; Rahaman, M.; Noll, B.; **K.C. Basnet, S.**; Teo, T.; Albrecht, H.; Milne, R. and Wang, S. Highly Potent,

Selective and Orally Bioavailable 4-Thiazol-*N*-(pyridin-2-yl)pyrimidin-2-amine CDK4/6 Inhibitors as Anti-cancer Drug Candidates: Design, Synthesis and Evaluation. *J. Med. Chem.* 2017, 60(5), 1892-1915.

10. Diab, S.; Abdelaziz, A.; Li, P.; Teo, T.; **K.C. Basnet, S.**; Noll, B.; Rahaman, M.; Lu, J.; Hou, J.; Yu, M.; Le, B. T.; Albrecht, H.; Milne, R. and Wang, S. Dual Inhibition of Mnk2 and FLT3 for the Treatment of Acute Myeloid Leukaemia. *Eur. J. Med. Chem.* 2017, 139, 762-772.

# Statement of Authorship

Chemical compounds described in this thesis were synthesised by Dr Sarah Diab, Dr Mingfeng Yu, Mr Todd Alexander Gillam, Mr Yuchao Yang, Mr Ahmed Magdy Abdelaziz and Ms Sapphire Le.

Ms Raffaella Schmid guided the preliminary steps in Mnk purification studies reported in **Section 4.2.2**. Ms Jingfeng Lu helped in later optimisation of purification steps. Ms Raffaella Schmid initiated the development and validation of the Mnk kinase assays in house. Ms Raffaella Schmid, Ms Jingfeng Lu and Mr Chen Seng Su performed approximately 1% of Mnk kinase assay-related experiments (**Appendix 4**). Some biochemical assays (FLT3 and CDK2A) described in **Appendix 5** were carried out by Eurofins Scientific or Reaction Biology Corp.

Cell viability assays described in **Appendix 5** were performed by me, Dr Peng Li and Dr Theodosia Theo.

# Acknowledgements

I appreciate and acknowledge the "Australian Government Research Training Program Scholarship" for providing me funding without which my dream of pursuing PhD studies would have been impossible.

Although the front page of this thesis presents only my name, many people have contributed to make this happen.

I am eternally grateful to my supervisor, Prof Shudong Wang, for believing in my potential. I was very fortunate to have her as my supervisor who gave me all the freedom to explore on my own and at the same time provided enormous support and guidance. Most importantly, she also granted her continuous support at difficult times, which was very important to accomplish this thesis. I am thankful to be part of her team.

My co-supervisor, Dr Hugo Albrecht, has been always there to listen and give suggestions. I am indebted to him for his continuous support and guidance, and sincerely appreciate his invaluable and innumerable support in every aspect of my work, from writing the original proposal, slide preparation for talks, writing manuscripts, detailing laboratory procedures, data analysis and interpretation to uncountable draft amendments of this thesis; just to name a few. His keen interest to deliver high quality research has always been my inspiration to move forward.

My sincere thanks go to my associate supervisor, Dr Tom Peat from CSIRO, Melbourne, for allowing me to visit his eminent lab and learn new skills under the supervision of friendly and skilled staff. I would also like to thank Ms Jo Caine from CSIRO for all the hard work she has done to help me.

Special thanks to Associate Professor Robert Milne for his constant support in coordinating the Higher Degree Research program and my research coordinator Dr Paul Anderson for his constructive advice.

I extend my appreciation to the present and former members of the group. Raffaella Schmid was my first teacher in the lab who introduced me to the enzymatic kinase assay, which was very important for my PhD work. I am indebted to her for giving me a lot of highly valuable advice. I would like to acknowledge Dr Mingfeng Yu and Dr Sarah Diab for innumerable help and support throughout my candidature, especially amendments to my journal article and thesis, and for being an emotional support.

This work would have been impossible without the invaluable support from many colleagues. I would like to thank Dr Frankie Lam, Dr Theodosia Teo, Dr Peng Li, Dr Julian Adams, Dr Malika Kumarasiri, Mr Ahmed Magdy, Mr Ben Noll, Mr Yuchao Yang, Mr Todd Alexander Gillam, Ms Jingfeng Lu, Ms Longjin Zhong, Mr Chen Seng Su, Ms Cheuk Ying Tai, Mr Md Saiful Islam, Mr Muhammad Hamidur Rahaman, Mr Laychiluh Bantie Mekonnen, Mr Stephen Phillip, Mr Solomon Tadesse Zeleke, Ms Sapphire Le, Mr Yi Long, Mr Goh Aik Wye and Dr Aleksandra Ochnik.

I am also grateful to the administrative and technical staff working at the Reid building - Ms Smitha Shridhar, Ms Jo Anne Planzer, Ms Karen Teague, Ms Carolyn Streckbein, Ms Helen Kenwright, Ms Hattie Li, and Ms Vicky Foreman. Without their support, this work could not be completed.

Thank you seems so little but this is all I have for my parents, Rupchan K.C. and Mathura K.C., and my husband, Harihar Basnet, for encouraging me in all of my pursuits and for inspiring me to follow my dreams. I would like to thank my parent-in-law, Lekhraj Basnet and Radha Basnet for all the support they have provided to me over the years was the

greatest gift that anyone has ever given me. Last, but not the least, I owe my greatest gratitude to the most important person in my life: my son, Babin Basnet, who is a powerful source of inspiration and positive energy.

There is a growing interest in mitogen-activated protein kinase (MAPK)-interacting kinases 1 and 2 (Mnk1 and Mnk2) as anti-cancer targets. Mnks integrate signals from several oncogenic and immune signalling pathways, including Ras/Raf/ERK, PI3K/AKT/mTOR, p38 and Toll-like receptor (TLR) pathways, by phosphorylating the eukaryotic initiation factor 4E (eIF4E) and other key effector proteins including heterogeneous nuclear ribonucleoprotein A1 (hnRNP A1), sprouty 2 and the polypyrimidine tract-binding protein-associated splicing factor (PSF). Through phosphorylation of these regulatory proteins, Mnks selectively regulate the stability and translation of a subset of cellular mRNAs.

Several studies, including animal models, suggested that eIF4E phosphorylation is essential for oncogenic transformation, but is of less importance to normal growth and development. Mnks are the only known kinases that phosphorylate eIF4E at Ser209 and therefore, pharmacological inhibition of Mnks provides a potentially effective strategy for treating cancer with minimal toxicity. However, the lack of selective inhibitors of Mnk has hampered the validation of pharmacological target(s) and drug development.

This thesis focused on the identification and characterisation of novel Mnk inhibitors, which can be used to gain pharmacological proof of concept for this anti-cancer strategy. For this purpose, a comprehensive profiling platform was developed with enzymatic and cellular assays.

Three series of novel Mnk inhibitors (series 1: thienopyrimidine, series 2: anilinopyrimydine and series 3: pyrazolo[3,4-*d*]pyrimidine) were synthesised using structure-guided design and medicinal chemistry (at the Centre for Drug Discovery and Development, University of South Australia, Adelaide). A screening cascade was established to assess the potency and selectivity of compounds, and to determine their

mode of inhibition. Screening of a library of one hundred sixty compounds resulted in fifty-three hits with a $K_i$ value of < 1 µM against either one or both Mnks. Among them, twenty-three compounds were dual inhibitors of Mnk1 and Mnk2. Remaining thirty compounds were identified as Mnk2 selective inhibitor with at least ten-fold more potency for Mnk2 over Mnk1. Twenty compounds with $K_i$ values of < 1 µM against Mnk2 were selected for ATP and peptide competition studies. Nine compounds interacted through an allosteric site without competing with the ATP and binding to the peptide substrate (-/- mode or type III). Other nine were ATP-competitive and non-substrate competitive (+/- mode or type I). Furthermore, while one compound (MNKI5-17) was shown to be ATP- and substrate- competitive (+/+ mode, or type I/II)), another *i.e.* MNKI-2-22, which is a type II inhibitor, targeted the substrate alone (-/+ mode). All -/- mode (type III) inhibitors (except MNKI-67) exhibited dual inhibition of Mnk1 and Mnk2. Interestingly, these ATP-competitive inhibitors were found to be highly selective for Mnk2 with little or no activity against Mnk1. The study suggests that Mnk1 and Mnk2 share a common structure at the allosteric binding site, but possess the distinct structural features within the ATP catalytic domain. These findings provide valuable assistance in the future design and development of Mnk-targeted anti-cancer therapeutics.

Enzymatic activity testing was followed by screening of compounds against prostate cancer (PCa) cell lines, since hyper-activation of the eIF4E is known to promote translation of key mRNAs that are indispensable for initiation, progression and metastasis of PCa. Earlier studies showed that knock-in mice expressing a mutant form of eIF4E, which cannot be phosphorylated by Mnks, were resistant to tumorigenesis in a PCa model. Therefore, twenty-seven compounds were tested for anti-proliferative effects against five PCa cell lines (*i.e.* 22RV1, DU145, LNCaP, PC3 and C4-2B) and nine demonstrated significant activities with $GI_{50}$ ranging from 0.085 µM - 10 µM. The

inhibitory effects of Mnk inhibitors on cellular eIF4E phosphorylation (*i.e.* inhibition of Mnks) well correlated with anti-proliferative activities against 22RV1 cells, supporting the significant role of Mnk in this type of PCa cells. However, inhibition of Mnks did not seem to be cytotoxic in LNCaP, PC3 and C4-2B cell lines, indicating a cell-type specific role of Mnks in cancers.

Previous studies have revealed the role of eIF4E phosphorylation in the progression and metastasis of PCa and inhibition of eIF4E phosphorylation resulted in down-regulation of several epithelial–mesenchymal transitions (EMT) proteins like *N*-cadherin, matrix metalloproteinases (MMPs), Snail, and Slug. These proteins are known to be essential for cancer cell migration. In line with this, this study confirmed the attenuated cell migration with Mnk inhibitors (*i.e.* MNKI-7 and MNKI-67) in C4-2B cells.

Acute myeloid leukaemia (AML) cells were found to be highly sensitive to some of the Mnk inhibitor leads. Moderate correlation between Mnk inhibition and anti-proliferative effects was observed in MV4-11 AML cells. Subsequently, more detailed mechanistic studies revealed that some of the Mnk inhibitors also targeted FMS-like tyrosine kinase 3 (FLT3). Given that FLT3-internal tandem duplication (ITD) mutations are found in approximately a quarter of AML cancers, the novel dual Mnk/FLT3 inhibitors offer new opportunities for developing new treatment of AML.

Overall, the presented work led to the identification of several classes of Mnk inhibitors with high potency and different selectivity profiles, and of their binding models. These compounds targeted Mnks by the means of ATP- or substrate-competitive or allosteric mechanism, the latter acting through a conserved but currently unknown site of the Mnks. The knowledge gained would be immensely valuable for the future drug design and development of Mnk targeted therapeutics. Moreover, the cellular mechanistic studies of

the selected compounds revealed that Mnk inhibition has different effects on types and sub-types of cancers. Identification of the appropriate cellular and pharmacological cancer models will be required in order to progress Mnk inhibitor drug candidates from the discovery towards the clinical applications.

| | |
|---|---|
| 4E-BP | 4E binding protein |
| 4E-SE | 4E sensitivity element |
| Ala | Alanine |
| ABC DLBCL | activated B-cell diffuse large B-cell lymphoma |
| Abl | Abelson |
| ADP | adenosine diphosphate |
| ADT | androgen deprivation therapy |
| AGC | protein kinase A, protein kinase B and protein kinase C family |
| AKT | Ak thymoma |
| Ala | Alanine |
| AML | acute myeloid leukaemia |
| ARE | AU-rich element |
| ATP | adenosine triphosphate |
| BAD | Bcl-xL/BCL-2-associated death promotor |
| Bak | BCL-2 homologous antagonist/killer |
| Bax | BCL-2-associated X protein |
| BC | blast crisis |
| BCL-2 | B-cell lymphoma-2 |
| BCL-$X_L$ | BCL-extra large |
| Bcr | breakpoint cluster region |
| BD | Becton Dickinson |
| BH3 | Bcl-2-homology domain 3 |
| BI-1 | Bax-inhibitor-1 |
| Bid | BH3-interacting-domain death agonist |
| Bik | Bcl-2-interacting killer |
| BLAST | basic local alignment search tool |
| Bmf | Bcl-2-modifying factor |
| Bok | Bcl-2 related ovarian killer |
| bp | base pair |
| BRAF | v-raf murine sarcoma viral oncogene homologue B1 |
| BSA | bovine serum albumin |
| *ca.* | circa |
| CAMK | calcium/calmodulin-dependent protein kinase |

| | |
|---|---|
| Caspase | cysteinyl aspartate-specific protease |
| CBP | cap-binding protein |
| CDK | cyclin-dependent kinase |
| cDNA | complementary deoxyribonucleic acid |
| CHO | chinese hamster ovary |
| CK1 | casein kinase 1 |
| c-Kit | cellular-Kit |
| CLK | CDC2/CDC28-like kinase |
| C-loop | catalytic-loop |
| CMGC | CAMK, CDK, MAPK, GSK-3, CLK families |
| CML | chronic myeloid leukaemia |
| cPLA2 | cytosolic phospholipase A2 |
| CRPC | castration resistant prostate cancer |
| *C*-terminal | carboxyl terminal |
| c-Myc | cellular-Myc |
| Cys | cysteine |
| Da | dalton |
| DC assay | detergent-compatible colourimetric assay |
| DMSO | dimethyl sulphoxide |
| DNA | deoxyribonucleic acid |
| ECL | enhanced chemiluminescence |
| $EC_{50}$ | half maximal effective concentration |
| EDTA | ethylenediaminetetraacetic acid |
| eIF | eukaryotic initiation factor |
| EGFR | Epidermal growth factor receptor |
| EMT | epithelial mesenchymal transition |
| ERα | oestrogen receptor alpha |
| ERK | extracellular-signal-regulated kinase |
| ESI | electrospray ionisation |
| Et | ethyl |
| FAB | French-American-British |
| FACS | fluorescence-activated cell sorting |
| FBS | foetal bovine serum |

| | |
|---|---|
| FDA | Food and Drug Administration |
| FGF | Fibroblast growth factor |
| FITC | fluorescein isothiocyanate |
| FLT3 | Feline McDonough sarcoma-like tyrosine kinase 3 |
| FMS | Feline McDonough sarcoma |
| g | gram |
| $G_0$ | gap zero phase or resting phase |
| $G_1$ | gap phase I |
| $G_2$ | gap phase II |
| GAPDH | glyceraldehyde 3-phosphate dehydrogenase |
| $GI_{50}$ | half maximal growth inhibitory concentration |
| Glu | glutamic acid |
| Gly | glycine |
| GPCR | G-protein coupled receptor |
| GR loop | glycine-rich loop |
| GSK | glycogen synthase kinase |
| GST | glutathione-S-transferase |
| GTP | guanosine-5′-triphosphate |
| H/His | histidine |
| HER2 | human epidermal growth factor receptor 2 |
| hnRNP A1 | heterogeneous nuclear RNA-binding protein A1 |
| Hrk | activator of apoptosis harakiri |
| HRMS | high-resolution mass spectrometry |
| HRP | horseradish peroxidase |
| IARC | international agency for research on cancer |
| $IC_{50}$ | half maximal inhibitory concentration |
| IGFIR | insulin-like growth factor 1 receptor |
| IPTG | isopropyl-β-D-thiogalactopyranoside |
| IMAP | immobilised metal ion affinity particle |
| ITD | internal tandem duplication |
| Jnk | c-Jun N-terminal kinase |
| $K_d$ | dissociation constant |
| $K_i$ | inhibition constant |

| | |
|---|---|
| $K_{m(app)}$ | apparent Michaelis-Menten constant |
| KR | kinase region |
| L | litre |
| LB | Lysogeny broth |
| LSC | leukaemia stem cell |
| $m^7G$ | 7-methylguanosine |
| MAPK | mitogen-activated protein kinase |
| Mcl-1 | myeloid cell leukaemia-1 |
| Me | methyl |
| MEF | mouse embryonic fibroblast |
| MEK | mitogen-activated protein kinase kinase |
| Met | methionine |
| Mnk | MAPK-interacting kinase |
| mRNA | messenger ribonucleic acid |
| MS | mass spectroscopy |
| mTOR | mammalian target of rapamycin |
| MTT | 3-(4,5-dimethylthiazol-2-yl)-2,5-diphenyltetrazolium bromide |
| mut | mutation |
| MW | molecular weight |
| *N*-terminal | amino terminal |
| ND | not determined |
| NLS | nuclear localisation sequence |
| NMR | nuclear magnetic resonance |
| p | phosphorylation |
| p70 S6K | p70 ribosomal protein S6 kinase |
| PARP | poly(adenosinediphosphate-ribose)polymerase |
| PBS | phosphate buffered saline |
| PCa | Prostate cancer |
| PCR | polymerase chain reaction |
| PDB | protein data bank |
| PDGFR | platelet-derived growth factor receptor |
| PDK1 | phosphoinositide-dependent kinase 1 |
| PEI | polyethylenimine |

| | |
|---|---|
| Phe | phenylalanine |
| PI | propidium iodide |
| PI3K | phosphoinositide-3-kinase |
| Pim | proviral integration site for Moloney murine leukaemia virus |
| PIP3 | phosphatidylionositol 3,4,5-triphosphate |
| PKB | protein kinase B |
| PMA | phorbol 12-myristate 13-acetate |
| PME | particle mesh Ewald |
| PML | promyelocytic leukaemia protein |
| PRAS40 | proline-rich AKT substrate 40 kDa |
| PRH | proline-rich homeodomain protein |
| PSF | polypyrimidine-tract binding protein-associated splicing factor |
| *PTEN* | phosphatase and tensin homologue |
| Puma | p53 up-regulated modulator of apoptosis |
| qRT-PCR | quantitative reverse transcription-polymerase chain reaction |
| R | arginine |
| Ref | reference |
| R-spine | regulatory-spine |
| Raf | rapidly accelerated fibrosarcoma |
| Raptor | protein regulatory associated protein of mTOR |
| Ras | rat sarcoma |
| Rb | retinoblastoma |
| RET | Rearranged during transfection |
| Rheb | ras homologue enriched in brain |
| RING | really interesting new gene |
| RNA | ribonucleic acid |
| rpm | rotations per minute |
| RPMI | Roswell Park Memorial Institute |
| rpS6 | ribosomal protein S6 |
| Rsk | ribosomal S6 kinase |
| SAPK | stress-activated protein kinase |
| S/B | Signal to background ratio |
| SD | standard deviation |

| | |
|---|---|
| SDS | sodium dodecyl sulphate |
| Ser | serine |
| siRNA | small interfering ribonucleic acid |
| Spry2 | sprouty 2 |
| Src | sarcoma |
| STE | homologues of yeast sterile 7, sterile 11 and sterile 20 |
| T | threonine |
| TAMRA | tetramethylrhodamine |
| TBE | Tris-borate-EDTA |
| TBS | Tris-buffered saline |
| TBST | Tris-buffered saline Tween®-20 |
| TGF-β | transforming growth factor β |
| Thr | threonine |
| TNFα | tumour necrosis factor α |
| TP53 | tumour protein 53 |
| TRAIL | TNF-related apoptosis-inducing ligand |
| TR-FRET | time resolved-fluorescence resonance energy transfer |
| Tris | tris(hydroxymethyl)aminomethane |
| TSC | tuberous sclerosis complex |
| TsOH | tosylic acid |
| Tyr | tyrosine |
| U | Unit |
| µM | micro molar |
| µs | micro second |
| UTR | untranslated region |
| v | version |
| VEGF | vascular endothelial growth factor |
| VEGFR | vascular endothelial growth factor receptor |
| WT | wild-type |
| Y | tyrosine |
| YT | yeast extract and tryptone |
| Z-DEVD | bis-(N-CBZ-L-aspartyl-L-glutamyl-L-valyl-L-aspartic acid amine |
| ZEB1 | zinc finger E-box binding homeobox 1 |

Figure 1.1: Regulation of eIF4E by two major cell-signalling pathways. .....6

Figure 1.2: Cap-dependent initiation of translation in eukaryotes.. .....11

Figure 1.3: mRNA discrimination in the translation by level of phosphorylated eIF4E.13

Figure 1.4: Schematic structure of Mnk1/2 and their sequence alignment of kinase domains. .....15

Figure 1.5: Examples of Mnk structures. .....18

Figure 1.6: Various substrates of human Mnks.....21

Figure 1.7: Chemical structures of Mnk inhibitors. .....24

Figure 2.1: Schematic representations of IMAP® assay principle. .....31

Figure 2.2: ADP-Glo™ assay principle. .....32

Figure 2.3: Screening cascade of Mnk inhibitor profiling.. .....34

Figure 2.4: Optimisation of the IMAP® assay conditions. .....37

Figure 2.5: ADP-Glo™ assay validation with Mnks. .....40

Figure 2.6: Hit identification by IMAP® assay. .....42

Figure 2.7: Robustness of IMAP® assay. .....43

Figure 2.8: Identification of dual and Mnk2 specific inhibitors. .....45

Figure 2.9: Determination of binding mode of inhibitor in Mnk2. .....49

Figure 2.10: Determination of the apparent $K_m$ and $V_{max}$ values at different compound concentrations.....50

Figure 2.11: Proposed binding modes of Mnk inhibitors.....58

Figure 3.1: Western blotting analysis of the levels of Mnk-eIF4E proteins in PCa cell lines. .....65

Figure 3.2: Schematic representation of HTRF based phospho – eIF4E (Ser209) cellular assay. .....66

Figure 3.3: HTRF assay is more sensitive than the classic Western blotting. .....67

Figure 3.4: Correlation of anti-proliferative effects with cellular eIF4E phosphorylation and Mnk kinase activity. ..... 69

Figure 3.5: Mnk inhibitors eliminate the phosphorylation of eIF4E by Western blotting analysis. ..... 71

Figure 3.6: Anti-migratory effect of MNKI-7 and MNKI-67 in C4-2B PCa cell line ... 73

Figure 3.7: Correlation between cellular anti-proliferation and Mnk enzyme inhibition ..... 78

Figure 3.8: Enzymatic Mnk inhibition and anti-proliferative effects correlation study with cellular eIF4E phosphorylation. ..... 80

Figure 3.9: Anti-proliferative effects correlated with FLT3 enzyme inhibition ..... 81

Figure 3.10: Effects of FLT3 inhibition on the phosphorylation of STAT-5 at Tyr694 and of eIF4E at Ser209 ..... 84

Figure 3.11: Study of apoptosis and cell death ..... 85

Figure 3.12: Caspase-3/7 activity in MV4-11 cells after 24-hours incubation with MNKI-7 and SL4-26 ..... 86

Figure 4.1: GST-Mnk1a and GST-Mnk1b expression vectors, pGEX-6P1 (*E. coli*, left) and pEBG-6P (HEK293T, right) ..... 93

Figure 4.2: Plasmid verification with agarose gel-electrophoresis. pGEX-6P1 (*E. coli*) and pEBG-6P (HEK293T) were cut with BamHI and NcoI ..... 94

Figure 4.3: Determination of optimal conditions for HEK293T cell transfection and IPTG induction with *E. coli* Bl-21 bacteria ..... 95

Figure 4.4: Gel image of samples collected at each stages of purification and assessment of protein purity with SDS-PAGE ..... 97

Figure 4.5: Western blot analysis of *E. coli*- and HEK293T-derived protein using total Mnk1 antibody and phospho-Mnk1 antibody ..... 99

Figure 4.6: Kinase activity testing with ADP-Glo™ assay .....101

Figure 8.1: ADP Glo assay validation with GST-Mnk2 .....163

Figure 8.2: Determination of interference of compounds to assay components.....165

Figure 8.3: ADP-Glo™ assay validation with CDK4/cyclin D1and CDK6/cyclin D1 166

Figure 8.4: ADP-Glo™ assay validation with CDK9/Cyclin T1.....167

Table 2.1: Common biochemical kinase assay technologies. ..... 29

Table 2.2: Kinetic constants for Mnks. ..... 41

Table 2.3: Summary of Mnk inhibitory activity and binding modes. ..... 47

Table 2.4: Selectivity of Mnk inhibitors against CDK2A and CDK9T1. ..... 52

Table 3.1: Characteristics of the prostate cancer cell lines. ..... 62

Table 3.2: $GI_{50}$ values calculated from MTT data in PCa cells in comparison to Mnk inhibitory activities. ..... 62

Table 3.3: Correlation of the p-eIF4E inhibitory activities of Mnk inhibitors in PCa cells with their anti-proliferative activities and enzymatic kinase inhibitory activities. . 68

Table 3.4: Anti-proliferative activity of CGP57380, MNKI-7, MNKI-85 and MNKI-57 against leukaemia cell lines and normal fibroblast cell line by 72 hours resazurin and MTT assay, respectively. ..... 76

Table 3.5: Kinase inhibitory and anti-proliferative profiles of MNKI-7 and SL4-26 .... 82

Table 4.1: Expression vectors and expression systems for the production of GST, GST-Mnk1a and GST-Mnk1b proteins. ..... 93

Table 4.2: Protein concentrations from *E. coli* and HEK293T purified protein assessed with DC protein assay ..... 96

Table 4.3: Purity of proteins assessed with SDS-PAGE. ..... 98

Table 6.1: List of 134 compounds with their chemical structures used in the study. ... 110

Table 6.2: List of recombinant proteins used in the kinase assay. ..... 118

Table 6.3: List of substrates used in the kinase assay. ..... 118

Table 6.4: List of assay kits, their suppliers and catalogue numbers. ..... 118

Table 6.5: List of chemicals and reagents, their suppliers and catalogue numbers. ..... 119

Table 6.6: List of antibodies used for Western blotting, their suppliers and catalogue numbers ..... 121

Table 6.7: List of general consumables, their suppliers and catalogue numbers .....122

Table 6.8: List of instruments, their suppliers and catalogue numbers. .....124

Table 6.9: Composition of kinase reaction buffer for Mnk1/2 and CDK4/6 assays .....126

Table 6.10: Composition of standard-assay-buffer (3.33 × stock) for CDK9 assay .....126

Table 6.11: Composition of kinase dilution buffer for CDK9 assay .....126

Table 6.12: Composition of lysis buffer used for Western blots .....127

Table 6.13: Composition of loading buffer (3 ×), 10 mL used for Western blots .....127

Table 6.14: Composition of running buffer (10 ×), 1 L used for Western blots .....127

Table 6.15: Composition of Tris buffer saline tween (TBST) 1 ×, 1 L used for Western blots .....127

Table 6.16: Composition of lysis buffer used for protein purification.....128

Table 6.17: Composition of wash buffer used for protein purification.....128

Table 6.18: Composition of elution buffer used for protein purification.....128

Table 6.19: Composition of activation buffer used for protein purification .....129

Table 6.20: Composition of storage buffer used for protein purification .....129

Table 6.21: List of primers used for DNA-sequencing of insert Mnk1a (HA1 and HA2) and Mnk1b (HA3 and HA4).....130

Table 8.1: GST and His tagged Mnk2 showed similar kinetic parameters.....164

Table 8.2: Compound profiling data from IMAP® and ADP-Glo™ assay for 160 compounds plus CGP57380 and cercosporamide are used as standards. .....168

Table 8.3: Summary of anti-proliferative effect, inhibition of cellular phosphorylation of eIF4E and kinase (Mnk1/2, CDK2A/9T1 and FLT3) inhibitory activity of compounds in MV4-11 cells. .....172

# 1. Introduction

Cancer is a term used to describe an uncontrolled growth and proliferation of cells due to genetic disease. These cancerous cells have the ability to invade and spread into other parts of the body through blood and lymph vessels, causing metastasis. As cancer cells can develop from any cell of almost all tissue types, there are more than one hundred types of cancers. Cancer is a leading cause of death worldwide. The most common types of cancer worldwide are lung, breast, prostate and colorectal cancers [1].

Development and progression of cancer occurs *via* several steps, which comprise six biological hallmarks including: (1) resisting cell death; (2) evading growth suppressors; (3) sustaining proliferative signalling; (4) enabling replicative immortality; (5) inducing angiogenesis and (6) activating invasion and metastasis [2]. In addition to the acquisition of these hallmarks by the tumour cells, the stromal cells also participate actively in developing certain characteristics of tumourigenesis rather than acting as passive bystanders [3]. Normal tissues carefully maintain the homeostasis of the organism by controlling the production and release of growth-promoting signals that direct the cells to enter from the resting phase into the cell growth-and-division cycle, and initiate programmed cell death (apoptosis) in response to DNA damage and other cellular stresses. However, in cancer cells this homeostatic regulation is highly compromised and

multiple pathways are employed to promote the abnormal cell proliferative and anti-apoptotic signalling [3, 4].

Two additional cancer-related cellular processes are gaining importance as emerging hallmarks of cancer as they are deemed functionally important for the development of cancer. They are: (1) the capacity of tumour cells to escape immunological surveillance by lymphocytes, macrophages and natural killer cells which pro-actively prevent tumour formation in the human body and (2) the ability of tumour cells to modify energy metabolism in order to support their continuous growth and survival [3, 5].

The acquisition of all these cancerous hallmarks is made possible by two enabling processes: the development of genomic instability and tumour-promoting inflammation. Genetic instability resulting from the mutations of functional genes confers a selective advantage and drives tumourigenesis. Classical examples of this are the Ras/Raf/MAPK and PI3K/AKT/mTOR signalling pathways which are frequently de-regulated in cancer (refer to section **1.2**). Inflammation mediated by innate immune cells, on the other hand, can inadvertently serve to promote tumour progression through supplying bioactive molecules to the tumour microenvironment while attempting to fight infections and heal wounds [3].

Along with surgery and radiotherapy, chemotherapy is the most commonly used therapeutic approach for many types of cancer. The traditional form of chemotherapy is based on cytotoxic effects leading to DNA modifications or targeted inhibition of nucleotide biosynthesis [6]. The most common drawbacks of chemotherapy are the serious side effects due to non-specific killing of cells, development of drug resistance and relapses. There is a pressing need to discover new drugs which target key molecules

involved in oncogenesis, possessing strong anti-tumour activity against cancer cells but reduced toxicity to normal cells.

There has been significant progress in understanding the molecular mechanisms and pathophysiology involved in cancer [7]. Many protein kinases such as MAP kinase-interacting kinases (Mnks), FMS-like tyrosine kinase-3 (FLT3), Abelson tyrosine kinase, human epidermal growth factor receptor 2 (HER2), Cyclin-dependent kinases (CDKs), phosphoinositide 3-kinase (PI3K) *etc.* have been associated with cancer development where they are deregulated by mutations, amplification and upregulation. As expected, the interest of many researchers has been drawn towards the development of kinase inhibitors including small molecule (*e.g.* imatinib) and monoclonal antibodies (*e.g.* trastuzumab) [8, 9]. Some of these drug molecules have shown the remarkable clinical advantages by selectively targeting cancer cells with minimal toxicity in normal cells.

## 1.1 Protein kinases as anticancer targets

Protein kinases are a very important class of enzymes present in the cell. They transfer the outermost phosphate (the gamma phosphate) from adenosine tri-phosphate (ATP) onto a serine, threonine or tyrosine residue of a target protein [10]. Protein kinases comprise the largest group of kinases with more than 500 different kinase genes encoded in the human genome. Protein kinases may be divided into two main categories: (1) serine/threonine kinases, which can phosphorylate both serine and threonine residues and (2) tyrosine kinases that are able to phosphorylate only tyrosine residues. These kinases play an important role in the control of fundamental cellular processes such as cell proliferation, differentiation and apoptosis *via* various signalling pathways. Alterations in the kinase activities that cause an imbalance of cellular signals which control these events may promote cell proliferation, prevent apoptosis and augment invasion. Their diverse

roles in various oncogenic signalling pathways make them important targets for the development of novel anti-cancer drugs [11, 12].

Development and approval of Imatinib, a tyrosine kinase inhibitor, for the treatment of chronic myeloid leukaemia (CML) patients [13] has inspired the scientific community to switch from non-specific chemotherapy to targeted cancer therapy, especially targeting protein kinases. Imatinib set new standards for cancer treatment, showing up to 80% response rates in CML patients [14]. At present, 28 small-molecule kinase inhibitors have been approved by the US Food and Drug Administration (FDA) for treating cancers, and many are in pre-clinical and clinical trials, potentially leading to considerable impact on future cancer therapy [15].

## 1.2 Major signalling pathways in cancer

The acquisition of a number of characteristic alterations (above section) during the course of cancer progression, are the reflections of the alterations in the cellular signalling pathways that in normal cells regulate diverse processes such as protein synthesis, cell growth and division, motility, and survival [16]. The rate of translation is controlled by a network of signalling pathways that regulate phosphorylation of translational proteins, and their dysregulation can lead to cellular dysfunction and disease including cancer. Two major signalling pathways involved in cancer development are:

### 1.2.1 Ras/Raf/MAPK signalling pathways

The Ras/Raf/MEK/ERK pathway is mainly stimulated by growth factors such as epidermal growth factor receptor (EGFR), insulin-like growth factor (IGF) type 1 receptor (IGF1R) leading to activation of Mnk1/2 (*vide infra*, **Section 1.4**) which eventually triggers eukaryotic initiation factor 4E (eIF4E) modulation *via*

phosphorylation in the eukaryotic initiation factor 4F (eIF4F) complex which is a heterotrimeric protein complex comprising of eIF4E, eIF4A and eIF4G (**Figure 1.1**). The activity of Ras is suppressed by neurofibromin-1 (NF-1) in normal conditions. Activated Ras is associated with a bound guanosine-5′-triphosphate (GTP) and is able to activate Raf kinase which in turn activates mitogen-activated protein kinase kinases (MEK) 1 and 2 by phosphorylation. Subsequently, activated MEK1/2 phosphorylates the extracellular signal-regulated kinases 1 and 2 (ERK1/2) [17]. Another downstream effector of Ras is the stress-driven p38 MAPK cascade. Activation of both ERK1/2 and p38 are involved in phosphorylating numerous cytoplasmic substrates which mediate many cellular mechanisms, including cell cycle progression, growth, migration, apoptosis and senescence [18, 19]. Additionally, aberrant Ras, Raf and MAPK proteins (primarily due to activating mutations and over-expression) were identified in cancers of pancreas, lung, thyroid, melanoma, breast, colorectal and acute myelogenous leukaemia (AML) [18, 20]. Therefore, blocking downstream effectors of Ras/MAPK signalling could be beneficial as a cancer treatment.

### 1.2.2 PI3K/AKT/mTOR signalling pathways

The PI3K/AKT/mTOR pathway is generally activated by extracellular growth factors, mitogens and cytokines, and is often involved in tumour development, as several components are prone to genetic modification. The tumour suppressor gene phosphatase and tensin homolog (*PTEN*) is often silenced by mutation in many cancers, and this promotes the activation of AKT and subsequently mTOR, resulting in increased phosphorylation of 4E binding proteins (4E-BPs) and ribosomal protein S6 kinases (S6Ks), therefore, leading to the release of eIF4E for the activation [11, 21]. S6Ks inhibit the phosphorylation of programmed cell death protein 4 (PDCD4) whose role is to inhibit

the interaction between eIF4A1 and eIF4G. Strategies to inhibit the activation of eIF4E are likely to be of advantage in *PTEN*-silenced cancers.

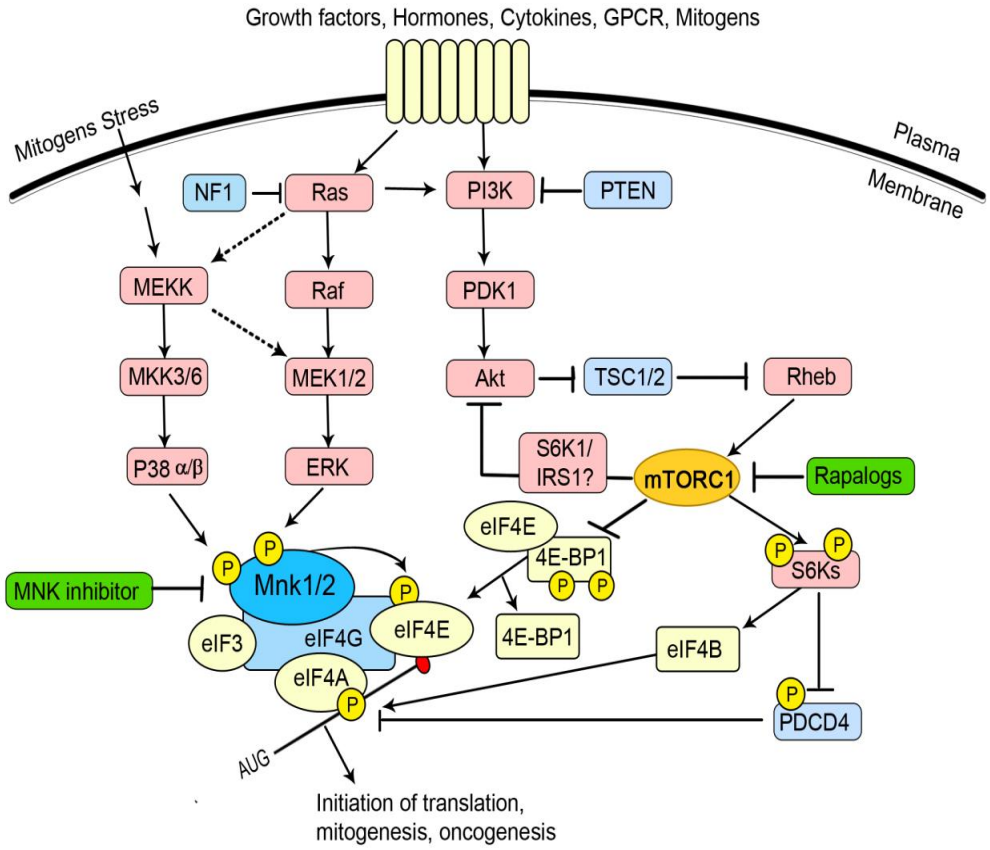



**Figure 1.1: Regulation of eIF4E by two major cell-signalling pathways.** Two intracellular signalling pathways, MAPK pathway and the PI3K/Akt/mTOR pathway modulate the activity of eIF4E. In response to extracellular stimuli such as growth factors, cytokines and stress, Mnks are phosphorylated by ERK1/2 and/or p38 MAPKs. Mnks activate eIF4E by phosphorylation at Ser209, which modulates translation with enhanced production of oncogenes. Furthermore, the PI3K/Akt/mTOR pathway regulates the availability of eIF4E. Triggering PI3K activates mTORC1, which in turn phosphorylates 4E-BPs and S6Ks. Hyper-phosphorylated 4E-BPs bind weakly to eIF4E, releasing it to bind to eIF4G to initiate cap-dependent translation. Activation of these signalling pathways leads to activation of the translational machinery in the cell. Reprinted with permission from Oncotarget, 3 March 2012, volume 3, pages 118-131 [22]. Copyright (2012) Impact Journals.

### 1.2.3 Node of convergence of two major signalling pathways

ERK1/2 and p38 MAPK in the Ras/Raf/MAPK pathway activate Mnks by phosphorylation of Thr209/214 and Thr244/249 located in the activation loops of Mnk1 and Mnk2, respectively [23]. The p38 stimulates mainly Mnk1 activity *via* a stress-activated cascade of kinases whereas ERK kinases can phosphorylate both Mnk1 and Mnk2 [24-26].

4E-BP1 plays a crucial role in regulating the availability of eIF4E for the formation of the eIF4F complex. 4E-BP1 is phosphorylated by mTOR and once hyper-phosphorylated, eIF4E is released, ensuring its availability for cap-dependent translation. Given that both the major signalling pathways (*i.e.* PI3K/AKT/mTOR and Ras/Raf/MAPK) lead to activation of eIF4E (**Figure 1.1**), and that Mnks are the only known kinase to activate eIF4E, Mnk inhibitors has potential to target both signalling pathways simultaneously [27].

Outcomes from anti-cancer treatment with inhibitors of the Ras/Raf/MAPK signalling pathway such as sorafenib (inhibitor of Raf kinase) [28] and PI3K/AKT/mTOR signalling pathways (rapalogs), such as rapamycin (inhibitor of mTOR) [29] are far from satisfactory due to the development of resistance. Inhibition of one pathway leads to the activation of the other [30]. Therefore, simultaneous targeting of the two signalling pathways appears an attractive therapeutic approach for cancer. The strategy advocated here involves the inhibition of eIF4E phosphorylation (common downstream effector of the two key signalling pathways) by targeting Mnk1 and 2.

## 1.3 Eukaryotic initiation factor 4E

eIF4E is a general translation factor involved in regulating the translation of mRNA at the 5′ terminal cap structure [31, 32]. Mnk1 and Mnk2 bind to eIF4G and phosphorylate eIF4E [33]. The availability of eIF4E is controlled by 4E-BPs, which in their non-phosphorylated form can interact with eIF4E and prevent it from binding with eIF4G (**Figure 1.1**). The hyper-phosphorylation of 4E-BPs releases eIF4E and allows it to integrate into the eIF4F complex. Moreover, eIF4E can be phosphorylated at Serine 209 by Mnk kinases, and it was supposed that this phosphorylation modulates the translational activity of malignancy-related "weak" mRNAs (*e.g.*, for VEGF, cyclin D1, c-Myc, survivin) [34]. Weak mRNAs contain long, structured, untranslatable regions at their 5' end which makes it difficult for ribosomes to initiate transcription. These weak mRNAs, that carry the code for proteins involved in oncogenesis, require cap-dependent translation which necessitates the cellular involvement of the eIF4E [35].

The availability of eIF4E to form the eIF4F complex and its phosphorylation by Mnk kinases are two important factors in controlling the rate of translation. In addition to its role in mRNA translation, eIF4E interacts with the 4E transporter (4E-T). This is a shuttling protein that regulates nuclear export to the cytoplasm of several mRNAs which contain the 4E-sensitivity element (4E-SE), including the mRNA for cyclin D1 [36]. Cyclin D1 is important for the progression from the G1 (Gap 1) to S (DNA synthesis) phase of the cell cycle [37, 38] . Furthermore, promyelocytic leukaemia protein (PML), a regulator of cell growth and apoptosis located inside the nucleus, binds to eIF4E and inhibits eIF4E-dependent transport of mRNA. These interactions can be associated with cell growth, proliferation and differentiation [39].

### 1.3.1 Regulation of eIF4E

The regulation of eIF4E activity is complex [40] but the two major mechanisms have been proposed: (1) interactions with eIF4E binding proteins (4E-BPs) and (2) phosphorylation by Mnk kinases (**Figure 1.1**). The 4E-BPs (4E-BP1, 4E-BP2 and 4E-BP3) bind reversibly to eIF4E and prevent formation of the eIF4F complex [20], leading to inhibition of cap-dependent translation [41]. Extracellular factors like hormones (*e.g.*, angiotensin, insulin), cytokines (*e.g.*, interleukin-3), amino acids, growth factors (*e.g.*, epidermal growth factor) and G-protein coupled receptors (GPCRs) stimulate the phosphorylation of 4E-BPs. In contrast, heat shock or infection by some viruses (*e.g.* picorna viruses) stimulate dephosphorylation of 4E-BPs and thus inhibit translation [20, 21, 42]. Moreover, p53 (an endogenous tumour suppressor protein) and various proteins of the TNF family, like Fas ligand, TNF-related apoptosis-inducing ligand (TRAIL) and TNFα, reduce the level of 4E-BP1 phosphorylation and thus block translation [8, 43].

Extracellular stimulators trigger a cascade of events where PI3K activates the 3-phosphoinositide dependent kinase-1 (PDK1), which triggers the activation of Akt, and in turn inactivates tuberous sclerosis complex 1 and 2 (TSC1/2) *via* phosphorylation of TSC2. TSC2 acts as the guanosine triphosphatase (GTPase) - activator protein for GTPase Rheb. Consequently, Rheb guanosine triphosphate (Rheb-GTP) accumulates which leads to activation of the PI3K/Akt/mTOR complex 1 (mTORC1) (**Figure 1.1**), and subsequently to phosphorylation of 4E-BP, release of eIF4E, and formation of the active eIF4F complex [44]. Altogether, phosphorylation of 4E-BP1 seems to be an early event controlling eIF4E-mediated tumourigenesis, which is emerging as a promising prognostic marker for cancer such as in astrocytoma [20, 21, 45].

MAP kinase pathways (refer to **Section 1.2.1**) activate the Mnks and mediate phosphorylation of eIF4E at Ser209 [45]. In addition, regulation of eIF4E phosphorylation by these upstream MAP kinases, constitutive Mnk activities also affect eIF4E activation. In particular, high basal activity of Mnk2 increases eIF4E phosphorylation, independently of the activation of the upstream ERK/p38 kinases. This may explain why insulin, which does not activate ERK but enhances eIF4F formation, increased only Mnk2-mediated phosphorylation of eIF4E [46].

### 1.3.2 Role of eIF4E in initiating translation

The levels of proteins in the cells are regulated by the rate of transcription, nuclear export of mRNA, mRNA stability, rate of translation and protein degradation. Among all these, rate of translation is described as one of the most important factors for determining the amount of protein [47]. Post-translational modification of proteins, such as phosphorylation, is especially important for regulating critical cellular functions like cell division, growth and metabolism. Deregulation of protein synthesis is often highlighted in oncogenesis, and eIF4E plays a key role in controlling protein synthesis. eIF4E is a mRNA cap-binding protein responsible for initiating translation in eukaryotic cells [23]. Eukaryotic translation is a process by which messenger RNAs (mRNAs) are translated into proteins in eukaryotes and is linked to cell growth, proliferation and differentiation [48]. There are two types of translation: (1) cap-dependent translation requiring eIF4E and (2) cap-independent translation mediated by internal ribosome entry sites (IRES). Protein translation involves three steps, *i.e.*, initiation, elongation and termination. Initiation of translation by various initiation factors, such as eIF4E, is often a rate-limiting step, which serves as a premium target for translational control [21].

The ribosome recruitment phase of translation initiation is mediated by the eIF4F complex which consists of: (1) eIF4E, the cap-binding protein responsible for directly binding to the cap structure of mRNA [49, 50]; (2) eIF4A, a helicase which unwinds local secondary structure and facilitates access of the 43S ribosomal complex to the mRNA complex [20, 49] and (3) eIF4G, a scaffold protein, which recruits the 40S ribosomal subunit to the mRNA *via* its interaction with eIF3 (a multi-subunit initiation factor) (**Figure 1.2**).

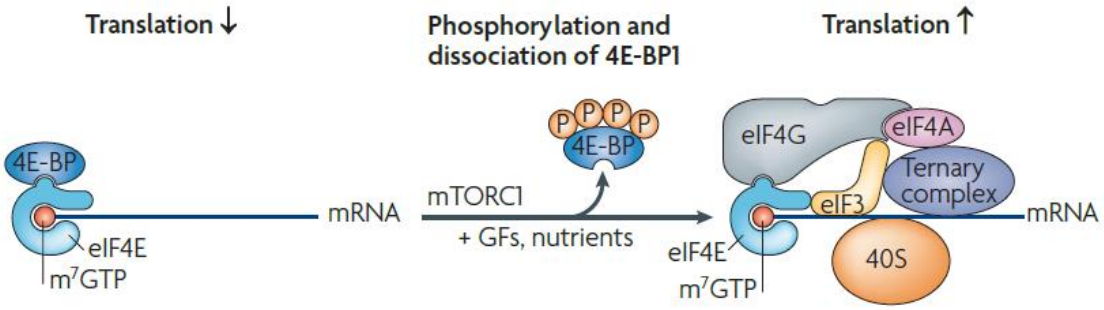



**Figure 1.2: Cap-dependent initiation of translation in eukaryotes.** Binding of eIF4E to hypo-phosphorylated 4EBPs acts as a rate-limiting step in cap-dependent translation initiation by preventing its interaction with eIF4G. mTORC1-mediated phosphorylation of 4E-BPs releases eIF4E, resulting in the recruitment of a 40S ribosomal subunit to the 5′ end of mRNA and eIF4G to the 5′ cap, facilitating recognition of the AUG-codon and thereby initiating the translation process **[46, 51, 52]**. Reprinted with permission from Nature Reviews Molecular Cell Biology, May 2009, volume 424, pages 307-318. Copyright (2009) Nature publishing group.

The assembly of the eIF4F complex is crucial for cap-dependent translation [53]. In eukaryotes, the initiation of cap-mediated translation involves recognition of the $m^7$GppN structure ($m^7$ = methyl group on position N7 on guanine, G = guanine, p = phosphate group and N = any nucleotide) by the cap-binding protein eIF4E at the 5′ end of the mRNA [49, 54]. This assists recruitment of the 40S ribosomal subunit with the ternary complex (of eIF2, GTP and the initiator methionyl tRNA) by eIF3 to the mRNA. Once this 40s subunit binds to the 5′ untranslated region (5′ UTR) of mRNA, it recognises and

locates the start codon AUG. The large ribosomal subunit 60S subsequently binds to give a complete ribosome, thus entering the elongation step of protein synthesis [55, 56].

### 1.3.3 Role of eIF4E in oncogenic translation

Recognition of the $m^7G$ cap structure by eIF4E at the 5′-UTR of mRNAs leads to initiation of cap-dependent translation of mRNAs [26]. A RNA helicase eIF4A and a scaffold protein eIF4G are then recruited to the system.The availability of eIF4E to participate in the formation of the eIF4F complex is critical for initiating the translation of most mRNAs. Given its restricted availability due to binding to 4E-BP1, eIF4E is considered as a rate-limiting factor for initiating translation in eukaryotic cells.

A low level of phosphorylated eIF4E is sufficient for the translation of short, unstructured 5'-UTR mRNAs (depicted as "strong" mRNAs), which are essential for the translation of housekeeping proteins required for normal growth, such as glyceraldehyde-3-phosphate-dehydrogenase (GAPDH) and β-actin [57]. In contrast, eIF4E phosphorylation greatly enhances the translation of "weak" mRNAs with long and structured 5'-UTRs, including proteins that play critical roles in tumour growth, proliferation and apoptosis (*e.g.*, c-Myc, EGF-2, VEGF and cyclin D1) [58] and anti-apoptotic proteins (*e.g.*, B-cell lymphoma 2 (Bcl-2) and survivin); (**Figure 1.3)** [59]. *In vivo* studies further supported these findings: transgenic mice with constitutive eIF4E expression controlled by the β-actin promotor showed a distinct increase in tumour formation [60]. Another finding has shown that the expression of eIF4E antisense RNA reduced proliferation of Hela cells [61]. In addition, inhibition of eIF4E phosphorylation by targeting Mnk1 activity by CGP57380 or downregulation of Mnk1 by shRNA blocked translation of VEGF mRNA [62]. An additional study demonstrated that unphosphorylatable eIF4E mutants reduced tumours [50] whereas phosphor-mimic eIF4E induced hypertrophy [63]. eIF4E has generated

significant interest in cancer research, since its overexpression has been implicated in various cancers including those of the breast, colon, head and neck, lung, bladder, prostate and gastrointestinal tract, Hodgkin's lymphomas and neuroblastomas [64].

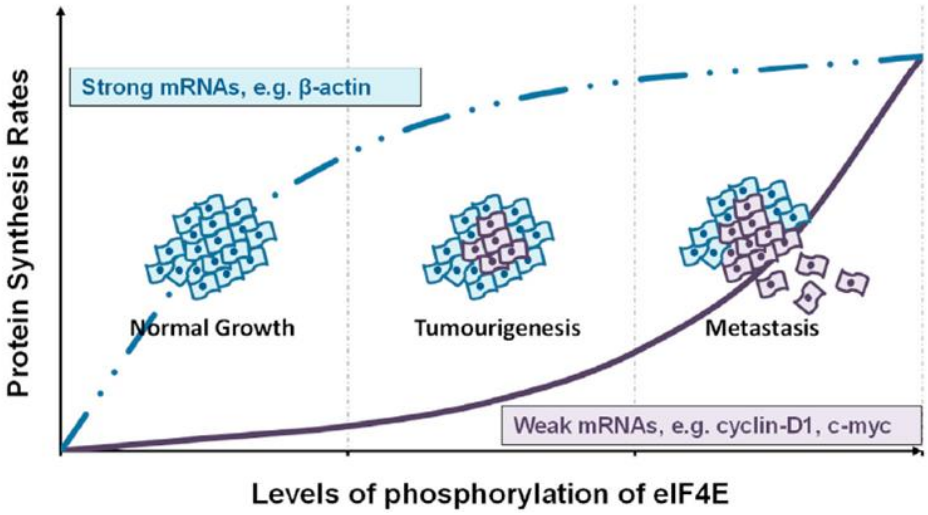



**Figure 1.3: mRNA discrimination in the translation by level of phosphorylated eIF4E.** Translation of "strong" mRNAs (blue dashed curve) is relatively independent of the level of phosphorylated eIF4E, whereas translation of "weak" mRNAs occurs only at much higher levels of phosphorylated eIF4E (purple solid curve). (Reprinted with permission from Cell Press, 24 Apr 2014, Volume 21, Issue 4, Pages 441-452 [23, 65].

### 1.3.4 eIF4E as a target for cancer therapy

Studies have shown that overexpression of eIF4E leads to oncogenic transformation and increased levels of oncogene products, *e.g.* c-Myc, cyclin D1, fibroblast growth factor 2 (FGF-2), and VEGF [36]. Transgenic mice with constitutive eIF4E expression showed an increase in tumour formation [66]. Conversely, antisense RNA to eIF4E decreased the proliferation of Hela cells and altered cell morphology [60], suggesting again that eIF4E contributes to oncogenesis. Reduced overall survival of patients diagnosed with non-small-cell lung carcinoma was linked to high level of eIF4E expression and to an acquired resistance to erlotinib [67]. Additionally, the degree of phosphorylation of eIF4E associated with the progression of the disease has a poor prognosis in prostate and

pancreatic cancers [68-70]. These studies provide proof-of-concept that deregulation of eIF4E may contribute to the formation tumour and maintenance of their growth.

Ribavirin, an $m^7$GppN mimetic, inhibited the activity of eIF4E after conversion to the triphosphate form in the cell [46, 71-73]. Ribavirin has also been reported to reduce the expression level of eIF4E in leukaemia patients [74]. A phase I clinical trial using the combination of ribavirin with low dose cytarabine in patients with overexpressed eIF4E showed that the combination was well tolerated and a marked clinical response was achieved by some patients [75, 76].

Moreover, Wagner *et al.* developed a compound, 4EG1-1, which blocked the interactions between eIF4E and EIF4G through binding with eIF4E, thereby inhibiting cap-dependent translation. This compound reduced the expression of growth and angiogenesis factors such as c-Myc and cyclin D1 [77, 78].

The eIF4E-specific antisense oligonucleotide, 2'-O-methyloxy-ether-gapmer, decreased the expression of oncogenic proteins including cyclin D1, c-Myc, VEGF, survivin and Bcl-2. Moreover, it did not affect body weight, organ weight, or liver transaminase levels in tumor xenograft models, thereby providing the *in vivo* evidence that cancers may be more susceptible to eIF4E inhibition than normal tissues [79, 80]. Given that the phosphorylation of eIF4E by Mnks seemed crucial for its oncogenic activity, targeting Mnks have emerged as a potential anti-cancer therapeutic strategy.

## 1.4 Mnks

Two Mnk genes *i.e. Mnk1* and *Mnk2*, alongside spliced variants (*i.e. Mnk1a*, *Mnk1b*, *Mnk2a* and *Mnk2b*) have been identified in humans (**Figure 1.4A**). All four isoforms contain a kinase domain, a nuclear localisation signal (NLS) and a binding region for

eIF4G [31, 81]. However, C-termini of these isomers are different: Mnk1a and Mnk2a isoforms contain a MAP kinase binding site, driving the phosphorylation of the respective Thr209 and Thr214 in the activation loop by p38 and/or ERK1/2 (*i.e.* Mnk1a binds to both ERK1/2 and p38 while Mnk2a binds to ERK1/2 only) [23]. The other two isoforms Mnk1b and Mnk2b have short C-terminal regions which lack the MAP kinase binding site, rendering them to be poor substrates for p38 and ERK1/2 kinases. There is 80% sequence similarity between the catalytic domains of Mnk1 and Mnk2 (**Figure 1.4B**) [82]. However, the conformation of the activation segments and the orientation of the lobes differ in crystallographic studies, revealing that the ATP binding site of Mnk1 is less accessible to ATP because the N-terminus is rotated by approximately 10°, producing a narrower interlobal cleft compared to Mnk2 [24, 83].

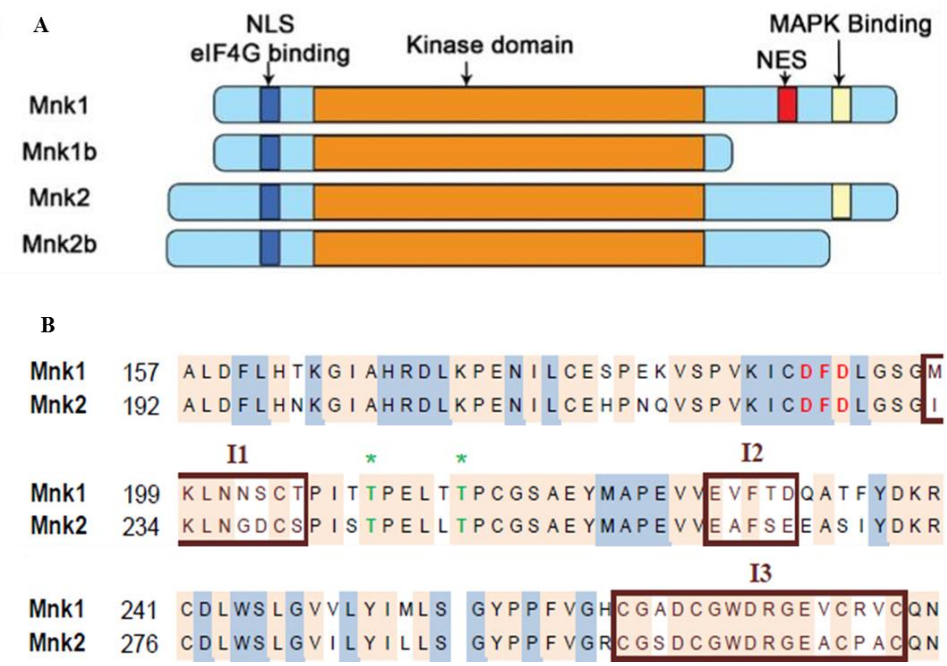



**Figure 1.4: Schematic structure of Mnk1/2 and their sequence alignment of kinase domains.** (A) The eIF4G binding site and NLS lie within the N-terminus and the MAPK binding site and nuclear export sequence (NES) within the C-terminus. (B) The DFD motif is shown in red, the phosphorylation sites in green asterisk, and the three insertions in line-edged brown boxes. The pink residues highlights the conserved residues between Mnk1 and Mnk2, and the blue residues conserved between other kinases like FLT3, and c-KIT. Reprinted with permission from Oncotarget, 3 March 2012, volume 3, pages 118-131 [23, 24]. Copyright (2012) Impact Journals).

### 1.4.1 Unique structural features of Mnk protein

Protein kinases have a $Mg^{2+}$-ATP binding site placed in a deep cleft between the hydrophobic C- and N-terminal lobes [23], which are connected by the hinge region. In general, protein kinases contain an activation loop designated by two conserved motifs namely the DFG (Asp-Phe-Gly) motif at the start of the loop and the APE (Ala-Pro-Glu) motif at the end [84]. The DFG motif plays a crucial role in modulating kinase activity and is able to adopt two extreme states; active state (DFG-in conformation) and inactive state (DFG-out conformation). Phosphorylation of the activation loop enables the Phe residue of the DFG motif to occupy a hydrophobic pocket in the groove between the two lobes, rendering it an active DFG-in conformation [8].

Similar to other protein kinases, Mnks have an ATP binding site sandwiched between the C- and N-lobes (**Figure 1.5A**). The N-terminal region consists of a small hydrophobic lobe comprising 80 amino acid residues where Lys78 seems to be crucial for ATP binding [84, 85]. This lobe consists of the binding region for eIF4G and the NLS. The C-terminal lobe contains the activation segment and the catalytic domain. The highly flexible activation segment encloses different elements essential for substrate binding and phosphate transfer, including the magnesium binding domain, activation loop containing the Thr residues which can be phosphorylated by MAPK, and the P+1 loop [24, 25]. In contrast with most other protein kinases, the Mnk1/2 activation segments start with a DFD motif (Asp191-Phe192-Asp193 in Mnk1 and Asp226-Phe227-Asp228 in Mnk2) within the magnesium binding loop instead of the DFG motif, resulting in distinct structural features of Mnks [86]. This unique structural feature offers an opportunity to develop highly selective Mnk inhibitors [87] by targeting the DFD motif.

Discovery of novel, potent and selective Mnk inhibitors has been limited by the unavailability of enough structural data. Only four crystal structures of Mnks are available in the public database (PDB) [24, 25]. The x-ray crystal structure of Mnk1 has been resolved in an auto-inhibited form (**Figure 1.5B**), where a Mnk-specific insertion (side chain of the Phe230) expels the preserved Phe192 of the DFD motif into the ATP-binding site from its hydrophobic pocket. This translocation imposes an inactive DFD-out conformation of the kinase. However, the corresponding structure of Mnk2 does not demonstrate this feature (**Figure 1.5C**) [88, 89]. The DFD to DFG mutation in Mnk2 partially stabilizes Mnk2 DFD/G-out conformation (**Figure 1.5D**) but suggested no enthalpy gains for the preference of the DFD/G-out conformation. Moreover, the distinct Mnks features from many other kinases can be exploited to design selective and potent novel drug candidate for cancer therapy [24, 25, 90].

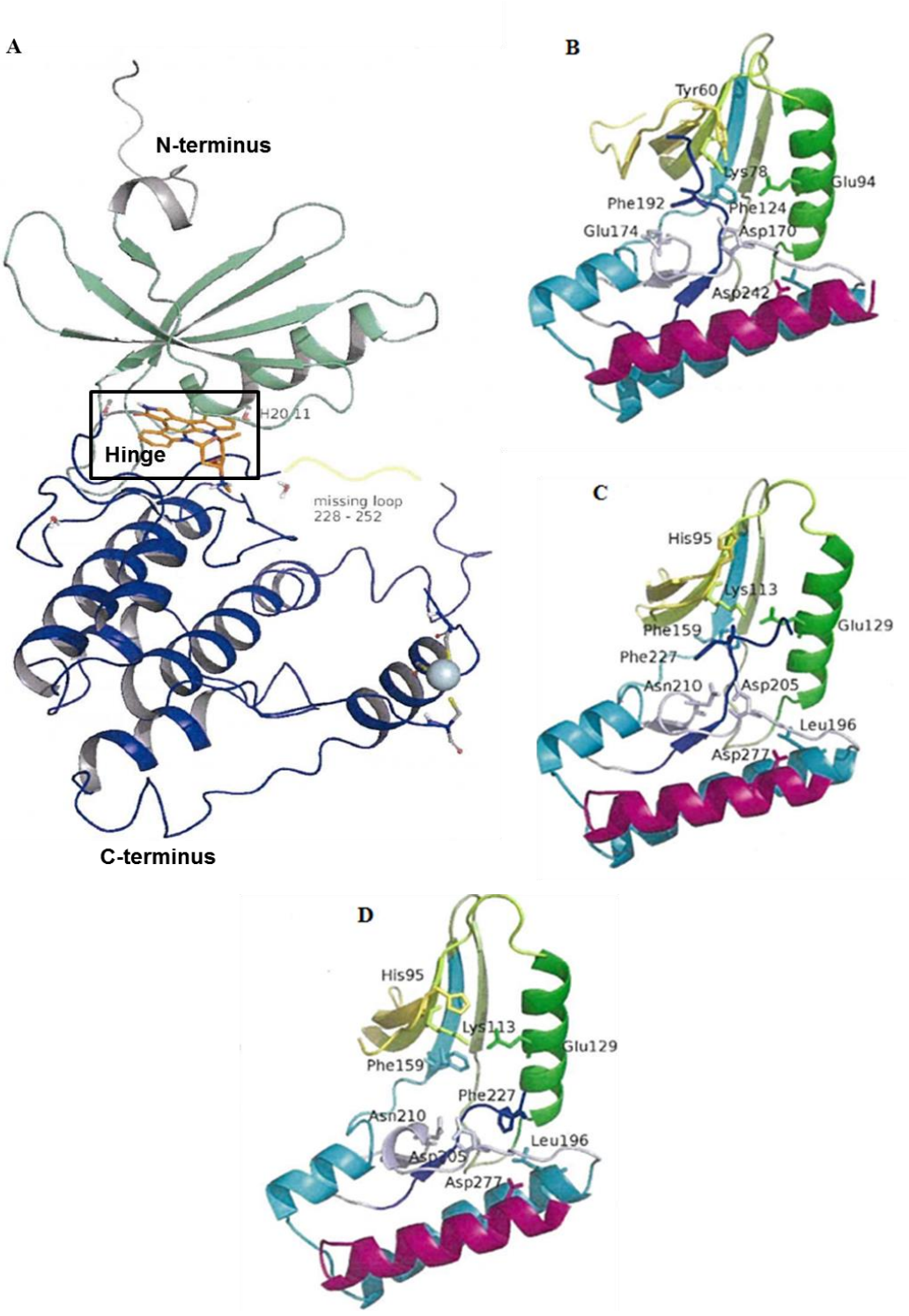



**Figure 1.5: Examples of Mnk structures.** (A) General structure of kinase domain of Mnks derived from the MNK2D228G/staurosporine complex (PDB ID 2HW7). The hinge region denoted by a black box lies between the N and C-terminal domain. The staurosporine represented by orange colour is bound in the ATP-binding site. Residues 228-252 are missing from the crystal structure. Water molecule which interacts with conserved side chain (Glu129 and Asp226 residues) is denoted as H2O11. (B) Mnk1in DFD-out conformation (PDB ID 2HW6). (C) Mnk2 in DFD-out conformation (PDB ID 2AC3)**.** (D) Mnk2 in DFD-in conformation (D228G mutant PDB ID 2AC5) [24, 25, 90].

### 1.4.2 Mnks as anti-cancer targets

Mnks are the only known kinases to phosphorylate eIF4E. Phosphorylation of eIF4E was not evident in mouse embryonic fibroblasts derived from a knock-in mouse where Ser209 had been replaced with the Alanine (Ala) residue (*i.e.* Ser209Ala). Moreover, approximately five-times fewer foci were formed in Ser209Ala mutant mice compared to fibroblasts from the wild-type mice after infection with a combination of Ras and c-Myc oncoprotein-expressing retroviruses [50, 91]. The same study showed that the knock-in mice with deficient eIF4E phosphorylation were resistant to prostate cancer induced by a loss of tumour suppressor *PTEN* gene. Another study where Mnk1/2 double knockout mice were crossed with a $PTEN^{-/-}$ lymphoma mouse model showed attenuated tumour formation, which correlated with reduced eIF4E phosphorylation. In contrast, $PTEN^{-/-}$ mice with intact Mnk1 and Mnk2 showed a higher incidence of tumours [32].

In addition, the role of Mnks in epithelial mesenchymal transition (EMT), a process that drives cancer cells to acquire metastatic capability, has also gained interest in recent research. Cell migration and invasion are key steps in metastasis, which are the major causes of death in cancer patients [92]. Studies showed that mutant (Ser209Ala) mice in which eIF4E cannot be phosphorylated were resistant to lung metastasis, and the cells derived from these mice showed impaired invasion [93]. The same study demonstrated that eIF4E phosphorylation induced by transforming growth factor-beta (TGFβ) promoted the translation of Snail and Mmp-3 mRNAs, thereby inducing EMT. The expression of these EMT-promoting proteins was observed to be selective, as the overall rate of translation was not affected.

Encouraging anti-tumour results have already been observed with compounds that selectively inhibit or degrade Mnks [32]. Mnk inhibition has gained further attention due

to the finding that the activity of Mnks is dispensable for normal growth and development [94-98]. Pharmacological inhibition of Mnks repressed the expression of vimentin, one of the classic markers of EMT, without increasing its mRNA level, suggesting that Mnks promoted the translation of vimentin [31, 99]. A recent study showed anti-migratory and anti-invasive activity of retinamides (*i.e.* the Mnk degrading agents) in MDA-MB-231 and MDA-MB-468 breast cancer cell lines [100]. Taken together, these studies suggest that Mnk-eIF4E signalling plays a major role in progressing tumour cells from benign to metastatic and inhibiting Mnks offers a promising therapeutic strategy against cancer.

### 1.4.3 Other Mnk substrates

Mnks regulate the activity of a number of other substrates besides eIF4E, such as polypyrimidine-tract binding protein-associated splicing factor (PSF) [95], RNA-binding proteins (*e.g.*, heterogeneous nuclear RNA-binding protein (hnRNP) A1 [101] and cytoplasmic proteins (*e.g.*, cytosolic phospholipase A2 (cPLA2) [102] and Sprouty 2 (Spry2) (**Figure 1.6)** [103].

The expression of tumour necrosis factor α (TNFα) has been shown to be modulated by Mnk1 through its effector hnRNP A1 (*i.e.* phosphorylation by Mnk1 at multiple Serine residues, Ser192, Ser310, Ser311 and Ser312). Experimental use of small interfering RNA (siRNA) to knock down Mnk1 in T cells inhibited the production of TNFα [104].

PSF was also reported to be phosphorylated by Mnks, and the role of this phosphorylation in exporting TNFα mRNA to the cytoplasm has been proposed [102]. Phosphorylation of cytosolic phospholipase A2 (cPLA2) at Ser727 by Mnk1 activated cPLA2 in a p38-dependent signalling pathway [101]. cPLA2 plays a major role in inducing the synthesis of eicosanoids by releasing arachidonic acid from glycerophospholipids, thereby implicating its role in the immune response, particularly inflammation [103]. Another

downstream effector of Mnks is Spry2, which is phosphorylated by Mnks at Ser112 and Ser121 [105]. Spry2 has been implicated as a inhibitor of multiple receptor tyrosine kinases and promotes down-regulation of the Ras-mediated ERK1/2 activation [106, 107].

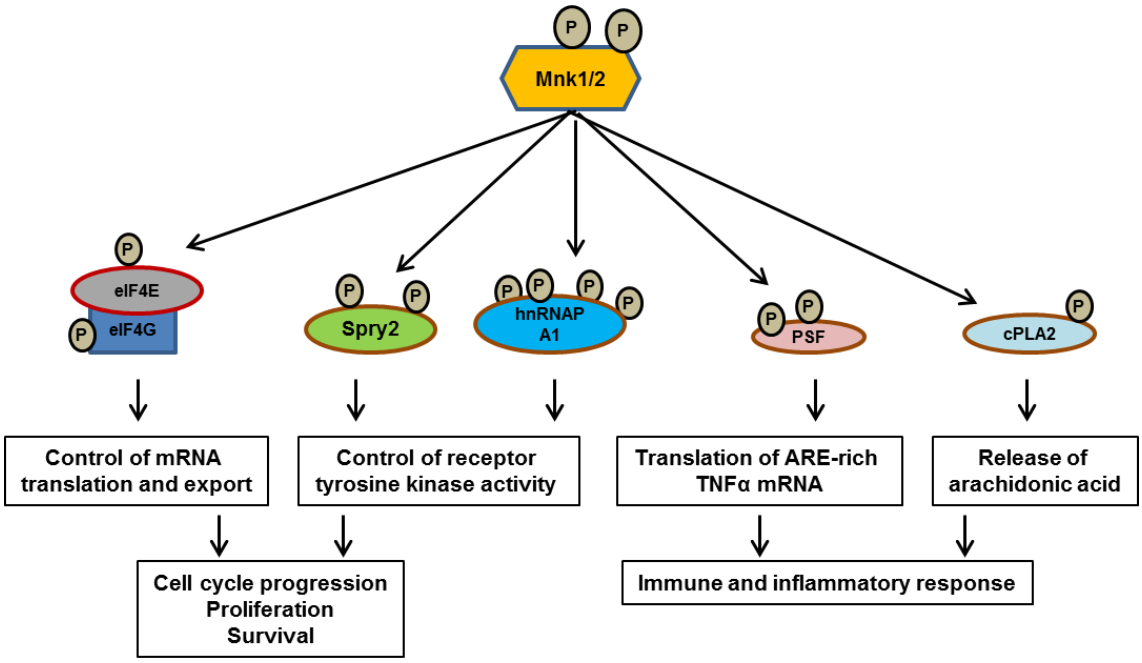



**Figure 1.6: Various substrates of human Mnks.** Upon phosphorylation by ERK1/2 and/or p38, Mnks are involved in regulating several downstream biological effectors by phosphorylating a number of substrates including eIF4E/eIF4G, Spry2, hnRNP A1, PSF, and cPLA2. Adapted from [107].

Overall, Mnk-mediated eIF4E phosphorylation promotes cancer development, progression and maintenance. Strong biological evidence supports Mnks as anti-cancer targets. Pharmacological inhibition of Mnks could represent an ideal mechanism-based and safe therapeutic strategy for cancer treatment since the kinase activity of Mnks seems to be of minor importance for normal growth and development. Comprehension of unique Mnk kinase structural features would guide inhibitor design, potency and selectivity optimisation.

### 1.4.4 Known Mnk inhibitors

At the commenement of this PhD project, only a few Mnk inhibitors *i.e.* CGP57380, CGP052088, cercosporamide and their analogues were available (**Figure 1.7**); yet none of them showed approporiate potency and selectivity. CGP57380 is a weak inhibitor with $K_i$ (inhibition constant) values of 1.01 and 0.87 μM against Mnk1 and Mnk2 respectively, and has been shown to block phosphorylation of eIF4E [108-110]. Cercosporamide, inhibiting Mnk1 and Mnk2 with $IC_{50}$ values of 0.116 and 0.011 μM respectively, also reduced eIF4E phosphorylation, induced apoptosis and inhibited the proliferation of various cancer cell lines. Furthermore, it blocked the phosphorylation of eIF4E in human xenograft tumour models and suppressed the outgrowth of B16 melanoma lung metastasis [111, 112].

Lack of kinase specificity is one of the major drawbacks of the kinase inhibitors. The ATP binding site is structurally conserved among kinases and is the target for many of their inhibitors (*i.e.* type I inhibitors). For example, in addition to Mnks, CGP57380 inhibited potently against several other kinases including Aurora B, serum- and glucocorticoid-induced kinase 1, lymphocyte cell-specific protein-tyrosine kinase, brain-specific kinase 2, CK1 and dual-specificity tyrosine-phosphorylated and -regulated kinase [113]. Cercosporamide also exerted non-specific inhibitory effects mainly on Janus kinase 3 (Jak3), proviral integration site for Moloney murine leukaemia virus 1 and 2 (Pim1/2) kinases and cyclin dependent kinases (CDKs) 2 and 9 [114]. Such broad off-target effects of these early Mnk inhibitors compromised the pharmacological proof of concept for Mnks as anti-cancer targets.

During this project, there have now been some advances made in developing novel Mnk inhibitors with higher potency and selectivity. A fragment-oriented virtual screening

protocol was applied to identify several compounds with potent inhibitory activity against Mnks, leading to the discovery of MnkI-1 (**Figure 1.7**) with $IC_{50}$ value of 0.646 and 0.575 μM against Mnk1 and Mnk2, respectively. MnkI-1 achieved some selectivity towards Mnks over a panel of twenty-two other protein kinases [113]. Recently, Han *et al*. reported a potent aminopyrazine benzimidazole derivative (**Figure 1.7**) with an $IC_{50}$ value of 0.003 μM against both Mnk1 and Mnk2 and was selective for Mnks over CDK1 and CDK2 (*i.e.* $IC_{50}$ > 25 μM) [83]. eFT508 inhibited both Mnks with $IC_{50}$ of 2 and 1 nM against Mnk1 and Mnk2 respectively. It is highly selective (≥ 100-fold) for Mnk1 and Mnk2 over 400 other protein and lipid kinases. This compound showed significant anti-tumour activity *in vivo* in multiple cancer models, including diffuse large B-cell lymphoma (DLBCL) with activating myeloid differentiation primary response 88 (MyD88) mutations, breast and lung cancers [115, 116]. Another compound, BAY 11433296 inhibited Mnk1 and Mnk2 with $IC_{50}$ of 0.040 μM and 0.904 μM, respectively [117]. This compound inhibited eIF4E phosphorylation in a range of 0.5- 2.6 μM in cancer cells and exhibited anticancer activity in patient-derived Non-Small Cell Lung Cancer (NSCLC) xenograft models. The chemical structure of the compound has not been revealed yet. eFT508 and BAY 11433296 have progressed to clinical trials [90].

In light of the oncogenic nature of Mnk in cancer it is crucial to identify selective Mnk inhibitors for pharmacologic target validation and drug development. One of the aims of the research presented in this thesis was to identify Mnk inhibitors with better selectivity and exhibit more potent anti-cancer activity.

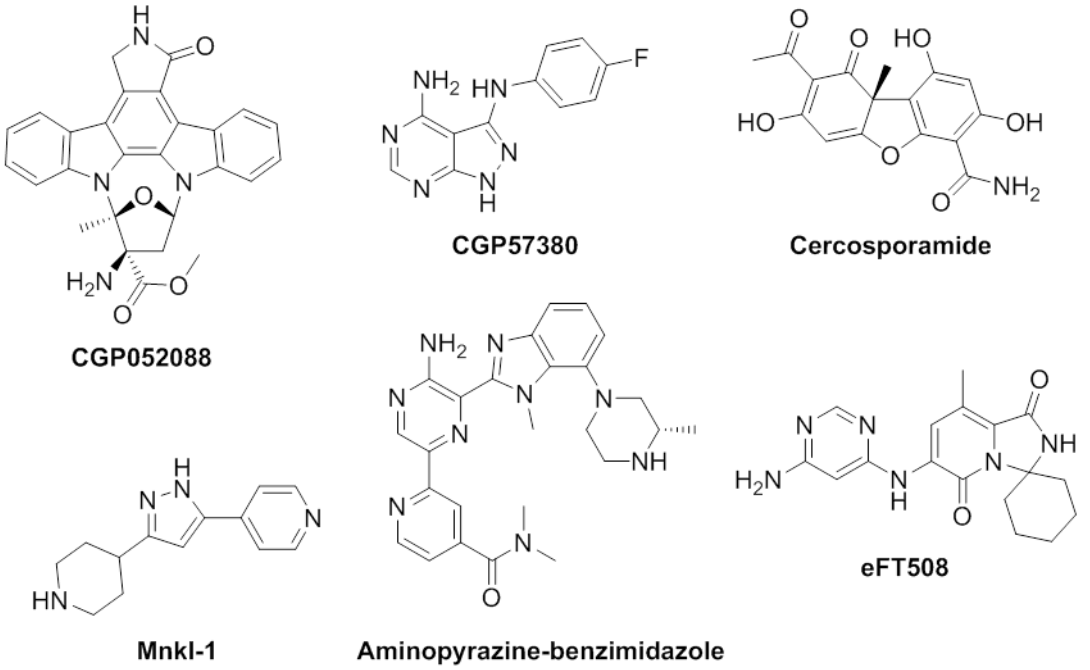



**Figure 1.7: Chemical structures of Mnk inhibitors.**

## 1.5 Selectivity of kinase inhibitors

Kinase inhibitors can be categorised from type I - VI according to the associated binding modes [118]. Type I inhibitors typically mimic the interaction of the adenine ring of ATP with residues located in the hinge region of their respective kinases [84], and bind to active (DFG-in) (DFD-in for Mnks) kinase conformation [84]. Unfortunately, the type I inhibitors often show a limited selectivity [119, 120], due to targeting the highly conserved structures of the ATP binding domain of kinases [121]. Nevertheless, many of the type I inhibitors are already approved as marketed drugs [90, 118, 122, 123].

Type II inhibitors, (*e.g.*, imatinib and BIRB-796), bind to the inactive DFG-out structure (DFD-out for Mnks). In most cases, type II inhibitors not only form one to three hydrogen bond(s) at the hinge region of the ATP binding site, but also interact with the adjacent DFD motif or the equivalent. [8, 124]. Type II inhibitors may have a higher selectivity than type I inhibitors, as there are substantial differences among the inactive conformations of kinases compared to their highly conserved ATP-activated structures.

Type III inhibitors may bind in the cleft between the small and large lobes adjacent to the ATP binding pocket and type IV inhibitors bind exclusively outside of the ATP binding site [125]. These binding sites are presumably non-conserved structural motifs among kinases, giving rise to a potentially higher degree of kinase selectivity compared to type I and type II inhibitors. Type III and IV inhibitors are also called allosteric inhibitors. The binding modalities are generally non-ATP-competitive and reversible [119-121, 126].

Bivalent inhibitors that span two regions of the protein kinase domain are labelled as type V inhibitors [118, 125].

Type VI inhibitors form irreversible, covalent bonds with the kinase active site [118]. Development of type VI inhibitors has been treated cautiously due to their indiscriminate and irreversible binding to proteins other than the target, therefore potentially incurring far more widespread off-target toxicities. More recently, there has been a renewed interest in the development of type VI inhibitors that form covalent bonds with a nucleophilic residue in the ATP-binding domain [124, 127]. By modulation and tailoring of chemical functionalities, there is a potential to develop type VI inhibitors as selective therapeutic agents [128-130]. Type VI inhibitors have several advantages, including high potency, prolonged pharmacodynamics and the ability to overcome the problem of drug resistance that may develop with their reversible counterparts. Irreversible inhibitors may maintain activity against drug resistant mutations that are acquired after treatment with reversible inhibitors [131, 132].

The human kinome contains over 500 kinases with evolutionarily conserved ATP binding sites and therefore, one of the aims of this project is to develop an important strategy to identify kinase inhibitors with high potency and selectivity in order to achieve improved safety profiles.

## 1.6 Hypothesis and research aims

The development of Mnk inhibitors is a multidisciplinary program, including medicinal chemistry, biochemical testing against Mnks, selectivity study against other kinases such as CDKs, cellular proliferation/apoptosis study, *in vivo* pharmacology experiments, run under the auspices of the Centre for Drug Discovery and Development at University of South Australia. The program is driven by the hypothesis that blocking of Mnk kinase activities will exert anti-cancer effects. In demonstrating this, the Centre has synthesised a large number of potential inhibitors of Mnks using analog-based and *in silico* protein structure-guided and ligand-based virtual screening approach. The focus on prostate cancer and leukaemia for the research studies described in this thesis was chosen based on previous studies establishing a link between Mnk activities and progression of these cancer types in animal models [32, 36, 96, 133-136]. The biological significance of eIF4E phosphorylation was established through developing prostate tumour in mice models upon the deletion of the tumour suppressor *PTEN* gene. The *PTEN*-loss lymphoma mice lacking Mnk1 and Mnk2 were resistant to tumour development [92]. Consistently, S209A knock in mice were resistance to prostate cancer [32]. Moreover, pharmacological inhibition of Mnks has been reported to reduce proliferation of prostate and leukaemia cells [36, 135-139].

The research presented in this thesis was conducted as a sub-project of the Mnk inhibitor program with the following research aims: (1) to identify novel Mnk inhibitors from a rationally designed compound library; (2) to characterise potency, selectivity and binding modes of the Mnk inhibitors; (3) to investigate the cellular mode of action in prostate cancer and leukaemia cell lines and (4) to evaluate the potential of lead inhibitors as single agent or combination therapy for treating cancers.

The identification of potent Mnk inhibitors has significant potential for the development of novel therapeutic agents for treating cancer. While the Mnk-mediated phosphorylation of eIF4E is important for its oncogenic activity, it seems redundant for normal growth. Therefore, pharmacological inhibition of Mnks may prove to be an effective and safe anti-cancer therapeutic approach. Novel and selective Mnk inhibitors can potentially be developed into anti-cancer agents leading to more effective cancer cures.

# 2. Identification and characterisation of Mnk inhibitors

## 2.1 Introduction

Protein kinases mediate protein phosphorylation, one of the major mechanisms for regulating growth, differentiation and metabolism in eukaryotic cells. They mediate transfer of the γ-phosphoryl group from ATP (a high energy donor), to the hydroxyl groups of serine, threonine or tyrosine residues in a specific protein substrate. Assessing the inhibitory activity of a chemical compound is a crucial step in guiding its design and optimisation in drug discovery. Some of the commonly used biochemical techniques to determine the potency of a kinase inhibitor are summarised in **Table 2.1** [32, 136-140]. Kinase activity assays need the co-factors like ATP, magnesium and a protein or peptide substrate. A technique to determine conversion of ATP to ADP, the disappearance of ATP or the formation of phospho-protein or phospho-peptide is necessary for evaluating kinase inhibitory potencies of a chemical compound [141].

**Table 2.1: Common biochemical kinase assay technologies.**

| Assay technology | Read out | Advantages/disadvantages | References |
|---|---|---|---|
| **Fluorescence Polarisation (FP), Version 1/2** | FP (Antibody/metal ion based) | High throughput, only one labelled substrate is required/ susceptible to compound interference, peptide must be relatively small | [142-144] |
| **Immunosorbent Assays (enzyme-linked or fluorescent linked assays** | Colourimetric /Fluorometric | Can be used as a sensitive probe for cell lysates in cell-based assays/ lower throughput and washing steps are required, must have suitable antibody pair | [145, 146] |
| **Luminescent Oxygen Channelling (Alpha Screen, Surefire assays)** | Luminescence oxygen channelling | Sensitive, high throughput can be applied to whole cell lysates. Lower potential artifacts than fluorescent compounds/ can be susceptible to interference by compounds which trap singlet oxygen. | [147, 148] |
| **Enzyme Fragment complementation** | Chemi-luminescence | High throughput, sensitive, amplified enzymatic, chemiluminescent signal less susceptible to interference/ can have interference with β-galactosidase-binding compounds, compound must be competitive with probe | [149-151] |
| **Scintillation Proximity assays** | Radioactive decay | High throughput, relatively artifact free in imaging-based systems, universal readout for kinases, versatile/ radioactive waste disposal | [152-155] |
| **IMAP® TR-FRET** | TR-FRET | Versatile without need for antibody, non-radioactive/ should be run at low ATP concentrations, peptide must be relatively small. | [112, 156] |
| **ADP- Glo™** | Luciferase based | Versatile and non-radioactive, use of high ATP concentrations is possible/ Susceptible to luciferase inhibitors | [112, 141, 152, 157] |

Each assay has its own advantages (**Table 2.1**) and selecting an assay technology is vast and challenging. Fluorescent assays are usually susceptible to interference from test compounds that either absorb light in the excitation or emission range of the assay or the compound themselves are fluorescent generating false negative results [158]. Immunosorbent assays require suitable antibody pair which can be used in cell-based

assays. However, this assay is low throughput and multiple washing steps are required [145, 146]. Luminescent oxygen channelling assay is sensitive, high throughput but can be susceptible to interference by compounds which trap singlet oxygen [147]. Enzyme fragment complementation assay is high-throughput and can be used for both cell-based and biochemical assay formats. It can have interference with β-galactosidase-binding compounds [149]. Radioisotope-based systems have been widely used for the longest time and have the advantage of measuring substrate phosphorylation directly with high sensitivity. However, the handling of radioactive materials, multiple washing steps and disposal of waste make these systems unfavourable for regular compound profiling [153, 155, 159]. In this project, Immobilised Metal Ion Affinity Particle (IMAP®) assay based on fluorescence and ADP-Glo™ assay based on luminescence were used. Running two different assays sequentially will eliminate false positive compounds which interfere with assay components such as luciferase enzyme in the ADP-Glo™ assay and false negatives such as fluorescent compounds blocking the fluorescence in the IMAP® assay. These assays are non-radiometric and homogenous, allowing to make an assay measurement by a simple mix and read procedure without the requirement to process samples by separation and/or by multiple washing steps [156, 157].

The working principle of IMAP® uses time-resolved fluorescence resonance energy transfer (TR-FRET) [160], which is based on the interaction of two chromophores called donor and acceptor. If a donor is excited by a photon of suitable wavelength, the energy can be transferred to an acceptor without the emission of photons by direct dipole-dipole interactions. There are three main conditions, which have to be met in order to obtain FRET. Firstly, the emission spectrum of the donor chromophore has to overlap with the excitation spectrum of the acceptor. Secondly, donor and acceptor must be orientated appropriately to enable dipole-dipole interaction. Thirdly, the distance between donor and

acceptor has to be minimal since the efficiency with which fluorescent energy is transferred is inversely proportional to the sixth power of the distance between them.

In the TR-FRET Progressive Binding System (Molecular Devices, Sunnyvale, CA, USA) the donor consists of a Terbium (Tb) complex, which is attached via a phosphorylated linker, to a nanoparticle consisting of trivalent metal (**Figure 2.1**). The acceptor used is the fluorescent 5-carboxytetramethylcarboxy rhodamine (TAMRA) which is attached to the C-terminal of a peptide substrate [161]. Following kinase-mediated phosphorylation to form the phospho-peptide, this binds to the nanoparticle, and thereby brings its fluorescent group into close proximity with the Tb-donor. The terbium donor is excited with a particular wavelength (330 nm), emitting electromagnetic radiation of 490 nm that is absorbed by the acceptor TAMRA linked to the phospho-peptide, which then emits fluorescent energy of 520 nm [162].

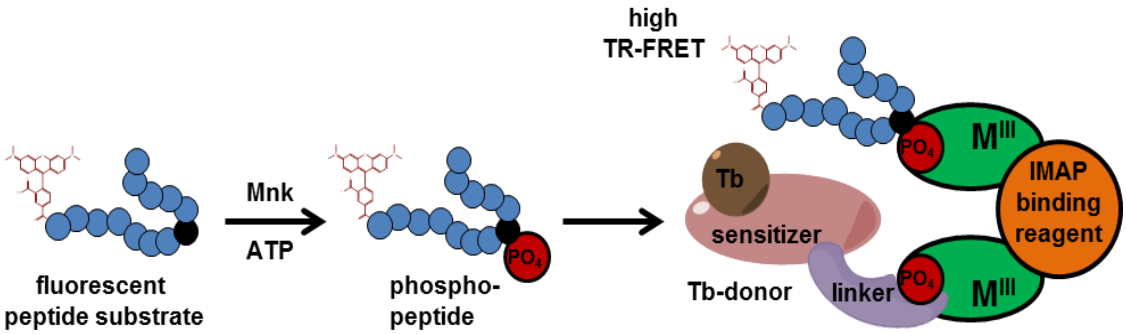



**Figure 2.1: Schematic representations of IMAP® assay principle.** The TAMRA-labelled peptide substrate is depicted as a chain of blue circles with residue Ser209 marked in black. The Mnk-phosphorylated peptide will bind specifically to trivalent metal ions of the IMAP® binding reagent. This will bring the TAMRA acceptor into close proximity with the Tb-donor (Tb-sensitiser complex). Reprinted with permission from Molecular Pharmacology, 2015, 88(5), 935-948 [112, 114, 141]. Copyright (2015) The American Society for Pharmacology and Experimental Therapeutics.

This method follows a direct approach by measuring the primary product of a kinase reaction. An additional advantage of this method is the long-lived fluorescence; the detection can be run in a time resolved mode with a delay of 200 µs which virtually

eliminates fluorescent background interferences from kinase inhibitors or other assay components.

The IMAP® assays are very robust at relatively low cost; however, they are not compatible with high ATP concentrations. The system generally tolerates ATP concentrations up to 200 µM (**Figure 2.4C**). Therefore, the ADP-Glo™ assay was established which measures the conversion of ATP to ADP during the kinase reaction (**Figure 2.2**). Following the kinase reaction, ADP Glo reagent is added to deplete the unused ATP in the reaction. Then, kinase detection reagent is added which converts the ADP formed in the reaction to ATP, allowing it to react with luciferase. The emitted photons by the luciferase reaction are measured as luminescence (**Figure 2.2**).

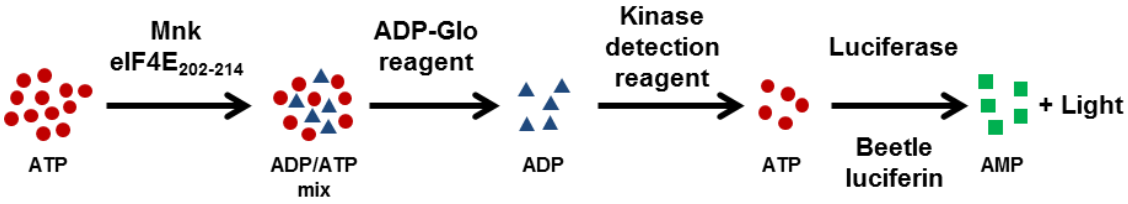



**Figure 2.2: ADP-Glo™ assay principle [112].** ATP is converted into ADP when exposed to Mnk and eIF4E$_{202-214}$. The ADP-Glo™ reagent is used to stop the reaction and enzymatically remove remaining ATP. Subsequently, the kinase detection reagent is applied to convert ADP back to ATP, which then drives a luciferase reaction turning over beetle luciferin to generate light.

This assay is suitable for determining $IC_{50}$ values (concentration at which the compounds inhibited 50% of the kinase activity) of kinase inhibitors at various ATP concentrations (up to 6 mM) which allows one to distinguish between ATP-competitive and non-competitive inhibitors. Furthermore, catalytic parameters such as $V_{max}$ (maximal reaction velocity) and $K_m$ (Michaelis-Mentens constant) can be determined. $V_{max}$ represents the maximum reaction velocity achieved by the system at saturating substrate concentration and the $K_m$ is the substrate concentration at which the enzymatic reaction rate is half of $V_{max}$ [163].

The first objective of this project was to establish a screening cascade as shown in **Figure 2.3.** The primary hits could be identified using the IMAP® assay followed by concentration-response determination with the ADP-Glo™ assay. The sequential uses of these mechanistically different assay technologies (identification of phosphorylated peptide *vs.* ATP depletion) were predicted to most likely exclude any false positives. As such, all compounds at concentrations of 1 and 10 μM were screened with the IMAP® assay. The compounds that inhibited Mnk1 or Mnk2 > 25% at 1 μM and/or > 90% inhibition at 10 μM were re-tested with the ADP-Glo™ assay to determine their $IC_{50}$ values. One of goals of this project was to distinguish between types I/II (ATP-competitive) and type III inhibitors (non-ATP competitive). This can be achieved by testing active compounds (*e.g.* $IC_{50}$ value < 2 μM) for substrate competition with changing the ATP and eIF4E-derived peptide concentrations using the ADP-Glo™ assay.

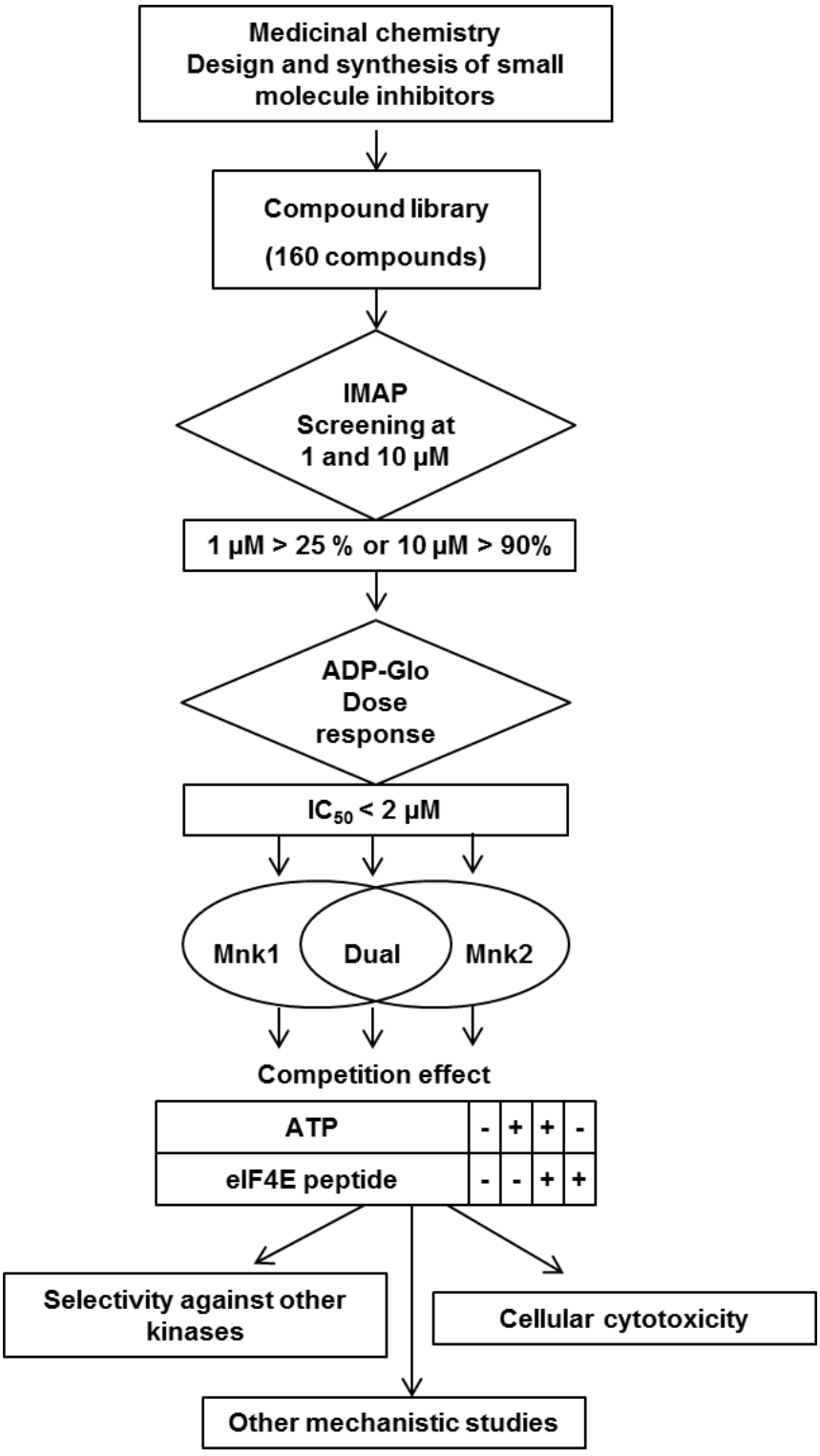



**Figure 2.3: Screening cascade of Mnk inhibitor profiling.** All compounds were tested with the IMAP® assays at 1 and 10 µM concentrations. Compounds that showed Mnk1 or Mnk2 inhibition > 25% at 1 µM and/or > 90% inhibition at 10 µM were further evaluated with the ADP-Glo™ assay to determine their $IC_{50}$ values. Mnk inhibitors with an $IC_{50}$ value < 2 µM were tested for substrate competition with ATP and eIF4E-derived peptide using the ADP-Glo™ assay. Some of the representative compounds were further evaluated for their mechanisms of cellular action.

The methods used to perform the assays are described (**Sections 6.2.1** and **6.2.2**), reliable results are gained from an optimised assay system that adheres to the following principles: (1) produce robust signals with reproducible data; (2) be time-efficient and (3) be of low labour intensity with easy and simple readout and cost-effective, especially with high throughput screening [141]. Assay parameters such as $V_{max}$ and $K_m$ for ATP and peptide substrate with the appropriate concentrations of kinase are determined to validate the assays, in order to find a balance between identifying a range of weaker and more potent inhibitors [164, 165].

Generally, good stringency of the system is obtained when test compounds are screened with the kinase substrates (ATP and peptide) adjusted to their respective $K_m$ values [166]. At $K_m$ levels, an enzyme shows 50% of its maximal velocity since 50% of the enzyme molecules are occupied with ATP or substrate molecules. Under these conditions, the enzyme is not saturated with ATP or substrate; hence the tested inhibitors are able to compete, allowing the detection of weak competitive inhibitors.

# 2.2 Results

## 2.2.1 Developing protocols to measure Mnk1/2 activities with IMAP® and ADP-Glo™ assays

Mnk1 (Life technologies, purity 95%) and Mnk2 (Merck Millipore, purity 83%) were used in the IMAP® and ADP-Glo™ assays. For the IMAP® assay, a peptide of thirteen amino acids ($eIF4E_{202-214}$) which contained the Mnk1/2 phosphorylated residue Ser209 at the C-terminal sequence of the eIF4E ($DTATKSGS_{209}TTKNR$) was custom synthesised. The peptide was N-terminally linked to the fluorescent FRET acceptor, TAMRA, generating the IMAP® kinase substrate TAMRA-$eIF4E_{202-214}$ (**Figure 2.1**). The fluorescently labelled peptide was shown to be phosphorylated by the Mnks and its

binding to trivalent metal-containing ($M^{III}$) nanoparticles evident from a robust TR-FRET signal between the Tb-donor and the TAMRA acceptor on the peptide.

For assay optimisation, 5 µM of the peptide substrate TAMRA-eIF4E$_{202-214}$ was incubated with different amounts of Mnk1 or Mnk2 in a standard kinase reaction using 100 µM ATP (**Figure 2.4A**). To obtain a sufficient signal-to-background ratio (S/B) and to minimise enzyme consumption, 100 ng of Mnk1 (S/B = 2.3) and 50 ng of Mnk2 (S/B = 2.5) were used in all subsequent experiments. The second step for optimisation was to test the TAMRA-eIF4E$_{202-214}$ substrate at three concentrations, and sufficient S/B ratios were detected at 5 µM (S/B = 2.4 for Mnk1 and S/B = 2.6 for Mnk2 (**Figure 2.4B**). Assay conditions were further optimised by testing ATP at various concentrations in the presence of Mnk1 or Mnk2, and increasing signals were detected with both kinases to approximately 200 µM ATP, followed by a rapid decrease of the signal (**Figure 2.4C**). The first five data points were used to determine concentrations of ATP suitable for the primary compound profiling. Iterative fitting to the Michaelis-Menten model [167] was carried out with Graphpad Prism software and it was estimated that half maximal signals would be achieved at concentrations of ATP of 165 and 80 µM for Mnk1 and Mnk2, respectively. These concentrations were applied to perform concentration-response experiments with two known inhibitors, CGP57380 and cercosporamide, using 100 ng of Mnk1 or 50 ng of Mnk2 and 5 µM TAMRA-peptide substrate. CGP57380 and cercosporamide showed an $IC_{50}$ value of 1.51 and 0.67 µM with Mnk1 and the corresponding values for Mnk2 were 1.87 and 0.16 µM (**Figure 2.4D**). The results obtained were comparable with the literature values [102, 113, 114].

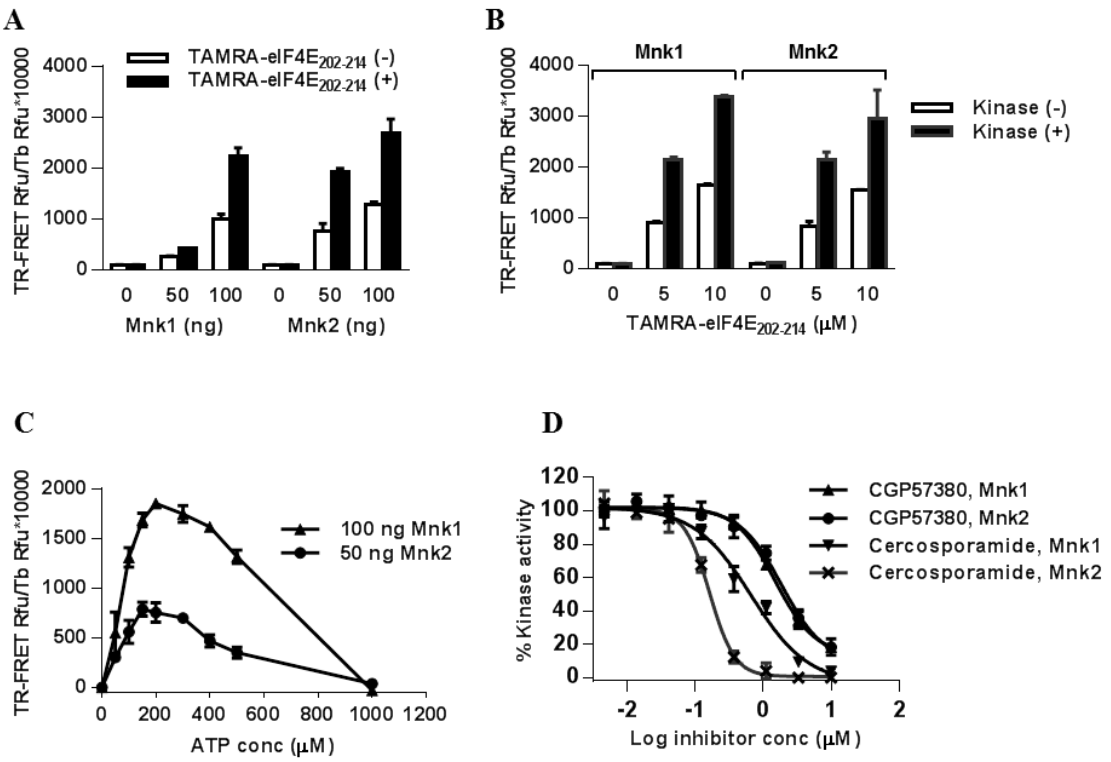



**Figure 2.4: Optimisation of the IMAP® assay conditions.** (A) Different quantities of recombinant Mnk1 or Mnk2 were incubated with 100 µM ATP and 5 µM TAMRA-eIF4E$_{202-214}$ to determine optimal assay conditions. Control reactions were performed without the substrate. (B) Determination of optimal concentrations of TAMRA-eIF4E$_{202-214}$ substrate in the IMAP® assay. 100 ng of Mnk1 or 50 ng of Mnk2 were incubated with 100 µM ATP and different concentrations of TAMRA-eIF4E$_{202-214}$ peptide substrate. Reactions without kinase acted as a control. (C) ATP titration for Mnks in the IMAP® assay. 100 ng of Mnk1 or 50 ng of Mnk2 were incubated with 5 µM TAMRA-eIF4E$_{202-214}$ substrate at different ATP concentrations. Control reactions without Mnk1 or Mnk2 were performed at the same time and used for background correction. (D) The control inhibitors CGP57380 and cercosporamide were tested in the IMAP® assay using optimal parameters obtained from (A), (B) and (C). Concentration-response curves were calculated by applying a four-parameter logistic, log (10) non-linear regression model.

For the IMAP® assay, a TAMRA-labelled eIF4E-derived peptide (eIF4E$_{202-214}$) was used to detect kinase activities of Mnk1 and Mnk2 successfully in the presence of tested compounds. However, the assay was incompatible with concentrations of ATP above 200 µM (**Figure 2.4C**). This effect was most likely due to the displacement of the phosphorylated substrate from the IMAP® nano-beads by ATP phosphate groups, leading to a reduced FRET signal. This inherent property of the IMAP® assay limits its suitability for experiments requiring high ATP concentrations (*e.g.* ATP competition testing) [168].

One advantage of using low ATP concentration in the assay is for identifying weak ATP-competitive and type II inhibitors, which would not be identified at higher ATP concentrations. Moreover, at relatively low ATP concentrations the assay was shown to be very robust and cost effective for initial compound profiling.

Similar to the IMAP® assay, the ADP-Glo™ assay was optimised for robust and reproducible data. Assay validation is usually achieved by performing a comprehensive matrix where combinations of different concentrations of ATP, kinase and substrate are evaluated. Due to the high complexity of kinase reactions, the validation was carried out in steps, which were performed independently. In the first step, suitable concentrations of Mnks were explored by incubating various amounts of Mnk1 or Mnk2 protein with 100 µM ATP and 100 µM $eIF4E_{202-214}$ substrate. The control reactions were performed without the substrate. Adequate robust signals were achieved using 100 ng Mnk1 and 30 ng Mnk2, which resulted in S/B ratios of 6.2 and 3.4, respectively (**Figure 2.5A**). In the next step $K_m$ and $V_{max}$ values were determined for the $eIF4E_{202-214}$ substrate (**Figure 2.5B** and **Table 2.2**) by fixing the ATP concentration to 2 mM testing a range of concentrations of $eIF4E_{202-214}$ substrate (**Figure 2.5B**).

The Michaelis-Menten curve fit revealed a $K_m$ value of 1.27 mM and the determined $V_{max}$ value was used to calculate a maximal specific activity (eIF4E-derived peptide turn over per minute) of 2172 nmol/min/mg for Mnk1. The respective values for Mnk2 were 609 µM and 1846 nmol/min/mg (**Table 2.2**). Subsequently, $K_m$ and $V_{max}$ values for ATP were determined using 100 ng Mnk1 or 30 ng Mnk2 with the eIF4E-derived peptide at a fixed concentration of 1.2 mM (**Figure 2.5D**). In all testing, control reactions were run without kinase and used for background correction.

The Michaelis-Menten curve fit resulted in a $K_m$ value of 2.094 mM and a specific activity of 1852 nmol/min/mg for Mnk1 under $V_{max}$ conditions. The corresponding values for Mnk2 were significantly lower at 216 µM for $K_m$ and 1075 nmol/min/mg, respectively (**Table 2.2**). Concentration-response testing with enzyme inhibitors is often carried out using substrate concentrations that correspond to the $K_m$ value. Mnk1 showed considerably higher $K_m$ values for ATP and the peptide substrate, therefore concentrations of ATP and peptide were reduced to values corresponding to 50% of the $K_m$ in order to minimise consumable costs. The S/B ratio under these conditions was 14.2 and seemed sufficient for dose response experiments (**Figure 2.5D**). For all further tests, the concentrations of ATP and peptide for incubation with Mnk1 were adjusted to 50% of the $K_m$ values while for Mnk2, concentrations equivalent to $K_m$ values were used.

Finally, the influence of concentration-response of the known inhibitors CGP57380 and cercosporamide on activity of both Mnks was investigated with the optimised ADP-Glo™ assay by using the aforementioned parameters in a final assay volume of 15 µL. $IC_{50}$ values were calculated by applying a four-parameter logistic non-linear regression model. Inhibition constants ($K_i$) were calculated from $IC_{50}$ values using the Cheng-Prusoff equation assuming the reversible ATP- competitive inhibition [169]. CGP57380 and cercosporamide inhibited Mnk1 with a $K_i$ value of 1.010 µM and 0.507 µM, respectively. The corresponding values against Mnk2 were 0.877 µM and 0.079 µM, respectively (**Figure 2.5E** and **Table 2.2**). The observed results were consistent with the literature data [102, 113, 114].

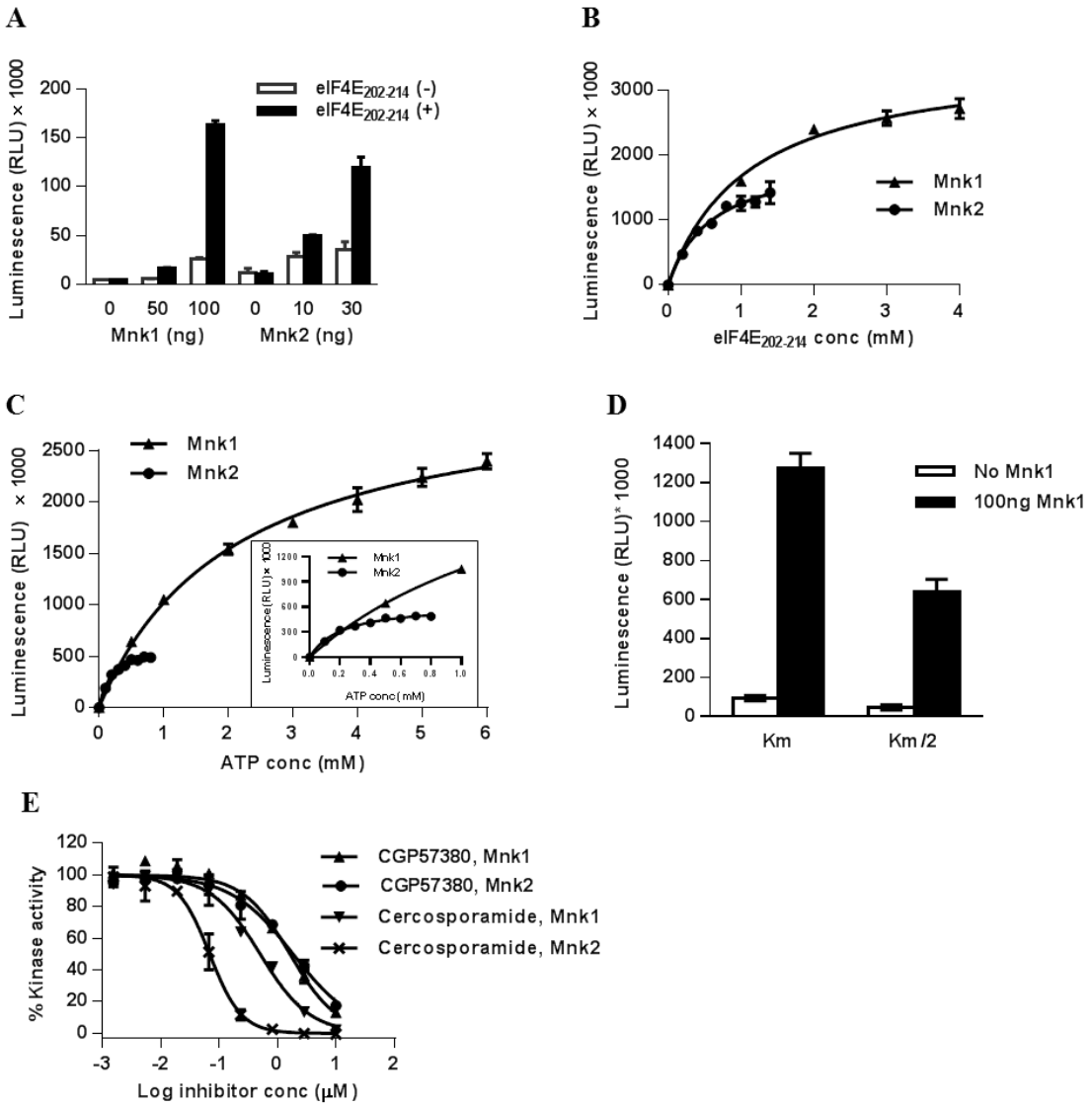



**Figure 2.5: ADP-Glo™ assay validation with Mnks.** (A) Different amounts of Mnk1 or Mnk2 were used in kinase reactions with fixed substrate concentrations of 100 µM ATP and 100 µM of eIF4E$_{202-214}$ peptide substrate. The obtained luminescence signals were compared to control reactions without the peptide substrate. The S/B ratios with 100 ng Mnk1 and 30 ng Mnk2 were 6.3 and 3.4, respectively. For all further experiments 100 ng Mnk1 and 30 ng Mnk2 were applied. (B) The $V_{max}$ and $K_m$ values were determined for the eIF4E$_{202-214}$ peptide substrate. The ATP concentration was adjusted to 2 mM and 100 ng Mnk1 or 30 ng Mnk2 were used in all reactions performed at different concentrations of eIF4E$_{202-214}$ peptide. (C) The determination of $V_{max}$ and $K_m$ values for ATP was carried out under identical conditions as described for panel C, with the difference being that the concentration of eIF4E$_{202-214}$ peptide was fixed at 1.2 mM while different ATP concentrations were used. Control reactions without kinase were performed at the same time and used for background correction prior to fitting with the Michaelis-Menten model. (D) Determination of signal to background ratio with 0.5 × $K_m$ with Mnk1. (E) the control inhibitors CGP57380 and cercosporamide were used for final validation of the ADP-Glo™ assays using above determined parameters. Concentration-response curves were calculated by iterative fitting to a four-parameter logistic non-linear regression model.

Surprisingly, the $K_m$ for ATP with Mnk1 was almost ten times higher than for Mnk2 (**Figure 2.5C** and **Table 2.2**). This lower affinity of ATP for Mnk1 than Mnk2 reflects most likely the structural differences between Mnk1 and Mnk2. The longer C-terminus of Mnk1 is known to affect its basal kinase activity and to repress phosphorylation of the activation loop, compared to Mnk2 and this structural difference may influence their affinity for ATP. In addition, Jauch *et al*. [82, 170] reported minor conformational differences between Mnk1 and Mnk2: for example, the N-lobe of Mnk2 is rotated by approximately by 10° further compared to Mnk1 creating a wider and, therefore, more accessible site in Mnk2 for the binding of ATP. The $K_i$ values for CGP57380 and cercosporamide (**Figure 2.5E** and **Table 2.2**) were determined as a final validation step and the data were comparable to literature values [24].

**Table 2.2: Kinetic constants for Mnks.**

| **Kinase** | **Mnk1** | | **Mnk2** | |
|---|---|---|---|---|
| **Substrate** | **ATP** | **eIF4E$_{202-214}$** | **ATP** | **eIF4E$_{202-214}$** |
| $K_m$ (μM) | 2094 | 1272 | 216 | 609 |
| $V_{max}$ (nmol/min) | 0.185 | 0.217 | 0.032 | 0.055 |
| Specific activity (nmol/min/mg) | 1852 | 2172 | 1075 | 1846 |
| **Compound** | **CGP57380** | **Cercosporamide** | **CGP57380** | **Cercosporamide** |
| $K_i$ value (μM) | 1.010 | 0.507 | 0.877 | 0.079 |

## 2.2.2 Identification of primary hits

A collection of 160 compounds was synthesized and assessed in this project. Series 1 compounds were derivatives of *N*-phenylthieno[2, 3-*d*] pyrimidin-4-amines (WO2010/023181) [113, 114]. Series 2 and 3 compounds were developed based on our privileged structures of 5-(2-(phenylamino)pyrimidin-4-yl)thiazol-2(3*H*)-one [98, 112, 171] and *N*-phenyl-1*H*-pyrazolo[3,4-*d*]pyrimidin-3-amine. Series 2 compounds were originally designed as cyclin-dependent kinase (CDK) inhibitors for previous projects.

Several CDK inhibitors were discovered to have strong inhibitory activities against Mnks also. For this project, derivatives of those CDK inhibitors were generated with the aim of increasing Mnk activity while reducing the CDK activity. Structures of the compounds evaluated in this thesis are provided in **Table 6.1** of **Section 6.1.1**. All these compounds were synthesised at the Centre for Drug Discovery and Development.

According to the screening cascade shown in **Figure 2.3**, all the compounds were tested at two concentrations (1 µM and 10 µM) in duplicate using the IMAP® assay, and the averages of relative activities were calculated for both concentrations (**Figure 2.6 A** and **B**).

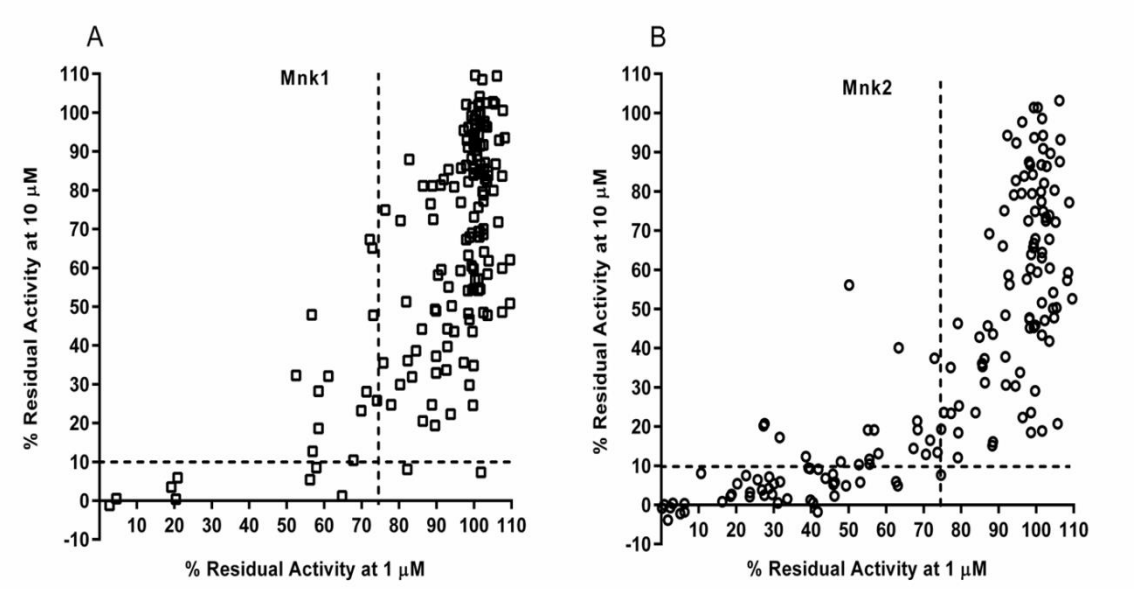



**Figure 2.6: Hit identification by IMAP® assay.** A collection of 160 compounds was tested for their inhibitory activities against Mnk1 (A) and Mnk2 (B) using the IMAP® assays. The compound concentrations used were 1 µM and 10 µM in duplicate and residual kinase activities were calculated as percentages relative to negative and positive controls (n = 4). The data are represented as means of two replicates for each compound. The dotted lines indicate the cut-off values of 75% and 10% residual kinase activity at 1 µM and 10 µM inhibitor concentrations, respectively.

The data are summarised in **Table 8.2**, **Appendix 8.4**. Overall, ninety-one compounds caused > 75% inhibition (at 1 µM) or > 90% (at 10 µM) reduction in the kinase activity

of Mnk1 and/or Mnk2. As hits, these compounds were further assessed for $IC_{50}$ values by ADP-Glo™ assay. Interestingly, there were more primary hits inhibiting Mnk2 than Mnk1, suggesting that the compounds were more selective for Mnk2 (**Figure 2.6 A and B**). This differential inhibition of Mnk1 and Mnk2 may be attributed to conformational differences between them [172].

Assay consistency and robustness were checked routinely by monitoring the correlation of duplicate data points (**Figure 2.7A** and **B**) and by calculating Z'-factors from four positive and negative controls which were included in all experiments (**Figure 2.7C**).

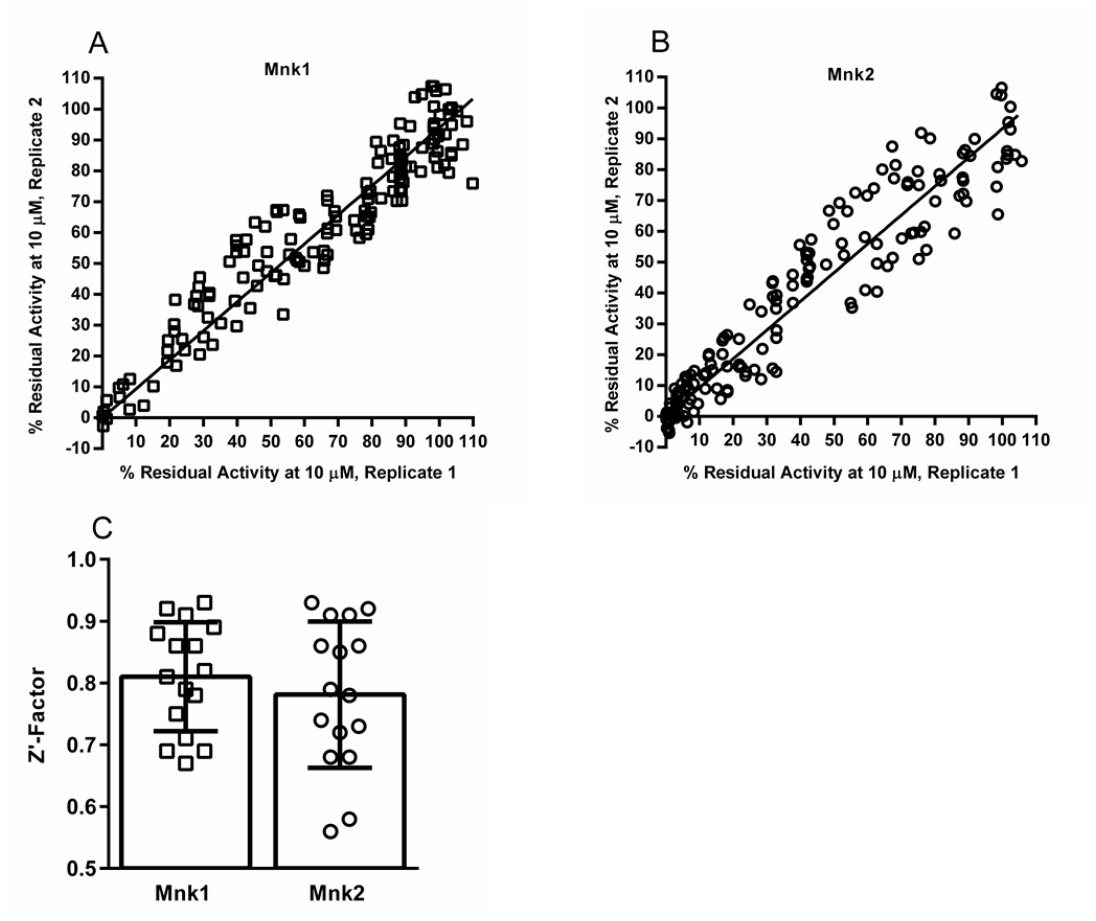



**Figure 2.7: Robustness of IMAP® assay.** In order to assess assay robustness, duplicate values were plotted against each other and linear regression was carried out (A and B). The calculated $R^2$ values were close to 0.9, indicating a good correlation between two duplicates and validating the sufficient robustness of the assays. To calculate Z'-factors, the data were collected from sixteen independent experiments for both Mnk1 and Mnk2. All experiments included four positive and four negative controls. The Z'-factors, were > 0.5 in all cases, indicating the sufficient robustness of the assays (C).

The Z'-factor is a screening window coefficient for measurement of assay performance, without the intervention of test compounds. This coefficient reflects both the dynamic range of assay signal and the data variation associated with signal measurements. A robust and reproducible assay is represented by a Z'-factor between 0.5 and 1.0 [173].

The calculated Z'-factors were all larger than 0.5, which indicated both Mnk1 and Mnk2 assays to be highly robust. Another statistical parameter, coefficient of determination ($R^2$) which is a measure of degree of relationship between two variables is also determined. The values of $R^2$ lie between zero to one. Higher the values of $R^2$, lower the variation between duplicates [174, 175]. The calculated $R^2$ values were 0.89 and 0.88 for Mnk1 and Mnk2 respectively, indicating a good correlation between the two duplicates and validating consistent assay results.

### 2.2.3 Dual Mnk1/2 and Mnk2 inhibitors

Ninety-one compounds which achieved the inhibition of > 75% and < 90% at 1 and 10 μM, respectively (**Figure 2.8)** were subjected to further analysis using the ADP-Glo™ kinase assay. Dose response experiments were performed to determine $IC_{50}$ values and there was particular emphasis on identifying dual Mnk1/2 and Mnk sub-type specific inhibitors. All results obtained from the ADP-Glo™ assay are summarised in **Table 8.2 (Appendix 8.4)**.

Fifty three compounds were identified with $K_i$ values ≤ 1 μM against Mnk1 and/or Mnk2. Among of them, thirty compounds showed selectivity for Mnk2 over Mnk1, being ≥ 10-fold more potent for Mnk2. Within the twenty-three dual Mnk1/2 inhibitors, thirteen of them showed $K_i$ values ≤ 1 μM (**Figure 2.8**). Interestingly, no Mnk1 selective inhibitors were identified, suggesting significant structural differences between Mnk1 and Mnk2.

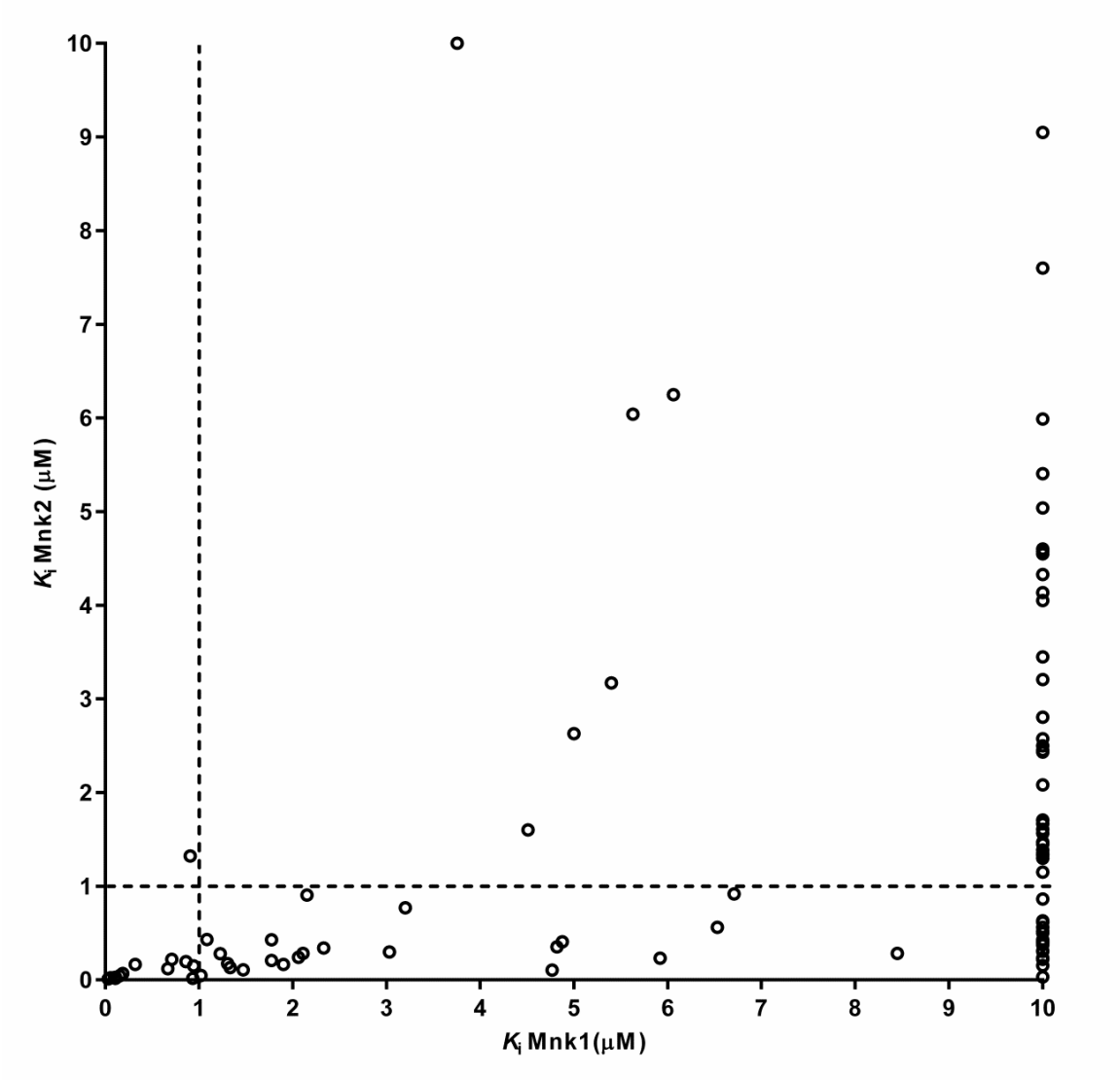



**Figure 2.8: Identification of dual and Mnk2 specific inhibitors.** Ninety-one compounds were tested with the ADP-Glo™ assay to determine $IC_{50}$ values. $K_i$ values were calculated from the $IC_{50}$ values at $K_m$ ATP and $K_i$ values against Mnk1 and Mnk2 plotted for each compound, represented by a circle. The dotted line represents the cut-off for $K_i$ values < 1 μM. For graphic presentation, compounds with $K_i$ values > 10 μM are shown as 10 μM.

### 2.2.4 Binding modes of Mnk1/2 inhibitors

It is generally believed that type III inhibitors may achieve higher specificity compared to type I/II inhibitors which target the highly conserved ATP binding pocket. In this project, a total of twenty inhibitors selected from each chemical class were investigated for competing characteristics at elevated ATP concentrations using the ADP-Glo™ assay.

All compounds were tested at ten concentrations ranging from 0.007 µM to 15 µM with 100 ng Mnk1 using 150, 2000 or 6000 µM ATP. In parallel the same range of concentrations was tested with 30 ng Mnk2 using 50, 200 or 2000 µM ATP. The selection of ATP concentrations was based on the $K_m$ values (**Table 2.2**) with one concentration lower and the other higher than the $K_m$. The eIF4E$_{202-214}$ peptide concentrations were fixed for Mnk1 and Mnk2 at 1.2 mM and 0.6 mM, respectively. The $IC_{50}$ values were calculated and the ratios ($IC_{50}$ ratio) between the highest and lowest ATP concentrations are given in **Table 2.3**.

Subsequently, a similar set of experiments were conducted to investigate competition effects of elevated eIF4E$_{202-214}$ concentrations. The peptide substrate was tested at 150, 600 and 3000 µM with ATP fixed at 2 mM for Mnk1 and 200 µM for Mnk2. The selection of eIF4E$_{202-214}$ concentrations was also based on the $K_m$ values (**Table 2.2**) where one concentration lower and the other higher than the $K_m$ value. The $IC_{50}$ values were routinely calculated and competing effects were assessed by the ratios obtained at the highest substrate concentration versus the one at the lowest substrate concentration (**Table 2.3** and **Figure 2.9**). A ratio of > 5 was arbitrarily set as a significant competing effect. With this criterion, four different inhibitory mechanisms were proposed:

(1) Non-substrate- and non-ATP-competitive inhibitors (mode -/-): These compounds did not show significant change in the $IC_{50}$ values when ATP or the eIF4E$_{202-214}$ substrate were used at increased concentrations. Compounds showing these types of inhibitory properties are depicted with mode -/- in **Table 2.3**. These type III inhibitors are most likely to offer selectivity among other kinases and exhibit more potent cellular inhibition of kinase since they need not compete with high intracellular ATP levels [176].

**Table 2.3: Summary of Mnk inhibitory activity and binding modes.**

| Compound | | $IC_{50}$ (μM) | | $IC_{50}$ ratio | | | | | |
|---|---|---|---|---|---|---|---|---|---|
| | | | | Mnk1 | | | Mnk2 | | |
| Code | Series | Mnk1 | Mnk2 | ATP ($\frac{6\ mM}{0.15\ mM}$) | eIF4E ($\frac{3\ mM}{0.15\ mM}$) | Mode | ATP ($\frac{2\ mM}{0.05\ mM}$) | eIF4E ($\frac{3\ mM}{0.15\ mM}$) | Mode |
| MNKI-6 | 1 | 0.047 | 0.020 | 2.2 | 1.9 | -/- | 1.9 | 1.1 | -/- |
| MNKI-7 | 1 | 0.083 | 0.044 | 1.5 | 1.2 | -/- | 1.0 | 1.0 | -/- |
| MNKI-5 | 1 | 0.147 | 0.050 | 1.8 | 1.0 | -/- | 1.1 | 0.9 | -/- |
| MNKI-57 | 1 | 0.159 | 0.036 | 2.4 | 1.7 | -/- | 4.1 | 1.5 | -/- |
| MNKI-8 | 1 | 0.164 | 0.052 | 1.8 | 1.5 | -/- | 4.1 | 0.9 | -/- |
| MNKI-19 | 1 | 0.279 | 0.136 | 1.7 | 1.0 | -/- | 1.6 | 1.3 | -/- |
| MNKI-83 | 1 | 0.480 | 0.328 | 2.3 | 2.8 | -/- | 2.4 | 0.8 | -/- |
| MNKI-67* | 1 | 1.40 | 0.036 | 2.2 | 1.4 | -/- | 1.5 | 1.0 | -/- |
| MNKI-37 | 1 | 1.53 | 0.219 | 1.9 | 1.1 | -/- | 1.1 | 0.8 | -/- |
| MNKI-15 | 1 | 2.85 | 0.328 | 14.5 | 1.5 | +/- | 6.4 | 2.0 | +/- |
| MNKI-2-22 | 1 | 3.09 | 0.480 | 7.2 | 1.9 | +/- | 3.5 | 7.6 | -/+ |
| MNKI-2-30 | 1 | 3.225 | 1.81 | 10.2 | 1.4 | +/- | 15.2 | 1.2 | +/- |
| MNKI-2-25 | 1 | 3.495 | 0.678 | 50.2 | 1.8 | +/- | 37.8 | 0.9 | +/- |
| MNKI-28* | 1 | 7.23 | 0.704 | NT | NT | | 11.6 | 1.1 | +/- |
| MNKI-85* | 1 | > 10 | 0.062 | NT | NT | | 15.2 | 1.2 | +/- |
| MNKI-4* | 1 | > 10 | 0.452 | NT | NT | | 12.9 | 1.0 | +/- |
| MNKI-12* | 1 | > 10 | 10 | NT | NT | | 18.6 | 2.3 | +/- |
| MNKI-7-50 | 3 | 4.80 | 1.54 | NT | NT | | 35.7 | 1.4 | +/- |
| MNKI-5-17* | 2 | > 10 | 0.618 | NT | NT | | 76.6 | 37.7 | +/+ |
| MNKI-4-61* | 2 | > 10 | 1.23 | NT | NT | | 16.4 | 1.3 | +/- |

Data shown are the mean values derived from at least two replicates.

NT; not tested. Series, compound series; eIF4E, $eIF4E_{202-214}$; Mode: ATP/$eIF4E_{202-214}$ competition; *mono-specific Mnk2 inhibitor.

(2) <u>ATP-competitive inhibitors (mode +/-):</u> These compounds showed a significant increase in the $IC_{50}$ values at elevated ATP concentrations, but showed none or only a marginally change in $IC_{50}$ values with increased $eIF4E_{202-214}$ concentrations. This group of compounds are apparently type I/II inhibitors which bind to ATP binding site. In addition to binding to ATP, type II inhibitors may extend beyond ATP binding sites.

(3) Dual substrate- and ATP-competitive inhibitors (mode +/+): $IC_{50}$ values were affected by increased ATP and peptide substrate levels. Only one compound *(i.e.* MNKI-5-17) showed this property and was only active against Mnk2. This category can be type II inhibitors as it seemed that the inhibitors also bind to the substrate binding sites.

(4) Substrate-competitive inhibitors (mode -/+): Only one compound (*i.e.*MNKI-2-22) was a moderate competitor of $eIF4E_{202-214}$ peptide, an effect observed with Mnk2 (**Table 2.3**). Surprisingly, when tested on Mnk1, the same compound was a moderate competitor of ATP but not of $eIF4E_{202-214}$. This class of compounds could probably be allosteric. However, further work is needed for more information.

A selection of compounds were further tested under the same conditions as outlined above using an extended range of ATP concentrations (**Figure 2.9A-C**) whilst the $eIF4E_{202-214}$ substrate concentrations were fixed at $K_m$. Data from individual dose response curves were analysed using Prism 6 Graphpad software and plotted as a function of log-transformed concentration of inhibitor. Representative examples are shown in (**Figure 2.9A-C**). A similar set of experiments were carried out to evaluate effects of the $eIF4E_{202-214}$ peptide; the ATP concentrations were fixed at $K_m$ value (**Figure 2.9D-F**). The data was further used to calculate apparent $K_m$ and $V_{max}$ values at various inhibitor concentrations.

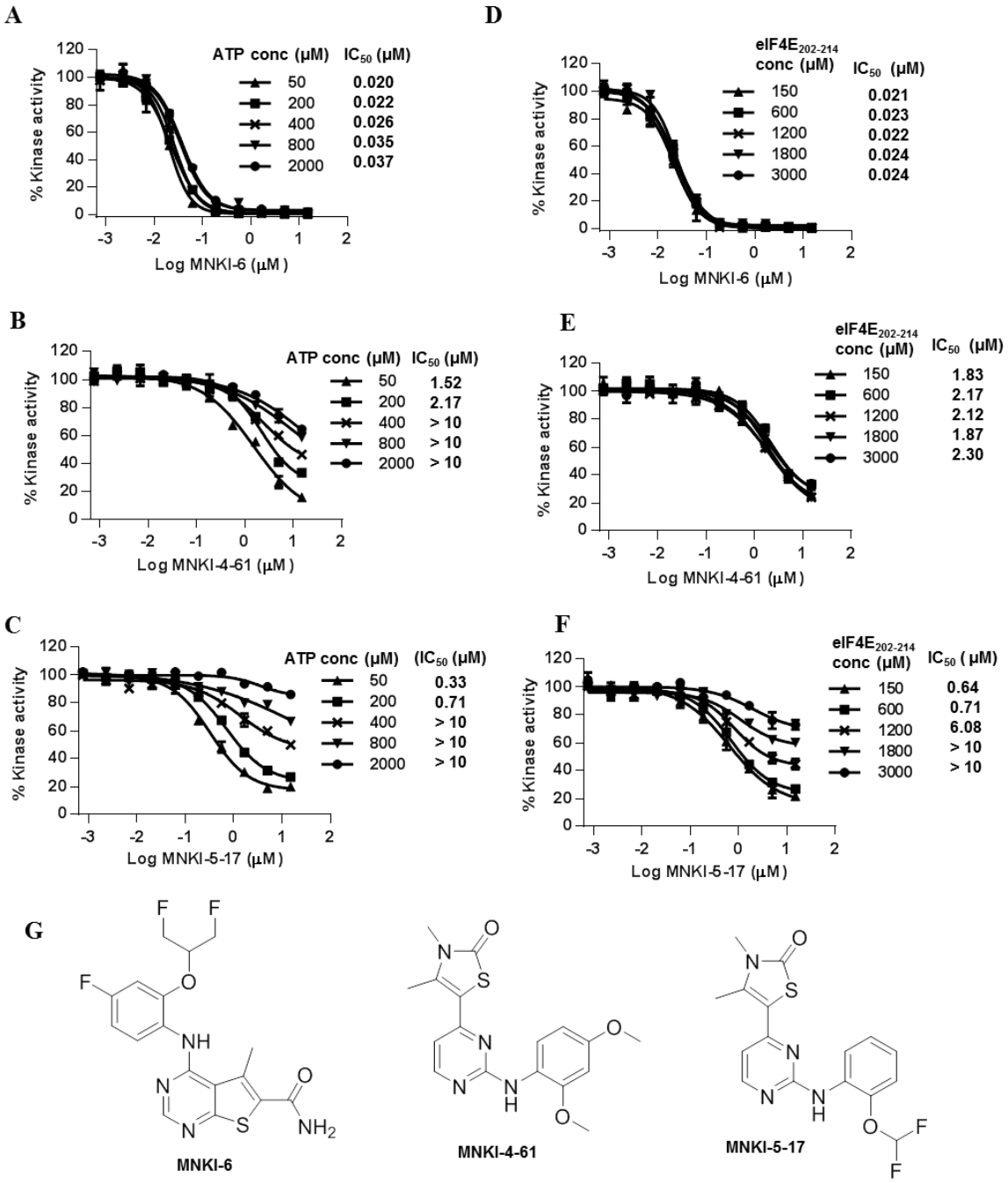
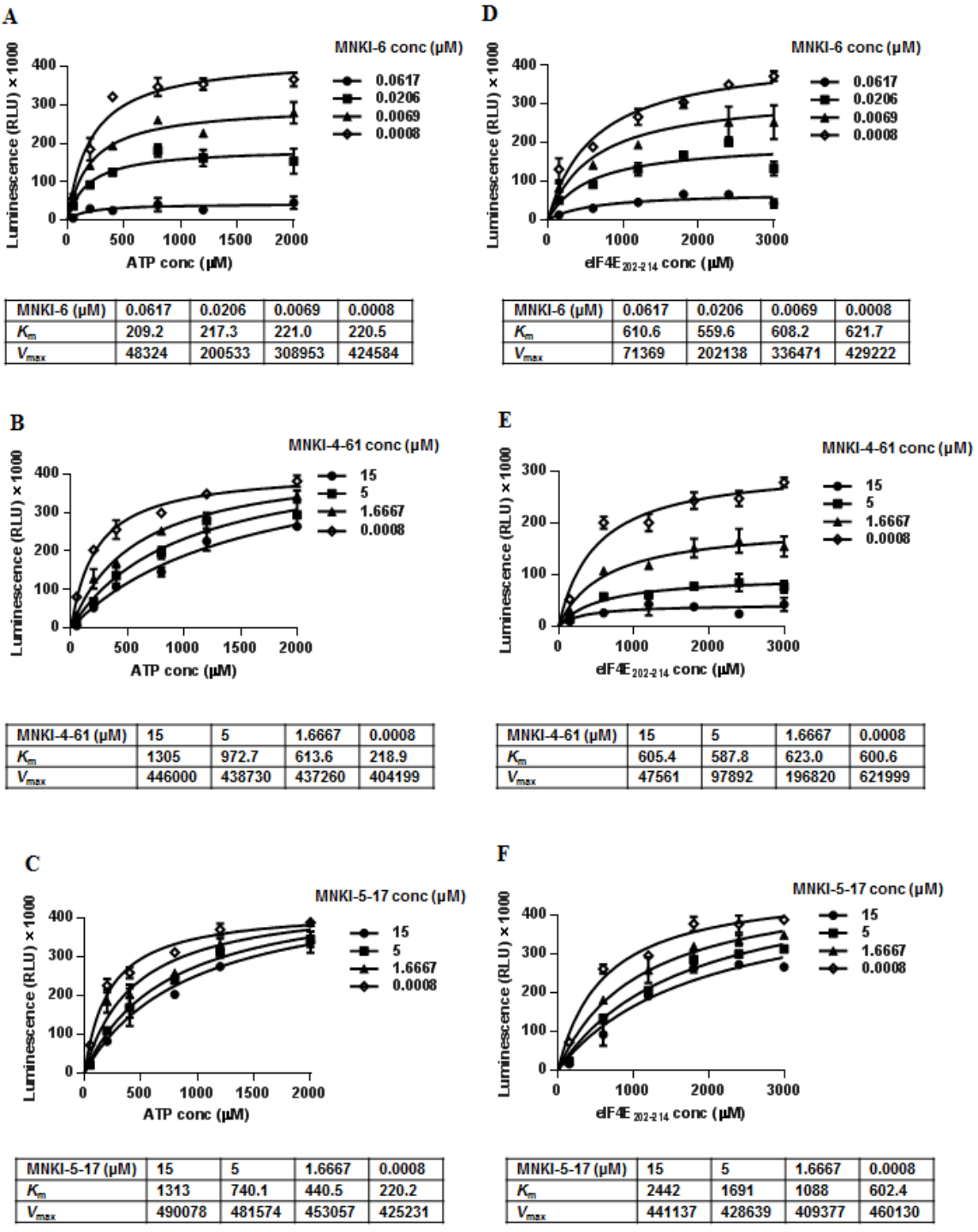



**Figure 2.9: Determination of binding mode of inhibitor in Mnk2.** 30 ng of Mnk2 was mixed with ten different concentrations of Mnk inhibitors and the ADP-Glo™ assay performed in the presence of increasing concentrations of ATP (A, B and C) and with increasing concentrations of eIF4E$_{202-214}$ peptide (D, E and F). All experiments were performed in duplicate and the values from individual samples analysed using the Prism 6 Graphpad software. The three compounds (G) were selected as examples for the different modes of inhibition (MNKI-6: -/-; MNKI-4-61: +/-; MNKI-5-17: +/+).

A representative example for mode -/- on Mnk2 is given in (**Figure 2.10A** and **D**). Increasing compound concentrations led to lower $V_{max}$ values for ATP and eIF4E$_{202-214}$

while the $K_m$ values remained unchanged, as it would be expected for a type III non-competitive inhibitory mechanism.




| MNKI-6 (μM) | 0.0617 | 0.0206 | 0.0069 | 0.0008 |
|---|---|---|---|---|
| $K_m$ | 209.2 | 217.3 | 221.0 | 220.5 |
| $V_{max}$ | 48324 | 200533 | 308953 | 424584 |

| MNKI-6 (μM) | 0.0617 | 0.0206 | 0.0069 | 0.0008 |
|---|---|---|---|---|
| $K_m$ | 610.6 | 559.6 | 608.2 | 621.7 |
| $V_{max}$ | 71369 | 202138 | 336471 | 429222 |

| MNKI-4-61 (μM) | 15 | 5 | 1.6667 | 0.0008 |
|---|---|---|---|---|
| $K_m$ | 1305 | 972.7 | 613.6 | 218.9 |
| $V_{max}$ | 446000 | 438730 | 437260 | 404199 |

| MNKI-4-61 (μM) | 15 | 5 | 1.6667 | 0.0008 |
|---|---|---|---|---|
| $K_m$ | 605.4 | 587.8 | 623.0 | 600.6 |
| $V_{max}$ | 47561 | 97892 | 196820 | 621999 |

| MNKI-5-17 (μM) | 15 | 5 | 1.6667 | 0.0008 |
|---|---|---|---|---|
| $K_m$ | 1313 | 740.1 | 440.5 | 220.2 |
| $V_{max}$ | 490078 | 481574 | 453057 | 425231 |

| MNKI-5-17 (μM) | 15 | 5 | 1.6667 | 0.0008 |
|---|---|---|---|---|
| $K_m$ | 2442 | 1691 | 1088 | 602.4 |
| $V_{max}$ | 441137 | 428639 | 409377 | 460130 |

**Figure 2.10: Determination of the apparent $K_m$ and $V_{max}$ values at different compound concentrations.** The Michaelis-Menten saturation curves are given for a range of ATP (panels A-C) and a range of eIF4E$_{202-214}$ concentrations (panels D-F). Selected compounds were used at the concentrations as indicated in the figure. The calculated kinetic parameters are given beneath the shown graphs.

Additional examples are given for modes +/- and +/+ in **Figure 2.10B, E, C** and **F**. Mode +/- showed increased $K_m$ values for ATP combined with unchanged $V_{max}$ values, which is an expected characteristic of competitive enzyme inhibition [24]. Lastly, for mode +/+ elevated $K_m$ values were calculated with increased ATP and $eIF4E_{202-214}$ concentrations. No major changes of the $V_{max}$ values were observed.

### 2.2.5 Selectivity of Mnk inhibitors

As described in **2.2.2**, series 2 compounds were developed based on the structures of 5-(2-(phenylamino)pyrimidin-4-yl)thiazol-2(3H)-one, which were originally designed for a drug discovery program targeting CDKs [177]. Thus, the selectivity of these compounds against CDK2-cyclin A (CDK2A) and CDK9-cyclin T (CDK9T1) were examined. CDK9T1 kinase assay was developed using our in-house ADP-Glo™ technology (**Appendix 8.3**), whereas CDK2A assay was performed with CROs (Eurofins Scientific, UK or Reaction Biology, USA). Of the fifty-three compounds with $K_i \leq 1$ μM for Mnk1 or Mnk2, thirty-seven compounds were tested against the CDK2A and CDK9T assays. All series 1 compounds (17 tested) and three out of four series 3 compounds were selective for Mnks over CDK2A and CDK9T1 (**Table 2.4**). However, ten out of sixteen series 2 compounds inhibited the CDKs with $K_i$ values < 10 μM.

**Table 2.4: Selectivity of Mnk inhibitors against CDK2A and CDK9T1.**

| | | $K_i$ (μM) | | | |
|---|---|---|---|---|---|
| **Compounds** | **Series** | **Mnk1**[a] | **Mnk2**[a] | **CDK2A**[b] | **CDK9T1**[a] |
| CGP57380 | | 1.01 | 0.877 | > 10 | > 10 |
| MNKI-2-22 | 1 | 2.06 | 0.24 | > 10 | > 10 |
| MNKI-2-25 | 1 | 2.33 | 0.339 | > 10 | > 10 |
| MNKI-2-30 | 1 | 2.15 | 0.905 | > 10 | > 10 |
| MNKI-4 | 1 | > 10 | 0.226 | > 10 | > 10 |
| MNKI-4-61 | 2 | > 10 | 0.615 | > 10 | 1.660 |
| MNKI-5 | 1 | 0.098 | 0.025 | > 10 | > 10 |
| MNKI-5-17 | 2 | > 10 | 0.309 | 5.359 | 0.131 |
| MNKI-6 | 1 | 0.031 | 0.01 | > 10 | > 10 |
| MNKI-7 | 1 | 0.055 | 0.022 | > 10 | > 10 |
| MNKI-7-7-2 | 2 | 0.859 | 0.195 | 0.230 | NT |
| MNKI-7-50 | 3 | 3.20 | 0.77 | > 10 | > 10 |
| MNKI-8 | 1 | 0.109 | 0.026 | > 10 | > 10 |
| MNKI-8-10 | 2 | 1.471 | 0.106 | 4.985 | > 10 |
| MNKI-8-81 | 2 | > 10 | 0.219 | NT | 0.345 |
| MNKI-8-88 | 2 | 5.918 | 0.232 | 0.930 | > 10 |
| MNKI-8-115 | 2 | > 10 | 0.398 | NT | > 10 |
| MNKI-9-18 | 2 | 0.942 | 0.15 | > 10 | > 10 |
| MNKI-9-42 | 2 | > 10 | 0.233 | NT | 0.0027 |
| MNKI-9-59 | 2 | 4.766 | 0.105 | 3.500 | > 10 |
| MNKI-10-1 | 2 | 0.71 | 0.219 | 0.8 | > 10 |
| MNKI-10-6 | 2 | > 10 | 0.304 | > 10 | > 10 |
| MNKI-10-22 | 2 | > 10 | 0.393 | NT | > 10 |
| MNKI-10-40 | 2 | 0.668 | 0.118 | 5.125 | 0.986 |
| MNKI-11-86 | 2 | 1.227 | 0.28 | NT | > 10 |
| MNKI-11-90 | 2 | 10 | 0.864 | > 10 | > 10 |
| MNKI-12-48 | 3 | 10 | 0.562 | > 10 | > 10 |
| MNKI-12-94 | 3 | NT | 0.429 | > 10 | > 10 |
| MNKI-12-95 | 3 | 1.772 | 0.429 | 4.700 | > 10 |
| MNKI-12 | 1 | > 10 | 0.500 | > 10 | > 10 |
| MNKI-15 | 1 | 1.400 | 0.164 | > 10 | > 10 |
| MNKI-19 | 1 | 0.186 | 0.068 | > 10 | > 10 |
| MNKI-28 | 1 | 4.82 | 0.352 | > 10 | > 10 |
| MNKI-37 | 1 | 1.02 | 0.048 | > 10 | > 10 |
| MNKI-57 | 1 | 0.106 | 0.018 | > 10 | > 10 |
| MNKI-67 | 1 | 0.933 | 0.018 | > 10 | > 10 |
| MNKI-83 | 1 | 0.32 | 0.164 | > 10 | > 10 |
| MNKI-85 | 1 | > 10 | 0.031 | > 10 | > 10 |

[a] $K_i$ values determined from ADP-Glo™ kinase assay in house. [b] $K_i$ values determined by Eurofins Scientific or Reaction Biology Corp. NT; not tested.

## 2.3 Discussion

The involvement of Mnk-eIF4E axis in oncogenic transformation and progression has been well studied [32, 92]. The identification and characterisation of Mnk inhibitors provides pharmacologic target validation and offers a novel approach for cancer therapy. Herein, a profiling platform (**Figure 2.3**) was developed where two enzymatic assay formats were established which complement one another as different detection modes were used. The IMAP® assay was used for initial screening followed upon by ADP-Glo™ assay. The screening cascade (**Figure 2.3**) was applied for one hundred sixty compounds. Mnk inhibitors showed more selectivity towards Mnk2 compared to Mnk1. This may be attributed to the difference in their conformation of the activation segments and their orientation, revealing that the ATP binding site of Mnk1 is less accessible because the N-terminus is rotated by approximately 10°, producing a narrower interlobal cleft compared to Mnk2 [24, 83]. These Mnk2 selective inhibitors provide valuable biochemical tools to dissect biological functions of Mnk1 *versus* Mnk2. It is currently not known whether individual or combined inhibition of Mnk1/2 would exert more potent anti-cancer activities.

Twenty compounds were tested for their ATP- and/or $eIF4E_{202-214}$ competitiveness according to the screening cascade prior the next stage of investigating their toxicity on cancer cell lines. $IC_{50}$ ratios of dose response experiments at high and low concentrations of ATP or $eIF4E_{202-214}$ were determined (**Table 2.3)**.

In this study, four groups of inhibitors based on inhibitor-kinase binding mode were identified:

(1) Nine compounds (**Table 2.3)** were found to be allosteric type III inhibitors which did not compete with either of the substrates (mode -/-). These compounds were

selective over CDK2A and CDK9T1 kinases (**Table 2.4**). Since allosteric binding sites are specific for a particular kinase, a high level of selectivity can be expected [122]. For example, CI-1040 (PD184352) is a highly selective allosteric inhibitor of MEK1/2 with significant *in vivo* anti-tumour activity against a range of human xenograft models, including colon, breast, pancreas, lung and kidney [178], other selective allosteric inhibitors include AKT inhibitor VIII, GNF-2 (Bcr-Abl inhibitor), JX401 (P38 inhibitor) [179-181]. These compounds are useful for pathway illustration and target validation in addition to lead discovery. The importance of non-ATP competitive kinase inhibitors has been widely recognised in the scientific community. Yet, there is paucity of direct screening methods to discover such compounds. The approach used in this study can be beneficial to identify such inhibitors.

(2) Nine compounds (**Table 2.3)** were characterised as type I/II that competed with the ATP (mode +/-). ATP-competitive inhibitors are generally expected to be non-selective due to structural similarities in ATP binding sites among kinases. However, many ATP antagonists have been successfully developed as marketed drugs [118, 122, 123]. Some ATP-competitive inhibitors have exhibited selective kinase inhibitory profiles. For example, eFT508, an ATP-competitive inhibitor of Mnk1 and Mnk2, is highly selective over 400 other kinases [87]. Another example of selective ATP-competitive inhibitor is skepinone-L, a p38 kinase inhibitor with excellent *in vivo* efficacy [182]. A number of kinases have unique active site characteristics such as rare amino acids in key positions, specific inserts (three inserts I1-I-3 in case of Mnks), different identity in key residue of ATP binding pocket called gatekeeper. Small gatekeeper residue, such as threonine, is present in 5% of kinases which may allow inhibitors to access a hydrophobic "back

pocket" [183]. In addition to selectivity, ATP-competitive inhibitors must compete with intracellular ATP which is generally in millimolar range. As a result of this, there is generally poor correlation between biochemical and cellular potency for ATP-competitive compounds, and a highly potent (nanomolar to picomolar) inhibitor is necessary for strong kinase inhibition in cells [184, 185]. Finally, the development of mutations in the ATP binding site residue may confer resistance to many ATP-competitive inhibitors [186-188].

(3) MNKI-5-17 competed with substrates, ATP and eIF4E$_{202-214}$ (mode +/+). Unlike ATP binding sites, the protein substrate binding site is less conserved among kinases. In addition, a high biochemical potency is not commonly required to produce strong cellular inhibition of kinase because the concentration of protein substrates are generally not higher than their $K_m$ value [189]. Bi-substrate-competitive inhibitors like macrocyclic Src kinase inhibitors attained remarkable kinase specificity and cellular potency [190]. Examples of other bi-substrate-competitive inhibitors include EGFR inhibitors (AG18 and AG99) exhibited potent inhibitory activity with good selectivity over the highly similar inflorescence and root apices receptor-like kinases (IRK) [188, 191, 192].

(4) Interestingly, MNKI-2-22 inhibited Mnk1 and did so in a competitive manner with ATP; meanwhile, it inhibited Mnk2 but did so in a competitive manner with eIF4E$_{202-214}$ (**Table 2.3**). A differential competitive nature of inhibitors among kinases has been previously reported for erbastin (EGFR inhibitor), a phenolic natural product isolated from *Streptomyces*. This compound has been shown to be a bi-substrate-competitive inhibitor for EGFR while ATP-competitive and peptide substrate non-competitive with other kinases [188, 193-195].

All compounds with mode -/- belonged to series 1 chemical class, showed $IC_{50}$ values < 1.6 µM and were dual inhibition of Mnk1 and Mnk2 (except MNKI-67). These findings suggest that these inhibitors act *via* an allosteric type III mechanism, and thus it may be concluded that an allosteric binding site is structurally conserved between Mnk1 and Mnk2. In contrast, all compounds with mode +/- had $IC_{50}$ values > 2.8 µM against Mnk1 and six of them were more selective against Mnk2. Most intriguingly, very subtle structural changes in the inhibitors resulted in switched activity modes. For example, MNKI-4-61 of series 2 changed from mode +/- to mode +/+ when 2,4-dimethoxyaniline was replaced with 2-(difluoromethoxy)aniline of MNKI-5-17 (**Figure 2.9G**). In the case of MNKI-5, removal of the 1,3-difluoropropan-2-ol group resulted in a change from mode -/- to a mode +/- for MNKI-15 and the potency against Mnk1 was reduced by a factor of almost twenty (**Figure 2.11A** and **Table 2.3**). Whilst, removal of the fluorides from the 1,3-difluoropropan-2-ol group (MNKI-37) maintained the -/- mode, it reduced the Mnk1 activity by almost ten-fold, demonstrating that the 1,3-difluoropropan-2-ol group prevents competition with ATP. Lastly, when the acetamide on the dihydrothiophene ring of MNKI-37 was replaced with *N*-(3-methoxypropyl) acetamide (MNKI-83), inhibition of Mnk1 was enhanced about three-fold. There is currently no structural data available for activated Mnk1 [96] and these inhibitory modes remain to be elucidated. The very subtle structural changes resulting in the different inhibitory modes lead one to believe that the binding site on the kinases for the inhibitors is in close proximity to the binding sites of ATP and the peptide.

Based on the experimental information, the binding modes were proposed as shown in **Figure 2.11B**). The inactive DFD-out conformation (**Figure 2.11B-1**) switches into the active DFD-in (**Figure 2.11B-2**) *via* phosphorylation of the activation segment by ERK1/2 or p38 kinases. The activated kinase coordinates contact of ATP and the substrate

(eIF4E) with catalytically important residues on the activation segment, the glycine-rich loop and the catalytic loop. MNKI-5 is an allosteric inhibitor but shares the same core scaffold (indicated as a black diamond in **Figure 2.11B - 3** and - **4**) with MNKI-15. The latter may have significant binding affinities to residues adjacent to and inside of the ATP binding pocket so that it exhibits a type II mechanism of inhibition (**Figure 2.11B-3**). MNKI-5 lacks the ability to compete with ATP, which may be caused by conformational changes arising from introduction of the 1,3-difluoropropan-2-ol moiety such that it moves away from interacting with the ATP binding site (**Figure 2.11B- 4**).

Taken together, this investigation suggests significant structural differences in the ATP catalytic domain between Mnk1 and Mnk2 leading to very different inhibitory mechanisms. However, both enzymes share a common structural feature of an allosteric binding site located in close proximity to the ATP and peptide binding sites. These results demonstrate that enzymatic kinase assays can be used to reveal Mnk inhibitors with dual and subtype-specific activities which showed a mostly ATP-competitive binding mode (this left some that blocked the peptide and some that were allosteric in their inhibitory mechanism). The findings will be invaluable for the future design, optimisation and development of highly selective Mnk inhibitors as anti-cancer therapeutic agents.

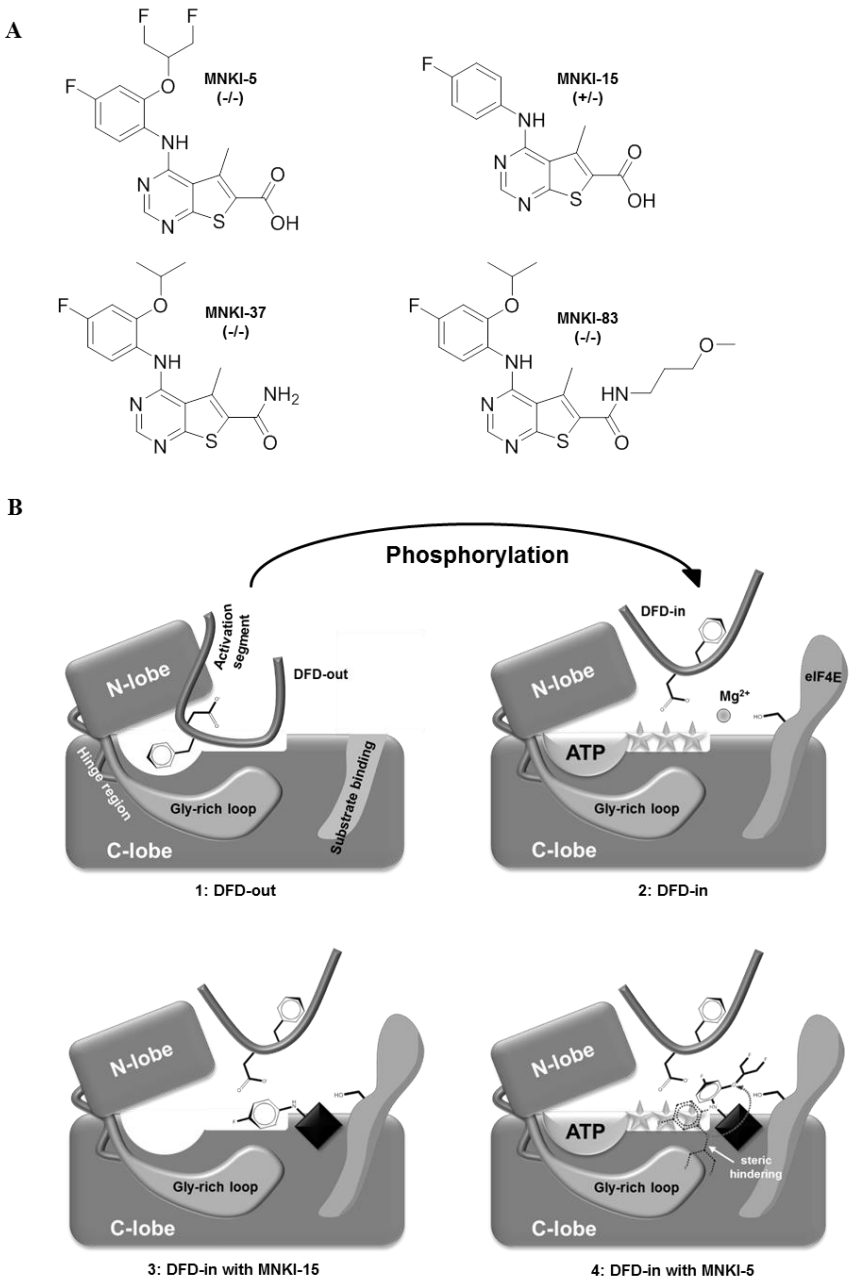



**Figure 2.11: Proposed binding modes of Mnk inhibitors.** (A) Structures of selected compounds. Subtle changes in the structure of MNKI-5 to form MNKI-15 induce a switch in mode of inhibition from mode -/- to mode +/- (MNKI-15) or dramatically reduce potency by more than a factor ten against Mnk1 (MNKI-37). The efficacy of MNKI-37 against Mnk1 was significantly improved through modification of the acetamide group as shown for MNKI-83 (B) Hypothetical working model for compound binding at the reactive site. The Mnks switch from the inactive DFD-out form 1) to the active DFD-in form 2) upon phosphorylation of the activation segment and subsequently bind the ATP substrate. 3) The cartoon depicts MNKI-15 as a Type II kinase inhibitor binding partly inside and partly adjacent to the ATP binding pocket. The black diamond represents the common core scaffold between MNKI-15 and 5, which occupies the postulated allosteric binding site. 4) Hypothetical binding modalities of MNKI-5: steric hindering from the larger side chain forces MNKI-5 (dashed structure) to adopt an alternative conformation with a non-ATP-competitive binding mode.

# 3. Effect of Mnk inhibition in a cellular context

## 3.1 Introduction

As discussed in the previous chapters, Mnks integrate several oncogenic signalling pathways within cells, such as MAP kinase, AKT/mTOR and toll-like receptors (TLRs) and activate the eIF4E mediated protein synthesis. In addition to eIF4E, Mnks also phosphorylate hnRNPA1 [102] which regulates the translation of mRNAs containing specific AU-rich elements in their 3′-untranslated regions (UTR) [196]. Phosphorylation of these substrates, such as eIF4E and hnRNPA1, modulates the expression of oncogenic proteins by regulating both the initiation of translation and stability of mRNA. In a lymphoma mouse model where a tumour suppressor *PTEN* gene was knocked-out, the tumour incidence was reduced with simultaneous *Mnk1/2* double knock-out when compared to mice with wild type Mnks [92]. In another study, *PTEN* knock-out mice harbouring a eIF4E Ser209Ala mutation were shown to be resistant to the development of prostate cancer (PCa) [32]. Therefore, inhibition of Mnks may provide an anti-cancer therapeutic strategy [95, 97, 98, 135, 136, 138, 197].

The aim of this chapter was to investigate the cellular mechanisms of the lead inhibitors identified in Chapter 2. PCa and AML cell lines were selected as model systems because upregulation of phosphorylated eIF4E and Mnks are linked to poor prognosis for patients with PCa [32, 90, 198] and hematological malignancies [90, 199, 200].

## 3.2 Mnk inhibition in prostate cancer cells

PCa is the second major cause of death in men in the Western world after heart disease. At the initial stage, PCa develops and proliferates locally, which can be counteracted by androgen deprivation therapy as the growth of cancer cells depends on androgen. Androgen signalling has been reported to promote translation of key mRNAs that are crucial in initiation and progression of PCa, and metastasis [201]. PCa cells can develop resistance to androgen deprivation therapy, thereby acquiring the capacity to proliferate independently of androgens (*i.e.* classified as hormone refractory disease). Currently, there are no effective treatments for late stage PCa, which proclaims a clinical need for the discovery of a new therapeutic approach. *PTEN*, a tumour suppressor gene, is often mutated in PCa [202]. This inactivating mutation in *PTEN* prompts the onset and progression of PCa by activation of PI3K/AKT/mTOR pathway (**Figure 1.1**); the latter increases 4E-BP phosphorylation and therefore releases eIF4E for phosphorylation by Mnks [203, 204]. Hyper-activation of eIF4E and overexpression of Mnks are common in hormone-refractory and metastatic prostate tumours and correlate with poor clinical outcome [32, 198, 205-207]. PCa progression to androgen independent stage involved increased eIF4E activation [198] and previous research has revealed that direct targeting of the translational machinery, especially eIF4E, is advantageous in inhibiting prostate cancer cell growth, cell migration and invasion, and induced cell apoptosis in castration resistant PCa (CRPC) cell lines [135, 208]. Collectively, these data imply the significant

role of eIF4E activation in PCa and suggest that targeting eIF4E may be attractive treatment strategy for PCa. As a part of further investigation into the role of Mnks in PCa, this chapter describes studies to determine the potential anti-proliferative and anti-migratory effects of Mnk inhibitors in PCa.

### 3.2.1 Effect of Mnk inhibitors on the viability of prostate cancer cells

PCa is a heterogeneous disease in terms of genetics, grade, ploidy and expression of tumour suppressor genes. A number of cell lines that depicts the stages and types of the disease will be used for experiments in this chapter. 22RV1 cells derived from the androgen dependent xenograft cell line (CRW22), expresses prostate-specific antigen (PSA), and is independent of androgen for its growth [209, 210]. LNCaP cells derived from lymph node metastasis, express PSA and are androgen dependent [210, 211]. DU-145 cells are moderately metastatic, derived from brain metastasis, does not express PSA and is independent of androgen for its growth [210, 212, 213]. PC-3 cells were derived from a vertebral metastatic, androgen independent and PSA negative tumour [213, 214] [213, 214]. C4-2B cells are highly metastatic, androgen-independent and were derived from an LNCaP xenograft in a nude mouse [215, 216]. The LNCaP, PC-3 and C4-2B cell lines were shown to contain inactivating *PTEN* mutations [213]. Overall, these five PCa cell lines represent different molecular characteristics of the disease based on the existence of the androgen receptor (AR), their production of PSA (an AR-regulated gene) and expression of *PTEN* [213, 217]. These characteristics of PCa cells under study are summarised in **Table 3.1**.

**Table 3.1: Characteristics of the prostate cancer cell lines.**

| Cell line | Tissue of origin | AR status | PSA | *PTEN* | References |
|---|---|---|---|---|---|
| 22RV1 | Derived from CRW22 xenograft | Positive (H875Y mutation) | Yes | +/+ | [209, 213] |
| LNCaP | Lymph node metastasis (from patient) | Positive (T877A mutation); Androgen dependent | Yes | -/- | [210, 211] |
| DU-145 | PCa brain metastasis (from patient) | Negative | No | +/- | [210, 212] |
| PC-3 | PCa vertebral metastasis (from patient) | Negative | No | -/- | [214] |
| C4-2B | LNCaP tumour in nude mouse | Positive | Yes | -/- | [215, 216] |

AR: androgen receptor; PSA: prostate-specific antigen; +/+: wild type; -/-: both alleles are missing and +/-: one of the allele is missing.

Twenty-seven inhibitors with $IC_{50}$ values < 0.5 µM against Mnk2 identified in **Chapter 2** (**Table 8.2, Appendix 8.4**) were selected for the initial assessment of anti-proliferative activity against the five PCa cell lines. A colorimetric assay called MTT (3-(4, 5-dimethylthiazolyl-2)-2, 5-diphenyltetrazolium bromide) was used to evaluate the cell viability (refer to **Chapter 6**). The metabolically active cells are capable of reducing the MTT to its insoluble formazan, which has a purple colour whereas the non-viable cells are unable to do so. Seven compounds showed anti-proliferative activity against 22RV1 and DU-145 cells with $GI_{50}$ values (the concentration of inhibitor that results in 50% reduction of the MTT signal) ranging from 0.5 to 8.9 µM. One compound was active against 22RV1only and one against DU-145 only. In addition, one compound inhibited the proliferation of LNCaP cells with a $GI_{50}$ value of 2.1 µM (**Table 3.2**).

**Table 3.2: $GI_{50}$ values calculated from MTT data in PCa cells in comparison to Mnk inhibitory activities.**

| | $K_i$ (µM) | $GI_{50}$ (µM), 72 hours | | | | |
|---|---|---|---|---|---|---|
| **Code** | **Mnk1/Mnk2** | **22RV1** | **LNCaP** | **DU-145** | **PC-3** | **C4-2B** |
| CGP57380 | 1.010/0.877 | > 10 | > 10 | > 10 | > 10 | > 10 |
| MNKI-2-22[1] | 2.060/0.240 | > 10 | > 10 | > 10 | > 10 | > 10 |
| MNKI-4[1] | NT/0.226 | 0.74 ± 0.03 | 2.12 ± 0.23 | 0.80 ± 0.13 | > 10 | > 10 |
| MNKI-5[1] | 0.098/0.025 | > 10 | > 10 | > 10 | > 10 | > 10 |
| MNKI-6[1] | 0.031/0.010 | > 10 | > 10 | 0.78 ± 0.22 | > 10 | > 10 |
| MNKI-7[1] | 0.055/0.022 | 6.75 ± 0.43 | > 10 | 6.11 ± 1.03 | > 10 | > 10 |
| MNKI-7-7-1[2] | NT/0.372 | > 10 | > 10 | > 10 | > 10 | > 10 |
| MNKI-7-7-2[2] | 0.859/0.195 | 8.84 ± 0.59 | > 10 | > 10 | > 10 | > 10 |
| MNKI-8[1] | 0.109/0.026 | 7.87 ± 1.83 | > 10 | 8.92 ± 0.19 | > 10 | > 10 |
| MNKI-9-18[2] | 0.942/0.150 | > 10 | > 10 | > 10 | > 10 | > 10 |
| MNKI-9-36[3] | 0.152/0.044 | > 10 | > 10 | > 10 | > 10 | > 10 |
| MNKI-9-41[2] | 1.773/0.206 | > 10 | > 10 | > 10 | > 10 | > 10 |
| MNKI-9-50[2] | >10/0.233 | > 10 | > 10 | > 10 | > 10 | > 10 |
| MNKI-9-66[3] | 1.083/0.432 | > 10 | > 10 | > 10 | > 10 | > 10 |
| MNKI-10-2[2] | 1.305/0.175 | > 10 | > 10 | > 10 | > 10 | > 10 |
| MNKI-10-6[2] | >10/0.304 | > 10 | > 10 | > 10 | > 10 | > 10 |
| MNKI-10-22[2] | >10/0.393 | > 10 | > 10 | > 10 | > 10 | > 10 |
| MNKI-11-86[2] | 1.227/0.280 | > 10 | > 10 | > 10 | > 10 | > 10 |
| MNKI-12-56[2] | 1.331/0.132 | > 10 | > 10 | >10 | > 10 | > 10 |
| MNKI-12-62[2] | 4.876/0.408 | > 10 | > 10 | > 10 | > 10 | > 10 |
| MNKI-15[1] | 1.900/0.164 | > 10 | > 10 | > 10 | > 10 | > 10 |
| MNKI-19[1] | 0.186/0.068 | > 10 | > 10 | > 10 | > 10 | > 10 |
| MNKI-28[1] | 4.820/0.352 | > 10 | > 10 | > 10 | > 10 | > 10 |
| MNKI-37[1] | 1.020/0.048 | 0.87 ± 0.08 | > 10 | 0.91 ± 0.25 | > 10 | > 10 |
| MNKI-57[1] | 0.106/0.018 | 0.51 ± 0.17 | > 10 | 6.32 ± 1.34 | > 10 | > 10 |
| MNKI-67[1] | 0.933/0.018 | 0.57 ± 0.06 | >10 | 0.99 ± 0.20 | >10 | >10 |
| MNKI-83[1] | 0.320/0.164 | > 10 | > 10 | > 10 | > 10 | > 10 |
| MNKI-85[1] | >10/0.031 | 4.77 ± 1.67 | > 10 | 7.04 ± 2.84 | > 10 | > 10 |

Data shown are the mean values from at least three independent experiments with three replicates each. NT: inactive from IMAP assay, therefore not tested (NT) for their $K_i$ values, [1]: compound series 1, [2]: compound series 2, [3]: compound series 3.

The growth inhibitory potential of Mnk inhibitors of series 1 (*N*-phenylthieno[2,3-*d*]pyrimidin-4-amines) were more potent compared to other chemical series. Eight out of nine potent inhibitors belonged to series 1 and one (MNKI-7-7-2) was from series 2 (3,4-

dimethyl-5-(2-(phenylamino)pyrimidin-4-yl)thiazol-2(3*H*)-ones). In addition, these eight inhibitors were selective for Mnk over CDK2A and CDK9T1 kinases ($K_i$ > 10 µM) whereas MNKI-7-7-2 had CDK2A inhibitory activity ($K_i$ CDK2A = 0.23 µM and $K_i$ CDK9T1 > 10 µM) (**Table 2.4**). Interestingly, six out of eight potent compounds from series 1 were allosteric inhibitors (MNKI-6, MNKI-7, MNKI-8, MNKI-37, MNKI-57 and MNKI-67) and two showed ATP competitive binding mode (MNKI-4 and MNKI-85) (**Table 2.3**). Allosteric inhibitors are expected to be more selective, implying the observed anti-proliferative activities for these compounds (**Table 3.2**) were due to inhibition of Mnks. However, none of the compounds were associated with any significant anti-proliferative activity against PC-3 and C4-2B cell lines ($GI_{50}$ > 10 µM).

To understand why these cell-lines had the different sensitivities towards Mnk inhibitors, we investigated the expression of proteins related to the Mnk-eIF4E axis. Western blotting analysis of 22RV1 and DU-145 PCa cells showed a high level of phosphorylated eIF4E (**Figure 3.1**) which was in line with the higher potency of the Mnk inhibitors. Both cell lines did not show significant phosphorylation of AKT at Ser473 which may be the possible reason for decreased phosphorylation of 4EBP1 (**Figure 3.1**). A consequence of low PI3K/AKT/mTOR pathway activity is eIF4E inactivation due to eIF4E remaining in an inactive complex bound to non-phosphorylated 4E-BP. However, the high constitutive eIF4E phosphorylation in 22RV1 and DU-145 cells can possibly be explained by a low expression of 4E-BP1. Previous reports have shown Mnk inhibition to be more effective in cell lines with low p-AKT activity [137]. Conversely, PC-3 and C4-2B cells express low levels of p-eIF4E which suggests that another mechanism, independent of MAPK/Mnk activity, may be responsible for uncontrolled growth. Therefore, a lack of anti-proliferative response in the PC-3 and C4-2B cells following Mnk-inhibitor treatment was not surprising. Lastly, LNCaP expressed higher levels of phosphorylated

eIF4E and their insensitivity to Mnk inhibitors may be due to their reliance on androgen for proliferation. Expression of Mnk1 protein was lower in 22RV1 cells compared to the other four cell lines (**Figure 3.1**), suggesting a predominant role of Mnk2 in this cell line.

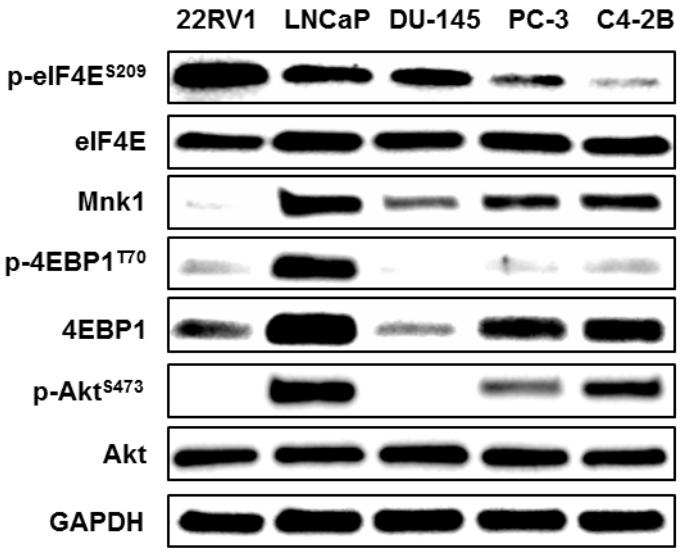



**Figure 3.1: Western blotting analysis of the levels of Mnk-eIF4E proteins in PCa cell lines.** Cells were lysed and probed with antibodies related to the Mnk and AKT signalling pathways. GAPDH was used as an internal loading control. A representative blot is selected from at least two independent repeats.

The correlation of the effect of Mnk inhibition on proliferation of PCa cells were further investigated by determining inhibition of eIF4E phosphorylation in PCa cells by Mnk inhibitors.

### 3.2.2 eIF4E phosphorylation as a biomarker

Phospho-eIF4E is a biomarker of Mnk inhibition, and therefore can be used to study whether there is a correlation between the anti-proliferative effects of Mnk inhibitors and eIF4E phosphorylation in PCa cells.

A fluorescence resonance energy transfer (FRET)-based approach for quantifying cellular eIF4E phosphorylation was established using a homogeneous time-resolved fluorescence (HTRF) format [218, 219]. After cell lysis, phosphorylated eIF4E is released and sandwiched between two monoclonal antibodies: the first is an anti-phospho-eIF4E

antibody labelled with $Eu^{3+}$ cryptate and the second an anti-eIF4E antibody labelled with d2 dye, an *N*-hydroxysuccinimide-activated organic dye. When the two antibodies are in close proximity, excitation of $Eu^{3+}$ cryptate triggers a FRET towards the d2 dye which fluoresces at a wavelength of 665 nm. The intensity of fluorescence is proportional to phosphorylated eIF4E (**Figure 3.2**). This assay is highly sensitive and quantitative, and therefore a robust, reliable and rapid alternative to more classical technologies such as Western blotting and enzyme-linked immunosorbent assay (ELISA).

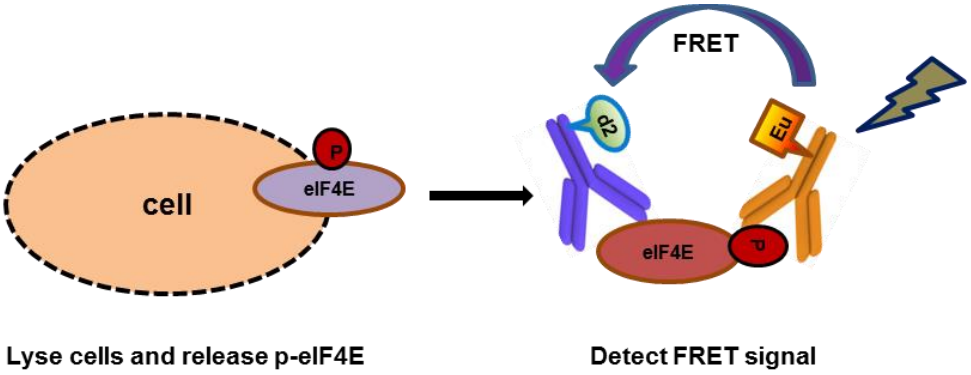



**Figure 3.2: Schematic representation of HTRF based phospho – eIF4E (Ser209) cellular assay.** The phosphorylated eIF4E is sandwiched between two monoclonal antibodies (an anti-phospho- eIF4E antibody labelled with $Eu^{3+}$ cryptate and an anti-eIF4E antibody labelled with d2). When the two antibodies bind to p-eIF4E, FRET occurs.

The assay was validated by comparison to Western blotting with one adherent PCa cell line (22RV1) and one suspension AML cell line (MV4-11). The lysates from both cell lines were serially diluted in 1:2 ratios and 16 µL of each lysate analysed in a side-by-side comparison between Western blotting and HTRF. The results indicated that the signal corresponding to p-eIF4E$^{S209}$ from Western blotting could not be detected from the last two dilutions whereas robust signals were observed with the HTRF assay, indicating the latter was more sensitive (**Figure 3.3A** and **B**).

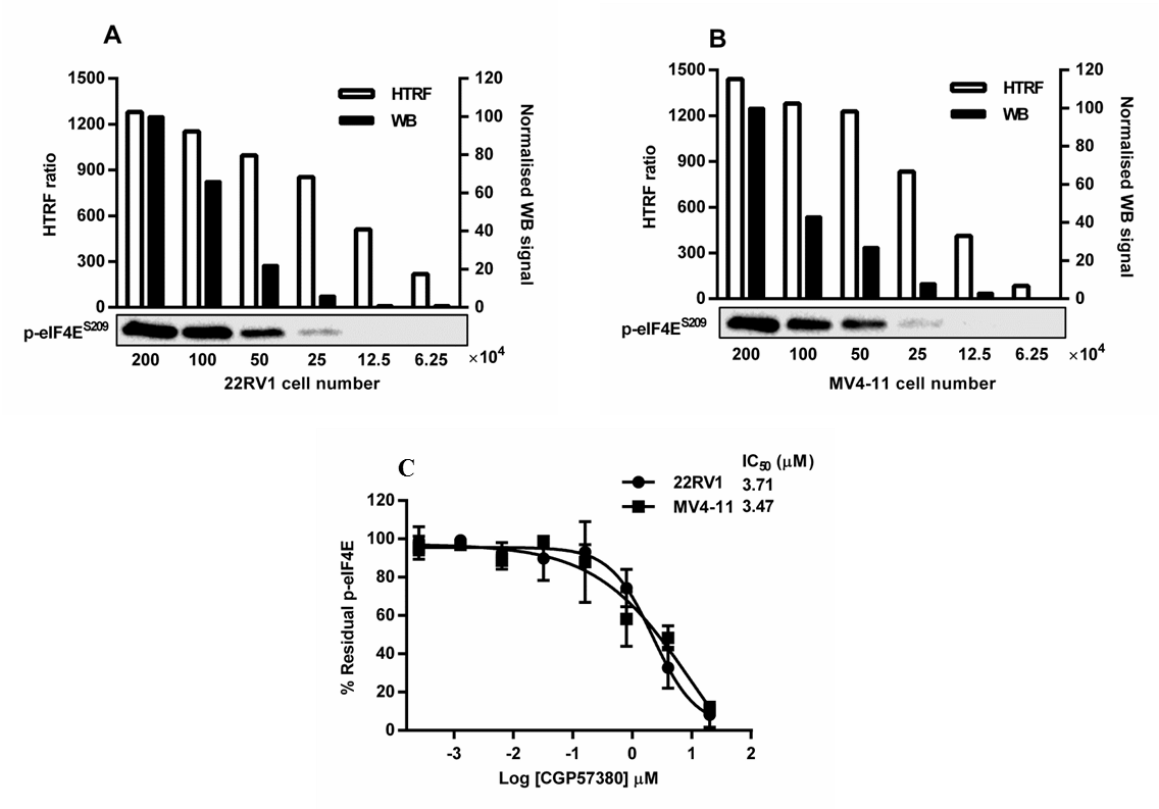



**Figure 3.3: HTRF assay is more sensitive than the classic Western blotting.** 22RV1 (**A**) and MV411 (**B**) cells were lysed and soluble supernatants were collected after centrifugation. Lysates were diluted at 1:2 serial dilutions and 16 µL were analysed in parallel by HTRF and Western Blot each. (C) Dose responses of 22RV1 and MV4-11 cells to CGP57380. 22RV1 and MV4-11 cells were incubated with various concentrations of CGP57380 for 1 hour at 37°C. After cell lysis, eIF4E phosphorylation was measured using the HTRF assay.

Using the HTRF assay, the effect of CGP57380 on 22RV1 and MV4-11 cell lines were investigated. The cells were treated with eight different serially-diluted (1:3 ratio) concentrations of the compound ranging from 0.009 to 20 µM. After 1 hour of incubation, the cells were lysed with 16 µL lysis buffer and transferred to an assay plate followed by addition of 4 µL premixed antibody (2 µL of anti-eIF4E antibody and anti-phospho- eIF4E antibody). Following incubation overnight, fluorescence from the plate was read at room temperature. $IC_{50}$ values were calculated by applying a four-parameter logistic non-linear regression model. CGP57380 showed an $IC_{50}$ value of 3.71 µM and 3.47 µM against 22RV1 and MV4-11 cells, respectively (**Figure 3.3C**). The data aligned closely with a

reported $IC_{50}$ value of ~3 µM for CGP57380 to inhibit phosphorylation of eIF4E determined using Western blotting [111].

The HTRF assay was applied to 22RV1 cells to study the cellular mode of action of Mnk inhibitors. Eight compounds with $GI_{50}$ values < 10 µM and one (MNKI-5) with $GI_{50}$ >10 µM against 22RV1 cells (**Table 3.2**) were selected to evaluate p-eIF4E related inhibitory responses. The 22RV1 cells were incubated with each compound for 1 hour at concentrations ranging from 10 to 0.0005 µM using 1:3 serial dilutions. Calculated $IC_{50}$ values are given in **Table 3.3.**

**Table 3.3: Correlation of the p-eIF4E inhibitory activities of Mnk inhibitors in PCa cells with their anti-proliferative activities and enzymatic kinase inhibitory activities.**

| Compounds | $IC_{50}$ (µM) | | 22RV1 | |
|---|---|---|---|---|
| | Mnk1[1)] | Mnk2[1)] | $IC_{50}$ (µM)[2)] | $GI_{50}$ (µM)[3] |
| MNKI-4 | > 10 | 0.452 | 0.276 | 0.749 |
| MNKI-7 | 0.083 | **0.044** | 0.097 | 6.756 |
| MNKI-7-7-2 | 1.718 | 0.390 | 0.876 | 8.848 |
| MNKI-8 | 0.164 | **0.052** | 0.564 | 7.871 |
| MNKI-37 | 1.530 | 0.219 | 0.274 | 0.874 |
| MNKI-57 | 0.159 | **0.036** | 0.164 | 0.515 |
| MNKI-67 | 1.400 | **0.036** | 0.114 | 0.571 |
| MNKI-85 | > 10 | **0.062** | 0.191 | 4.773 |
| MNKI-5 | 0.147 | **0.050** | 2.512 | >10 |

[1)] $IC_{50}$ values by ADP-Glo™ kinase assay (refer to chapter 2).

[2)] $IC_{50}$ values of phospho-eIF4E inhibition by HTRF assay.

[3)] $GI_{50}$ values by MTT assay.

The Pearson correlation coefficient (also referred to as the Pearson's r) was determined. It is a measure of the linear correlation between two variables. The value of r is measured between -1 and +1, where -1 is total negative correlation, 0 is no correlation, and 1 is total positive correlation [220-222]. There was a moderate correlation between eIF4E phosphorylation and anti-proliferative response of Mnk inhibitors on 22RV1 cells (Pearson correlation r = 0.658, **Figure 3.4A**) while much lower correlation was observed

with enzymatic Mnk inhibitory activity (Pearson correlation r = -0.138 for Mnk1 and 0.006 for Mnk2, **Figure 3.4B** and **C**). Since 22RV1 cells express low level of Mnk1 protein (**Figure 3.1**), Mnk2 inhibitors were expected to have a similar effect as dual Mnk1/2 inhibitors.

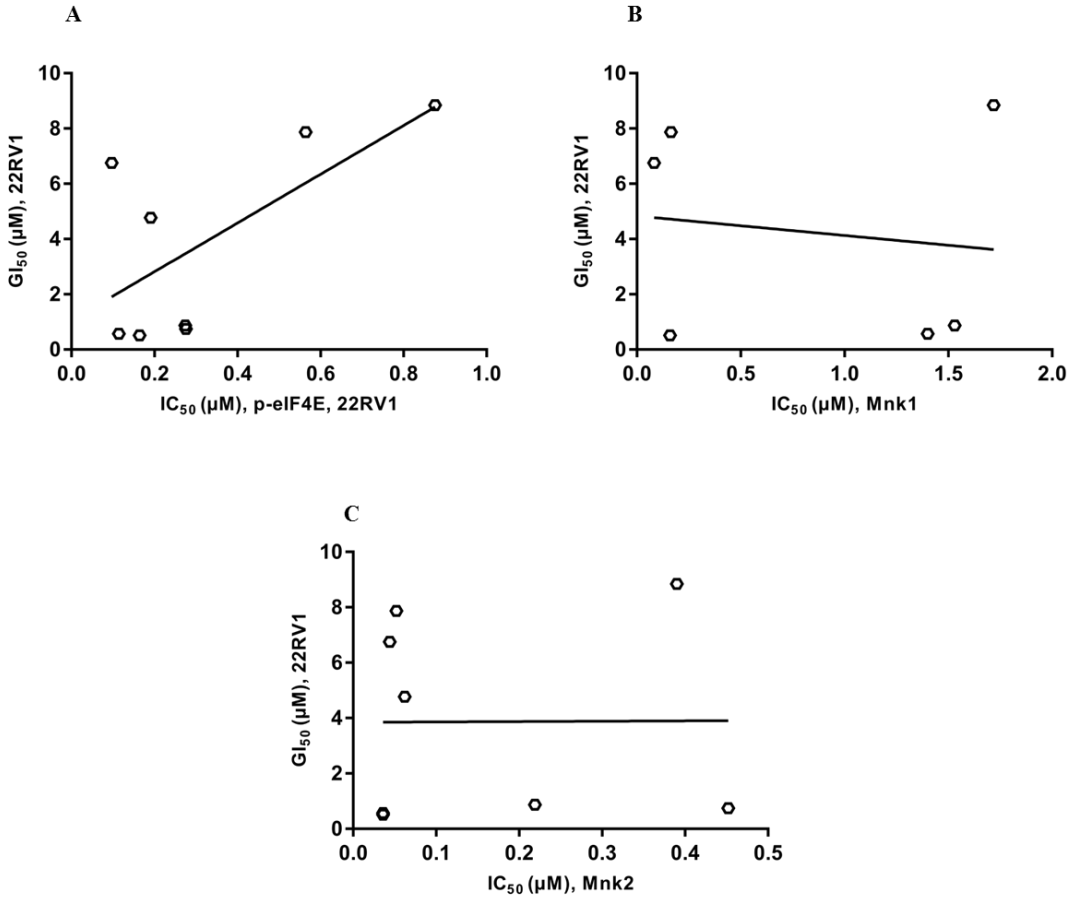



**Figure 3.4: Correlation of anti-proliferative effects with cellular eIF4E phosphorylation and Mnk kinase activity.** Cells were exposed to each compound for 72 hours. The MTT assay was used to test cell viability of 22RV1 cells. HTRF assay was used to determine the phosphor-eIF4E after 1 hour of incubation with each compound. (A) The $IC_{50}$ values for cellular phosphorylation of eIF4E were plotted against the $GI_{50}$ values against 22RV1 cells. The data are given for eight compounds with a $GI_{50}$ value of < 10 μM against 22RV1 cells. Pearson correlation coefficient (r = 0.658; n = 8; one-tailed p = 0.037). (B) A similar plot with six compounds (two compounds with $IC_{50}$ > 10 μM were excluded) against $IC_{50}$ Mnk1 was generated. Pearson correlation coefficient (r = -0.138; n = 6; one-tailed p = 0.396) and (C) Correlation between anti-proliferative effects and $IC_{50}$ against Mnk2 (r = 0.006; n = 8; one-tailed p = 0.494).

As shown in **Table 3.3** there are six compounds with Mnk2 inhibitory activity $IC_{50}$ < 0.1 μM (*i.e.* MNKI-5, MNKI-7, MNKI-8, MNKI-57, MNKI-67 and MNKI-85; shown in

bold and underlined). The two most potent of these (MNKI-57 and MNKI-67) showed an approximately three to five-fold increase between the $IC_{50}$ values based on enzyme activity and eIF4E phosphorylation. Approximately fifteen-fold increase in $GI_{50}$ values (0.5 µM) was observed when comparing with enzymatic activities (0.03µM). Whilst MNKI-7 and MNKI-85 showed comparable ratios between enzymatic and p-eIF4E inhibition, much larger effects were seen for the increase of $GI_{50}$ values. MNKI-5 which did not show anti-proliferative activity up to 10 µM was the weakest inhibitor of eIF4E phosphorylation. The observed anti-proliferative effects in the 22RV1 cells appeared to correlate better with the inhibition of eIF4E phosphorylation. eIF4E phosphorylation correlates with reduced cell viability, hence this supports that Mnk inhibition can have strong anti-cancer activity against PCa cells. However, other factors in addition to HTRF-determined p-eIF4E status need to be considered to give a better prediction of outcome.

### 3.2.3 Mnk inhibition blocks migration of prostate cancer cells

Inflammation has been proposed as one of the hallmarks of cancer [3] and recognised as a driving force for progression and metastasis of some types of cancers. Recent studies have revealed that there are links between Toll-like receptors (TLRs) and cancer [223, 224]. TLRs form a family of transmembrane protein receptors that recognise several endogenous (low density lipoproteins, beta-defensins, heat shock protein, hyaluronan, biglycan) and exogenous bacterial lipopolysaccharides (LPS), viral proteins ligands [225, 226]. Studies have further demonstrated an increased expression of TLR4 in human prostate epithelial cancer cells [227, 228] which promoted their malignant transformation [229, 230]. This observation is in agreement with the finding that LPS-stimulated TLR4 activated Mnk1 and up-regulated phosphorylation of eIF4E which promote cell migration

[31], thereby establishing the potential of Mnk inhibitors to interfere with TLR4-induced migration of PCa cells.

LPS has been reported to activate ERK and p38 [231] which in turn suggests that these may activate Mnks and enhance eIF4E phosphorylation. LPS was used as TLR4 ligand in five PCa cell lines (**Table 3.1**) in order to determine whether LPS could increase the level of Mnk-mediated p-eIF4E. **Figure 3.5A** showed a significant increase in eIF4E phosphorylation in C4-2B cells only, and thus were selected for further experimental studies. C4-2B cells were incubated with 100 ng/mL LPS for 30 minutes, followed by incubation with Mnk inhibitor for 1 hour (1 μM of MNKI-67 or MNKI-7). The compounds prevented the phosphorylation of eIF4E (p-eIF4E$^{S209}$), confirming the cellular Mnk inhibition (**Figure 3.5B**).

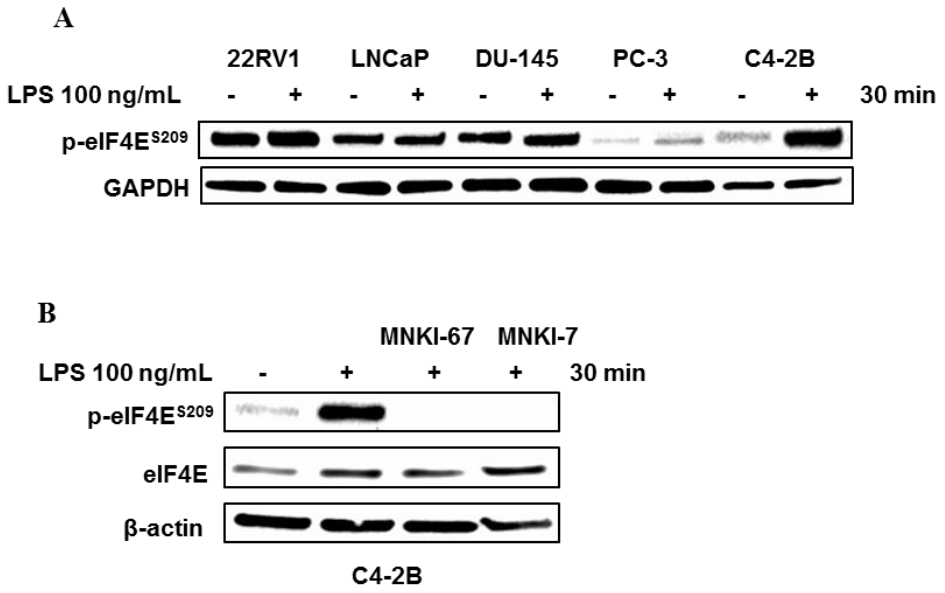



**Figure 3.5: Mnk inhibitors eliminate the phosphorylation of eIF4E by Western blotting analysis.** (A) Treatment of various prostate cancer cell lines with 100 ng/mL LPS for 30 minutes increased the eIF4E phosphorylation in C4-2B cells dramatically. (B) C4-2B cells were treated with 100 ng/mL LPS for 30 minutes, and then with 1 μM of MNKI-67 or MNKI-7 for 1 hour. A representative blot is selected from at least two independent repeats.

Subsequently, the effects of MNKI-7 and MNKI-67 on cell migration using wound healing [232-234] and trans-well migration assays [235-237] were studied. In the wound healing assay, C4-2B cells were cultured until fully confluent and the monolayers scratched in a straight line to create the wounded monolayers (refer to **Section 6.2.11**). These monolayers were then cultured in the presence or absence of 100 ng/mL LPS and/or 1 µM Mnk inhibitors. The wounded areas were photographed immediately after scratch and twenty-four hours later. For the control image at time zero, the distance between the edges at 10 separate locations was averaged. Similar averages were then calculated after 24 hours using the same ten locations. The percentage of wound closure was calculated by subtracting the wound distance at twenty-four hour from zero hour and divided by the distance at time zero then multiplied by one hundred. As shown in **Figure 3.6A**, treatment with LPS significantly induced migration of C4-2B cells into the scratch area (100% wound closure) when compared to the untreated cells (73%) after 24 hours whereas co-incubation with MNKI-7 (49%) or MNKI-67 (34%) for 24 hours supressed C4-2B cell migration to the scratched area, revealing the potential role of Mnk inhibitors in preventing the motility of C4-2B cells.

The effects on cell migration by the Mnk-inhibitors were also confirmed with the trans-well migration assay (refer to **Section 6.2.12**), the cells invading the matrigel-coated polycarbonate filter in the Boyden chamber were analysed (**Figure 3.6B)**. C4-2B cells were pre-treated with LPS before seeding on a Boyden chamber, and subsequently treated with 1 µM of MNKI-7 or MNKI-67 each. After 24 hours, cells that invaded through the matrigel matrix and porous membrane were fixed, stained and counted using ImageJ software Version K1.45 within five random fields. Cells treated with LPS were found to migrate to the other side of the membrane readily (mean of 63 cells/field compared to mean of 11 cells/field in control). In contrast, Mnk inhibitors, MNKI-7 and MNKI-67,

prevented the migration of C4-2B cells as shown by the reduced number of migrated cells through the chamber (mean of 5 and 7 cells/field for MNKI-7 and MNKI-67 respectively).

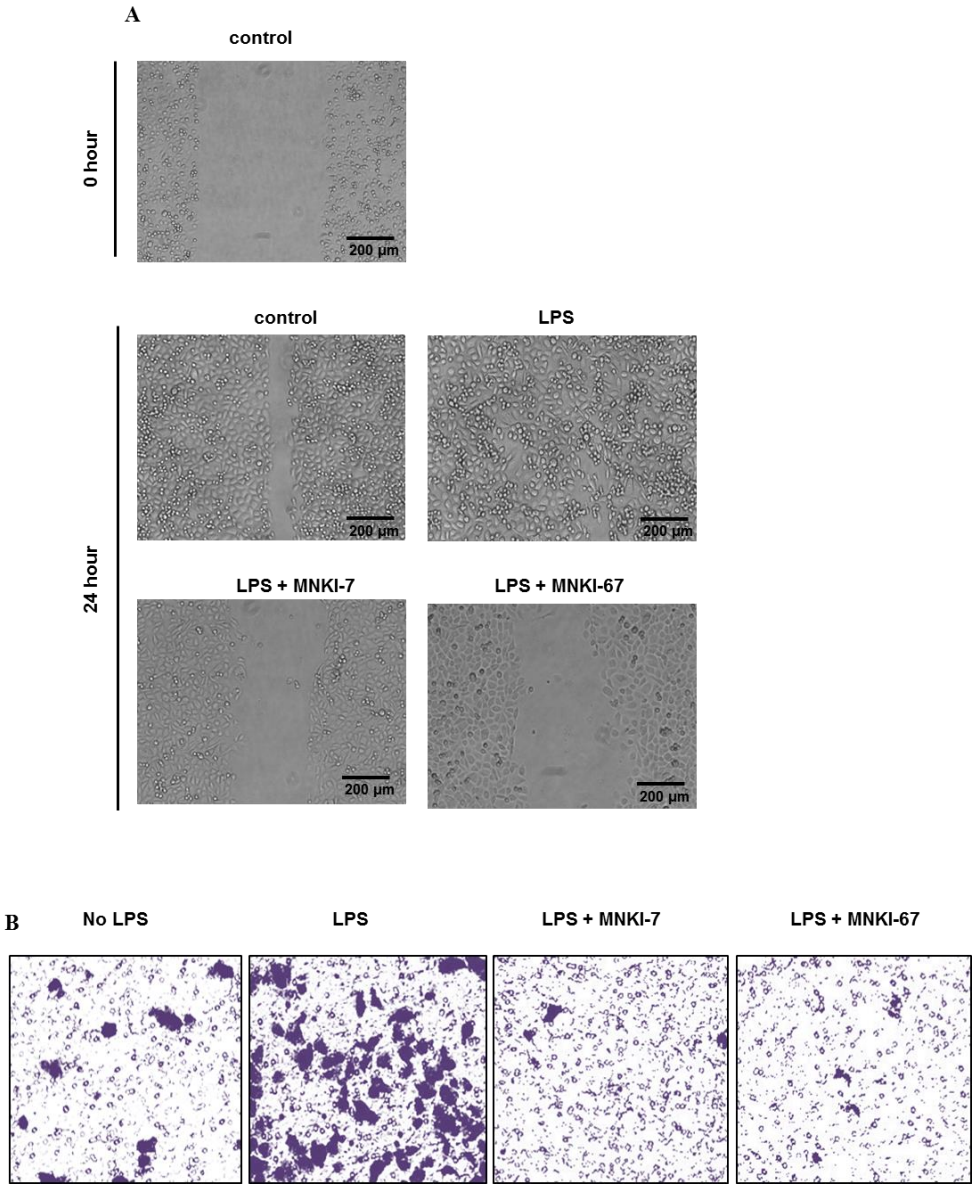



**Figure 3.6: Anti-migratory effect of MNKI-7 and MNKI-67 in C4-2B PCa cell line.** (A) Cells were cultivated in 6-well plates until full confluency was achieved. The monolayers were scratched in a straight line, and the wounded monolayers were then given culture medium with or without 100 ng/mL LPS and 1 µM of MNKI-7 or MNKI-67 each. The wound area was inspected after 24 hours using an inverted phase contrast microscope and representative images are shown. (B) Effect of MNKI-7 and MNKI-67 on the invasion of the C4-2B was evaluated by trans-well migration assay. LPS pre-treated C4-2B cells were seeded on a matrigel coated Boyden chamber and treated with MNKI-7 or MNKI-67. After 24 hours, cells that invaded through the matrigel matrix and porous membrane were fixed, stained and counted within five random fields. Photographs represent the extent of cell invasion in each of the treated and untreated cells.

Earlier studies support the Mnk-eIF4E pathway as being crucial for the progression to metastatic cancer, by facilitating the translation of migration related proteins like vimentin in mesenchymal cells, also known as mucous connective cells [95, 100]. Pharmacologic and genetic targeting of Mnks using Mnk inhibitor CGP57380 and knockdown of Mnks, respectively, has previously been shown to reverse epithelial-mesenchymal transition (EMT), to decrease cell migration and to reduce protein expression of zinc finger E-box binding homeobox 1 (ZEB1) (an EMT inducer) [238]. Another report revealed that eIF4E Ser209Ala knock-in mice were resistant to lung metastases, and that cells isolated from these mice exhibited impaired invasion [93]. Preliminary data discussed in this chapter suggests that Mnk-inhibition could be beneficial for preventing PCa cell migration and invasion.

## 3.3 Inhibition of Mnk in leukaemia cells

AML is a highly heterogeneous disease characterised by a set of mutations and chromosomal translocations in immature myeloid cells that contribute to impede the survival or proliferative pathways [239]. The Ras/Raf/MAPK and PI3K/AKT/mTOR signalling pathways are over-activated in AML [240, 241], suggesting potential therapeutic advantage of targeting the Mnk/eIF4E axis for AML. Generally, a single genetic alteration is insufficient to induce leukaemogenesis in most cases [242, 243]. Constitutively activated signalling pathways resulting from the mutated genes that normally regulate haematopoietic cell growth and homeostasis are an additional contributor to the development and progression of AML [244]. Mutations in the FLT3 gene are very common, including the internal tandem duplication (ITD) in the juxta membrane domain, accounting for about a quarter of all AML cases [245][246].

Therefore, these signal transduction cascades may represent promising opportunities for therapeutic intervention in AML.

### 3.3.1 Anti-proliferative activity of Mnk inhibitors against leukaemia cell lines

Based on previous studies showing cytotoxic activity of Mnk inhibitors against leukaemia cells [136, 138, 247], the anti-proliferative activities of MNKI-7, MNKI-57 and MNKI-85 were assessed on a panel of leukaemia cell lines including four AML, two acute promyelocytic leukaemia (APL) ), one histiocytic lymphoma (HL)) and one CML, as well one normal fibroblast cell line (WI-38) using resazurin and MTT proliferation assays conducted over 72 hours (**Table 3.4**). MNKI-7 and MNKI-57 were dual Mnk1/2 inhibitors ($K_i$ Mnk1 = 0.055 µM, $K_i$ Mnk2 = 0.022 µM for MNKI-7 and $K_i$ Mnk1 = 0.106 µM, $K_i$ Mnk2 = 0.018 µM for MNKI-57) whereas MNKI-85 was selective for Mnk2 ($K_i$ = 0.031 µM) over Mnk1 ($K_i$ > 10 µM). CGP57380 was included in the assays as a comparator which modestly suppressed cell proliferation with $GI_{50}$ values ranging from 3.8 - 9.4 µM. Of all the leukaemia cell lines tested, AML cell lines were most sensitive towards the Mnk inhibitors ($GI_{50}$ < 10 µM). MNKI-57 exhibited its strongest effect on KG1 cells ($GI_{50}$ = 0.49 µM) whereas MNKI-7 and MNKI-85 were most effective against MV4-11 cells with $GI_{50}$ values of 0.81 µM and 7.44 µM respectively (**Table 3.4**).

**Table 3.4: Anti-proliferative activity of CGP57380, MNKI-7, MNKI-85 and MNKI-57 against leukaemia cell lines and normal fibroblast cell line by 72 hours resazurin and MTT assay, respectively.**

| Cell line | | FLT3 | 72 hours $GI_{50}$ (μM) ± SD | | | |
|---|---|---|---|---|---|---|
| | | | CGP57380 | MNKI-7 | MNKI-85 | MNKI-57 |
| MV4-11 | AML | ITD | 4.52 ± 0.90 | 0.81 ± 0.03 | 7.44 ± 0.77 | 6.10 ± 0.79 |
| MOLM-13 | AML | ITD/WT | 8.81 ± 0.80 | 1.59 ± 0.20 | > 10 | 5.76 ± 1.10 |
| PL-21 | AML | ITD/WT | 9.39 ± 0.11 | 8.75 ± 0.32 | > 10 | 7.21 ± 4.41 |
| KG-1 | AML | WT | 3.78 ± 1.11 | 4.97 ± 0.17 | > 10 | 0.49 ± 0.38 |
| HL-60 | APL | WT | > 10 | > 10 | > 10 | > 10 |
| NB4 | APL | WT | > 10 | > 10 | > 10 | > 10 |
| U937 | HL | WT | > 10 | > 10 | > 10 | > 10 |
| K562 | CML | WT | > 10 | > 10 | > 10 | > 10 |
| WI-38 | normal fibroblasts | - | > 10 | > 10 | > 10 | > 10 |

Data shown are the mean values from at least three independent experiments with three replicates each. ITD; internal tandem duplication, WT; wild type, AML; acute myeloid leukaemia, APL; acute promyelocytic leukaemia, HL; histiocytic lymphoma, CML; chronic myeloid leukaemia.

While MV4-11 cells were sensitive to the Mnk inhibitors ($GI_{50}$ < 10 μM), they had minimal effects on the growth of non-AML HL-60, U937, NB4 and K562 cells. The differences in the sensitivity to the Mnk-inhibitors between the AML cell lines is likely to be attributed to the different subtypes, which are classified based on the immunohistochemistry and morphology of myeloid neoplasms [248]. MV4-11 and MOLM-13 are acute monoblastic leukaemia cells (classified as M5/M5a in the French–American–British classification system) [249] that carry the respective t(9,11) and t(4,11) chromosomal translocations, resulting in the fusion proteins MLL-AF9 and MLL-AF4, respectively [250, 251]. Importantly, this subtype of AML is correlated with aberrant up-regulation of eIF4E protein expression [252]. KG-1 cells are a minimally differentiated acute myeloblastic leukaemia cell line (M0) whereas PL-21 is derived from AML, M3 subtype. The higher sensitivity of KG-1 cells compared to PL-21 may be attributed to other factors independent of FLT-3 mutational status. Our recent study revealed the

sensitivity of KG-1 cells was correlated with the level of phosphorylated 4EBP1 at Thr70 [97].

MV4-11 cells were found to be sensitive to all three compounds tested and were, therefore, chosen for exploring anti-proliferative activity of a further one-hundred and four additional compounds identified in chapter 2 and the results are summarised in **Appendix 8.5, Table 8.3**. The data are shown in clusters of five distinct groups i.e. **A-E**. Of the one-hundred and four compounds, seventy-seven showed $GI_{50}$ values < 10 µM, ranging from 0.007 to 9.7 µM (**Appendix 8.5, Table 8.3, Groups A, B and D**). **Group A** and **B** compounds inhibited Mnks with $K_i$ < 10 µM, however 21 compounds from **group D** were non-inhibitors of Mnk ($K_i$ < 10 µM) suggesting the anti-proliferative result was due to the consequence of off-target effect in this group. Thirteen compounds in **group C** showed discrepancy between Mnk inhibitory activities and anti-proliferative effects suggesting the requirement of direct biomarker of Mnk inhibition in the cells.

In order to study the correlation between inhibition of Mnks and anti-proliferative effect against MV4-11 cells, Mnk inhibitors from compound series 1 and 2 with $K_i$ and $GI_{50}$ values < 10 µM were selected (Groups **A** and **B**, **Table 8.3, Appendix 8.5**). Compounds from series 3 were excluded from the study since almost all inhibitors (except MNKI-9-36 and MNKI-12-94) were weak inhibitors of Mnk ($K_i$ > 1 µM). Compounds with CDK2/9 activities ($K_i$ < 10 µM) were also excluded. The remaining thirty compounds were analysed for correlation of anti-proliferative activities *versus* Mnk1 and Mnk2 inhibitory potencies. Anti-proliferative activities of the compounds seemed to be in good correlation with Mnk inhibition (**Figure 3.7**). Mnk2 was more dominant for eIF4E phosphorylation compared to Mnk1since the compounds showed good anti-proliferative activities despite of no Mnk1 inhibitory activities. However, some potent inhibitors of Mnks (MNKI-37 to MNKI-67) as shown in **Figure 3.7** showed discrepancy between anti-

proliferative activities and Mnk inhibition. Enzymatic kinase activities are not always directly translated to cellular outcomes which can be due to the cellular effects on the compounds (active/passive transport), intracellular degradation and also the potency of an ATP-competitive inhibitor in cells depends significantly on the affinity between the kinase and ATP which is reflected by the $K_m$ value [184]. The intracellular concentration of ATP is assumed to range from 1-5 mM [253, 254] and therefore exceeds the $K_m$ of ATP and the $IC_{50}$ increases at approximately the similar rate [184]. Therefore, evaluation of intracellular biomarker is more relevant to establish the correlation.

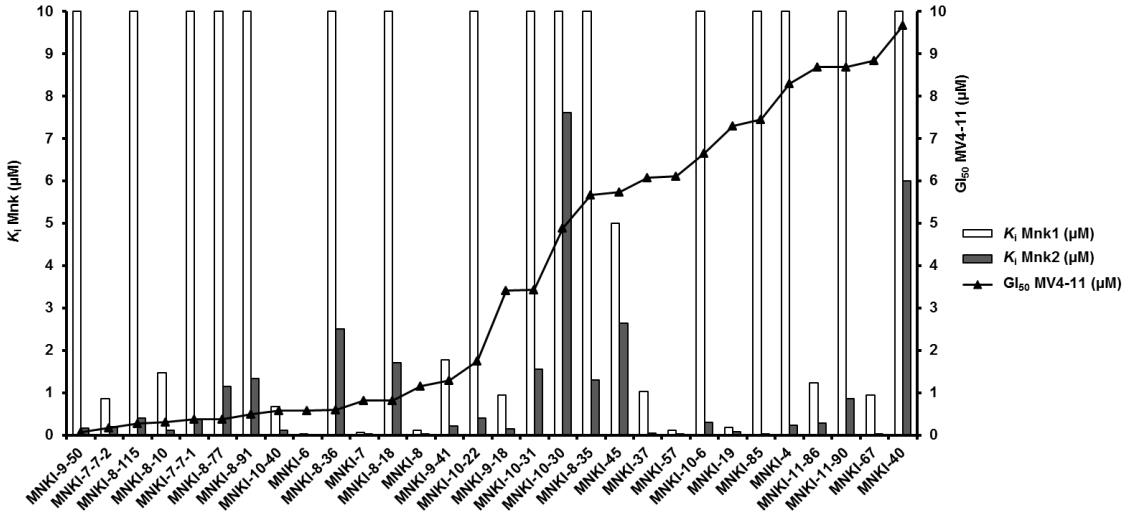



**Figure 3.7: Correlation between cellular anti-proliferation and Mnk enzyme inhibition.** MV4-11 cells were exposed to each compound for 72 hours. The resazurin assay was used to test cell viability in concentration-response experiments, and $GI_{50}$ values were calculated (**Table 8.3**). $K_i$ values were determined from ADP-Glo™ assay (**Table 8.2**). $K_i$ values for Mnk1and Mnk2 were plotted against $GI_{50}$ values. Compounds with $K_i$ values of > 10 µM against Mnk1 are shown as 10 µM and the data are given for thirty compounds.

In the next step, seventeen compounds from series 1 without inhibiting CDK2/9 activity were selected to study the correlation of the eIF4E phosphorylation assessed by cellular HTRF assay described in **Section 3.2.2**. Series 2 compounds were excluded since ten out of sixteen tested compounds from this series were CDK2/9 modulators (**Table 2.4**). Only fourteen inhibitors were used for Mnk1 study after exclusion of three Mnk2 selective

compounds. As shown in **Figure 3.8A** and **B**, the inhibitory activity by the biochemical assays correlated well with cellular Mnk inhibition i.e. phosphorylated eIF4E with a Pearson correlation for Mnk1, r = 0.603 (n=14) and Mnk2, r = 0.637 (n=17). In addition, there was moderate correlation for the same compounds (Compounds with $GI_{50}$ values >10 µM were excluded) when anti-proliferative effects were compared to inhibition of eIF4E phosphorylation in MV4-11 cells (Pearson's correlation r = 0.581, n=10) (**Figure 3.8C**). However, four compounds with low inhibitory activity on eIF4E phosphorylation (< 0.2 µM) showed $GI_{50}$ values above 6 µM suggesting some other activity maintaining the viability of these cells. Since the anti-proliferative potency of a compound is the consequence of its overall effect in the cells and merely any compound is absolutely specific, some disparities between anti-proliferative activity and kinase potency are expected. For example, seven compounds out of twenty-nine compounds were found to inhibit CDK2A and/or CDK9T1 [36]. The data are summarised in **Table 8.3 Appendix 8.5** (**Group A, B and C**). In addition, fifteen compounds displayed potent FLT3 inhibitory activities with $K_i$ values ranging from 0.005 to 0.207 10 µM (**Table 8.3, Appendix 8.5, Group B)**. Therefore, the observed anti-proliferative activities can potentially be the combined effects of the kinase inhibitors on multiple signalling pathways in cancer cells.

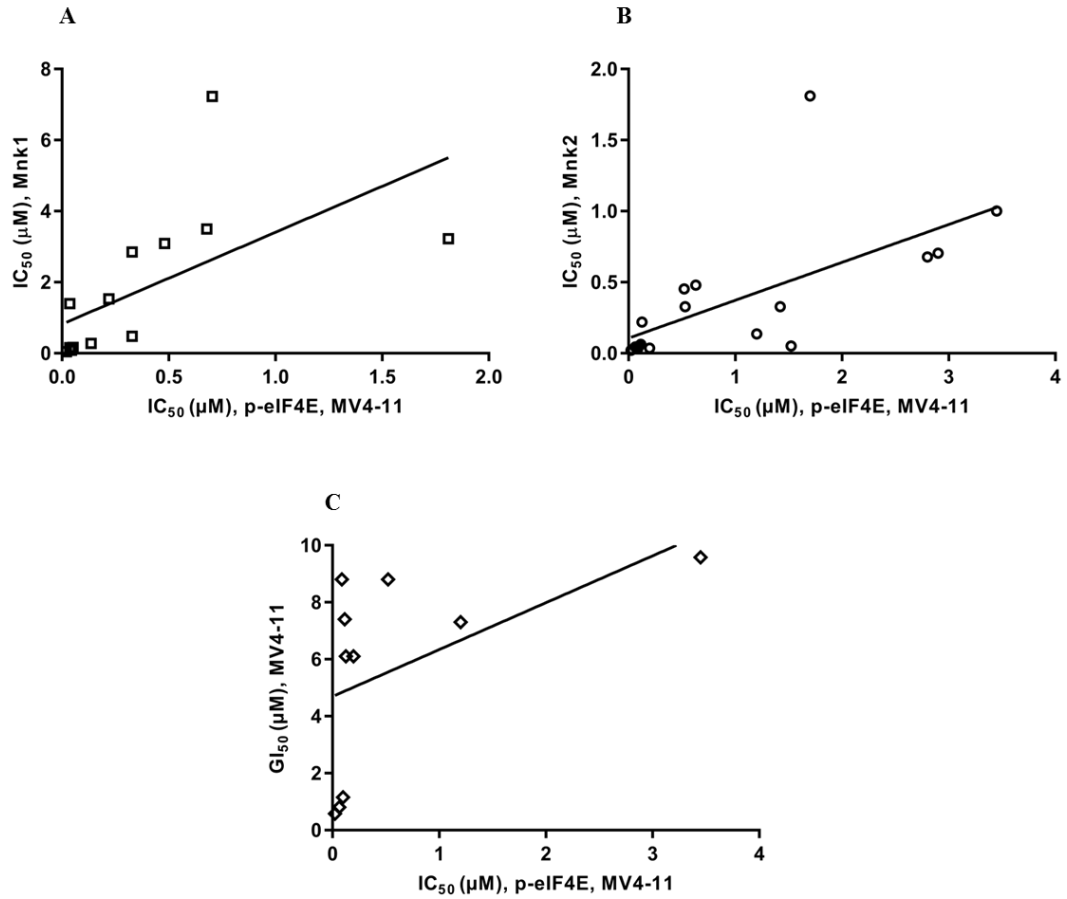



**Figure 3.8: Enzymatic Mnk inhibition and anti-proliferative effects correlation study with cellular eIF4E phosphorylation.** (A) MV4-11 cells were exposed for 1 hour to each Mnk inhibitor at 8 serial (1:3) dilutions. Inhibition of eIF4E phosphorylation was detected using the HTRF assay (**Section 3.2.2**). Enzymatic Mnk1 inhibition (**Table 8.2**) was plotted versus cellular eIF4E inhibition (**Table 8.3**) in MV4-11 cells and the Pearson correlation coefficient was determined ($r = 0.603$, $n = 14$; one-tailed $p = 0.011$). (B) A graph similar to (A) was plotted for Mnk2 activity ($r = 0.637$, $n = 17$; one-tailed $p = 0.003$). (C) $IC_{50}$ values for cellular eIF4E inhibition were plotted against $GI_{50}$ values. Compounds with $GI_{50}$ values >10 µM were excluded. The trend line is shown and the Pearson correlation coefficient has been calculated ($r = 0.581$, $n = 10$; one-tailed $p = 0.007$).

Since cytotoxic effects were only observed in AML but no other type of leukaemia cells (**Table 3.4**), specific genetic traits of AML cells were investigated from published literature [249, 255]. FLT3-ITD mutations occur in approximately 30% of AML patients therefore we tested the inhibitors in MV4-11, MOLM-13 and PL-21 AML cells which carry the FLT3-ITD mutation (**Table 3.4**) [249]. For comparison, HL-60, NB4, U937 and K562 AML cells, which do not express ITD mutations, were insensitive to all three

compounds. These results are in agreement with a previous study, in which the $GI_{50}$ value of Mnk inhibitor cercosporamide was > 10 µM against the FLT3-ITD-negative U937 and K562 AML cells [138].

We further investigated whether there is any correlation between FLT3 kinase inhibition and cellular anti-proliferative activity in MV4-11 cells. Anti-proliferative activity of twelve compounds from **Appendix 8.5**, **Group B** were plotted (three compounds with CDK2/9 activities were excluded) against FLT3 kinase inhibitory activity (10). The results showed a positive correlation with a Pearson's correlation coefficient r = 0.768 (n=12, $p$ = 0.0018) (**Figure 3.9**). This opens up the prospective for combining Mnk and FLT3 inhibition for better anti-cancer potencies. One of our studies revealed dual inhibition of FLT3 and Mnk2 caused the increased apoptotic cell death of MV4-11 cells compared to inhibition of FLT3 or Mnk2 alone. As eIF4E is a focal point of the MAPK and mTOR pathways, suppressing its translational function might interrupt mechanisms responsible for the development of resistance following FLT3 inhibition [256].

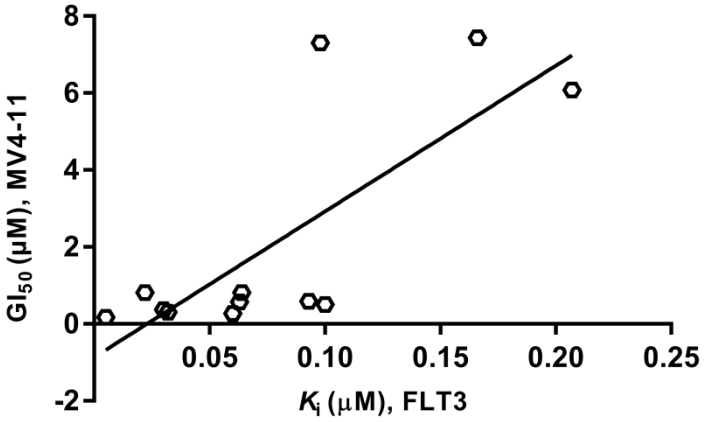



**Figure 3.9: Anti-proliferative effects correlated with FLT3 enzyme inhibition**. MV4-11 cells were exposed to each compound for 72 hours. The resazurin assay was used to test cell viability in dose response experiments and $GI_{50}$ values were calculated. $K_i$ values for FLT3 were plotted against $GI_{50}$ values. Compounds with CDK2/9 activity were excluded and the data are given for 12 compounds. The trend lines are shown and the Pearson correlation coefficient was determined (r = 0.768, n = 12; one-tailed p = 0.0018).

FLT3 is a well-established therapeutic target in AML and several FLT3 inhibitors are currently in clinical trials (ClinicalTrials.gov Identifiers: NCT00651261, NCT01565668, NCT01468467 and NCT01522469) for the treatment of AML patients [257]. However, development of these compounds has been hampered by resistance as a result of secondary mutations in FLT3 which can overcome the compounds inhibitory actions [258-260]. Therefore, it is important to identify novel strategies to overcome resistance. This project provides an opportunity to investigate potential beneficial effects of dual FLT3 and Mnk2 inhibition in AML cell lines.

### 3.3.2 Effects of combined inhibition of Mnk and FLT3 in MV4-11 cells

In order to address the question whether combined inhibition of FLT3 and Mnk leads to synergistic anti-proliferative effects, MNKI-7, a dual Mnk and FLT3 inhibitor, and SL4-26, a FLT3 inhibitor were selected. MNKI-7 is a potent inhibitor of Mnk1/2 ($K_i$ = 0.055 and 0.022 μM, respectively) and FLT3 ($K_i$ = 0.022 μM). It is approximately thirty-fold selective over CDK4/6 and showed no activity against CDK2A and CDK9T1 ($K_i$ > 10 μM) (**Table 3.5**). SL4-26 was designed and synthesised at our Centre for Drug Discovery and Development, yet due to intellectual property issues, the structure of this molecule cannot be disclosed. SL4-26 is a highly potent FLT3 inhibitor ($K_i$ = 0.0007) with an appreciable selectivity for FLT3 over Mnk1/2, CDK2A, CDK4D1, CDK6D1 and CDK9T1 (**Table 3.5**).

**Table 3.5: Kinase inhibitory and anti-proliferative profiles of MNKI-7 and SL4-26**

| Code | $K_i$ (μM) | | | | | | | $GI_{50}$ (μM) |
|---|---|---|---|---|---|---|---|---|
| | Mnk1 | Mnk2 | CDK2A | CDK4D1 | CDK6D1 | CDK9T1 | FLT3 | MV4-11 |
| MNKI-7 | 0.055 | 0.022 | > 10 | 0.882 | 0.619 | > 10 | 0.022 | 0.810 |
| SL4-26 | > 10 | 4.03 | > 10 | 7.67 | 5.63 | > 10 | 0.0007 | 0.075 |

It also showed potent anti-proliferative activity against MV4-11 with a $GI_{50}$ value of 0.075 μM as determined by 72 hour resazurin assay. The anti-proliferative activity of SL4-26 is approximately ten-fold more potent than that of MNKI-7 (**Table 3.5**).

FLT3 has downstream effects on MAPK, PI3K and signal transducer and activator of transcription-5 (STAT-5) pathways, resulting in the increased proliferation and reduced apoptosis. STAT-5 is constitutively activated by mutated FLT3 and the cytotoxic effect of FLT3 inhibitors is correlated to inhibition of STAT-5 activity [261, 262]. Western blot analysis of MV4-11 cells post-treated with SL4-26 showed that the compound reduced the phosphorylation of STAT-5 (p-$STAT5^{T694}$) within 1 hour in a dose-dependent manner starting from 0.01 μM and abolished the level of p-$STAT5^{T694}$ at 0.2 μM (**Figure 3.10**). Given its low activity against Mnk1/2 (**Table 3.5**); SL4-26 was not expected to inhibit Mnk activity. However, the p-eIF4E was abolished at concentrations > 0.5 μM, indicating that SL4-26 could potentially be inhibiting the upstream kinases like ERK1/2 and/or AKT. In the same experiment, MNKI-7 was found to be 10-fold less potent in reducing STAT-5 phosphorylation, which was in line with its lower inhibitory potency against FLT3 (**1A**) and eIF4E phosphorylation was completely inhibited at concentration > 1 μM without affecting the total eIF4E protein (**1B**). Since 2 μM of MNKI-7 was enough to abolish both STAT-5 and eIF4E phosphorylation and 0.2 μM of SL4-26 abolished STAT-5 phosphorylation, these concentrations were chosen for cell survival experiments.

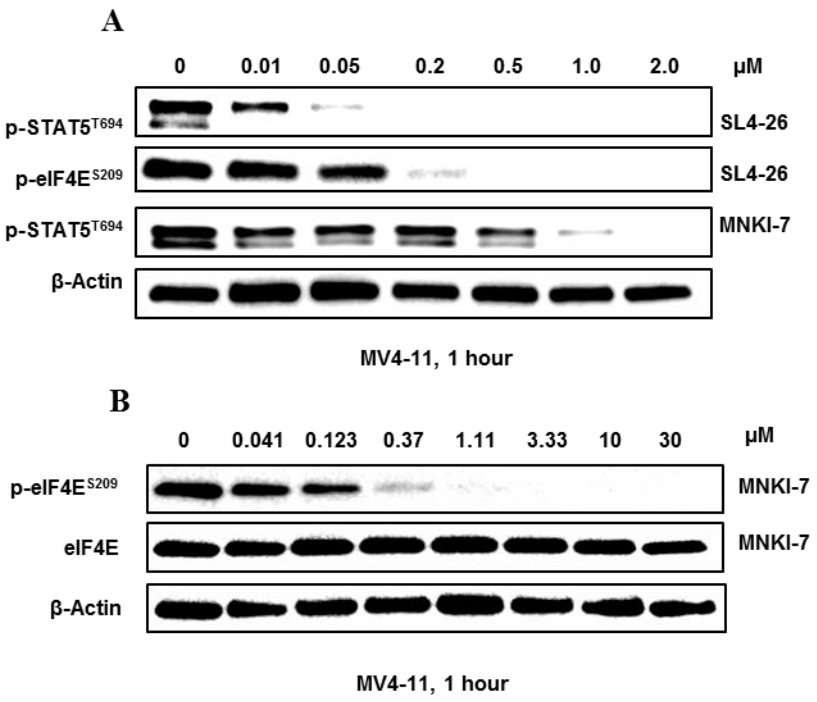



**Figure 3.10: Effects of FLT3 inhibition on the phosphorylation of STAT-5 at Tyr694 and of eIF4E at Ser209.** MV4-11 cells were treated with MNKI-7 or SL4-26 for 1 hour at the concentrations shown and the cells were lysed for Western blot analysis. ß-actin was used as loading control and a representative blot selected from at least two independent repeats.

In order to investigate the synergistic effects of Mnk and FLT3 inhibition, MV4-11 cells 48 h post-treatment with 2.0 μM MNKI-7 or 0.2 μM SL4-26 were stained with dual annexin V-FITC/PI and analysed by flow cytometry [263]. One of the early events in the apoptotic cell death is the loss of cell membrane asymmetry. In early apoptotic cells, the membrane phospholipid phosphatidylserine (PS) is translocated from the inner to the outer lipid layer of the plasma membrane, thereby exposing PS to the external cellular environment. Annexin V when labelled with a fluorescent marker, such as fluorescein isothiocyanate (FITC), binds with PS and can be used with flow cytometry to measure early apoptotic cells. Propidium iodide (PI) is a membrane impermeable dye that is normally excluded from viable cells and binds to double stranded DNA by intercalating between base pairs. Compared to the untreated control, the percentage of apoptotic cells, as indicated by annexin V-positive and PI-negative and both positive, increased

approximately 30% upon incubation of MV4-11 cells with MNKI-7 and approximately 50% with SL4-26 (**Figure 3.11A** and **B**). To confirm these results, similar experiments were performed using trypan blue stain, which is also a cell membrane impermeable dye excluded by the intact cells. The percentages of live/dead cells were analysed with an automatic cell counter and the obtained results (**Figure 3.11C**) were similar to those from annexin V/PI staining. Results from both Annexin V and trypan blue exclusion assay were consistent with the anti-proliferative effect of these compounds; SL4-26 exhibiting stronger anti-apoptotic effects compared to MNKI-7, suggesting that anti-proliferative activity is the consequence of apoptosis.

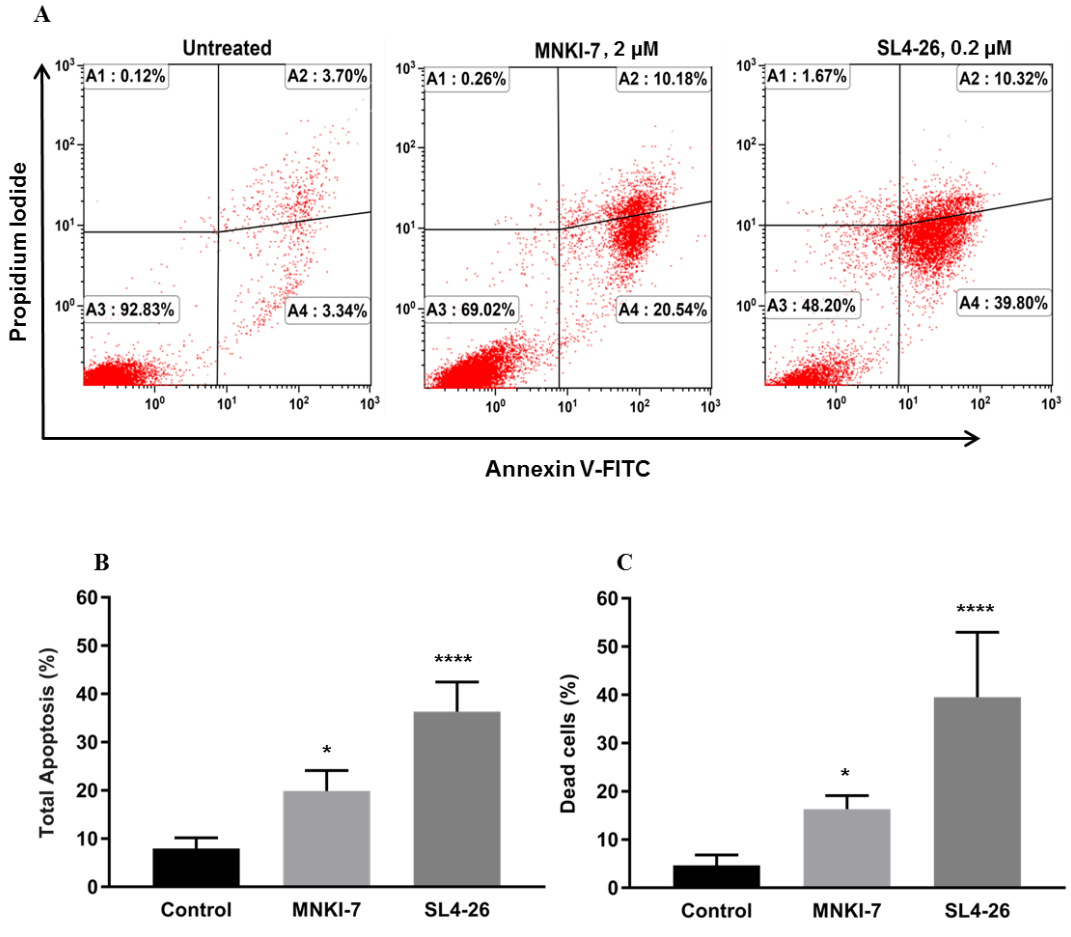



**Figure 3.11: Study of apoptosis and cell death.** (A, B) Cells were treated with MNKI-7 and SL4-26 for 48 hours and stained with annexin V-FITC and PI to be detected by flow cytometry. (C) The trypan blue exclusion method was used to determine the numbers of dead cells (%) after incubation with each compound for 48 hours. Vertical bars represent the mean ± SD of three independent experiments, *P < 0.05 and ****P < 0.0001.

### 3.3.3 Caspase dependent cytotoxicity of Mnk and/or FLT3 inhibition

A group of intracellular proteases called caspases are responsible for the deliberate disassembly of the cell into apoptotic bodies during apoptosis and are implicated in physiological and pathological processes. Caspase 3 and 7 are crucial effectors of apoptotic cell death process [264]. Cell death induced by the kinase inhibitors can be caspase-dependent or caspase-independent apoptotic pathways. The involvement of the caspase activation in apoptosis mediated by MNKI-7 and SL4-26 were studied. MV4-11 cells were treated with 2.0 μM MNKI-7 or 0.2 μM SL4-26 for 24 hours, and the activity of caspases 3 and 7 was measured (**Figure 3.12**). Carbobenzoxy-valyl-alanyl-aspartyl-[*O*-methyl]- fluoromethylketone (Z-VAD-FMK), which is a cell-permeable pan-caspase inhibitor that irreversibly binds to the catalytic site of caspase proteases [265, 266], was used as a negative control to investigate the apoptotic mechanisms.

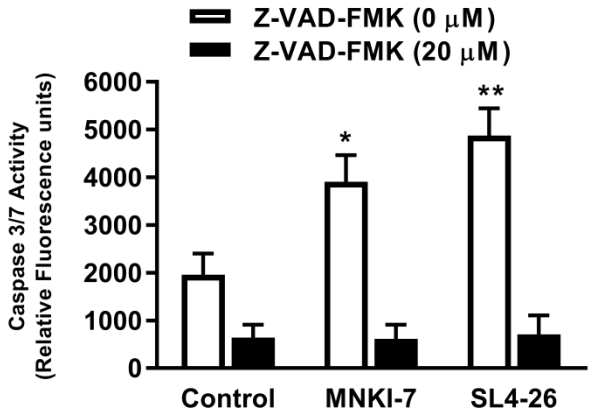



**Figure 3.12: Caspase-3/7 activity in MV4-11 cells after 24-hours incubation with MNKI-7 and SL4-26.** MV4-11 cells were treated with 2 μM MNKI-7 or 0.2 μM SL4-26 for 24 hours, and the activity of caspases 3 and 7 was measured. Z-VAD-FMK was used as a pan-caspase inhibitor. Vertical bars represent the mean ± SD of three independent experiments, * $P < 0.05$, ** $P < 0.01$.

The compounds induced activation of caspase 3/7 and as expected, Z-VAD-FMK inhibited caspase 3/7 activity in non-drug-treated MV4-11 cells along with drug-treated

ones. These results indicate that both compounds induced caspase-dependent apoptosis. The activation of caspase 3/7 induced by SL4-26 was higher than induced by MNKI-7, consistent with previous results from anti-proliferative, Annexin V and trypan blue assays.

## 3.4 Discussion

In this chapter, the anti-proliferative effects of Mnk inhibitors on various PCa and leukaemia cells were studied. Five PCa cell lines with various genetic traits were used to test twenty-seven Mnk inhibitors with $K_i$ values less than 0.5 μM. Results revealed that 22RV1 and DU-145 cells are the most sensitive whereas LNCaP, PC-3 and C4-2B are resistant to Mnk inhibitors tested. A frequent feature in PCa is characterised by inactivating mutations in *PTEN*. This gene supresses the proliferative signal exerted by the PI3K in response to growth factors [202, 267]. Therefore, inactivating mutation of *PTEN* leads to increased activation of the PI3K /AKT pathway [204]. 22RV1 and DU-245 have low basal levels of AKT/mTOR activity due to the expression of the *PTEN* gene. In contrast, LNCaP, PC3 and C4-2B cells have constitutively active PI3K/AKT/mTOR pathway with mutated *PTEN*. The activity of the mTOR and Mnk pathways are under a controlled balance in PCa cells and downregulation of the former is correlated with activation of the latter [137].The Mnk inhibitors were found more efficient in preventing proliferation of *PTEN*-expressing cells (22RV1 and DU-145). In these cells, AKT/mTOR activity is low and it is not adequate for full activation of mTOR, such that the pathway is unable to phosphorylate 4E-BP1 (**Figure 3.1**). In an attempt to compensate for the lower levels of activity of the AKT/mTOR pathway, Mnk/eIF4E pathway is activated which are demonstrated by the high levels of phosphorylated eIF4E in these cells (**Figure 3.1**). 22RV1 expressed both wild type *PTEN* alleles while DU-145

express one wild type and one mutated (+/-) (+/+) [268, 269] (**Table 3.1**), which is reflected by the lower expression of phosphorylated eIF4E in DU-145 cells compared to 22RV1 cells (**Figure 3.1**). Therefore, the Mnk inhibitors had a potent effect on proliferation of 22RV1 and DU145 cells. The results suggested that the Mnk/eIF4E pathway is specifically relevant in PCa cells expressing wild-type *PTEN*, such as 22RV1 and DU145. Inhibition of Mnk is an important tool to regulate cell proliferation in PCa and its efficacy might depend on the PI3K/AKT/mTOR activity in the cell.

In addition to Mnks, androgen signalling has a major role in PCa development and progression [270]. LNCaP cells being androgen dependent for their proliferation, sole inhibition of Mnks may not be sufficient for inducing anti-proliferative effects. Ramamurthy *et. al*., have highlighted the significance of simultaneous targeting of androgen and Mnk signalling in androgen-dependent and castration-resistant PCa [135].

The anti-proliferative activity of Mnk inhibitors against 22RV1 cells correlated well with their inhibitory effects on cellular eIF4E which strongly supports the significant role of elevated eIF4E activation [198] which promotes tumourigenesis [32]. However, enzymatic kinase inhibitory potencies showed low correlation with the anti-proliferative activities. The variations of $GI_{50}$ values are most likely due to synergistic off-target effects of the compounds such as CDK inhibition. Identification of the responsible off-target effects could be promising avenue for the development of potential drug combinations for future PCa treatment.

Earlier reports have substantiated that phosphorylated eIF4E plays a role in stimulating prostate cell metastasis [261, 262]. EMT is a critical process in developing metastasis [271] which is modulated, in part, by the cap-dependent Mnk–eIF4E translational complex [93, 100]. Phosphorylation of eIF4E is implicated in EMT and translation of

biomarkers of metastasis (MMP-3, MMP-9, Cox-2, Cyclin D1, Snail and Slug) [134, 272]. The two Mnk inhibitors (MNKI-7 and MNKI-67) used in this study reduced migration of C4-2B PCa cells induced by elevated eIF4E phosphorylation. Beggs *et. al.,* reported the Mnk1/2 knocked-down MEFs significantly decreased motility in scratch wound-healing assays indicating an important role for Mnk1/2 in cell migration. In addition to these genetic data, the same study showed that pharmacological inhibitors of the Mnks prevented the migration of breast (MDA-MB-231) and tongue squamous cell carcinoma (SCC25) cells [100]. Other study using the eIF4E (S209A) knock-in mouse model revealed that lack of eIF4E phosphorylation impedes EMT and thus inhibits metastasis [93]. Therefore, Mnks are potentially valuable targets for managing tumour metastasis, a major determinant to cancer-associated patient mortality.

The effects of Mnk inhibitors on the proliferation of various leukaemia cell lines were subsequently investigated. The compounds showed anti-proliferative effects most consistently in AML cells, particularly those with FLT3-ITD mutations. This leukaemia cell-type specificity of Mnk inhibitors can be attributed to the disparity in cellular expression of certain proteins, genetic traits and deregulation of multiple signalling pathways in AML. Four Mnk inhibitors from compound series 1 (MNKI-4, MNKI-19, MNKI-57 and MNKI-85) has been studied in detail against leukaemia cells [97, 136]. These compounds were selective for Mnks over CDK2A, CDK4D1 and CDK9T1 ($K_i$ > 10 µM) and among them two (MNKI-4 and MNKI-85) are Mnk2 subtype selective ($K_i$ > 10 µM against Mnk1) **(Table 2.3).** Screening of MNKI-19 and MNKI-85 against six AML cell lines and MNKI-4 and MNKI-57 against twenty-eight cell lines from various cancer types revealed cell type specific anti-proliferative effect with higher inhibitory potencies against FLT3-expressing cells like MV4-11 and MOLM-13. Mnk inhibitors induced cell cycle arrest in the $G_1$ phase of the cell cycle *via* downregulation of cyclin D3

induced and apoptosis *via* downregulation of anti-apoptotic protein (Mcl-1) and/or increase in poly (ADP-ribose) polymerase cleavage. While MNKI-19 induced cell cycle accumulation, MNKI-85 failed to do so, suggesting a combined role of both Mnk subtypes in cell cycle progression [136].

MV4-11 cells harbour the FLT3-ITD mutation; therefore, study of the effect of inhibiting Mnks alone or in combination with FLT3 was pursued. SL4-26, a selective FLT3 inhibitor, is approximately thirty-fold more potent for FLT3 as measured by *in vitro* enzymatic activity assay (**Table 3.5**) and 10-fold more potent in reducing p-STAT-5 compared to MNKI-7 (**Figure 3.10**). Thus, SL4-26 was found to be more effective in inducing apoptosis compared to Mnk inhibitor, MNKI-7. In addition, MNKI-7 also inhibits CDK4D1 and CDK6D1 at concentrations that might drive cell cycle arrest and consequently to senescence which may be reason for MNKI-7 to induce less cell apoptosis compared to SL4-26. Overall, the results suggest a more critical role of FLT3 than that of Mnks in driving cell proliferation in MV4-11 cells.

Collectively, plenty of biological evidence supports Mnks as anti-cancer targets; however their pharmacological validation needs further investigation. Given cancer being a multi-factor-network disease, a combination of Mnk inhibitor with other agent(s) aiming at crucial signalling pathways might be considered as an additional therapeutic intervention. However, an impetuous multi-target activity might present considerable risks due to unpredictable adverse effects. A rationally designed combination strategy based on the selective inhibition on a specific set of kinase targets would potentially reduce these risks.

# 4. Isolation and purification of Mnk proteins

## 4.1 Introduction

The development of specific Mnk inhibitors has been hampered by the lack of structural information of Mnks despite advances in understanding their biological roles in association to cancer development. Mnk subtype selective inhibitors will be invaluable to investigate the precise biological roles of individual Mnks. Jauch *et al*. provided Mnk1/ 2 structures using truncated proteins without activation loop phosphorylation (*i.e.* inactive (DFD-out) conformation). Among three characteristic insertions of Mnk (I1, I2 and I3), I1 is a vital part of activation loop, but to date the crystal structure has not been identified [273, 274]. In addition, our recent study using computational dynamic simulations suggested that the interaction between the DFD motif and the insertion I1 plays a crucial role in instigating and stabilising the DFD-out conformation [24, 25]. However, the binding of small molecule kinase inhibitors can be activation state specific with allosteric inhibitors favouring inactive DFD-out conformation while type I inhibitors generally favour active DFD-in conformation [275]. The information about DFD-in conformation which is gained by phosphorylation of Mnks is also unknown hindering the structure-

guided Mnk inhibitor design, which may lead to effective anti-cancer therapy and has led to the studies undertaken in this chapter

In Chapter 2, we successfully identified a class of allosteric Mnk inhibitors and their binding modes (1-4) have been proposed. To further substantiate our proposed binding mechanisms, understanding protein structure and its interactions with ligands would prove inhibitor-kinase binding modality. Therefore, this chapter attempted to: (1) produce protein for crystallography studies; and (2) perform site directed mutagenesis to identify Mnk binding sites.

## 4.2 Results

### 4.2.1 Expression systems

*Escherichia coli* (*E. coli)* BL-21 and human embryonic kidney 293T (HEK293T) cells were chosen as recombinant expression systems for Mnk1 protein (**Table 4.1** and **Figure 4.1)**. Each system has its own advantages and disadvantages. Firstly, the *E. coli*-based system requires simple experimental operation, is time-and cost-efficient, and the purification procedure can easily be paused by freezing bacterial pellets at -80°C. A disadvantage of this system is the need of the *in vitro* activation of *E. coli*-derived proteins (*i.e.* Mnk1 activated by ERK1 in this study). By comparison, Mnk1 protein isolated from HEK293T cells is of much greater biological relevance since the cell line is of human origin, and the kinase activation is readily achieved by treating cells with phorbol 12-myristate 13-acetate (PMA) prior to harvesting. PMA is an activator of the signal transduction enzyme protein kinase C (PKC) which is routinely used in biomedical research to induce cellular proteins [121, 276, 277]. However, this system is more expensive and time-consuming and interrupting the process was not feasible for our study.

**Table 4.1: Expression vectors and expression systems for the production of GST, GST-Mnk1a and GST-Mnk1b proteins.**

| Plasmids | Expression system |
|---|---|
| pGEX-6P1<br>pGEX-6P1-hMnk1a<br>pGEX-6P1-hMnk1b | *E. coli* BL-21 |
| pEBG-6P<br>pEBG-6P-hMnk1a<br>pEBG-6P-hMnk1b | HEK293T |

In our studies Mnk1a and Mnk1b were expressed in HEK293T cells with a pEBG-6P expression vector, while the pGEX-6P1 expression vector was used for the *E. coli*-based expression system. All Mnk proteins were expressed with an N-terminal glutathione-S-transferase (GST) fusion (*e.g.*, GST-Mnk1a and GST-Mnk1b, protein (**Table 4.1** and **Figure 4.1**).

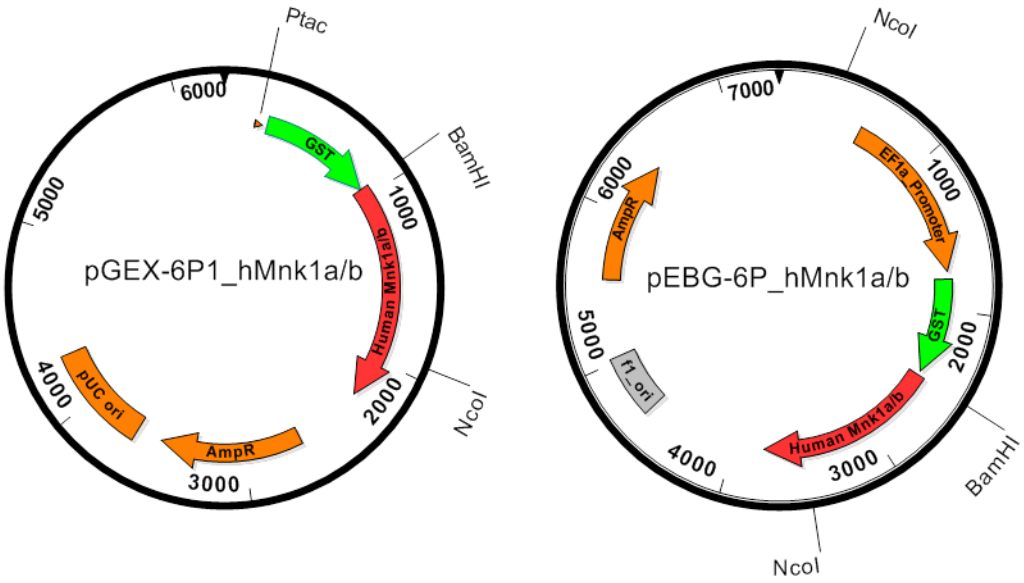



**Figure 4.1: GST-Mnk1a and GST-Mnk1b expression vectors, pGEX-6P1 (*E. coli*, left) and pEBG-6P (HEK293T, right).** Resistance-genes (AmpR), promoters (Ptac in *E. coli* and EF1a in HEK293T), and BamHI and NcoI restriction sites are shown.

The plasmid vectors were obtained from the Proud laboratory (University of Southampton, United Kingdom) and a heat shock transformation method [278-280] was

used for amplification of plasmids. This method allows the incorporation of the target plasmid DNA into the rapidly dividing, competent bacterial cell by a sudden increase in temperature which propels a plasmid into a bacterial cell where it gets replicated. The plasmid DNA was purified using a maxiprep method [281, 282]. The purified plasmids were cut with the restriction enzymes BamHI (GGATCC) and NcoI (CCATGG) for verification of expected DNA fragments. The correct insert sizes of the Mnk1a and Mnk1b DNA-fragments were confirmed by agarose-gel electrophoresis (**Figure 4.2**). pGEX-6P1 vector for expressing GST was linearised which was about 4.9 kilobase pairs (kb) whereas pGEX-6P1-hMnk1a and pGEX-6P1-hMnk1b expressing GST-Mnk1a and GST-Mnk1b were cut into fragments of 1.0 kb and 4.9 kb (**Figure 4.2A**). pEBG-6P expressing GST was cut into fragments of 2.1 kb and 4.0 kb. These two fragments along with a third fragment of 1.0 kb were also observed for GST-Mnk1a and GST-Mnk1b expressed from the corresponding pEBG-6P vectors (**Figure 4.2B**).

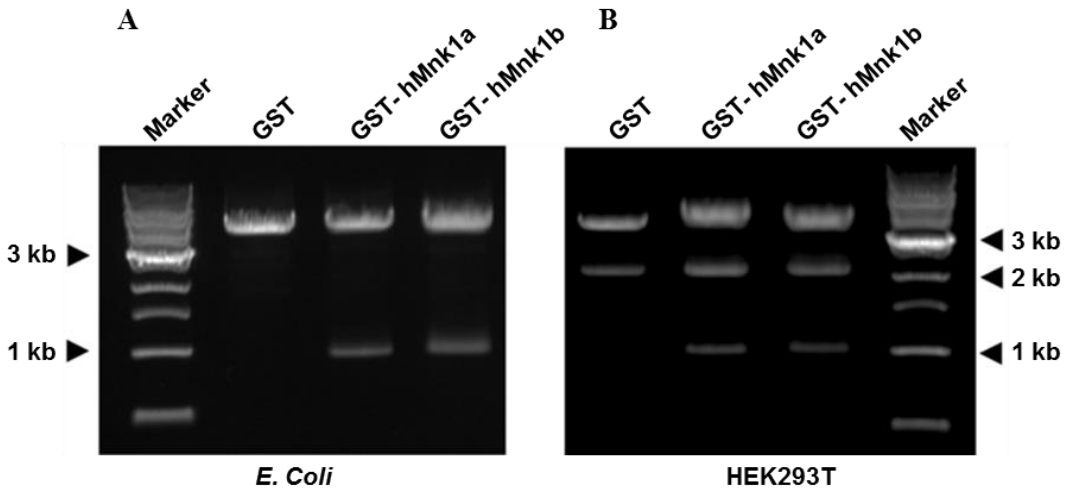



**Figure 4.2: Plasmid verification with agarose gel-electrophoresis.** pGEX-6P1 (*E. coli*) and pEBG-6P (HEK293T) were cut with BamHI and NcoI. (A) pGEX-6P1 vector for expressing GST was linearised (4.9 kb) whereas pGEX-6P1-hMnk1a and pGEX-6P1-hMnk1b expressing GST-Mnk1a and GST-Mnk1b were cut into fragments of 1.0 kb and 4.9 kb. (B) pEBG-6P expressing GST was cut into two fragments of 2.1 kb and 4.0 kb. GST-Mnk1a and GST-Mnk1b expressed from pEBG-6P-hMnk1a and pEBG-6P-hMnk1b were cut into three fragments of 1.0 kb, 2.1 kb and 4.0 kb.

To further confirm the correctness of the amplified plasmids, the restriction digest was followed by full-length sequencing of the insert. Sequencing was performed by the Australian Genome Research Facility Ltd (AGRF) in Adelaide.

Transient transfection of HEK293T cells was achieved with polyethylenimine (PEI). The pEBG-6P plasmid vector, driving the expression of green fluorescent protein (GFP), was used as transfection control (**Figure 4.3A**). Protein induction was carried out 48 hours after transfection and 16 hours post serum starvation with 0.5 µM PMA for 30 minutes. In parallel, *E. coli* BL-21 cells were transformed with a heat shock method [283]. Isopropyl-*β*-D-thiogalactopyranoside (IPTG) was used for protein induction, which was added at log phase when the optical density at 600 nm ($OD_{600}$) had reached about 1.0 and incubated at 30°C for 4 hours (**Figure 4.3B**).

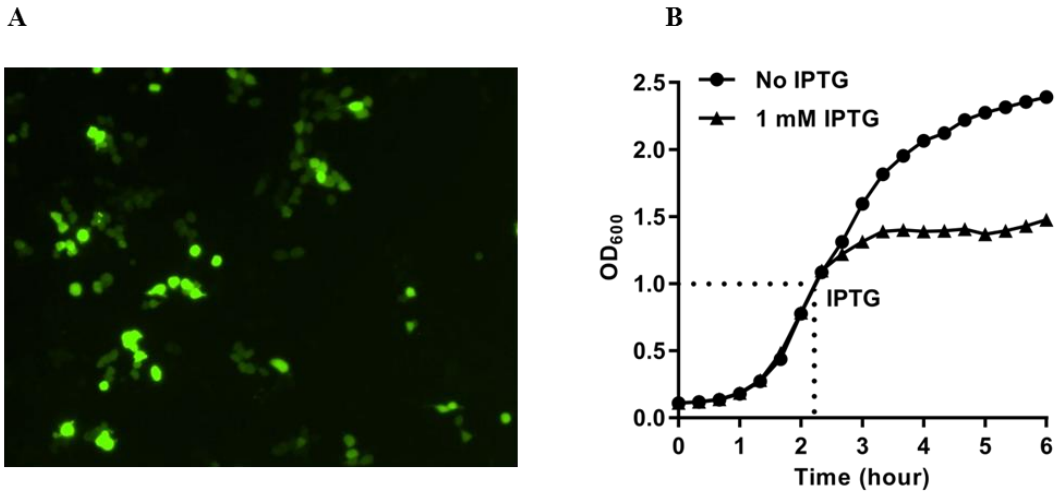



**Figure 4.3: Determination of optimal conditions for HEK293T cell transfection and IPTG induction with *E. coli* Bl-21 bacteria.** (A) Expression of GFP after 48 hours transfection of HEK293T cells under optimised transfection conditions. (B) *E. coli* was cultured at 37°C and the optical density at 600 nm was measured every 20 minutes. Dotted lines show an $OD_{600}$ value and a time at which IPTG was added.

### 4.2.2 Protein purification and activation

Affinity chromatography was used to purify the Mnk proteins [281]. The glutathione tri-peptide (Glu-Cys-Gly) covalently immobilised on Glutathione HiCap Matrix support

beads was used. The interaction of GST with its ligand glutathione retains proteins with a GST-tag on the matrix. Once bound, the proteins can be purified with a large amount of wash buffer prior to elution with an elution buffer containing an excess of reduced L-glutathione which has stronger affinity with GST compared to GST and Glutathione HiCap Matrix support beads. The purified Mnks from *E. coli* were activated by ERK1 as the bacterial cellular machinery is unable to effect post-translational modifications such as phosphorylation. Samples from *E. coli* and HEK293T cells were collected at each stage and analysed by the sodium dodecyl sulphate (SDS) polyacrylamide gel electrophoresis (PAGE) (**Figure 4.4**).

After collecting the purified proteins, total protein concentrations were assessed by using a detergent compatible (DC) protein assay (Bio-Rad) according to the manufacturer's protocol, and the results are presented in **Table 4.2**. The concentrations of proteins obtained from *E.coli* ranged from 0.32 to 0.54 mg/mL whereas in the case of HEK293T cells they were between 0.24-0.35 mg/mL and no GST protein was detected.

**Table 4.2: Protein concentrations from *E. coli* and HEK293T purified protein assessed with DC protein assay**

| Expression | Protein | Concentration (mg/mL) |
|---|---|---|
| *E.coli* | GST | 0.54 |
| | GST-hMnk1a (activated with ERK1) | 0.32 |
| | GST-hMnk1b | 0.38 |
| HEK293T | GST | ND |
| | GST-hMnk1a | 0.24 |
| | GST-hMnk1b | 0.35 |

In order to optimise the purification steps, samples were run through SDS-PAGE. In addition to the purified protein, samples collected from each step of purification, for

example cleared lysate (CL), column flow- through (FT) and wash fraction (WF) were loaded to track the purification process (**Figure 4.4**). Flow through was the unbound fraction which was collected after the lysate-matrix mix had been loaded onto the column and contained all non-GST-binding proteins. The wash fraction was collected when the column was washed with wash buffer to remove remaining protein impurities.

GST-Mnk1a and GST-Mnk1b proteins were visible on SDS-PAGE after the purification of the lysates from *E. coli* or HEK293T cells. In contrast, non-fused GST was detected only in the case of *E. coli* (**Figure 4.4**).

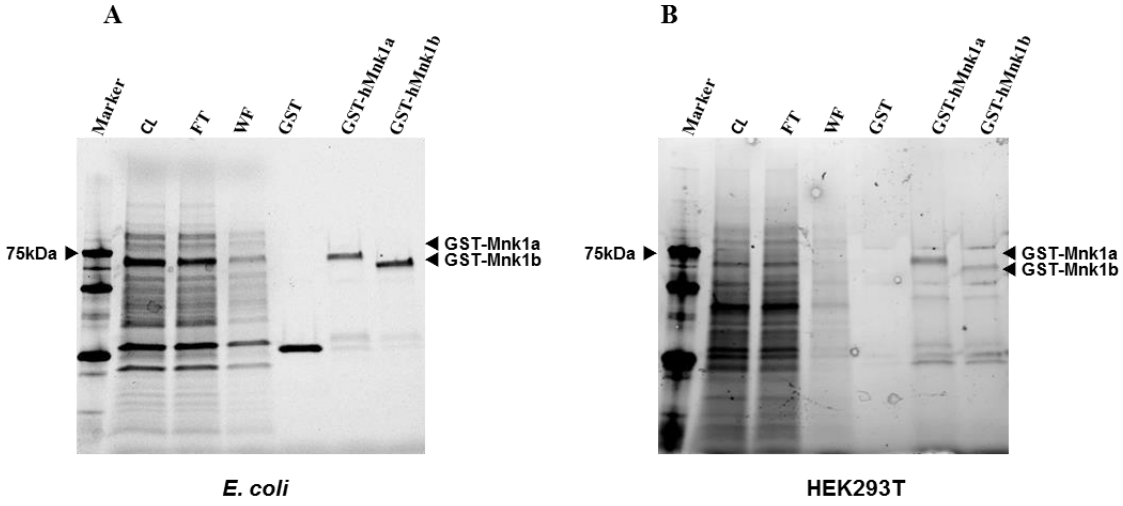



**Figure 4.4: Gel image of samples collected at each stages of purification and assessment of protein purity with SDS-PAGE**. (A) *E.coli* derived proteins and (B) HEK293T derived proteins. Proteins can be distinguished according to their molecular weights. GST: 24 kDa, GST-Mnk1a: 71 kDa and GST-Mnk1b: 61 kDa. Purity was assessed by using the software Image Lab 4.1. CL = cleared lysate, FT= column flow-through, WF = wash fraction. CL, FT, and WF was shown for only GST-hMnk1a protein.

Although SDS-PAGE was repeated more than three times using different batches of purified protein originated from HEK293T cells, GST could never be detected and the underlying reason is not clear. As the non-fused GST protein was used as a negative control, the fraction was still used even though GST was not detected. Importantly for the negative control we used the same purification procedure to the GST-Mnk proteins in order to obtain a similar protein background. GST-Mnk1a and GST-Mnk1b were

distinguished according to their molecular weights: GST-Mnk1a is 71 kDa whereas GST-Mnk1b is a shorter isoform with a size of 61 kDa (GST: 24 kDa).

The purity of the proteins was assessed by SDS-PAGE and stain-free protein detection and calculated as relative quantity using the software Image Lab 4.1. The band of interest was selected as a reference band and the area under the curve (AUC) of the corresponding peak was set to 100%. AUCs of all other peaks (impurities) were calculated relative to the reference peak and expressed as a percentage. Subtraction of the impurities from the reference peak revealed the percentage of purity of the protein of interest. Proteins isolated from *E. coli* seemed to be purer than those from HEK293T cells with a purity of 95.4% for GST, 60.3% for GST-Mnk1a and 67.8% for GST-Mnk1b (**Table 4.3**). This can be explained by the reduced complexity of the *E. coli*-based expression system. Proteins from HEK293T cells showed a purity of 43.2% and 32.6% for GST-Mnk1a and GST, respectively.

**Table 4.3: Purity of proteins assessed with SDS-PAGE.**

| Protein | *E. coli* (%) | HEK293T (%) |
|---|---|---|
| GST | 95.4 | ND |
| GST-Mnk1a | 60.3 | 43.2 |
| GST-Mnk1b | 67.8 | 32.6 |

**ND; not determined.**

GST-Mnk1a expressed in *E. coli* needs to be activated via phosphorylation at Thr209 and Thr214 with upstream kinases like ERK or p38 as *E. coli* lacks machinery for post-translational modifications of eukaryotic proteins [284, 285]. Therefore, GST-Mnk1a protein expressed in *E. coli* was activated before the purification while still bound to the

GST beads. Mnk1b lacks the ERK-binding site on its short C-terminus and is therefore known to be a poor substrate for ERK [286].

Western blot analysis was carried out to prove the existence of the GST-Mnk1a and GST-Mnk1b proteins as well as to confirm their phosphorylation states using antibodies to against both non-phosphorylated (i.e. total) and phosphorylated Mnk1 protein (**Figure 4.5**). Mnk1 antibody readily bound to purified GST-Mnk1a isolated from *E. coli.*, however did not bind to GST-Mnk1b because it is raised against an epitope which is lacking on the C-terminus of GST-Mnk1b. Phospho-Mnk1 antibody bound only to activated GST-Mnk1a from *E. coli.* GST was used as a negative control and no binding was detected to either total Mnk1 and phospho-Mnk1 antibodies. Similar results were obtained for protein expression in HEK293T cells. Total Mnk1 antibody recognised GST-Mnk1a but not GST-Mnk1b. Importantly, a band approximately 24 kDa smaller than GST-Mnk1 was detected. Given that the molecular weight of GST is 24 kDa, this band was considered to be endogenous Mnk1a (**Figure 4.5B**).

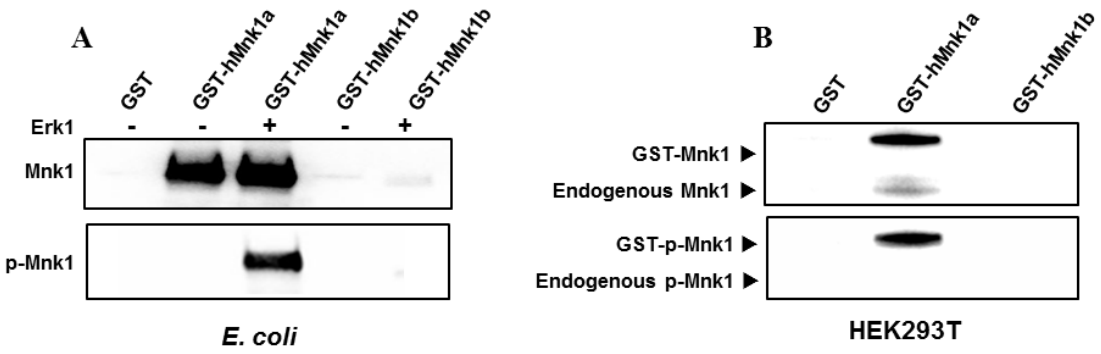



**Figure 4.5: Western blot analysis of *E. coli*- and HEK293T-derived protein using total Mnk1 antibody and phospho-Mnk1 antibody.** (A) Antibody binding to *E. coli*-derived proteins. Mnk1a antibody bound to both ERK1 activated and non-activated GST-Mnk1a but did not recognise GST-Mnk1b. Phospho-Mnk1a antibody bound only to ERK1 activated GST-Mnk1a. (B) Antibody binding to HEK293T–derived protein (cells activated with PMA prior to purification). Mnk1 antibody bound to GST-Mnk1a but not to GST-Mnk1b. Phospho-Mnk1a antibody recognised phosphorylated GST-Mnk1a readily. Non-fused GST was used as a negative control for both experiments.

Western blot analysis confirmed that the activated GST-Mnk1a was obtained, but failed to detect GST-Mnk1b. As a result, the presence of GST-Mnk1b was not further assessed as it has less relevance for the development of Mnk inhibitors. Since Mnk1b is not activated by ERK1 [287], it can be speculated that alternative kinase(s) is (are) involved in the activation under certain circumstances. Currently, the potential roles of Mnk1b and the mechanisms of its activation have not been fully investigated. It has been reported that Mnk1b phosphorylation at the T loop sites is not necessary for its eIF4E kinase activity [66] while the role of Ala344 in the C-terminal region of Mnk1b is reported to be crucial for the kinase activity of the protein [66]. Activating mutations in Ras or loss of function of the Ras GTPase-activator protein NF1 often plays a central role in the over-activation of the Ras/Raf/ERK pathway leading to tumourigenesis [288]. In this context, Mnk1a can be considered a more important anti-cancer target than Mnk1b, since it is strongly affected by ERK-mediated over-stimulation.

### 4.2.3 Kinase activity testing with ADP-Glo™ system

In order to evaluate the enzymatic activity of the purified proteins derived from *E. coli* and HEK293T, GST-hMnk1a was reacted with ATP and $eIF4E_{202-214}$ peptide substrate at concentration of 1 mM as described in Materials and Methods Section 4.2.1.2, and the kinase activity was determined using an ADP-Glo™ assay [23] (**Figure 4.6**). ADP-Glo™ assay is non-radioactive and feasible to run with high ATP concentrations. The S/B ratio was best optimised using 4 µg of protein in 15 µL of assay volume. Therefore, this concentration was used for all other proteins including commercial GST-Mnk1 produced in insect cells for comparison with Mnk1 produced in-house. The result showed approximately 10 times less activity than the commercial one (**Figure 4.6B** and **D**). Mnk1 derived from HEK293T cells gave rise to more background noise compared to the one isolated from *E. coli* (**Figure 4.6A** and **C**), which can at least partially be attributed to the

lower purity of the former and the lower level of phosphorylated Mnk1 protein. One of the possible causes for less activity of the obtained kinase is incomplete phosphorylation. An attempt was made to detect the phosphorylation status of the purified kinase using mass spectrometry, but without success.

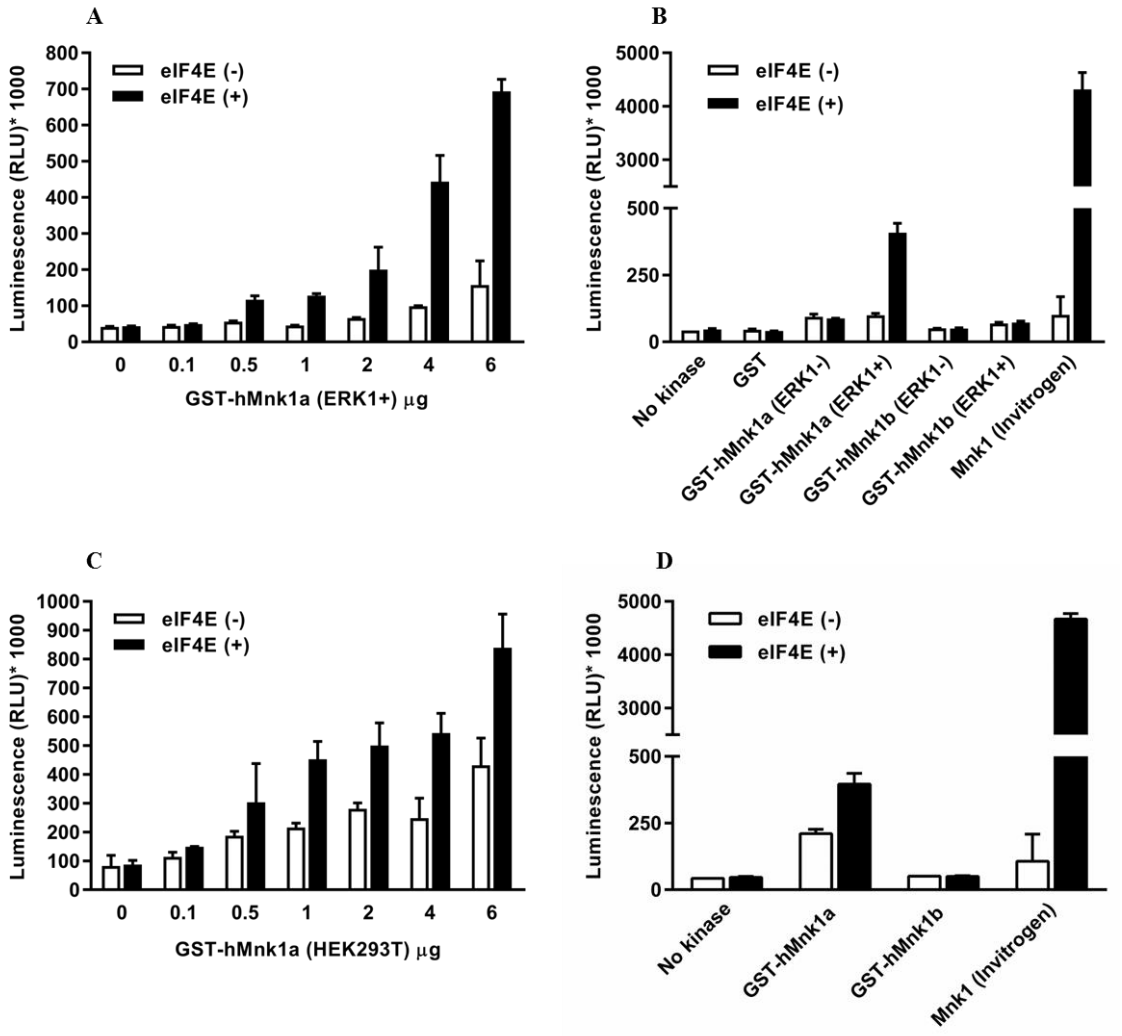



**Figure 4.6: Kinase activity testing with ADP-Glo™ assay.** (A) Various amounts of GST-hMnk1a derived from *E. coli* were used in kinase reaction with ATP and eIF4E$_{202-214}$ peptide substrate at a concentration of 1 mM for each. The luminescence signals thus obtained were compared with control reactions in the absence of the peptide substrate. (B) Similar experiment to (A) was repeated along with other kinases including commercial Mnk1 and non-fused GST as positive and negative controls respectively. (C) Various amounts of GST-hMnk1a purified from HEK293T were used in kinase reaction with fixed substrate concentrations of ATP and eIF4E$_{202-214}$ peptide substrate of 1 mM each. The obtained luminescence signals were compared with control reactions without the peptide substrate. (D) Similar experiment to (C) was repeated along with GST-hMnk1b including commercial Mnk1 and without any kinase as control.

## 4.3 Discussion

In this chapter, we successfully produced phosphorylated recombinant wild type Mnk. However, due to time constraints; the mutagenesis studies could not be performed. Nevertheless, the presented protein expression work has provided an excellent basis to undertake the studies in the future. Specifically, it would be of interest to pursue the binding modalities of allosteric inhibitors, as these are most likely to be specific due to their unique binding site. As such, Mnk inhibitors with high selectivity may be developed.

In-house production of activated protein kinases can be cost effective and facilitate site-directed mutagenesis experiments for detailed investigation on kinase inhibitory mechanisms and help to better understand the structural basis of the enzyme activity. GST-Mnk1a was successfully purified from both bacterial and mammalian expression systems. Protein obtained from *E. coli* was activated using ERK1. GST-Mnk1b was also isolated from both expression systems; however, Western blot analysis failed to verify their presence since the Mnk1 antibody did not bind or bound very weakly to Mnk1b as the antibody was raised against an epitope on C-terminus which is lacking in Mnk1b.

Proteins derived from *E. coli* showed a purity of 60-70% whereas those isolated from HEK293T cells were less pure (*i.e.* 30-45%). Since a high purity is a prerequisite for good quality crystallisation [289-291], this impacted on obtaining the Mnk-crystal structure for the studies undertaken in this chapter. To circumvent this issue for future studies, it is important to re-optimise the expression and purification procedures by additional cleaning which can then be used to confirm inhibitor or proposed hypothetical binding models. Some purification steps such as affinity and ion-exchange chromatography were performed, yet regrettably, no further improvements in the protein purity could be achieved. Due to time constraints, no further investigation of the protein production was

undertaken in this thesis. Nevertheless, the established methods will be of importance for the future work in line with the studies described for the development of more specific Mnk inhibitors for cancer therapy. Comprehensive understanding of Mnk kinase structural elements would rationally lead inhibitor design and selectivity optimisation.

# 5. Discussion, Future work and Conclusion

## 5.1 Discussion

The main findings of this thesis have given insight into: (1) the identification of Mnk subtype specific inhibitors; (2) their binding modes with Mnk protein and; (3) their anti-cancer mechanisms in prostate and leukaemia cancer cell lines.

Firstly in this study, most of the ATP-competitive inhibitors (type I/II) were preferential inhibitors of Mnk2. Secondly, type III inhibitors targeted both Mnk1 and Mnk2, suggesting that both proteins share an identical allosteric binding site. In addition, some type III and many type I inhibitors were also potent inhibitors of FLT3. The combined inhibition of Mnk and FLT3 can present a good opportunity to develop new therapeutics for treating some types of haematological malignancies. Thirdly, the study of correlation between Mnk inhibition and cellular cytotoxicity suggested the potential of Mnk inhibitors to promote the cancer treatment strategies.

This thesis represents the very first line of comprehensive profiling of Mnk inhibitors. Two enzymatic assay formats, IMAP® TR-FRET progressive binding system and ADP-

Glo™ kinase assay, were established, which were capable of delivering robust and reliable results. Importantly, the two systems complement one another as different detection modes are used, and therefore eliminated false positives at the very early stage of testing and profiling. The established screening cascade (**Figure 2.3**) was successfully applied to characterise one-hundred and sixty novel kinase inhibitors developed in our laboratory, and to further identify type I/II and type III inhibitors. Despite limited published protein structural data (only crystal structures of truncated, non-phosphorylated Mnk1/2 are available); the identification of these inhibitors, in particular, allosteric inhibitors, is a significant achievement.

Our results showed that a rational design and advanced medicinal chemistry could generate highly potent Mnk inhibitors, but achieving the appreciable selectivity for Mnks was a challenging task. For example, even the allosteric inhibitors (MNKI-7 and MNKI-19) inhibited other kinases including FLT3 (**Table 2.3 and Table 8.3, Appendix 8.5, Group B**). To elucidate the Mnk targeted mechanism, thus, it is important to develop the appropriate cell-based assays so that the association between the molecular markers for example, phosphorylation of the eIF4E by Mnk, and cellular activity can be assessed.

Moderate correlation between the inhibition of Mnks and anti-proliferation activities were observed in PCa and leukaemia cells. Cell culture approaches cannot mimic the complexity of the reciprocal interaction between the growing tumour and the microenvironment (*i.e.* stromal-epithelial cell interactions). Since Mnks may drive cancer progression through complex mechanisms *in vivo* including cell migration, effects on the immune system and stromal cells, additionally 3-dimensional experimental systems and/or co-culture approaches which allow for the maintenance of stromal-epithelial interactions are likely to more informative [112]. Tumour cells *in vivo* secrete a variety

of cytokines which can lead to a pro-inflammatory and pro-tumorigenic state [95, 100] and Mnks regulate the production of Interleukin-6 (IL-6) which is one of the key regulators of tumour initiation and development [292]. Other cytokines modulated by Mnks such as IL-8, IL1-ß, IL-17, IL-4 and TNFα have also been shown to positively control cancer progression and metastasis [273, 293]. Therefore, inhibiting Mnks can also potentially exert anti-tumour effects by supressing the production of multiple cytokines involved in oncogenesis *in vivo*.

This work has highlighted the potential for agents which modulate dysregulated translation by acting through eIF4E for therapeutic intervention in prostate cancer and leukaemia. Other reports have focussed on the application of Mnk inhibitors on different types of cancer such as breast cancer [95] and lymphoma [87]. The vast majority of Mnk inhibitors are classified as type I, ATP-competitive molecules, and the approaches presented in this thesis are a useful set of tools for identifying allosteric inhibitors; with the advantage of higher selectivity. Altogether, novel strategies may result in discovering compounds with superior efficacy and safety, which in turn could also be applicable for the treatment of other chronic diseases beyond oncology.

## 5.2 Future work

Identification of Mnk inhibitors for pharmacological target validation has so far been hampered by the paucity of structural knowledge of Mnks. Crystal structures of activated Mnks would enable the design of selectivity inhibitors. To achieve this, a huge amount of highly pure and homogenous protein is required. Fundamental steps for purification of recombinant Mnk protein have been accomplished as part of the presented work and will be beneficial for further optimisation procedures. Protein purity can be improved by optimisation of gel filtration and/or ion exchange procedures.

One of the future objectives is to develop type II Mnk inhibitors which target a hydrophobic pocket adjacent to the ATP binding site and increase the selectivity. From the assays established in the current study, the ADP-Glo™ assay could distinguish between ATP-competitive and non-ATP-competitive inhibitors by varying concentrations of ATP in the kinase reaction. However, type II inhibitors are most likely to show behaviour between an ATP-competitive and non-ATP-competitive inhibitor depending on the extent of ATP cleft binding, and in this regard, the ADP-Glo™ assay is not suitable to differentiate type I and II mechanisms. Other techniques need to be established and one of approaches is the use of surface plasmon resonance (SPR).

There are several lines of evidence suggesting that inhibition of Mnks is beneficial to prevent cancer cell migration and invasion [294-297]. Thus, future work can be directed towards studying the role of Mnk inhibition in cancer metastasis. Our preliminary finding on MNKI-mediated inhibition of migration of C4-2B PCa cells was encouraging, but needs to be further confirmed in animal models and other cell types. Given the complex mechanisms involved in anti-cancer effects, study of Mnk inhibition *in vivo* cancer models could provide useful insights on targeting Mnks for cancer management. In addition, fluorescent proteins like green and red fluorescent proteins (GFP and RFP) can be used in animal xenograft models which will allow us to visualise, in real time, important aspects of cancer in living animals, including tumour cell invasion, metastasis and angiogenesis. These multi-coloured proteins facilitate the colour-coding of cancer cells growing *in vivo* and enable the distinction between a specific genotype and phenotype. For instance, the behaviour of highly metastatic cancer cells labelled with RFP and low metastatic cancer cells labelled with GFP can be directly compared.

The investigation of the effects of Mnk inhibitors in leukaemia cells indicates that inhibiting Mnks induces anti-proliferative activity on MV4-11 cells where FLT3-ITD might be a determinant of cell growth and proliferation. Moreover, isolated cell culture may not reflect the effect on the complex mechanisms involved in the organism since the tumour microenvironment may also play crucial role in oncogenesis [93, 95, 100]. Therefore, an animal model with *PTEN* -/- can be used to gain insight into Mnk inhibition in the organism.

Finding a novel molecular target will provide new direction for drug discovery. We found twenty-one compounds (Mnk $K_i$ >10 μM) exhibiting potent anti-proliferative activity with $GI_{50}$ ranging from 0.5 – 9.0 μM (**Table 8.3, Appendix 8.5 Group D**). Further study of these compounds may lead to identification of other targets for cancer. Besides phosphorylating eIF4E, Mnks also have downstream effects *via* other substrates like hnRNPA1, sprouty and PSF. Research in this area has been less pursued, thus it is important to focus not only on eIF4E-mediated mechanisms in cancer but also on other mechanisms and associated therapeutic implications.

## 5.3 Conclusion

After the Bcr-Abl tyrosine kinase inhibitors have revolutionised the treatment of CML patients, a huge amount of research has been directed towards finding new targets for effective cancer therapies. Inhibitors of Mnks offer a potential opportunity for the safe treatment of cancer. Collectively, the studies performed in this thesis have provided a framework for future studies investigating and developing Mnk-inhibitors for cancer therapy. Future studies aimed at effectively targeting Mnk activity for cancer treatment are required since Mnk is a known oncogenic factor in cancer and has significant potential to advance to the current management of cancer therapy.

# 6. Materials and Methods

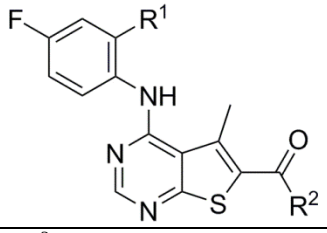
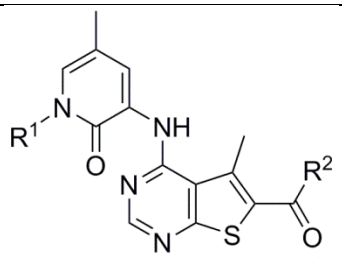
Drug discovery is driven by multi-disciplinary research, which interlinks medicinal chemistry, molecular and cell biology and pharmacology. This chapter summarises the techniques used for the studies described in this thesis.

## 6.1 Materials

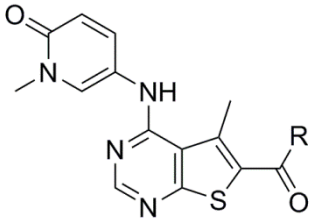
### 6.1.1 Compounds

Cercosporamide and $N^3$-(4-fluorophenyl)-1*H*-pyrazolo-[3,4-*d*]pyrimidine-3,4-diamine (CGP57380) were supplied by BioAustralis (Smithfield, NSW, Australia) and Sigma (Castle Hill, NSW, Australia), respectively. These compounds were used as references for Mnk1/2 inhibition. Compounds of series 1 (*N*-phenylthieno[2,3-*d*]pyrimidin-4-amines), series 2 (3,4-dimethyl-5-(2-(phenylamino)pyrimidin-4-yl)thiazol-2(3*H*)-ones) and series 3 (*N*-phenyl-1*H*-pyrazolo[3,4-*d*]pyrimidin-3-amine) were synthesised in our laboratory as reported previously [298, 299] and were dissolved in dimethylsulfoxide (DMSO) to give stock solutions of 10 mM concentration which were stored at -20°C.

**Table 6.1: List of 134 compounds with their chemical structures used in the study.**

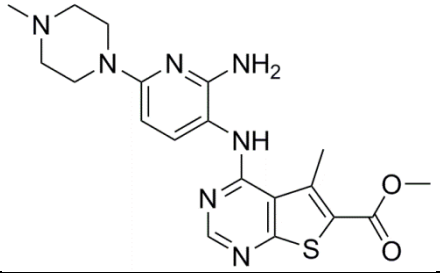
| Code | Chemical structure |
|---|---|
| **Series 1** |  |
| MNKI-4 | $R^1 = OCH(CH_2F)_2$, $R^2 = OCH_3$ |
| MNKI-5 | $R^1 = OCH(CH_2F)_2$, $R^2 = OH$ |
| MNKI-6 | $R^1 = OCH(CH_2F)_2$, $R^2 = NH_2$ |
| MNKI-7 | $R^1 = OCH(CH_2F)_2$, $R^2 = NHCH_3$ |
| MNKI-8 | $R^1 = OCH(CH_2F)_2$, $R^2 = NHCH_2CH_3$ |
| MNKI-11 | $R^1 = CH_3$, $R^2 = OCH_3$ |
| MNKI-12 | $R^1 = CH_3$, $R^2 = OH$ |
| MNKI-14 | $R^1 = H$, $R^2 = OCH_3$ |
| MNKI-15 | $R^1 = H$, $R^2 = OH$ |
| MNKI-9 | $R^1 = OCH(CH_3)_2$, $R^2 = OCH_3$ |
| MNKI-19 | $R^1 = OCH(CH_3)_2$, $R^2 = OH$ |
| MNKI-37 | $R^1 = OCH(CH_3)_2$, $R^2 = NH_2$ |
| MNKI-57 | $R^1 = OCH(CH_3)_2$, $R^2 = NHCH_3$ |
| MNKI-67 | $R^1 = OCH(CH_3)_2$, $R^2 = NHCH_2CH_3$ |
| MNKI-85 | $R^1 = OCH(CH_3)_2$, $R^2 = NHCH_2CH_2OCH_3$ |
| MNKI-83 | $R^1 = OCH(CH_3)_2$, $R^2 = NHCH_2CH_2CH_2OCH_3$ |
| |  |
| MNKI-32 | $R^1 = CH_3$, $R^2 = OCH_3$ |
| MNKI-28 | $R^1 = CH_3$, $R^2 = OH$ |
| MNKI-42 | $R^1 = CH_3$, $R^2 = NH_2$ |
| MNKI-41 | $R^1 = CH_3$, $R^2 = NHCH_3$ |
| MNKI-40 | $R^1 = CH_3$, $R^2 = NHCH_2CH_3$ |
| MNKI-44 | $R^1 = CH_3$, $R^2 = NHCH_2CH_2OCH_3$ |

| | |
|---|---|
| MNKI-45 | $R^1 = CH_3$, $R^2 = NHCH_2CH_2CH_2OCH_3$ |
| MNKI-58 | $R^1 = CH_2CH_2OCH_3$, $R^2 = OCH_3$ |
| MNKI-2-22 | $R^1 = CH_2CH_2OCH_3$, $R^2 = OH$ |
| MNKI-2-25 | $R^1 = CH_2CH_2OCH_3$, $R^2 = NH_2$ |

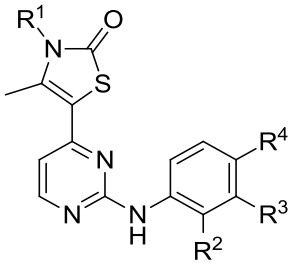


| | |
|---|---|
| MNKI-64 | $R = OCH_3$ |
| MNKI-2-30 | R = OH |
| MNKI-2-32 | $R = NH_2$ |

MNKI-2-11



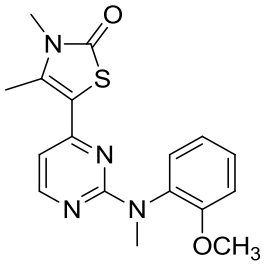
**Series 2**

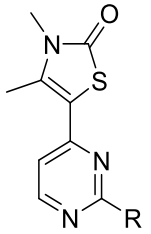


| | |
|---|---|
| MNKI-4-6 | $R^1 = CH_2CH_2N(CH_3)_2$, $R^2 = H$, $R^3 = COCH_3$, $R^4 = H$ |
| MNKI-4-61 | $R^1 = CH_3$, $R^2 = OCH_3$, $R^3 = H$, $R^4 = OCH_3$ |
| MNKI-4-63 | $R^1 = CH_3$, $R^2 = OCH_3$, $R^3 = H$, $R^4 = Cl$ |
| MNKI-4-73 | $R^1 = CH_3$, $R^2 = H$, $R^3 = H$, $R^4 = OCH_3$ |
| MNKI-4-77 | $R^1 = CH_3$, $R^2 = CH_3$, $R^3 = H$, $R^4 = H$ |
| MNKI-4-79 | $R^1 = CH_3$, $R^2 = CH_2CH_3$, $R^3 = H$, $R^4 = H$ |
| MNKI-4-81 | $R^1 = CH_3$, $R^2 = H$, $R^3 = H$, $R^4 = H$ |
| MNKI-4-89 | $R^1 = CH_3$, $R^2 = H$, $R^3 = H$, $R^4 = CH_3$ |
| MNKI-4-91 | $R^1 = CH_3$, $R^2 = H$, $R^3 = H$, $R^4 = CH_2CH_3$ |
| MNKI-5-1 | $R^1 = CH_3$, $R^2 = OCH_2CH_3$, $R^3 = H$, $R^4 = H$ |
| MNKI-5-13 | $R^1 = CH_3$, $R^2 = CH_3$, $R^3 = H$, $R^4 = F$ |

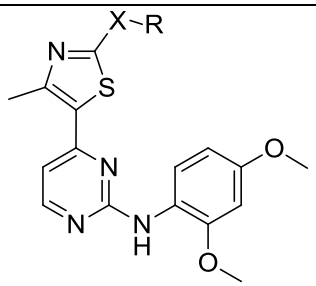
| | |
|---|---|
| MNKI-5-17 | $R^1 = CH_3$, $R^2 = OCHF_2$, $R^3 = H$, $R^4 = H$ |
| MNKI-5-59 | $R^1 = CH_3$, $R^2 = CH_3$, $R^3 = NHSO_2CH_3$, $R^4 = H$ |
| MNKI-5-61 | $R^1 = CH_3$, $R^2 = H$, $R^3 = COCH_3$, $R^4 = H$ |
| MNKI-5-65 | $R^1 = CH_3$, $R^2 = H$, $R^3 = OCH_3$, $R^4 = H$ |
| MNKI-5-71 | $R^1 = CH_3$, $R^2 = H$, $R^3 = NHSO_2CH_3$, $R^4 = H$ |
| MNKI-5-73 | $R^1 = CH_3$, $R^2 = H$, $R^3 = CH_3$, $R^4 = H$ |
| MNKI-6-10 | $R^1 = CH_3$, $R^2 = OCH_3$, $R^3 = H$, $R^4 = H$ |
| MNKI-6-16 | $R^1 = CH_3$, $R^2 = CF_3$, $R^3 = H$, $R^4 = H$ |
| MNKI-7-76 | $R^1 = CH_3$, $R^2 = OCF_3$, $R^3 = H$, $R^4 = H$ |
| MNKI-7-77 | $R^1 = CH_3$, $R^2 = OCF_3$, $R^3 = H$, $R^4 = OCH_3$ |
| MNKI-9-62 | $R^1 = CH_3$, $R^2 = H$, $R^3 = SO_2NH_2$, $R^4 = H$ |
| MNKI-8-81 | $R^1 = H$, $R^2 = OCH_3$, $R^3 = H$, $R^4 = OCH_3$ |
| MNKI-10-9 | $R^1 = H$, $R^2 = OCH_3$, $R^3 = F$, $R^4 = OCH_3$ |

MNKI-7-83



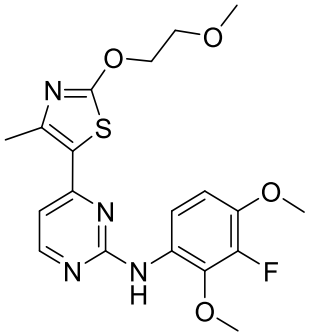


| | |
|---|---|
| MNKI-6-44 | $R = NH_2$ |
| MNKI-6-77 | $R = NHCH_3$ |
| MNKI-6-78 | $R = N(CH_2CH_2OCH_3)_2$ |
| MNKI-6-82 | $R = NHCH_2CH_2SO_2CH_3$ |
| MNKI-6-86 | $R = OCH_3$ |
| MNKI-6-87 | $R = NCH_2CH_2OCH_3$ |

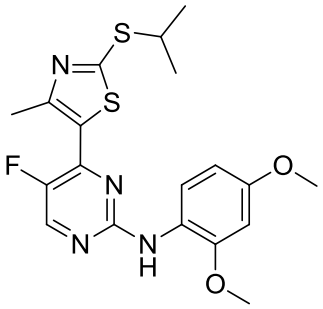


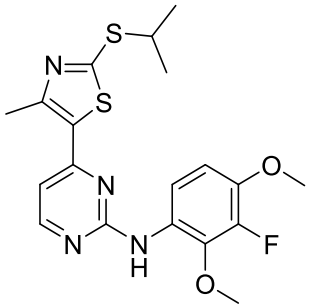
| | |
|---|---|
| MNKI-7-115 | X = S, R = $CH_3$ |
| MNKI-8-17 | X = S, R = $CH_2CH_3$ |
| MNKI-8-18 | X = S, R = $CH_2CH_2OCH_3$ |
| MNKI-8-25 | X = S, R = $CH_2CH_2CH_3$ |
| MNKI-8-35 | X = S, R = $CH(CH_3)_2$ |
| MNKI-8-36 | X = S, R = $CH_2CH_2$morpholine |
| MNKI-8-77 | X = S, R = $CH_2CH_2CH_2N(CH_3)_2$ |
| MNKI-8-88 | X = S, R = $CH_2CH_2N(CH_3)_2$ |
| MNKI-8-91 | X = S, R = $CH_2CH_2$piperazine |
| MNKI-8-115 | X = S, R = 2-$CH_3$-pyridine |
| MNKI-7-7-1 | X = $NCH_3$, R = H |
| MNKI-7-7-2 | X = $NCH_3$, R = $CH_3$ |
| MNKI-11-62 | X = O, R = $CH_3$ |
| MNKI-11-67 | X = O, R = $CH_2CH_3$ |
| MNKI-11-86 | X = O, R = $CH(CH_3)_2$ |
| MNKI-11-90 | X = O, R = $CH_2CH_2OCH_3$ |
| MNKI-11-84 | X = S, R = $CH_2CH_2CH_2CH_3$ |

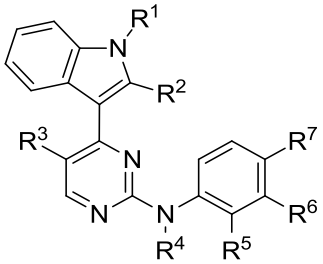
MNKI-9-81



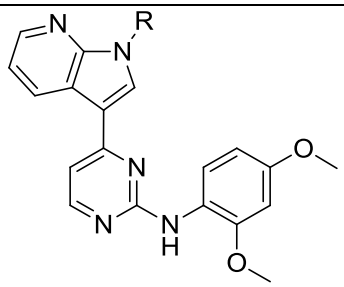
MNKI-9-7



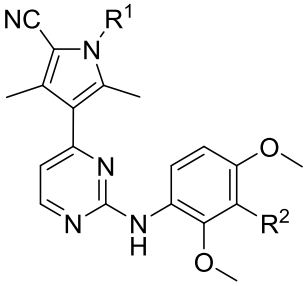
| | |
|---|---|
| MNKI-10-10 |  |



| | |
|---|---|
| MNKI-9-9 | $R^1$ = H, $R^2$ = H, $R^3$ = CN, $R^4$ = H, $R^5$ = $OCH_3$, $R^6$ = H, $R^7$ = $OCH_3$ |
| MNKI-9-10 | $R^1$ = H, $R^2$ = $CH_3$, $R^3$ = CN, $R^4$ = H, $R^5$ = $OCH_3$, $R^6$ = H, $R^7$ = $OCH_3$ |
| MNKI-9-18 | $R^1$ = H, $R^2$ = H, $R^3$ = H, $R^4$ = H, $R^5$ = $OCH_3$, $R^6$ = H, $R^7$ = $OCH_3$ |
| MNKI-9-45 | $R^1$ = $CH_3$, $R^2$ = H, $R^3$ = CN, $R^4$ = H, $R^5$ = $OCH_3$, $R^6$ = H, $R^7$ = $OCH_3$ |
| MNKI-9-59 | $R^1$ = $CH_3$, $R^2$ = H, $R^3$ = H, $R^4$ = H, $R^5$ = $OCH_3$, $R^6$ = H, $R^7$ = $OCH_3$ |
| MNKI-9-60 | $R^1$ = $CH_3$, $R^2$ = $CH_3$, $R^3$ = CN, $R^4$ = H, $R^5$ = $OCH_3$, $R^6$ = H, $R^7$ = $OCH_3$ |
| MNKI-12-94 | $R^1$ = $CH_2CH_3$, $R^2$ = $CH_3$, $R^3$ = CN, $R^4$ = H, $R^5$ = $OCH_3$, $R^6$ = H, $R^7$ = $OCH_3$ |
| MNKI-12-95 | $R^1$ = $CH_2CH_2CH_3$, $R^2$ = $CH_3$, $R^3$ = CN, $R^4$ = H, $R^5$ = $OCH_3$, $R^6$ = H, $R^7$ = $OCH_3$ |
| MNKI-10-1 | $R^1$ = $CH(CH_3)_2$, $R^2$ = H, $R^3$ = CN, $R^4$ = H, $R^5$ = $OCH_3$, $R^6$ = H, $R^7$ = $OCH_3$ |
| MNKI-10-2 | $R^1$ = $CH_2CH_2OCH_3$, $R^2$ = H, $R^3$ = CN, $R^4$ = H, $R^5$ = $OCH_3$, $R^6$ = H, $R^7$ = $OCH_3$ |
| MNKI-10-5 | $R^1$ = $CH_3$, $R^2$ = H, $R^3$ = H, $R^4$ = H, $R^5$ = $OCH_3$, $R^6$ = F, $R^7$ = $OCH_3$ |
| MNKI-10-6 | $R^1$ = $CH_2CH_2$morpholine, $R^2$ = H, $R^3$ = CN, $R^4$ = H, $R^5$ = $OCH_3$, $R^6$ = H, $R^7$ = $OCH_3$ |
| MNKI-10-22 | $R^1$ = cyclopentane, $R^2$ = H, $R^3$ = CN, $R^4$ = H, $R^5$ = $OCH_3$, $R^6$ = H, $R^7$ = $OCH_3$ |
| MNKI-10-26 | $R^1$ = $CH_2CH_2OCH_3$, $R^2$ = H, $R^3$ = CN, $R^4$ = H, $R^5$ = $OCH_3$, $R^6$ = H, $R^7$ = $OCH_2CH_3$ |
| MNKI-10-27 | $R^1$ = $CH_2CH_2OCH_3$, $R^2$ = H, $R^3$ = CN, $R^4$ = H, $R^5$ = $OCH_3$, $R^6$ = F, $R^7$ = $OCH_3$ |
| MNKI-10-30 | $R^1$ = $CH_2CH_2OCH_3$, $R^2$ = H, $R^3$ = CN, $R^4$ = H, $R^5$ = $OCF_3$, $R^6$ = H, $R^7$ = $OCH_3$ |
| MNKI-10-31 | $R^1$ = $CH_2CH_2OCH_3$, $R^2$ = H, $R^3$ = CN, $R^4$ = H, $R^5$ = $OCHF_2$, $R^6$ = H, $R^7$ = H |
| MNKI-10-34 | $R^1$ = $CH_3$, $R^2$ = H, $R^3$ = H, $R^4$ = $CH_3$, $R^5$ = $OCH_3$, $R^6$ = H, $R^7$ = $OCH_3$ |
| MNKI-10-40 | $R^1$ = H, $R^2$ = H, $R^3$ = H, $R^4$ = H, $R^5$ = $OCHF_2$, $R^6$ = H, $R^7$ = H |

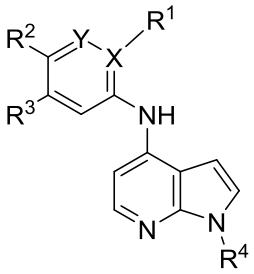


| | |
|---|---|
| MNKI-9-41 | R = $CH_3$ |
| MNKI-9-42 | R = H |



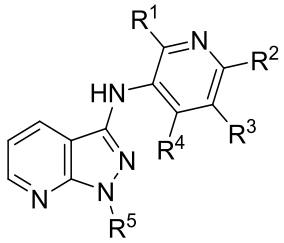
| | |
|---|---|
| MNKI-9-50 | $R^1$ = H, $R^2$ = H |
| MNKI-12-56 | $R^1$ = $CH(CH_3)_2$, $R^2$ = H |
| MNKI-12-62 | $R^1$ = $CH_2CH_2OCH_3$, $R^2$ = H |
| MNKI-12-78 | $R^1$ = $CH_3$, $R^2$ = H |
| MNKI-12-81 | $R^1$ = $CH_2CH_2CH_3$, $R^2$ = H |
| MNKI-12-86 | $R^1$ = $CH_2CH_3$, $R^2$ = H |
| MNKI-12-90 | $R^1$ = cyclopentane, $R^2$ = H |
| MNKI-12-93 | $R^1$ = Cyclopropyl methyl, $R^2$ = H |
| MNKI-12-72 | $R^1$ = $CH_2CH_2OCH_3$, $R^2$ = F |

**Series 3**

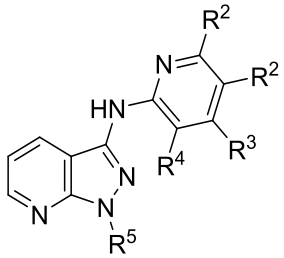


| | |
|---|---|
| MNKI-7-50 | X = N, Y = C, $R^1$ = H, $R^2$ = F, $R^3$ = H, $R^4$ = H |
| MNKI-7-52 | X = N, Y = C, $R^1$ = H, $R^2$ = F, $R^3$ = H, $R^4$ = $CH_3$ |
| MNKI-7-54 | X = C, Y = N, $R^1$ = $OCH_3$, $R^2$ = H, $R^3$ = $CH_3$, $R^4$ = H |
| MNKI-7-56 | X = C, Y = N, $R^1$ = $OCH_3$, $R^2$ = H, $R^3$ = H, $R^4$ = H |

| | |
|---|---|
| MNKI-9-25 | X = C, Y = N, $R^1$ = H, $R^2$ = H, $R^3$ = H, $R^4$ = H |

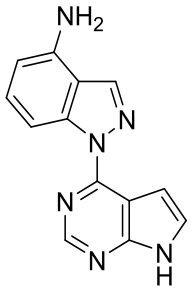



| | |
|---|---|
| MNKI-7-117 | $R^1$ = $OCH_3$, $R^2$ = H, $R^3$ = $CH_3$, $R^4$ = H, $R^5$ = $CH_3$ |
| MNKI-7-118 | $R^1$ = $OCH_3$, $R^2$ = H, $R^3$ = $CH_3$, $R^4$ = H, $R^5$ = H |
| MNKI-8-29 | $R^1$ = H, $R^2$ = H, $R^3$ = H, $R^4$ = $OCH_3$, $R^5$ = H |
| MNKI-8-30 | $R^1$ = H, $R^2$ = H, $R^3$ = H, $R^4$ = $OCH_2CH_3$, $R^5$ = H |
| MNKI-8-55 | $R^1$ = H, $R^2$ = H, $R^3$ = $CH_3$, $R^4$ = H, $R^5$ = H |
| MNKI-8-56 | $R^1$ = H, $R^2$ = H, $R^3$ = H, $R^4$ = $CH_3$, $R^5$ = H |
| MNKI-8-66 | $R^1$ = $CH_3$, $R^2$ = H, $R^3$ = H, $R^4$ = H, $R^5$ = H |
| MNKI-8-67 | $R^1$ = H, $R^2$ = F, $R^3$ = H, $R^4$ = H, $R^5$ = H |
| MNKI-8-78 | $R^1$ = H, $R^2$ = $OCH_3$, $R^3$ = H, $R^4$ = H, $R^5$ = H |
| MNKI-8-79 | $R^1$ = H, $R^2$ = $OCH_2CH_3$, $R^3$ = H, $R^4$ = H, $R^5$ = H |
| MNKI-9-13 | $R^1$ = H, $R^2$ = *N*-$CH_3$piperazine, $R^3$ = H, $R^4$ = H, $R^5$ = H |

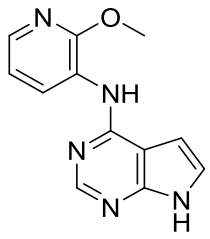



| | |
|---|---|
| MNKI-9-15 | $R^1$ = H, $R^2$ = H, $R^3$ = F, $R^4$ = H, $R^5$ = H |
| MNKI-9-23 | $R^1$ = H, $R^2$ = H, $R^3$ = H, $R^4$ = H, $R^5$ = H |

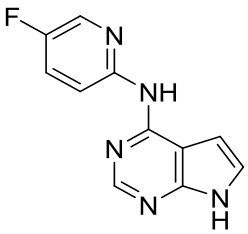
MNKI-9-36



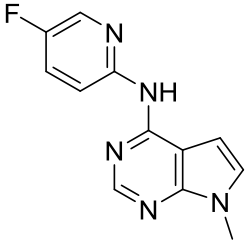
MNKI-9-38



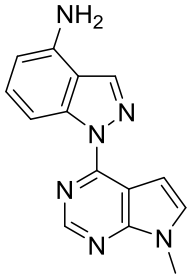
MNKI-9-66



MNKI-9-67



MNKI-9-68



Structures of the remaining 26 compounds cannot be disclosed due to intellectual property infringements.

### 6.1.2 Recombinant protein kinases

**Table 6.2: List of recombinant proteins used in the kinase assay.**

| Protein | Supplier | Catalogue Number |
|---|---|---|
| GST-Mnk1 | Life technologies | PR9138A |
| GST-Mnk2 | Life technologies | PR8046A |
| His-Mnk2 | Merck Millipore | 14-664M |
| GST-CDK4/cyclin D1 | ProQinase | 0142-0143-1 |
| GST-CDK6/cyclin D1 | ProQinase | 0051-0143-1 |
| GST-CDK9/cyclin T1 | ProQinase | 0371-0345-1 |

### 6.1.3 Kinase substrates

**Table 6.3: List of substrates used in the kinase assay.**

| Substrate | Supplier | Catalogue Number |
|---|---|---|
| TAMRA-eIF4E | Mimotopes Pty.Ltd. | 2366001 |
| TAMRA-Phospho eIF4E | Mimotopes Pty.Ltd. | 2366002 |
| $eIF4E_{202-204}$ | Mimotopes Pty.Ltd. | 2366003 |
| RB-CTF | ProQinase | 0040-0000-6 |
| RBER-IRStide | ProQinase | 0863-0000-1 |

### 6.1.4 Assay kits

**Table 6.4: List of assay kits, their suppliers and catalogue numbers.**

| Assay kit | Supplier | Catalogue Number |
|---|---|---|
| ADP-Glo™ kinase assay | Promega Corporation | V9101 |
| ADP-Glo™ - Max kinase assay | Promega Corporation | V7001 |
| Amersham ECL prime Western blotting detecting | GE | RPN2236 |
| Amersham ECL select Western blotting detecting | GE | RPN2235 |
| Annexin V-FITC apoptosis detection kit | BD Pharmingen™ | 556547 |
| Apo-ONE® homogenous caspase-3/7 assay | Promega Corporation | G7791 |
| Bio-Rad detergent-compatible clourimetric (DC) | Bio-Rad Laboratories | 500-0112 |
| Phospho-eIF4E (Ser209) cellular assay kit | Cisbio assays | 64EF4PEG |
| FlowClean cleaning agent | Beckman Coulter Inc. | A70449 |

| | | |
|---|---|---|
| IMAP® TR-FRET evaluation kit | Molecular devices | R8161 |
| IsoFlow™ sheath fluid | Beckman Coulter Inc. | 8546859 |
| Plasmid plus midi kit | Qiagen | 12943 |
| Plasmid maxi kit | Qiagen | 12863 |
| Qiaprep spin miniprep kit | Qiagen | 27106 |
| Trans-Blot® Turbo™ Mini polyvinylidene | Bio-Rad Laboratories. | 170-4156 |

## 6.1.5 Chemicals and Reagents

**Table 6.5: List of chemicals and reagents, their suppliers and catalogue numbers.**

| Chemicals/reagents | Supplier | Catalogue |
|---|---|---|
| Agarose-1000 (UltraPure™) | Life Technologies | 16550-100 |
| Adenosine-triphosphate | Sigma – Aldrich | A2383 |
| Ampicillin sodium salt | Sigma – Aldrich | A9518 |
| Bacto-Agar | BD Biosciences | 214010 |
| Bacto-Tryptone | BD Biosciences | 211705 |
| Bacto-Yeast Extract | BD Biosciences | 212750 |
| β-Glycerophosphate disodium salt hydrate | Sigma – Aldrich | G9422 |
| 2- mercaptoethanol | Sigma – Aldrich | M6250 |
| 3-(4,5-dimethylthiazol-2-yl)-2,5-diphenyl | Life Technologies | M-6494 |
| Bovine serum albumin (BSA) | Sigma – Aldrich | A7030 |
| Brij S20 | Sigma – Aldrich | B7920 |
| Bromophenol Blue | Sigma – Aldrich | B0126 |
| Caspase inhibitor IV | Merck Millipore | 219007 |
| cOmplete™ protease inhibitor cocktail tablets | Roche Diagnostics | 11697498001 |
| CGP57380 | Sapphire Biosciences | AB120365 |
| Dimethyl sulphoxide (DMSO) | Bacto laboratories | AJA2225 |
| Dithiothreitol (DTT) | Sigma – Aldrich Corporation | D9779 |
| DNA ladder 1 kb | NEB | B7021S |
| Ethanol absolute | Bacto laboratories | AJA214 |
| Ethylenediaminetetraacetic acid (EDTA) | Sigma – Aldrich | E6758 |
| Foetal Bovine Serum (FBS) | Sigma – Aldrich | 12003C |
| Gel loading solution | Sigma – Aldrich | G7654 |
| Glutathione HiCap Matrix | Qiagen | 30900 |

| | | |
|---|---|---|
| Glycerol | Sigma – Aldrich | G9012 |
| Glycine | Sigma – Aldrich | G7126 |
| HEPES | Sigma – Aldrich | H3375 |
| Hydrochlororic acid (Hcl) | Sigma – Aldrich | 258148 |
| IPTG | Sigma – Aldrich | I5502 |
| L-glutamine solution | Sigma – Aldrich | G7513 |
| Magnesium chloride | Sigma – Aldrich | M8266 |
| Minimum Essential Medium Eagle | Sigma – Aldrich | M2279 |
| Minimum Essential Medium non-essential | Sigma – Aldrich | M7145 |
| Methanol | Merck-Millipore | 106018 |
| MOPS | Sigma – Aldrich | M1254 |
| Polyethylene amine (PEI) | Sigma – Aldrich | P4417 |
| Penicillin-Streptomycin | Sigma – Aldrich | P0718 |
| Phosphate Buffered Saline (PBS) | Sigma – Aldrich | P4417 |
| Precision plus Protein™ WesternC™ standards | Bio-Rad Laboratories | 161-0376 |
| Propidium Iodide (PI) | Sigma – Aldrich | P4170 |
| Rapamycin | Sigma – Aldrich | 37094 |
| Resazurin sodium salt | Sigma – Aldrich | R7017 |
| Roswell Park Memorial Institute (RPMI)- | Sigma – Aldrich | R8758 |
| Sodium Chloride | Sigma – Aldrich | S5886 |
| Sodium citrate tribasic dehydrate | Sigma – Aldrich | C7254 |
| Sodium deoxycholate | Sigma – Aldrich | D6750 |
| Sodium Dodecyl Sulphate (SDS) | Sigma – Aldrich | L3771 |
| Sodium hydroxide | Sigma – Aldrich | 306576 |
| Sodium orthovanadate | Sigma – Aldrich | S6508 |
| Sucrose | Sigma – Aldrich | T1503 |
| Triton™ X-100 | Sigma – Aldrich | X100 |
| Trizma® base | Sigma – Aldrich | T1503 |
| Trizma® hydrochloride | Sigma – Aldrich | T3253 |
| Trypan blue solution (0.4%) | Bio-Rad Laboratories | T8154 |
| Trypsin-EDTA solution | Sigma – Aldrich | 59430C |
| Tween®20 | Sigma – Aldrich | P7949 |

### 6.1.6 Antibodies

**Table 6.6: List of antibodies used for Western blotting, their suppliers and catalogue numbers**

| Antibody | Mol. WT | Supplier | Catalogue |
|---|---|---|---|
| β-actin (13E5) rabbit monoclonal | 45 | Cell Signalling | 4970L |
| 4E-BP1 (53H11) rabbit monoclonal | 20 | Cell Signalling | 9644S |
| AKT (pan) (C67E7) rabbit monoclonal | 60 | Cell Signalling | 4691S |
| Bcl-2 (Clone 124) mouse monoclonal | 26 | DAKO | M0887 |
| Caspase -3 (8G10) rabbit monoclonal | 17,19,35 | BD Biosciences | 9665S |
| cleaved PARP (Asp214) (D64E10) XP® | 89 | Cell Signalling | 5625S |
| c-Myc (D84C12) XP® rabbit monoclonal | 57-65 | Cell Signalling | 5605P |
| eIF4E (C46H6) rabbit monoclonal | 25 | Cell Signalling | 2067S |
| Mcl-1 (D35A5) rabbit monoclonal | 40 | Cell Signalling | 5453S |
| Mnk1 (C4C1) rabbit monoclonal | 50 | Cell Signalling | 2195S |
| mTOR (7C10) rabbit monoclonal | 289 | Cell Signalling | 2983S |
| Mnk2 rabbit monoclonal | 50 | Sigma-Aldrich | 6889 |
| p38 MAPK (D13E1) XP® rabbit | 38 | Cell Signalling | 8690S |
| p44/42 MAPK (ERK1/2) (137F5) rabbit | 44,42 | Cell Signalling | 4695S |
| P70 S6 kinase (49D7) rabbit monoclonal | 70, 85 | Cell Signalling | 2708S |
| PARP (46D11) rabbit monoclonal | 116, 89 | Cell Signalling | 9532S |
| Phospho-4E-BP1 (Ser65) rabbit | 15-20 | Cell Signalling | 9451S |
| Phospho-4E-BP1 (Thr70) rabbit | 15-20 | Cell Signalling | 9455S |
| Phospho-4E-BP1 (Thr37/46) rabbit | 15-20 | Cell Signalling | 9459S |
| Phospho-AKT (Ser473) (D9E) XP®rabbit | 60 | Cell Signalling | 4060P |
| Phospho-eIF4E (Ser209) rabbit | 25 | Cell Signalling | 9741S |
| Phospho- Mnk1 (Thr197/202) rabbit | 50 | Cell Signalling | 2111S |
| Phospho- mTOR (Ser2448) (D9C2) XP® | 289 | Cell Signalling | 5536P |
| Phosphor-p38 MAPK (Thr180/Tyr182) | 38 | Cell Signalling | 4511S |
| Phospho-p44/42 MAPK (ERK1/2) | 44, 42 | Cell Signalling | CS:4370S |
| Phospho-P70 S6 kinase (Thr389) (49D7) | 70, 85 | Cell Signalling | 9205S |
| Phospho-S6 ribosomal protein | 32 | Cell Signalling | 5364S |
| Polyclonal goat anti-mouse | - | DAKO | P044701 |
| Polyclonal swine anti-rabbit | - | DAKO | P021702 |

| | | | |
|---|---|---|---|
| RNA polymerase II 8WG16, mouse | 220 | BioLegend® | MMS-126R |
| RNA polymerase II H5, mouse | 220-240 | BioLegend® | MMS-129R |
| RNA polymerase II H14, mouse | 220-240 | BioLegend® | MMS-134R |
| S6 ribosomal protein (5G10) rabbit | 32 | Cell Signalling | 2217S |

### 6.1.7 General consumables

**Table 6.7: List of general consumables, their suppliers and catalogue numbers**

| Consumable | Supplier | Catalogue |
|---|---|---|
| Assay plates, 96 well half area, flat bottom, non-binding, white | Sigma – Aldrich | 3992 |
| 1 mL tuberculin syringe | BD Biosciences | 302100 |
| 10 mL syringe | BD Biosciences | 302143 |
| BD Microlance™ 3 needles 21G × 2” | BD Biosciences | 301155 |
| BD PrecisionGlide needles 25G × 1” | BD Biosciences | 301807 |
| BD PrecisionGlide needles 25G × 1.5” | BD Biosciences | 301808 |
| Bijou sample container (Sterlin 129B-7 mL) | Sigma – Aldrich | Z645346 |
| 0.2 µM sterilised filter | John Morris Scientific | F1077526 |
| 0.2 mL thin wall PCR® tube with flat top cap | Thermo Fisher Scientific | 431-Q |
| 0.6 mL graduated microcentrifuge tubes with flat top cap | Thermo Fisher Scientific | 502-GRD-Q |
| 1.5 mL Snapseal microcentrifuge tubes | Scientific Specialties | 126000 |
| 81-well cryogenic racks with lid | Thermo Fisher Scientific | 8800 |
| CELLSTAR® 96 well cell culture plate, sterile, flat bottom with lid | Greiner-Bio-One | 655 180 |
| CELLSTAR® cell culture flask, 50 mL, 25 $cm^2$ polystyrene, filter screw cap red, clear, sterile | Greiner-Bio-One | 690 175 |
| CELLSTAR® cell culture flask, 520 mL, 75 $cm^2$ polystyrene, filter screw cap red, clear, sterile | Greiner-Bio-One | 658 175 |
| Corning® CellBIND surface culture dishes | Sigma – Aldrich | CLS3294 |
| Corning® Cell scrapers | Sigma – Aldrich | CLS3010 |
| Corning® Pasteur pipettes, non-sterile | Sigma – Aldrich | CLS7095B9 |
| Cryo.s™ 1 mL support rim internal thread natural cap vial | Greiner-Bio-One | 123263 |
| D10 Diamond® Eco-Pack™ | John Morris Scientific | F161630 |
| D200 Diamond® Eco-Pack™ | John Morris Scientific | F161930 |

| | | |
|---|---|---|
| D200 Diamond® Tipack™ | John Morris Scientific | F171300 |
| D300 Diamond® Eco-Pack™ | John Morris Scientific | F161730 |
| D1000 Diamond® Eco-Pack™ | John Morris Scientific | F161670 |
| D1000 Diamond® Tipack™ | John Morris Scientific | F171500 |
| D5000 Diamond® Easy-Pack™ | John Morris Scientific | F161571 |
| D5000 Diamond® Tipack™ | John Morris Scientific | F161370 |
| DF10ST Diamond® Tipack™ | John Morris Scientific | F171103 |
| DF100ST Diamond® Tipack™ | John Morris Scientific | F171403 |
| DFL10ST Diamond® Tipack™ | John Morris Scientific | F171203 |
| Dual solution® pipetting reservior | Sigma – Aldrich | Z676012 |
| Enviro-Safe® thermometer | Sigma – Aldrich | Z253006 |
| Falcon® 5 mL round bottom tube, high clarity polypropylene, 12×75 mm, no cap, non-sterile | In Vitro Technologies | FAL352002 |
| Falcon® 6 well clear flat bottom tissue culture-treated multiwall cell culture plate, with lid, sterile | In Vitro Technologies | FAL353046 |
| Falcon® 100 × 20 mm standard tissue culture-treated cell culture dishes, sterile | In Vitro Technologies | FAL353003 |
| Falcon® 15 mL conical polypropylene, centrifuge tube, sterile | In Vitro Technologies | FAL352096 |
| Falcon® 24 well clear flat bottom tissue culture-treated multiwall cell culture plate, with lid, sterile | In Vitro Technologies | FAL353047 |
| Falcon® 50 mL conical polypropylene, centrifuge tube, sterile | In Vitro Technologies | FAL352070 |
| Floating tube rack rectangular | Sigma – Aldrich | R776 |
| Micro spoon and spatula weighing set | Sigma – Aldrich | Z648299 |
| Minisart® high flow syringe | Sartorius | 16532K |
| Nunc™ F96 MicroWell™ black and white plystyrene plates | Thermo Fisher Scientific | NUN137101 |
| Nunc™ Sealing tapes plystyrene | Thermo Fisher Scientific | 250050 |
| PD-10 desalting column | GE Healthcare | 17-0851-01 |
| Polypropylene column | Qiagen | 34924 |
| Promed® nitrile gloves | Thermo Fisher Scientific | JCMPMD17007 |
| Reversible 96 well rack | Sigma – Aldrich | R6276 |
| Sample container with flow seal cap (Sterlin 128C-30 mL) | Sigma – Aldrich | Z645362 |

| | | |
|---|---|---|
| Sciencewarware® heavy-duty test-tube rack | Sigma – Aldrich | Z178128 |
| Serological pipette, 10 mL, sterile | Sarstedt | 86.1254.001 |

### 6.1.8 Instruments

**Table 6.8: List of instruments, their suppliers and catalogue numbers.**

| Instrument | Supplier | Catalogue |
|---|---|---|
| All-purpose tweezer set | Sigma – Aldrich | Z162507 |
| Assistant- hemocytometers and counting chambers | Karl Hecht GmbH & Co KG "Assistant" | 422/12 |
| Cell culture $CO_2$ incubator (SafeCell™ Ultraviolet system) | SANYO Electric | MCO-19AIC(UV) |
| ChemiDoc™ multiplexing imaging system | Bio-Rad Laboratories | 170-8280 |
| Corning® LSE™ digital dry bath heater, dual block | Corning Inc. | 6785-DB |
| Counting chambers, bright lined, Neubauer-improved | Hirschmann® EM Techcolor | 8100204 |
| Eclipse TS100 inverted routine microscope | Nikon Corporation | - |
| Envision® multilabel reader | PerkinElmer | 2104-0010 |
| Excellence analytical balances | Mettler Toledo | XS64 |
| Gallios™ flowcytometer | Beckman Coulter Inc. | B43620 |
| Gilson® Pipetman Classic™ P10, 10 µL | John Morris Scientific | F144802 |
| Gilson® Pipetman Classic™ P100, 100 µL | John Morris Scientific | F123615 |
| Gilson® Pipetman Classic™ P5000, 5 mL | John Morris Scientific | F123603 |
| Gilson® Pipetman Concept® multichannel 8×10 µL | John Morris Scientific | F31032 |
| Gilson® Pipetman Concept® multichannel 12×10 µL | John Morris Scientific | F31042 |
| Gilson® Pipetman L12 ×200, 20-200 µL | John Morris Scientific | FA10012 |
| Gilson® Pipetman Macroman™ | John Morris Scientific | F100755 |
| Gilson® Pipetman Motorised P200M, 200 µL | John Morris Scientific | F81003 |
| Gilson® Pipetman Neo® Multichannel 8×200 µL | John Morris Scientific | F14403 |
| Gilson® Pipetman Neo® P200N | John Morris Scientific | F144565 |
| Gilson® pipetteman starter kit | John Morris Scientific | F167300 |
| Heraeu™ FRESCO™ 21 centrifuge | Thermo Scientific | 75003424 |

| | | |
|---|---|---|
| Heraeu™ MegaFuge™ 40R centrifuge | Thermo Scientific | 75003067 |
| Heraeu™ PICO™ 17 centrifuge | Thermo Scientific | 75003424 |
| Heraeu™ BioFuge™ Primo R centrifuge | Thermo Scientific | 75007591 |
| Infinity® Class II microbiological safety cabinet | Esco Corporation | FC2-4K1 |
| Large 3-D rotator | Thermo Scientific | 4631-1CE |
| Midsize inverter sensor microwave oven in white | Sharp Corporation | R350YW |
| Mini-PROTEAN tetra cell for precast gels | Bio-Rad Laboratories | 1658004EDU |
| Mini Trans-Blot® electrophoretic transfer cell | Bio-Rad Laboratories | 170-3930 |
| MS3 basic vortex mixer | IKA® | 3617000 |
| MTS 2/4 digital microtiter Shaker | IKA® | 3208000 |
| Multi-purpose rotator | Thermo Scientific | 2314-1CE |
| MultiSUB midi 96 STRETCH gel system | Cleaver Scientific | MS110822 491 |
| NanoDrop 2000c Ultraviolet-Visible spectrophotometer | Thermo Scientific | - |
| Ratek digital heated water bath | Adelab Scientific | WB14D |
| SevenMulti™ pH meter | Mettler Toledo | S40K |
| T100™ thermal cycler | Bio-Rad Laboratories | 180-1096 |
| T10™ automatic cell counter | Bio-Rad Laboratories | 145-0001 |
| T10™ counting slides, dual chamber | Bio-Rad Laboratories | 145-0015 |
| Trans-Blot® Turbo™ transfer system | Bio-Rad Laboratories | 170-4155 |
| Tube supporting ring | Bio-Rad Laboratories | 186-2000 |

The buffers and reagents used for IMAP® assay were provided in the assay kit namely IMAP® progressive binding buffer A and B, IMAP® progressive binding reagent and IMAP® TR-FRET donor [Terbium (Tb) based phospho conjugate].

## 6.1.9 Buffers

### 6.1.9.1 Buffers for ADP-Glo™ kinase assays

**Table 6.9: Composition of kinase reaction buffer for Mnk1/2 and CDK4/6 assays**

| Ingredients | Concentration |
|---|---|
| Tris, pH 7.5 | 40 mM |
| $MgCl_2$ | 20 mM |
| DTT | 0.4 mM |

**Table 6.10: Composition of standard-assay-buffer (3.33 × stock) for CDK9 assay**

| Ingredients | Concentration |
|---|---|
| HEPES-NaOH, pH 7.5 | 167 mM |
| $MgCl_2$ | 10 mM |
| $MnCl_2$ | 10 mM |
| DTT | 3.33 mM |

**Table 6.11: Composition of kinase dilution buffer for CDK9 assay**

| Ingredients | Concentration |
|---|---|
| HEPES-NaOH, pH 7.5 | 500 mM |
| $PEG_{20,000}$ | 2.5 mg/mL |
| DTT | 10 mM |

### 6.1.9.2 Buffers for IMAP® TR-FRET assay

The buffers and reagents used for IMAP® assay were provided in the assay kit namely IMAP® progressive binding buffer A and B, IMAP® progressive binding reagent and IMAP® TR-FRET donor [Terbium (Tb) based phospho conjugate].

### 6.1.9.3 Buffers for Western blots

**Table 6.12: Composition of lysis buffer used for Western blots**

| Ingredients | Concentration |
|---|---|
| HEPES-NaOH, pH 7.5 | 25 mM |
| NaCl | 300 mM |
| EDTA pH 7.5 | 0.2 mM |
| DTT | 0.5 mM |

**Table 6.13: Composition of loading buffer (3 ×), 10 mL used for Western blots**

| Ingredients | Amount |
|---|---|
| Tris-Cl pH 6.8 | 2.4 mL |
| Glycerol | 3 mL |
| 20% SDS | 3 mL |
| β-Mercaptoethanol | 1.6 mL |
| Bromophenol blue | 0.006 g |

**Table 6.14: Composition of running buffer (10 ×), 1 L used for Western blots**

| Ingredients | Amount |
|---|---|
| Tris (Trizma Base) | 30.3 g |
| Glycine | 144 g |
| Sodium dodecyl sulphate | 10 g |
| $dH_2O$ | to make 1 L |

**Table 6.15: Composition of Tris buffer saline tween (TBST) 1 ×, 1 L used for Western blots**

| Ingredients | Amount |
|---|---|
| NaCl | 8 g |
| Tris (Trizma Base) | 2.42 g |
| Tween-20 | 500 µL |
| $dH_2O$ | to make 1 L |

#### 6.1.9.4 Buffers for protein purification

**Table 6.16: Composition of lysis buffer used for protein purification**

| Ingredients | Concentration |
|---|---|
| Tris Base, pH 8.0 | 50 mM |
| $MgCl_2$ | 10 mM |
| Triton X-100 | 1% |
| DTT | 5 mM |
| Lysozyme/DNase | 1 × |
| Complete protease inhibitor | 1 × |

Lysozyme 50 mg/mL, DNase 1mg/mL in $dH_2O$ (Lysozyme/DNase stock 200 × stock) stored at -20 °C. One complete protease inhibitor tablet is sufficient for the inhibition of the proteolytic activity in 50 mL extraction solution.

**Table 6.17: Composition of wash buffer used for protein purification**

| Ingredients | Concentration |
|---|---|
| Tris base, pH 8.0 | 50 mM |
| NaCl | 0.5 mM |
| DTT | 5 mM |

**Table 6.18: Composition of elution buffer used for protein purification**

| Ingredients | Concentration |
|---|---|
| Tris base, pH 8.0 | 50 mM |
| NaCl | 0.15 mM |
| DTT | 5 mM |
| Glutathione reduced | 20 mM |

Reduced glutathione should be added freshly.

**Table 6.19: Composition of activation buffer used for protein purification**

| Ingredients | Concentration |
|---|---|
| Tris, pH 8.0 | 40 mM |
| $MgCl_2$ | 20 mM |
| DTT | 5 mM |

**Table 6.20: Composition of storage buffer used for protein purification**

| Ingredients | Concentration |
|---|---|
| Tris, pH 8.0 | 40 mM |
| NaCl | 0.15 mM |
| EDTA | 0.5 mM |
| DTT | 2 mM |

### 6.1.10 Primers used for DNA sequencing and quantitative reverse transcription-polymerase chain reaction (qRT-PCR)

**Table 6.21: List of primers used for DNA-sequencing of insert Mnk1a (HA1 and HA2) and Mnk1b (HA3 and HA4).**

| Name | Sequence | Purpose |
|---|---|---|
| HA1 | 5-TACATGGACCCAATGTGCCTGG-3 | Fwd seq pEBG-6P |
| HA2 | 5-GTTCGGGAGTCAAACCATGTCC-3 | Rev seq pEBG-6P |
| HA3 | 5-GGGCTGGCAAGCCACGTTTGGTG-3 | pGEX 5′ Seq |
| HA4 | 5-CCGGGAGCTGCATGTGTCAGAGG-3 | pGEX 3′ Seq |

## 6.2 Methods

### 6.2.1 IMAP® TR-FRET kinase assay

The kinase reaction was performed in 1 × IMAP® reaction buffer with Tween-20, dithiothreitol (DTT) and distilled $H_2O$ according to manufacturer's protocol using the TAMRA-eIF4E$_{202-214}$ peptide substrate. Each test compound was added to the above kinase reaction mixture at final concentrations of 1 and 10 µM with DMSO content of 0.5%. Mnk kinase stock solution was diluted with 1 × IMAP® reaction buffer containing Tween-20 and added to the reaction mixture. The kinase reaction was started by final addition of ATP and incubated at 30°C for 90 min in a total assay volume of 20 µL. The reaction was stopped by adding 60 µL of progressive binding solution (30% binding buffer A, 70% binding buffer B, progressive binding reagent (1:600) and terbium (Tb)-donor (1:400)) and the plate was then read in an EnVision Multilabel plate reader (PerkinElmer, Buckinghamshire, UK) following 5 hours of incubation in the dark. The excitation wavelength for the Tb-donor was set at 330 nm and the emissions of the Tb-donor and the TAMRA-eIF4E$_{202-214}$ substrate (TR-FRET signal) were recorded at 545 and 572 nm, respectively. The emission was measured in a time resolved mode with a

delay of 200 µsec. Positive and negative controls were carried out in 0.5% DMSO in the presence and absence of each Mnk kinase, respectively. For dose response experiments with control Mnk inhibitors (CGP57380 and cercosporamide), the kinase reaction was run in a similar way with an inhibitor dilution factor of 1:3 for 8 concentrations ranging from 10 µM to 4.5 nM with 0.5% DMSO.

### 6.2.2 ADP-Glo™ kinase assay

Assay kits were used according to instructions and adapted as outlined in the results and discussion section. Test compounds were generally prepared with 1:3 serial dilutions for 8 concentrations (from 10 µM to 4.5 nM); 10 concentrations were used (15 µM to 0.7 nM) for competition experiments. The kinase reaction was performed with 1 × kinase reaction buffer (40 nM Tris base pH 7.5, 20 mM $MgCl_2$, 0.4 mM DTT), 0.1 mg/mL BSA, distilled $H_2O$, $eIF4E_{202-214}$ substrate and each Mnk kinase in a total assay volume of 15 µL following the manufacturer's protocol, Briefly, the kinase reactions were started by addition of ATP, incubated for 45 min at 30°C and then stopped by adding 15 µL of ADP Glo reagent. After incubation at room temperature in the dark for 40 min, 30 µL of kinase detection reagent was added to each well and incubated for 30-60 min depending on the ATP concentration used in the kinase reaction (10-100 µM: 30 min, 100-500 µM: 40 min, 500-1000 µM: 60 min). For higher concentrations of ATP (up to 6 mM), the ADP-Glo™ max kit was used which is similar to ADP-Glo™ kinase assay but adapted for high ATP concentrations as used in ATP competition experiments. The incubation time after addition of the detection reagent was 60 min for this assay. Luminescence was measured using an EnVision Multilabel plate reader (PerkinElmer, Buckinghamshire, UK) with an integration time of 1 sec per well. Positive and negative controls were performed in 0.5% DMSO in the presence and absence of each Mnk kinase, respectively. Standard curves

with defined ADP/ATP ratios were routinely performed and used to convert relative light units (RLUs) into reaction velocities (*e.g.*, $V_{max}$ calculation).

### 6.2.3 CDK and FLT3 kinase assays

Inhibition of CDK was measured using a radiometric assay by Eurofins Pharma Discovery Services UK Limited using ATP concentration within 15 μM of $K_m$ for each kinase. The half maximal inhibitory concentration ($IC_{50}$) value was determined from a 10 data point dose response experiment, and inhibitory constant ($K_i$) was calculated from the corresponding $IC_{50}$ and $K_m$ (ATP) values of each kinase. The kinase reaction for CDK4/CyclinD1 and CDK6/CyclinD1 was performed with kinase reaction buffer similar to that used in Mnk kinase assay and with RB-CTF substrate. For CDK9/CyclinT1, the kinase reaction was performed with standard assay buffer and kinase dilution buffer from ProQinase (**Table 6.10** and **Table 6.11**). RBER-IRStide substrate was used for the CDK9/CyclinT assay. Inhibition of CDK2/CyclinA1 and FLT3 was measured by radiometric assays using the Reaction Biology KinaseProfiler services, USA.

### 6.2.4 Cell culture

All leukaemia cell lines were kindly provided by Professor Richard D'Andrea (University of South Australia) and maintained in Roswell Park Memorial Institute (RPMI)-1640 medium with 10% foetal bovine serum (FBS) in a 37°C incubator with 5% carbon dioxide.

### 6.2.5 Cell viability assay

In this thesis, resazurin (Sigma Aldrich, Castle Hill, NSW, Australia) and MTT (Life Technologies, Mulgrave, VIC, Australia) assays were performed for suspension cells and adherent cells respectively.

Resazurin reduction is one of the methods for measuring metabolic activity, which serves as a marker of viable cells. Resazurin is a non-fluorescent but cell permeable redox dye that can be easily dissolved in physiological buffers. This can be added directly to wells containing cultured cells in a homogeneous format where resazurin is reduced by viable cells to a pink and highly fluorescent product called resorufin. A linear relationship is quantified between the amounts of resorufin and the viable cells through a fluorometer with excitation and emission wavelengths of 560 and 590 nm, respectively.

MTT is a soluble pale yellow substrate which is converted to an insoluble purple formazan precipitate in the presence of living cells with active metabolism. The formazan can be dissolved by a number of organic solvents, but DMSO is preferred as it provides better solubilisation of formazan and gives more stable output readings [96-98, 171]. The absorbance of the coloured solution that reflects the number of living cells can be measured preferably at 570 nm by a spectrophotometer.

Leukaemia cell lines were seeded in triplicates at a density of $6 \times 10^3$ cells per well into 96 well plates and incubated overnight. To determine $GI_{50}$ (the inhibitor concentration required to reduce cell viability by 50%), five-fold serial dilutions of test compounds were prepared and added to the cells which were then incubated for indicated time points. For resazurin assays, indicated amounts of compounds were added. 20 μL of resazurin (0.1 mg/mL) was added to each well and incubated in dark at 37°C incubator with 5% carbon dioxide. After 4 hours fluorescence was measured with excitation/emission at 570/585 nm using the EnVision Multilabel plate reader (PerkinElmer, Buckinghamshire, UK). For MTT assays, 50 μL of MTT (2 mg/mL) was added, after 4 hours incubation medium was removed and DMSO was added to dissolve formazan crystals and the absorbance was measured at 570 nm. $GI_{50}$ values were calculated using a non-linear 4-parameter logistic analysis using GraphPad Prism software (version 6.0, San Diego USA).

### 6.2.6 HTRF assay

The principle of the HTRF assay is based on Fluorescence Resonance Energy Transfer (FRET); the transfer of energy between two fluorophores, a donor and an acceptor when in close proximity. Molecular interactions between biomolecules can be assessed by coupling each partner with a fluorescent label and by detecting the level of energy transfer. This immunoassay involves two monoclonal antibodies: an anti-eIF4E antibody labelled with d2 and an anti-phospho-eIF4E antibody labelled with $Eu^{3+}$ cryptate.

An optimized number of cells were seeded in a 96 well plate containing 100 µL medium one day prior to adding inhibitors. Serial dilutions of inhibitors with a dilution factor of 1:3 was prepared to give eight concentrations ranging from 20 to 0.0091 µM with 1% DMSO in the medium and 50 µL added to respective wells. After 1 h of incubation at 37°C, cells were lysed with lysis buffer by shaking at room temperature for 30 minutes. Lysate (16 µL) was mixed with 4 µL of premixed antibody (D2 and cryptate antibody 2 µL each) and incubated at room temperature overnight. Then the plate was read at two different wavelengths (665 nm and 620 nm) using the EnVision Multilabel plate reader (PerkinElmer, Buckinghamshire, UK).

### 6.2.7 Caspase 3/7 activation assay

A non-fluorescent caspase substrate, Z-DEVD-R110 (R110: rhodamine 110, bis-(*N*-CBZ-L-aspartyl-L-glutamyl-L-valyl-L-aspartic acid amine) was used in this assay. In the presence of caspase-3/7 activity, the substrate is cleaved by caspase-3/7 protease, and the DEVD peptides are removed from rhodamine 110 to produce a highly fluorescent substrate. The Apo-ONE® homogeneous caspase-3/7 buffer has a dual role in efficiently lysing the cells and supporting optimal caspase-3/7 activity. The Apo-ONE® homogenous caspase-3/7 kit (Promega, Madison, WI, USA) was used to determine caspase-3/7 activity

according to manufacturer's instructions. Briefly, MV4-11 cells were seeded at a density of 1800 cells per well in a 96 well plate. Compounds and pan-Caspase inhibitor (Z-VAD-FMK) were added after 24 hours. Caspase substrate Z-DEVD-R110 was added after indicated time points and incubated for 2 hours at room temperature and then fluorescence was measured with excitation/emission at 499/521 nm using the EnVision Multilabel plate reader (PerkinElmer, Buckinghamshire, UK).

### 6.2.8 Trypan blue exclusion assay

The viable healthy cells possess intact cell membranes that are impermeable to certain dyes, such as trypan blue, eosin, and Propidium, whereas dead cells are permeable for these dyes and can be stained. Cells were seeded at a density of $3 \times 10^4$ cells per well in a 24 well cell culture plate and treated with each kinase inhibitor. At indicated time points, cells were harvested, centrifuged and re-suspended in 100 µL of cell culture medium. Samples were mixed with 0.4% trypan blue (Bio-Rad) at a 1:1 ratio, and cell counting was performed using a TC10 cell counter (Bio-Rad, Gladesville, NSW, Australia).

### 6.2.9 Bio-Rad DC Assay

To determine the protein concentration, Bio-Rad's Detergent Compatible (DC) Assay (Biorad, Gladesville, NSW, Australia) was used according to a micro-plate assay protocol. Protein standard serial dilution of BSA with 8 data point ranging from 0.23 mg/mL up to 1.44 mg/mL was generated. The purified protein samples were 1:2 diluted in storage buffer, which was also used as blank control. Absorbance was read at 750 nm using the PerkinElmer EnVision Multilabel plate reader. Protein concentration was calculated using the standard curve.

### 6.2.10 Western blotting

MV4-11 cells were seeded at $8\times10^5$ cells/10 mL of RPMI-1640 medium and cultured for 24 hours. Subsequently the cells were treated, with kinase inhibitors for 24 hours and further centrifuged and lysed for preparation of protein. Protein concentration was determined by DC assay (Bio-Rad) and a total of 20 µg protein was separated by SDS-PAGE. 20 µg of protein was mixed with 6.6 µL of 3 × gel loading dye, and the final volume was made up to 20 µL. The proteins were denatured at 95°C for 5 minutes, centrifuged and loaded onto the polyacrylamide gel cassette (Bio-Rad Mini PROTEAN Tetra System, Gladesville, NSW, Australia). 5 µL of protein standard (Bio-Rad, Precision Plus Protein WesternC Standards) was loaded to distinguish the separated proteins according to their molecular weights. The gel was run for approximately 80 minutes at 120 V and the purity of the protein was assessed in a Bio-Rad ChemiDoc™ MP System by using an exposure time of 5 sec. The proteins were electro-transferred onto a nitrocellulose membrane (Bio-Rad, Gladesville, NSW, Australia) for 7 minutes using the Bio-Rad Trans-Blot Turbo Transfer Starter. The membrane was washed for 5 minutes with Tris-buffered saline Tween®-20 (TBST), blocked for 1 hour with 1x TBST 10% skim milk powder and incubated with the primary antibody-solution for 15 minutes at room temperature, then overnight at 4°C and followed by 1 hour at room temperature the following day. After incubation the membrane was washed for 4 × 20 minutes in 1x TBST before the secondary antibody-solution was added. After incubation for 1-2 hours at room temperature with secondary-antibody, the blot was again washed for 4 × 20 minutes in 1x TBST to remove excess antibodies. The blot was then developed by using Amersham ECL Western blotting detecting reagent.

Primary antibodies against phosphorylated STAT-5 (p-STAT5$^{Y694}$), STAT-5, phosphorylated ERK1/2 (p-ERK1/2$^{T202/Y204}$), ERK1/2, phosphorylated p38 (p-

p38$^{T180/Y182}$), p38, Mnk1, phosphorylated 4EBP1 (p-4EBP1$^{T37/46}$, p-4EBP1$^{T70}$, p-4EBP1$^{S65}$), 4EBP1, phosphorylated eIF4E (p-eIF4E$^{S209}$), eIF4E, Mcl-1, phosphorylated histone 2AX (p-H2A.X$^{S139}$), β-actin (Cell Signalling Technologies, Danvers, MA, USA), Bcl-2 (Dako, Glostrap, Denmark), Mnk2 (Sigma Aldrich, Castle Hill, NSW, Australia). A secondary anti-rabbit immunoglobulin G (IgG) horseradishperoxidase (HRP)-conjugated antibody (Dako, Glostrap, Denmark and Cell Signalling Technologies Danvers, MA, USA) was used to develop the Western blot with Enhanced Chemiluminescence (ECL) reagents (GE Life Sciences).

### 6.2.11 Wound healing assays

*In vitro* study of cell migration was performed using a wound healing assay (also called wound-scratch assay) which is a straightforward and economical method to study cell migration. In this method, a new artificial gap, so called "scratch", is created on a confluent cell monolayer, and the cells on the edge of the scratch will move toward the opening to close the scratch until new cell–cell contacts are established again. The PCa cell line C4-2B was cultured in a 24 well cell culture plate until confluency. P200 pipette tips were used to make scratch, images were captured at the beginning and regular intervals during cell migration to close the scratch. The percentage of wound closure was calculated by subtracting the wound distance at twenty-four hour from zero hour and divided by the distance at time zero then multiplied by one hundred.

### 6.2.12 Cell invasion assay

Invasive capacity of the tumour cells as they penetrate an extracellular matrix (ECM) is the most important characteristic that is typically associated with cancer cell metastasis. Transmembrane cell invasion assay is a physiologically relevant cell-based assay to study cell migration. The human prostate cell line C4-2B was evaluated by transwell migration

assay. LPS pre-treated C4-2B cells were seeded on matrigel coated Boyden chamber and treated with each Mnk inhibitor. After 24 hours, cells that invaded through the matrigel matrix and porous membrane were fixed with 5% glutaraldehyde for 10 minutes, and stained on the lower side of the insert filter with 1% crystal violet in 2% ethanol for 20 minutes. The excess crystal violet was removed by quickly merging the insert in $dH_2O$ for 5 seconds and the excess water was drained from the top side of the insert using a cotton swab and the invaded cells were counted within five random fields using a fluorescence microscope.

### 6.2.13 Detection of apoptosis

Detection of cells undergoing apoptosis was detected using the annexin V-FITC/PI dual staining assay. An early feature of the apoptosis process is the translocation of membrane phospholipid phosphatidylserine from the inner side of the plasma membrane to the surface. Annexin V is a phospholipid binding protein with a high affinity for phosphatidylserine. Flowcytometric detection of early apoptotic cells makes the use of this annexin V being a sensitive probe which can also be conjugated to fluorochromes while maintaining its high affinity for phosphatidylserine.

PI is a fluorescent molecule that intercalates between the DNA bases *via* binding to nucleic acids. Since, dead or damaged cells are permeable to PI, it has been extensively used to stain cells and quantify their DNA contents. In this assay, annexin V is used in combination with PI to assess the level of apoptosis. Viable healthy cells with intact cell membrane are not stained with either stain while early apoptotic cells are stained with annexin V but not with PI. Cells in late apoptosis or necrosis are stained with both dyes. This assay was performed with an annexin V-FITC apoptosis detection kit following the manufacturer' instructions (Becton Dickinson, Australia).

MV4-11 cells were seeded at a density of $8 \times 10^4$ cells/well in a 6-well plate and incubated overnight at 37°C with 5% $CO_2$. The next day, cells were treated with each compound incubated for indicated time period and harvested with 1 mL fresh medium. The harvested cells were washed with 1x PBS, collected in FACS tubes, and centrifuged at a speed of 300 × *g* for 5 minutes at room temperature. The cell pellets were resuspended in 1 mL of 1x PBS, and the number of cells in each sample was counted using a TC10™ automatic cell counter. $1 \times 10^5$ cells were transferred into a fresh FACS tube with 1 mL of cold 1x PBS, centrifuged at a speed of 300 × *g* for 5 minutes at room temperature. Cell pellets were again re-suspended in 1 mL of cold 1x PBS, and centrifuged at 300 × *g* for 5 minutes. Then the cell pellet was stained with 3 µL of annexin V-FITC and 3 µL of PI with 100 µL of 1 × annexin V binding buffer in each sample, and incubated in the dark at room temperature for 15 minutes. An extra 200 µL of 1 × annexin V binding buffer was added into each tube, and the percentage of apoptotic cells was measured by a Gallios™ flow cytometer. Data were analysed using the Kaluza® flow analysis software v1.2.

### 6.2.14 Plasmid transformation and cryo stocks

Transformation is the process by which foreign DNA that is introduced into bacteria is amplified or cloned. Bacterial cells having the ability to readily take up foreign plasmid are called competent cells. In order to amply the plasmids, 10 ng plasmid-DNA of GST, GST-Mnk1a or GST-Mnk1b was transformed into BL-21 Star™ (DE3) One Shot Chemically Competent Cells (Invitrogen, Mulgrave, VIC, Australia) using heat shock method. Plasmids were mixed gently with 50 µL of competent cells in a microcentrifuge tube. The competent cell/plasmid mixture was kept on ice for 20-30 minutes then heat shock each transformation tube by placing the tube onto a 42°C water bath for 60 seconds. The tubes were then kept back on ice for 2 minutes and 1 mL of LB media without antibiotic was added to the bacteria, and the mix was incubated at 37°C in a shaking

incubator for 1 hour. 50 µL of the mixture was plated onto a 10 cm LB agar plate containing ampicillin. After incubation at 37°C for 16-18 hours, one colony was picked and inoculated into 30 mL of LB media with ampicillin (50 µg/mL). After incubation at 37°C (150 rpm) until an optical density at 600 nm ($OD_{600}$) of 0.8-1.0 was reached (*ca*. 5-6 hours), the culture was transferred to 1 mL of LB with ampicillin for large culture and incubated at 37°C overnight, and the next day plasmids were purified from bacterial pellet using Midi prep method (Qiagen). Cryo stocks were prepared in 50% glycerol. 700 µL of bacterial culture at $OD_{600}$ of 0.8-1.0 and 300 µL of 50% glycerol were mixed in a cryo vial and put on -20°C for 1 hour. After that, the vials were transferred to -80°C for long-term storage.

### 6.2.15 Plasmid purification

Plasmid purification was performed using Qiagen plasmid Midi kits: a modified alkaline lysis procedure, followed by binding of plasmid DNA to a resin under appropriate low-salt and pH conditions. RNA, proteins, dyes, and low-molecular-weight impurities are removed by a medium-salt wash. Plasmid DNA is eluted with a high-salt buffer and then concentrated and desalted by isopropanol precipitation.

The bacterial pellet from Section 4.2.13 was re-suspended in 4 mL of buffer P1 containing RNase and mixed well by vortexing until all clumps were dispersed well. Subsequently, 4 mL of buffer P2 was added and mixed thoroughly by vigorously inverting the stubs 4–6 times, and incubated at room temperature for 5 minutes. Vortexing should be avoided at this stage in order to avoid shearing of genomic DNA. When the lysate appeared viscous, 4 mL of chilled buffer P3 was added, mixed immediately and thoroughly by vigorously inverting 4–6 times, and incubated on ice for 15 minutes. Precipitation was enhanced by using chilled buffer P3 and incubating on ice, and a fluffy white material

formed while the lysate became less viscous. The precipitated material contains genomic DNA, proteins and cell debris. The suspension was centrifuged at 20,000 × *g* for 30 minutes at 4°C and the supernatant containing plasmid DNA was collected promptly. Centrifugation step was repeated in order to clear the lysate completely from precipitated material. Subsequently, the DNA was precipitated by adding 42 mL of isopropanol to the lysate. The resultant suspension was centrifuged at 15,000 × *g* for 30 minutes at 4°C, and the supernatant was decanted. The precipitated DNA pellet was re-dissolved in 500 μL Tris EDTA (TE) buffer (pH 8.0), and QBT buffer was added to obtain a final volume of 5 mL. TE buffer was used to facilitate re-dissolving of DNA whereas QBT buffer provided optimal DNA binding conditions.

The DNA solution was then applied to the Qiagen tip previously equilibrated with 4 mL of QBT buffer and washed with 2 × 10 mL of QC buffer, then eluted with 5 mL of QF buffer. The eluted DNA is precipitated by adding 3.5 mL of isopropanol, mixed and centrifuged at 15,000 × *g* for 30 minutes at 4°C. The DNA was then washed with 2 mL of 70% ethanol, and centrifuged at 15,000 × *g* for 10 minutes. The 70% ethanol removed precipitated salt and replaced isopropanol with the more volatile ethanol, making the DNA easier to be re-dissolved. Lastly, the DNA was air-dried and dissolved in distilled water, and concentration of plasmid was determined using NanoDrop.

### 6.2.16 Manual protein purification and buffer exchange

The manual protein purification was carried out using affinity chromatography according to Glutathione Affinity Handbook provided by Qiagen. The glutathione tri-peptide (Glu-Cys-Gly) covalently immobilised on Glutathione HiCap Matrix support beads was purchased. Proteins carrying a GST-tag were retained on the matrix due to the interaction of the Glutathione-S-transferase with its ligand glutathione. Once bound, the proteins

could be easily removed by disrupting their interaction with the glutathione. This was achieved by adding excess reduced L-glutathione into the elution buffer to compete with the immobilised glutathione for the binding site on the GST. The lysate was mixed with 1 mL of Glutathione HiCap Matrix slurry (Qiagen, Chadstonecentre, VIC, Australia), previously equilibrated with 10 column volumes (CVs) of lysis buffer in polypropylene gravity flow columns and incubated on an end-over-end shaker for at least 1 hour at 4°C in 50 mL falcon tubes. The lysate-matrix mix was centrifuged at 1000 × *g* for 2 minutes (4°C) and 80% of the supernatant was removed. The glutathione matrix was re-suspended and the remaining 20% lysate-matrix mix was equally divided into two polypropylene columns. Only purified protein from *E. coli* was activated with ERK1 (Sigma-Aldrich, New Castle Hill, NSW, Australia) to obtain active GST-Mnk (phosphorylated) whereas protein obtained from HEK293T did not require activation. After activation with ERK1 (refer to **Section 6.2.17**), both columns were washed with 6 CVs of lysis buffer to remove unbound material and eluted in 2.5 mL of elution buffer. PD 10 desalting columns (GE Healthcare, Parramatta, NSW, Australia) were used according to protocol to change from elution buffer into storage buffer. Aliquots of 50 µL were shock frozen in liquid nitrogen and stored at -80°C.

### 6.2.17 Activation of GST-Mnk1a with ERK1

Activation of GST-Mnk1a was carried out in activation buffer (20 mM HEPES/KOH pH 7.4, 10 mM $MgCl_2$, 0.25 mM DTT, 0.05% Brij S20, 50 mM β-glycerophosphate, 1 mM $Na_3VO_4$ and Roche protease inhibitor cocktail). GST-Mnk1a was kept immobilised on the Glutathione HiCap matrix during activation. The column was washed prior to activation with 6 CVs of activation buffer to remove unbound material. Then the matrix was re-suspended in 2 mL activation buffer, which contained 1 mM ATP and 500 nM ERK1. The matrix was incubated for 1 hour at 30°C with continuous shaking at 200 rpm.

### 6.2.18 Purity assessment

To assess the purity of the protein, sodium dodecyl sulphate-polyacrylamide gel electrophoresis (SDS-PAGE) was used. SDS-PAGE was run with Bio-Rad Mini-Protean TGX Stain-Free Gels (Biorad, Gladesville, NSW, Australia) where a specific trihalo compound present in the gel bound covalently to tryptophan residues of proteins upon activation with UV light. Thus, the visualisation of the protein bands was achieved without using other staining agents such as Coomassie. The gel could be directly used for assessment of the proteins. Western blotting was carried out according to **Section 6.2.10.**

### 6.2.19 Data analysis

Microsoft Excel or GraphPad Prism software (version 6.0) was used for data analysis.

The normalised TR-FRET signal was calculated by dividing the relative fluorescence units (Rfu) measured from the TR-FRET emission (572 nm) by the Tb emission (545 nm) and multiplying by 10,000:

$$TR\text{-}FRET = \frac{TR\text{-}FRET\ Rfu}{Tb\ Rfu} \times\ 10{,}000$$

Determination of the maximal velocity ($V_{max}$) and Michaelis-Menten constant ($K_m$) was carried out using Michaelis-Menten curve fitting.

$$v = \frac{V_{max} \times [S]}{K_m + [S]}$$

Where v = reaction velocity and [S] = concentration of substrate.

Dose response curves were used to calculate $IC_{50}$ and $GI_{50}$ values using a 4-parameter logistic non-linear regression model and the conversion to $K_i$ values was done using the Cheng-Prusoff equation [169]:

The Z'-factor [300, 301] was routinely calculated to quantify the assay performance according to the following equation:

$$Z' = 1 - \frac{3 \times (\sigma_p + \sigma_n)}{(\mu_p - \mu_n)}$$

Where $\sigma_p$ = standard deviation (SD) of positive controls; $\sigma_n$ = SD of negative controls; $\mu_p$ = mean of positive controls; $\mu_n$ = mean of negative controls.

Pearson correlation coefficient was calculated using the following formula:

$$Correl(x, y) = \frac{\sum(x - \overline{x})(y - \overline{y})}{\sqrt{\sum(x - \overline{x})^2 \sum(y - \overline{y})^2}}$$

Where x and y were the $IC_{50}$ and $GI_{50}$ values respectively.

# 7. References


1. Bray, F., et al., *Global estimates of cancer prevalence for 27 sites in the adult population in 2008.* International Journal of Cancer, 2013. **132**(5): p. 1133-1145.
2. Hanahan, D. and R.A. Weinberg, *The hallmarks of cancer.* Cell, 2000. **100**(1): p. 57-70.
3. Hanahan, D. and R.A. Weinberg, *Hallmarks of cancer: the next generation.* Cell, 2011. **144**(5): p. 646-674.
4. Jin, Z. and W.S. El-Deiry, *Overview of cell death signaling pathways.* Cancer Biology & Therapy, 2005. **4**(2): p. 147-171.
5. Vajdic, C.M. and M.T. van Leeuwen, *Cancer incidence and risk factors after solid organ transplantation.* International Journal of Cancer, 2009. **125**(8): p. 1747-1754.
6. Gibbs, J.B., *Mechanism-based target identification and drug discovery in cancer research.* Science, 2000. **287**(5460): p. 1969-1973.
7. Wang, Y. and G. Giaccone, *Challenges in cancer molecular targets and therapeutics.* Frontiers in Oncology, 2011. **1**(4): p. 1-4.
8. Zhang, J., P.L. Yang, and N.S. Gray, *Targeting cancer with small molecule kinase inhibitors.* Nature Reviews Cancer, 2009. **9**(1): p. 28-39.
9. Hudis, C.A., *Trastuzumab—mechanism of action and use in clinical practice.* New England Journal of Medicine, 2007. **357**(1): p. 39-51.
10. Schlessinger, J., *Cell signaling by receptor tyrosine kinases.* Cell, 2000. **103**(2): p. 211-225.
11. Dhillon, A.S., et al., *MAP kinase signalling pathways in cancer.* Oncogene, 2007. **26**(22): p. 3279-3290.
12. Sangwan, V. and M. Park, *Receptor tyrosine kinases: role in cancer progression.* Current Oncology, 2006. **13**(5): p. 191-193.
13. Dagher, R., et al., *Approval summary imatinib mesylate in the treatment of metastatic and/or unresectable malignant gastrointestinal stromal tumors.* Clinical Cancer Research, 2002. **8**(10): p. 3034-3038.
14. Kantarjian, H.M., et al., *Long-term survival benefit and improved complete cytogenetic and molecular response rates with imatinib mesylate in Philadelphia chromosome–positive chronic-phase chronic myeloid leukemia after failure of interferon-α.* Blood, 2004. **104**(7): p. 1979-1988.

15. Wu, P., T.E. Nielsen, and M.H. Clausen, *FDA-approved small-molecule kinase inhibitors.* Trends in Pharmacological Sciences, 2015. **36**(7): p. 422-439.
16. Martin, G.S., *Cell signaling and cancer.* Cancer cell, 2003. **4**(3): p. 167-174.
17. Calkhoven, C.F., C. Müller, and A. Leutz, *Translational control of gene expression and disease.* Trends in Molecular Medicine, 2002. **8**(12): p. 577-583.
18. Downward, J., *Targeting RAS signalling pathways in cancer therapy.* Nature Reviews Cancer, 2003. **3**(1): p. 11-22.
19. De Luca, A., et al., *The RAS/RAF/MEK/ERK and the PI3K/AKT signalling pathways: role in cancer pathogenesis and implications for therapeutic approaches.* Expert Opinion on Therapeutic Targets, 2012. **16**(sup2): p. S17-S27.
20. Raught, B. and A.-C. Gingras, *eIF4E activity is regulated at multiple levels.* The International Journal of Biochemistry & Cell Biology, 1999. **31**(1): p. 43-57.
21. Mamane, Y., et al., *eIF4E–from translation to transformation.* Oncogene, 2004. **23**(18): p. 3172-3179.
22. Chappell, W.H., et al., *Ras/Raf/MEK/ERK and PI3K/PTEN/Akt/mTOR inhibitors: rationale and importance to inhibiting these pathways in human health.* Oncotarget, 2011. **2**(3): p. 135-164.
23. Hou, J., et al., *Targeting Mnks for cancer therapy.* Oncotarget, 2012. **3**(2): p. 118-131.
24. Jauch, R., et al., *Mitogen-activated protein kinases interacting kinases are autoinhibited by a reprogrammed activation segment.* The EMBO Journal, 2006. **25**(17): p. 4020-4032.
25. Jauch, R., et al., *Crystal structures of the Mnk2 kinase domain reveal an inhibitory conformation and a zinc binding site.* Structure, 2005. **13**(10): p. 1559-1568.
26. Waskiewicz, A.J., et al., *Mitogen-activated protein kinases activate the serine/threonine kinases Mnk1 and Mnk2.* The EMBO journal, 1997. **16**(8): p. 1909-1920.
27. Pettersson, F., S.V. del Rincon, and W.H. Miller Jr, *Eukaryotic translation initiation factor 4E as a novel therapeutic target in hematological malignancies and beyond.* Expert Opinion on Therapeutic Targets, 2014. **18**(9): p. 1035-1048.
28. Liu, L., et al., *Sorafenib blocks the RAF/MEK/ERK pathway, inhibits tumor angiogenesis, and induces tumor cell apoptosis in hepatocellular carcinoma model PLC/PRF/5.* Cancer research, 2006. **66**(24): p. 11851-11858.
29. Thoreen, C.C., et al., *An ATP-competitive mammalian target of rapamycin inhibitor reveals rapamycin-resistant functions of mTORC1.* Journal of Biological Chemistry, 2009. **284**(12): p. 8023-8032.
30. Zielinski, R., et al., *The crosstalk between EGF, IGF, and Insulin cell signaling pathways-computational and experimental analysis.* BMC systems biology, 2009. **3**(1): p. 88.
31. Ueda, T., et al., *Mnk2 and Mnk1 are essential for constitutive and inducible phosphorylation of eukaryotic initiation factor 4E but not for cell growth or development.* Molecular and Cellular Biology, 2004. **24**(15): p. 6539-6549.
32. Furic, L., et al., *eIF4E phosphorylation promotes tumorigenesis and is associated with prostate cancer progression.* Proceedings of the National Academy of Sciences, 2010. **107**(32): p. 14134-14139.

33. MacKay, J.A., et al., *Self-assembling chimeric polypeptide–doxorubicin conjugate nanoparticles that abolish tumours after a single injection.* Nature Materials, 2009. **8**(12): p. 993-999.
34. Zuberek, J., et al., *Phosphorylation of eIF4E attenuates its interaction with mRNA 5' cap analogs by electrostatic repulsion: Intein-mediated protein ligation strategy to obtain phosphorylated protein.* RNA, 2003. **9**(1): p. 52-61.
35. De Benedetti, A. and A.L. Harris, *eIF4E expression in tumors: its possible role in progression of malignancies.* The international journal of biochemistry & cell biology, 1999. **31**(1): p. 59-72.
36. Diab, S., et al., *MAP kinase-interacting kinases—emerging targets against cancer.* Chemistry & Biology, 2014. **21**(4): p. 441-452.
37. Wheater, M.J., P.W. Johnson, and J.P. Blaydes, *The role of MNK proteins and eIF4E phosphorylation in breast cancer cell proliferation and survival.* Cancer Biology & Therapy, 2010. **10**(7): p. 728-735.
38. Culjkovic, B., I. Topisirovic, and K.L. Borden, *Controlling gene expression through RNA regulons: the role of the eukaryotic translation initiation factor eIF4E.* Cell Cycle, 2007. **6**(1): p. 65-69.
39. Culjkovic, B., et al., *eIF4E promotes nuclear export of cyclin D1 mRNAs via an element in the 3' UTR.* The Journal of Cell Biology, 2005. **169**(2): p. 245-256.
40. Cohen, N., et al., *PML RING suppresses oncogenic transformation by reducing the affinity of eIF4E for mRNA.* The EMBO journal, 2001. **20**(16): p. 4547-4559.
41. Meric, F. and K.K. Hunt, *Translation initiation in cancer: a novel target for therapy 1 FM is supported by The University of Texas MD Anderson Cancer Center Physician-Scientist Program and by NIH Grant 1KO8-CA 91895-01. KKH is supported by Department of Defense Award DAMD-17-97-1-7162. 1.* Molecular Cancer Therapeutics, 2002. **1**(11): p. 971-979.
42. Vries, R.G., et al., *Heat shock increases the association of binding protein-1 with initiation factor 4E.* Journal of Biological Chemistry, 1997. **272**(52): p. 32779-32784.
43. Goodfellow, I.G. and L.O. Roberts, *Eukaryotic initiation factor 4E.* The International Journal of Biochemistry & Cell Biology, 2008. **40**(12): p. 2675-2680.
44. Lachance, P.E., et al., *Phosphorylation of eukaryotic translation initiation factor 4E is critical for growth.* Molecular and Cellular Biology, 2002. **22**(6): p. 1656-1663.
45. Korkolopoulou, P., et al., *Phosphorylated 4E-binding protein 1 (p-4E-BP1): a novel prognostic marker in human astrocytomas.* Histopathology, 2012. **61**(2): p. 293-305.
46. Scheper, G.C. and C.G. Proud, *Does phosphorylation of the cap-binding protein eIF4E play a role in translation initiation?* European Journal of Biochemistry, 2002. **269**(22): p. 5350-5359.
47. Schwanhäusser, B., et al., *Global quantification of mammalian gene expression control.* Nature, 2011. **473**(7347): p. 337-342.
48. Jones, R.M., et al., *Assignment of the human gene encoding eukaryotic initiation factor 4E (EIF4E) to the region q21-25 on chromosome 4.* Somatic cell and molecular genetics, 1997. **23**(3): p. 221-223.
49. Pyronnet, S., et al., *Human eukaryotic translation initiation factor 4G (eIF4G) recruits mnk1 to phosphorylate eIF4E.* The EMBO journal, 1999. **18**(1): p. 270-279.

50. Wendel, H.-G., et al., *Dissecting eIF4E action in tumorigenesis.* Genes & development, 2007. **21**(24): p. 3232-3237.
51. Sonenberg, N., *eIF4E, the mRNA cap-binding protein: from basic discovery to translational research This paper is one of a selection of papers published in this Special Issue, entitled CSBMCB-Systems and Chemical Biology, and has undergone the Journal's usual peer review process.* Biochemistry and Cell Biology, 2008. **86**(2): p. 178-183.
52. Ma, X.M. and J. Blenis, *Molecular mechanisms of mTOR-mediated translational control.* Nature reviews Molecular cell biology, 2009. **10**(5): p. 307-318.
53. Sonenberg, N. and A.G. Hinnebusch, *Regulation of translation initiation in eukaryotes: mechanisms and biological targets.* Cell, 2009. **136**(4): p. 731-745.
54. Waskiewicz, A.J., et al., *Phosphorylation of the cap-binding protein eukaryotic translation initiation factor 4E by protein kinase Mnk1 in vivo.* Molecular and Cellular Biology, 1999. **19**(3): p. 1871-1880.
55. Hernandez, G., *Was the initiation of translation in early eukaryotes IRES-driven?* Trends in Biochemical Sciences, 2008. **33**(2): p. 58-64.
56. Pickering, B.M. and A.E. Willis. *The implications of structured 5′ untranslated regions on translation and disease*. in *Seminars in Cell & Developmental Biology*. 2005. Elsevier.
57. Rhoads, R.E., *Cap recognition and the entry of mRNA into the protein synthesis initiation cycle.* Trends in Biochemical Sciences, 1988. **13**(2): p. 52-56.
58. De Benedetti, A. and J.R. Graff, *eIF-4E expression and its role in malignancies and metastases.* Oncogene, 2004. **23**(18): p. 3189-3199.
59. Saito, H., et al., *Activation of the c-myc gene by translocation: a model for translational control.* Proceedings of the National Academy of Sciences, 1983. **80**(24): p. 7476-7480.
60. Ruggero, D., et al., *The translation factor eIF-4E promotes tumor formation and cooperates with c-Myc in lymphomagenesis.* Nature medicine, 2004. **10**(5): p. 484-486.
61. De Benedetti, A., et al., *Expression of antisense RNA against initiation factor eIF-4E mRNA in HeLa cells results in lengthened cell division times, diminished translation rates, and reduced levels of both eIF-4E and the p220 component of eIF-4F.* Molecular and cellular biology, 1991. **11**(11): p. 5435-5445.
62. Korneeva, N.L., et al., *Mnk mediates integrin (α6β4) dependent eIF4E phosphorylation and translation of VEGF mRNA.* Molecular Cancer Research, 2010: p. molcanres. 0091.2010.
63. Das, F., et al., *TGFβ-induced PI 3 kinase-dependent Mnk-1 activation is necessary for Ser-209 phosphorylation of eIF4E and mesangial cell hypertrophy.* Journal of cellular physiology, 2013. **228**(7): p. 1617-1626.
64. Pardo, O.E., et al., *Fibroblast Growth Factor-2 Induces Translational Regulation of Bcl-XL and Bcl-2 via a MEK-dependent Pathway correlation with resistance to etoposide-induced apoptosis.* Journal of Biological Chemistry, 2002. **277**(14): p. 12040-12046.
65. Fan, S., et al., *Phosphorylated eukaryotic translation initiation factor 4 (eIF4E) is elevated in human cancer tissues.* Cancer Biology & Therapy, 2009. **8**(15): p. 1463-1469.

66. O'Loghlen, A., et al., *Identification and molecular characterization of Mnk1b, a splice variant of human MAP kinase-interacting kinase Mnk1*. Experimental Cell Research, 2004. **299**(2): p. 343-355.

67. Honer, M., et al., *18F-labeled bombesin analog for specific and effective targeting of prostate tumors expressing gastrin-releasing peptide receptors.* Journal of Nuclear Medicine, 2011. **52**(2): p. 270-278.

68. Li, Y., et al., *Elevated expression of eukaryotic translation initiation factor 4E is associated with proliferation, invasion and acquired resistance to erlotinib in lung cancer.* Cancer Biology & Therapy, 2012. **13**(5): p. 272-280.

69. Yoshizawa, A., et al., *Overexpression of phospho-eIF4E is associated with survival through AKT pathway in non–small cell lung cancer.* Clinical Cancer Research, 2010. **16**(1): p. 240-248.

70. Seki, N., et al., *Prognostic significance of expression of eukaryotic initiation factor 4E and 4E binding protein 1 in patients with pathological stage I invasive lung adenocarcinoma.* Lung Cancer, 2010. **70**(3): p. 329-334.

71. MacKay, J.A., et al., *Quantitative model of the phase behavior of recombinant pH-responsive elastin-like polypeptides.* Biomacromolecules, 2010. **11**(11): p. 2873-2879.

72. Costa, C., et al., *Negative feedback regulation of Rac in leukocytes from mice expressing a constitutively active phosphatidylinositol 3-kinase γ.* Proceedings of the National Academy of Sciences, 2007. **104**(36): p. 14354-14359.

73. Wang, X., et al., *Inhibition of mammalian target of rapamycin induces phosphatidylinositol 3-kinase-dependent and Mnk-mediated eukaryotic translation initiation factor 4E phosphorylation.* Molecular and Cellular Biology, 2007. **27**(21): p. 7405-7413.

74. Fischer, P.M., *Cap in hand: targeting eIF4E.* Cell Cycle, 2009. **8**(16): p. 2535-2541.

75. Borden, K.L. and B. Culjkovic-Kraljacic, *Ribavirin as an anti-cancer therapy: acute myeloid leukemia and beyond?* Leukemia & Lymphoma, 2010. **51**(10): p. 1805-1815.

76. Zahreddine, H.A., et al., *The sonic hedgehog factor GLI1 imparts drug resistance through inducible glucuronidation.* Nature, 2014. **511**(7507): p. 90-93.

77. Borden, K.L., *Targeting the oncogene eIF4E in cancer: From the bench to clinical trials.* Clinical & Investigative Medicine, 2011. **34**(6): p. 315-319.

78. Assouline, S., et al., *A phase I trial of ribavirin and low-dose cytarabine for the treatment of relapsed and refractory acute myeloid leukemia with elevated eIF4E.* Haematologica, 2015. **100**(1): p. e7-e9.

79. Graff, J.R., et al., *Targeting the eukaryotic translation initiation factor 4E for cancer therapy.* Cancer Research, 2008. **68**(3): p. 631-634.

80. Moerke, N.J., et al., *Small-molecule inhibition of the interaction between the translation initiation factors eIF4E and eIF4G.* Cell, 2007. **128**(2): p. 257-267.

81. Graff, J.R., et al., *Therapeutic suppression of translation initiation factor eIF4E expression reduces tumor growth without toxicity.* The Journal of Clinical Investigation, 2007. **117**(9): p. 2638-2648.

82. Goto, S., Z. Yao, and C.G. Proud, *The C-terminal domain of Mnk1a plays a dual role in tightly regulating its activity.* Biochemical Journal, 2009. **423**(2): p. 279-290.

83. Oyarzabal, J., et al., *Discovery of mitogen-activated protein kinase-interacting kinase 1 inhibitors by a comprehensive fragment-oriented virtual screening approach.* Journal of Medicinal Chemistry, 2010. **53**(18): p. 6618-6628.

84. Liu, Y. and N.S. Gray, *Rational design of inhibitors that bind to inactive kinase conformations.* Nature Chemical Biology, 2006. **2**(7): p. 358-364.

85. Huang, D., et al., *Kinase selectivity potential for inhibitors targeting the ATP binding site: a network analysis.* Bioinformatics, 2010. **26**(2): p. 198-204.

86. Buxade, M., J.L. Parra-Palau, and C.G. Proud, *The Mnks: MAP kinase-interacting kinases (MAP kinase signal-integrating kinases).* Frontiers in Bioscience, 2008. **13**: p. 5359-5373.

87. Webster, K.R., et al. *eFT508, a potent and selective mitogen-activated protein kinase interacting kinase (MNK) 1 and 2 inhibitor, is efficacious in preclinical models of diffuse large B-cell lymphoma (DLBCL).* in *57th American Society of Hematology Annual Meeting and Exposition, Orlando, FL*. 2015.

88. Kannan, S., et al., *Probing the binding mechanism of Mnk inhibitors by docking and molecular dynamics simulations.* Biochemistry, 2014. **54**(1): p. 32-46.

89. Dreas, A., et al., *Mitogen-activated protein kinase (MAPK) interacting kinases 1 and 2 (MNK1 and MNK2) as targets for cancer therapy: recent progress in the development of MNK inhibitors.* Current medicinal chemistry, 2017. **24**: p. 1-28.

90. Dreas, A., et al., *Mitogen-activated protein kinase (MAPK) interacting kinases 1 and 2 (MNK1 and MNK2) as targets for cancer therapy: recent progress in the development of MNK inhibitors.* Current medicinal chemistry, 2017.

91. Nolen, B., S. Taylor, and G. Ghosh, *Regulation of protein kinases: controlling activity through activation segment conformation.* Molecular Cell, 2004. **15**(5): p. 661-675.

92. Ueda, T., et al., *Combined deficiency for MAP kinase-interacting kinase 1 and 2 (Mnk1 and Mnk2) delays tumor development.* Proceedings of the National Academy of Sciences, 2010. **107**(32): p. 13984-13990.

93. Robichaud, N., et al., *Phosphorylation of eIF4E promotes EMT and metastasis via translational control of SNAIL and MMP-3.* Oncogene, 2015. **34**(16): p. 2032-2042.

94. Bhat, M., et al., *Targeting the translation machinery in cancer.* Nature Reviews Drug Discovery, 2015. **14**(4): p. 261-278.

95. Ramalingam, S., et al., *First MNK degrading agents block phosphorylation of eIF4E, induce apoptosis, and inhibit cell growth, migration and invasion in triple-negative and HER2-overexpressing breast cancer cell lines.* Cancer Research, 2014. **74**(19 Supplement): p. 756-756.

96. Diab, S., et al., *Discovery of 5-(2-(Phenylamino) pyrimidin-4-yl) thiazol-2 (3H)-one Derivatives as Potent Mnk2 Inhibitors: Synthesis, SAR Analysis and Biological Evaluation.* ChemMedChem, 2014. **9**(5): p. 962-972.

97. Teo, T., et al., *Pharmacologic co-inhibition of Mnks and mTORC1 synergistically suppresses proliferation and perturbs cell cycle progression in blast crisis-chronic myeloid leukemia cells.* Cancer Letters, 2015. **357**(2): p. 612-623.

98. Yu, M., et al., *Discovery of 4-(dihydropyridinon-3-yl) amino-5-methylthieno [2, 3-d] pyrimidine derivatives as potent Mnk inhibitors: synthesis, structure–activity relationship analysis and biological evaluation.* European Journal of Medicinal Chemistry, 2015. **95**: p. 116-126.

99. Curiel, T.J., et al., *Specific recruitment of regulatory T cells in ovarian carcinoma fosters immune privilege and predicts reduced survival.* Nature Medicine, 2004. **10**(9): p. 942-949.

100. Beggs, J.E., et al., *The MAP kinase-interacting kinases regulate cell migration, vimentin expression and eIF4E/CYFIP1 binding.* Biochemical Journal, 2015. **467**(1): p. 63-76.

101. Buxadé, M., et al., *The PSF· p54nrb Complex is a novel Mnk substrate that binds the mRNA for tumor necrosis factor α.* Journal of Biological Chemistry, 2008. **283**(1): p. 57-65.

102. Buxadé, M., et al., *The Mnks are novel components in the control of TNFα biosynthesis and phosphorylate and regulate hnRNP A1.* Immunity, 2005. **23**(2): p. 177-189.

103. Hefner, Y., et al., *Serine 727 phosphorylation and activation of cytosolic phospholipase A2 by MNK1-related protein kinases.* Journal of Biological Chemistry, 2000. **275**(48): p. 37542-37551.

104. Joshi, S. and L.C. Platanias, *Mnk kinase pathway: cellular functions and biological outcomes.* World Journal of Biological Chemistry, 2014. **5**(3): p. 321-333.

105. Funk, C.D., *Prostaglandins and leukotrienes: advances in eicosanoid biology*. Science, 2001. **294**(5548): p. 1871-1875.

106. Edwin, F., K. Anderson, and T.B. Patel, *HECT domain-containing E3 ubiquitin ligase Nedd4 interacts with and ubiquitinates Sprouty2.* Journal of Biological Chemistry, 2010. **285**(1): p. 255-264.

107. DaSilva, J., et al., *Regulation of sprouty stability by Mnk1-dependent phosphorylation.* Molecular and Cellular Biology, 2006. **26**(5): p. 1898-1907.

108. Mason, J.M., et al., *Sprouty proteins: multifaceted negative-feedback regulators of receptor tyrosine kinase signaling.* Trends in Cell Biology, 2006. **16**(1): p. 45-54.

109. Kim, H.J. and D. Bar-Sagi, *Modulation of signalling by Sprouty: a developing story.* Nature Reviews Molecular Cell Biology, 2004. **5**(6): p. 441-450.

110. Cabrita, M.A. and G. Christofori, *Sprouty proteins, masterminds of receptor tyrosine kinase signaling.* Angiogenesis, 2008. **11**(1): p. 53-62.

111. Knauf, U., C. Tschopp, and H. Gram, *Negative regulation of protein translation by mitogen-activated protein kinase-interacting kinases 1 and 2.* Molecular and Cellular Biology, 2001. **21**(16): p. 5500-5511.

112. Basnet, S.K., et al., *Identification of a highly conserved allosteric binding site on Mnk1 and Mnk2.* Molecular Pharmacology, 2015. **88**(5): p. 935-948.

113. Konicek, B.W., et al., *Therapeutic inhibition of MAP kinase interacting kinase blocks eukaryotic initiation factor 4E phosphorylation and suppresses outgrowth of experimental lung metastases.* Cancer Research, 2011. **71**(5): p. 1849-1857.

114. Bain, J., et al., *The selectivity of protein kinase inhibitors: a further update.* Biochemical Journal, 2007. **408**(3): p. 297-315.

115. Han, W., et al., *Discovery of a Selective and Potent Inhibitor of Mitogen-Activated Protein Kinase-Interacting Kinases 1 and 2 (MNK1/2) Utilizing Structure-Based Drug Design.* Journal of Medicinal Chemistry, 2016. **59**(7): p. 3034-3045.

116. Webster, K.R., et al. *eFT508: An oral, potent and highly selective inhibitor of MNK1 and MNK2, promotes anti-tumor immunity as a monotherapy and in combination with immune checkpoint blockade*. in *Cancer Research*. 2017. Amer Association Cancer Research 615 Chestnut St, 17th floor, Philadelphia, PA 19106-4404 USA.

117. Santag, S., et al., *Preclinical anti-tumor efficacy and mode of action of a novel, orally available, selective MKNK1 inhibitor [BAY 1143269]*. 2015, AACR.

118. Roskoski, R., *Classification of small molecule protein kinase inhibitors based upon the structures of their drug-enzyme complexes.* Pharmacological research, 2016. **103**: p. 26-48.

119. Nagar, B., et al., *Crystal structures of the kinase domain of c-Abl in complex with the small molecule inhibitors PD173955 and imatinib (STI-571).* Cancer Research, 2002. **62**(15): p. 4236-4243.

120. Vogtherr, M., et al., *NMR characterization of kinase p38 dynamics in free and ligand-bound forms.* Angewandte Chemie International Edition, 2006. **45**(6): p. 993-997.

121. Wodicka, L.M., et al., *Activation state-dependent binding of small molecule kinase inhibitors: structural insights from biochemistry.* Chemistry & Biology, 2010. **17**(11): p. 1241-1249.

122. Backes, A., et al., *Small-molecule inhibitors binding to protein kinases. Part I: exceptions from the traditional pharmacophore approach of type I inhibition.* Expert opinion on drug discovery, 2008. **3**(12): p. 1409-1425.

123. Zhao, Z., et al., *Exploration of type II binding mode: a privileged approach for kinase inhibitor focused drug discovery?* ACS Chemical Biology, 2014. **9**(6): p. 1230-1241.

124. Blanc, J., R. Geney, and C. Menet, *Type II kinase inhibitors: an opportunity in cancer for rational design.* Anti-Cancer Agents in Medicinal Chemistry 2013. **13**(5): p. 731-747.

125. Gavrin, L.K. and E. Saiah, *Approaches to discover non-ATP site kinase inhibitors.* MedChemComm, 2013. **4**(1): p. 41-51.

126. Tokarski, J.S., et al., *The structure of Dasatinib (BMS-354825) bound to activated ABL kinase domain elucidates its inhibitory activity against imatinib-resistant ABL mutants.* Cancer Research, 2006. **66**(11): p. 5790-5797.

127. Eglen, R. and T. Reisine, *Drug discovery and the human kinome: recent trends.* Pharmacology & Therapeutics, 2011. **130**(2): p. 144-156.

128. Liu, Q., et al., *Developing irreversible inhibitors of the protein kinase cysteinome.* Chemistry & Biology, 2013. **20**(2): p. 146-159.

129. Ou, S.-H.I., *Second-generation irreversible epidermal growth factor receptor (EGFR) tyrosine kinase inhibitors (TKIs): a better mousetrap? A review of the clinical evidence.* Critical Reviews in Oncology/Hematology, 2012. **83**(3): p. 407-421.

130. Sequist, L.V., et al. *First-in-human evaluation of CO-1686, an irreversible, highly selective tyrosine kinase inhibitor of mutations of EGFR (activating and T790M)*. in *ASCO Annual Meeting Proceedings*. 2014.

131. Kwak, E.L., et al., *Irreversible inhibitors of the EGF receptor may circumvent acquired resistance to gefitinib.* Proceedings of the National Academy of Sciences of the United States of America, 2005. **102**(21): p. 7665-7670.

132. Pao, W., et al., *Acquired resistance of lung adenocarcinomas to gefitinib or erlotinib is associated with a second mutation in the EGFR kinase domain.* Public Library of Science one Medicine, 2005. **2**(3): p. e73.

133. Serafimova, I.M., et al., *Reversible targeting of noncatalytic cysteines with chemically tuned electrophiles.* Nature Chemical Biology, 2012. **8**(5): p. 471-476.

134. Kwegyir-Afful, A.K., et al., *Galeterone and VNPT55 disrupt Mnk-eIF4E to inhibit prostate cancer cell migration and invasion.* The FEBS Journal, 2016. **283**(21): p. 3898-3918.

135. Ramamurthy, V.P., et al., *Simultaneous targeting of androgen receptor (AR) and MAPK-interacting kinases (MNKs) by novel retinamides inhibits growth of human prostate cancer cell lines.* Oncotarget, 2015. **6**(5): p. 3195-3210.

136. Teo, T., et al., *Pharmacologic inhibition of Mnks in acute myeloid leukemia.* Molecular Pharmacology, 2015. **88**(2): p. 380-389.

137. Bianchini, A., et al., *Phosphorylation of eIF4E by MNKs supports protein synthesis, cell cycle progression and proliferation in prostate cancer cells.* Carcinogenesis, 2008. **29**(12): p. 2279-2288.

138. Altman, J.K., et al., *Inhibition of Mnk kinase activity by cercosporamide and suppressive effects on acute myeloid leukemia precursors.* Blood, 2013. **121**(18): p. 3675-3681.

139. Lim, S., et al., *Targeting of the MNK–eIF4E axis in blast crisis chronic myeloid leukemia inhibits leukemia stem cell function.* Proceedings of the National Academy of Sciences, 2013. **110**(25): p. E2298-E2307.

140. Kosciuczuk, E.M., et al., *Merestinib blocks Mnk kinase activity in acute myeloid leukemia progenitors and exhibits antileukemic effects in vitro and in vivo.* Blood, 2016. **128**(3): p. 410-414.

141. Glickman, J.F., *Assay development for protein kinase enzymes.* Assay Guidence Manual 2012.

142. Turek-Etienne, T.C., et al., *Development of a fluorescence polarization AKT serine/threonine kinase assay using an immobilized metal ion affinity-based technology.* Assay and Drug Development Technologies, 2003. **1**(4): p. 545-553.

143. Turek-Etienne, T.C., et al., *Evaluation of fluorescent compound interference in 4 fluorescence polarization assays: 2 kinases, 1 protease, and 1 phosphatase.* Journal of Biomolecular Screening, 2003. **8**(2): p. 176-184.

144. Newman, M. and S. Josiah, *Utilization of fluorescence polarization and time resolved fluorescence resonance energy transfer assay formats for SAR studies: Src kinase as a model system.* Journal of Biomolecular Screening, 2004. **9**(6): p. 525-532.

145. Waddleton, D., C. Ramachandran, and Q. Wang, *Development of a time-resolved fluorescent assay for measuring tyrosine-phosphorylated proteins in cells.* Analytical Biochemistry, 2002. **309**(1): p. 150-157.

146. Zhang, Y., et al., *Preparation of anti-tetracycline antibodies and development of an indirect heterologous competitive enzyme-linked immunosorbent assay to detect residues of tetracycline in milk.* Journal of Agricultural and Food Chemistry, 2007. **55**(2): p. 211-218.

147. Von Leoprechting, A., et al., *Miniaturization and validation of a high-throughput serine kinase assay using the alpha screen platform.* Journal of Biomolecular Screening, 2004. **9**(8): p. 719-725.

148. Warner, G., et al., *AlphaScreen™ kinase HTS platforms.* Current Medicinal Chemistry, 2004. **11**(6): p. 721-730.

149. Eglen, R.M., *Enzyme fragment complementation: a flexible high throughput screening assay technology.* Assay and Drug Development Technologies, 2002. **1**(1): p. 97-104.

150. Golla, R. and R. Seethala, *A homogeneous enzyme fragment complementation cyclic AMP screen for GPCR agonists.* Journal of Biomolecular Screening, 2002. **7**(6): p. 515-525.

151. Zhao, X., et al., *A homogeneous enzyme fragment complementation-based β-arrestin translocation assay for high-throughput screening of G-protein-coupled receptors.* Journal of Biomolecular Screening, 2008. **13**(8): p. 737-747.

152. Park, Y.-W., et al., *Homogeneous proximity tyrosine kinase assays: scintillation proximity assay versus homogeneous time-resolved fluorescence.* Analytical Biochemistry, 1999. **269**(1): p. 94-104.

153. Choi, C.W., *Scintillation Proximity Assay.* Korean Journal of Nuclear Medicine, 1999. **33**(6): p. 461-465.

154. Sills, M.A., et al., *Comparison of assay technologies for a tyrosine kinase assay generates different results in high throughput screening.* Journal of Biomolecular Screening, 2002. **7**(3): p. 191-214.

155. Von Ahsen, O., et al., *Assay concordance between SPA and TR-FRET in high-throughput screening.* Journal of Biomolecular Screening, 2006. **11**(6): p. 606-616.

156. Turek, T.C., et al., *Development and validation of a competitive AKT serine/threonine kinase fluorescence polarization assay using a product-specific anti-phospho-serine antibody.* Analytical biochemistry, 2001. **299**(1): p. 45-53.

157. Koresawa, M. and T. Okabe, *High-throughput screening with quantitation of ATP consumption: a universal non-radioisotope, homogeneous assay for protein kinase.* Assay and drug development technologies, 2004. **2**(2): p. 153-160.

158. Palmier, M.O. and S.R. Van Doren, *Rapid determination of enzyme kinetics from fluorescence: overcoming the inner filter effect.* Analytical Biochemistry, 2007. **371**(1): p. 43-51.

159. Glickman, J.F., A. Schmid, and S. Ferrand, *Scintillation proximity assays in high-throughput screening.* Assay and drug development technologies, 2008. **6**(3): p. 433-455.

160. Hall, M.D., et al., *Fluorescence polarization assays in high-throughput screening and drug discovery: a review.* Methods and Applications in Fluorescence, 2016. **4**(2): p. 022001.

161. Mergny, J.L. and J.C. Maurizot, *Fluorescence resonance energy transfer as a probe for G-quartet formation by a telomeric repeat.* ChemBioChem, 2001. **2**(2): p. 124-132.

162. Sapsford, K.E., L. Berti, and I.L. Medintz, *Materials for fluorescence resonance energy transfer analysis: beyond traditional donor–acceptor combinations.* Angewandte Chemie International Edition, 2006. **45**(28): p. 4562-4589.

163. Johnson, K.A. and R.S. Goody, *The original Michaelis constant: translation of the 1913 Michaelis–Menten paper.* Biochemistry, 2011. **50**(39): p. 8264-8269.

164. London, J.W., et al., *A systematic approach to enzyme assay optimization, illustrated by aminotransferase assays.* Clinical Chemistry, 1975. **21**(13): p. 1939-1952.

165. Acker, M.G. and D.S. Auld, *Considerations for the design and reporting of enzyme assays in high-throughput screening applications.* Perspectives in Science, 2014. **1**(1): p. 56-73.

166. Brooks, H.B., et al., *Basics of enzymatic assays for HTS.* 2012.

167. Goličnik, M., *Evaluation of enzyme kinetic parameters using explicit analytic approximations to the solution of the Michaelis–Menten equation.* Biochemical Engineering Journal, 2011. **53**(2): p. 234-238.

168. Loomans, E.E., et al., *High-throughput screening with immobilized metal ion affinity-based fluorescence polarization detection, a homogeneous assay for protein kinases.* Assay and drug development technologies, 2003. **1**(3): p. 445-453.

169. Twentyman, P. and M. Luscombe, *A study of some variables in a tetrazolium dye (MTT) based assay for cell growth and chemosensitivity.* British Journal of Cancer, 1987. **56**(3): p. 279.

170. Parra, J.L., M. Buxadé, and C.G. Proud, *Features of the catalytic domains and C termini of the MAPK signal-integrating kinases Mnk1 and Mnk2 determine their differing activities and regulatory properties.* Journal of Biological Chemistry, 2005. **280**(45): p. 37623-37633.

171. Teo, T., et al., *An integrated approach for discovery of highly potent and selective Mnk inhibitors: Screening, synthesis and SAR analysis.* European Journal of Medicinal Chemistry, 2015. **103**: p. 539-550.

172. Diab, S., et al., *Discovery of 5-(2-(Phenylamino) pyrimidin-4-yl) thiazol-2 (3H)-one Derivatives as Potent Mnk2 Inhibitors: Synthesis, SAR Analysis and Biological Evaluation.* ChemMedChem, 2014. **9**(5): p. 962–972.

173. Zhang, J.-H., T.D. Chung, and K.R. Oldenburg, *A simple statistical parameter for use in evaluation and validation of high throughput screening assays.* Journal of biomolecular screening, 1999. **4**(2): p. 67-73.

174. Altman, D.G., *Practical statistics for medical research*. 1990: CRC press.

175. Carpenter, R., *Principles and procedures of statistics, with special reference to the biological sciences.* The Eugenics Review, 1960. **52**(3): p. 172.

176. Garuti, L., M. Roberti, and G. Bottegoni, *Non-ATP competitive protein kinase inhibitors.* Current medicinal chemistry, 2010. **17**(25): p. 2804-2821.

177. Gumireddy, K., et al., *A non-ATP-competitive inhibitor of BCR-ABL overrides imatinib resistance.* Proceedings of the National Academy of Sciences of the United states of America, 2005. **102**(6): p. 1992-1997.

178. Allen, L.F., J. Sebolt-Leopold, and M.B. Meyer. *CI-1040 (PD184352), a targeted signal transduction inhibitor of MEK (MAPKK)*. in *Seminars in oncology*. 2003. Elsevier.

179. Noble, M.E., J.A. Endicott, and L.N. Johnson, *Protein kinase inhibitors: insights into drug design from structure.* Science, 2004. **303**(5665): p. 1800-1805.

180. Adrián, F.J., et al., *Allosteric inhibitors of Bcr-abl–dependent cell proliferation.* Nature Chemical Biology, 2006. **2**(2): p. 95-102.

181. Calleja, V., et al., *Role of a novel PH-kinase domain interface in PKB/Akt regulation: structural mechanism for allosteric inhibition.* Public Library of Science one Biology, 2009. **7**(1): p. e1000017.

182. Koeberle, S.C., et al., *Skepinone-L is a selective p38 mitogen-activated protein kinase inhibitor.* Nature chemical biology, 2012. **8**(2): p. 141-143.

183. Müller, S., et al., *The ins and outs of selective kinase inhibitor development.* Nature Chemical Biology, 2015. **11**(11): p. 818-821.

184. Knight, Z.A. and K.M. Shokat, *Features of selective kinase inhibitors.* Chemistry & Biology, 2005. **12**(6): p. 621-637.

185. Scapin, G., *Protein kinase inhibition: different approaches to selective inhibitor design.* Current Drug Targets, 2006. **7**(11): p. 1443-1454.

186. Krishnamurty, R. and D.J. Maly, *Biochemical mechanisms of resistance to small-molecule protein kinase inhibitors.* ACS Chemical Biology, 2010. **5**(1): p. 121-138.

187. Daub, H., K. Specht, and A. Ullrich, *Strategies to overcome resistance to targeted protein kinase inhibitors.* Nature reviews drug discovery, 2004. **3**(12): p. 1001-1010.

188. Breen, M.E. and M.B. Soellner, *Small molecule substrate phosphorylation site inhibitors of protein kinases: approaches and challenges.* ACS Chemical Biology, 2014. **10**(1): p. 175-189.

189. Lawrence, D.S. and J. Niu, *Protein kinase inhibitors: the tyrosine-specific protein kinases.* Pharmacology & Therapeutics, 1998. **77**(2): p. 81-114.

190. Georghiou, G., et al., *Highly specific, bisubstrate-competitive Src inhibitors from DNA-templated macrocycles.* Nature Chemical Biology, 2012. **8**(4): p. 366-374.

191. Yaish, P., et al., *Blocking of EGF-dependent cell proliferation by EGF receptor kinase inhibitors.* Science, 1988. **242**(4880): p. 933.

192. Gazit, A., et al., *Tyrphostins I: synthesis and biological activity of protein tyrosine kinase inhibitors.* Journal of Medicinal Chemistry, 1989. **32**(10): p. 2344-2352.

193. Bishop, W.R., et al., *Inhibition of protein kinase C by the tyrosine kinase inhibitor erbstatin.* Biochemical Pharmacology, 1990. **40**(9): p. 2129-2135.

194. Hsu, C.-Y.J., et al., *Inhibition kinetics and selectivity of the tyrosine kinase inhibitor erbstatin and a pyridone-based analogue.* Biochemical Pharmacology, 1992. **43**(11): p. 2471-2477.

195. Posner, I., et al., *Kinetics of inhibition by tyrphostins of the tyrosine kinase activity of the epidermal growth factor receptor and analysis by a new computer program.* Molecular Pharmacology, 1994. **45**(4): p. 673-683.

196. Hamilton, B., et al., *Association of heterogeneous nuclear ribonucleoprotein A1 and C proteins with reiterated AUUUA sequences.* Journal of Biological Chemistry, 1993. **268**(12): p. 8881-8887.

197. Diab, S., et al., *Unveiling new chemical scaffolds as Mnk inhibitors.* Future Medicinal Chemistry, 2016. **8**(3): p. 271-285.

198. Graff, J.R., et al., *eIF4E activation is commonly elevated in advanced human prostate cancers and significantly related to reduced patient survival.* Cancer Research, 2009. **69**(9): p. 3866-3873.

199. Worch, J., et al., *The serine-threonine kinase MNK1 is post-translationally stabilized by PML-RARα and regulates differentiation of hematopoietic cells.* Oncogene, 2004. **23**(57): p. 9162-9172.

200. Pellagatti, A., et al., *Gene expression profiling in polycythemia vera using cDNA microarray technology.* Cancer Research, 2003. **63**(14): p. 3940-3944.

201. Chen, C.D., et al., *Molecular determinants of resistance to antiandrogen therapy.* Nature Medicine, 2004. **10**(1): p. 33-39.

202. Sansal, I. and W.R. Sellers, *The biology and clinical relevance of the PTEN tumor suppressor pathway.* Journal of Clinical Oncology, 2004. **22**(14): p. 2954-2963.

203. Trotman, L.C., et al., *Pten dose dictates cancer progression in the prostate.* Public Library of Science One Biology, 2003. **1**(3): p. e59.

204. Majumder, P.K. and W.R. Sellers, *Akt-regulated pathways in prostate cancer.* Oncogene, 2005. **24**(50): p. 7465-7474.

205. Lapointe, J., et al., *Gene expression profiling identifies clinically relevant subtypes of prostate cancer.* Proceedings of the National Academy of Sciences of the United States of America, 2004. **101**(3): p. 811-816.

206. Tomlins, S.A., et al., *Integrative molecular concept modeling of prostate cancer progression.* Nature Genetics, 2007. **39**(1): p. 41-51.

207. Varambally, S., et al., *Integrative genomic and proteomic analysis of prostate cancer reveals signatures of metastatic progression.* Cancer Cell, 2005. **8**(5): p. 393-406.

208. Tasseff, R., et al., *Analysis of the molecular networks in androgen dependent and independent prostate cancer revealed fragile and robust subsystems.* Public Library of Science one, 2010. **5**(1): p. e8864.

209. Sramkoski, R.M., et al., *A new human prostate carcinoma cell line, 22Rv1.* In Vitro Cellular & Developmental Biology-Animal, 1999. **35**(7): p. 403-409.

210. Russell, P.J. and E.A. Kingsley, *Human prostate cancer cell lines.* Prostate Cancer Methods and Protocols, 2003: p. 21-39.

211. Horoszewicz, J., et al., *The LNCaP cell line--a new model for studies on human prostatic carcinoma.* Progress in Clinical and Biological Research, 1980. **37**: p. 115.

212. Stone, K.R., et al., *Isolation of a human prostate carcinoma cell line (DU 145).* International Journal of Cancer, 1978. **21**(3): p. 274-281.

213. Rahaman, M.H., et al., *Targeting CDK9: a promising therapeutic opportunity in prostate cancer.* Endocrine-Related Cancer, 2016: p. ERC-16-0299.

214. Kaighn, M., et al., *Establishment and characterization of a human prostatic carcinoma cell line (PC-3).* Investigative Urology, 1979. **17**(1): p. 16-23.

215. Wu, H.C., et al., *Derivation of androgen-independent human LNCaP prostatic cancer cell sublines: Role of bone stromal cells.* International Journal of Cancer, 1994. **57**(3): p. 406-412.

216. Thalmann, G.N., et al., *Androgen-independent cancer progression and bone metastasis in the LNCaP model of human prostate cancer.* Cancer Research, 1994. **54**(10): p. 2577-2581.

217. Cunningham, D. and Z. You, *In vitro and in vivo model systems used in prostate cancer research.* Journal of Biological Methods, 2015. **2**(1).

218. Degorce, F., et al., *HTRF: a technology tailored for drug discovery–a review of theoretical aspects and recent applications.* Current Chemical Genomics and Translational Medicine, 2009. **3**(1).

219. Mathis, G., *HTRF® technology.* Journal of Biomolecular Screening, 1999. **4**(6): p. 309-313.

220. Pearson, K., *Note on regression and inheritance in the case of two parents.* Proceedings of the Royal Society of London, 1895. **58**: p. 240-242.

221. Goodwin, L.D. and N.L. Leech, *Understanding correlation: Factors that affect the size of r.* The Journal of Experimental Education, 2006. **74**(3): p. 249-266.

222. Rummel, R.J., *Understanding correlation.* Honolulu: Department of Political Science, University of Hawaii, 1976.

223. De Marzo, A.M., et al., *Inflammation in prostate carcinogenesis.* Nature Reviews Cancer, 2007. **7**(4): p. 256-269.

224. Wu, Y. and B.P. Zhou, *Inflammation: a driving force speeds cancer metastasis.* Cell Cycle, 2009. **8**(20): p. 3267-3273.

225. Aggarwal, B.B., *Signalling pathways of the TNF superfamily: a double-edged sword.* Nature Reviews Immunology, 2003. **3**(9): p. 745-756.

226. Brubaker, S.W., et al., *Innate immune pattern recognition: a cell biological perspective.* Annual Review of Immunology, 2015. **33**: p. 257-290.

227. Andreani, V., et al., *Activation of Toll-like receptor 4 on tumor cells in vitro inhibits subsequent tumor growth in vivo.* Cancer Research, 2007. **67**(21): p. 10519-10527.

228. Kundu, S.D., et al., *The toll-like receptor pathway: a novel mechanism of infection-induced carcinogenesis of prostate epithelial cells.* The Prostate, 2008. **68**(2): p. 223-229.

229. Yu, L. and S. Chen, *Toll-like receptors expressed in tumor cells: targets for therapy.* Cancer Immunology, Immunotherapy, 2008. **57**(9): p. 1271-1278.

230. Huang, B., et al., *Toll-like receptors on tumor cells facilitate evasion of immune surveillance.* Cancer Research, 2005. **65**(12): p. 5009-5014.

231. Cherla, R.P., et al., *Shiga toxin 1-induced cytokine production is mediated by MAP kinase pathways and translation initiation factor eIF4E in the macrophage-like THP-1 cell line.* Journal of Leukocyte Biology, 2006. **79**(2): p. 397-407.

232. Liang, C.-C., A.Y. Park, and J.-L. Guan, *In vitro scratch assay: a convenient and inexpensive method for analysis of cell migration in vitro.* Nature Protocols, 2007. **2**(2): p. 329-333.

233. Rodriguez, L.G., X. Wu, and J.-L. Guan, *Wound-healing assay.* Cell Migration: Developmental Methods and Protocols, 2005: p. 23-29.

234. Broughton 2nd, G., J.E. Janis, and C.E. Attinger, *The basic science of wound healing.* Plastic and Reconstructive Surgery, 2006. **117**(7 Suppl): p. 12S-34S.

235. Kramer, N., et al., *In vitro cell migration and invasion assays.* Mutation Research/Reviews in Mutation Research, 2013. **752**(1): p. 10-24.

236. Justus, C.R., et al., *In vitro cell migration and invasion assays.* Journal of Visualized Experiments, 2014(88): p. e51046-e51046.

237. Marshall, J., *Transwell® invasion assays.* Cell Migration: Developmental Methods and Protocols, 2011: p. 97-110.

238. Kumar, K., et al., *Differential Regulation of ZEB1 and EMT by MAPK-Interacting Protein Kinases (MNK) and eIF4E in Pancreatic Cancer.* Molecular Cancer Research, 2016. **14**(2): p. 216-227.

239. Gilliland, D.G., C.T. Jordan, and C.A. Felix, *The molecular basis of leukemia.* ASH Education Program Book, 2004. **2004**(1): p. 80-97.

240. Martelli, A., et al., *Phosphoinositide 3-kinase/Akt signaling pathway and its therapeutical implications for human acute myeloid leukemia.* Leukemia, 2006. **20**(6): p. 911-928.

241. Milella, M., et al., *Therapeutic targeting of the MEK/MAPK signal transduction module in acute myeloid leukemia.* Journal of Clinical Investigation, 2001. **108**(6): p. 851.

242. He, L.-Z., et al., *Acute leukemia with promyelocytic features in PML/RARα transgenic mice.* Proceedings of the National Academy of Sciences, 1997. **94**(10): p. 5302-5307.

243. Yuan, Y., et al., *AML1-ETO expression is directly involved in the development of acute myeloid leukemia in the presence of additional mutations.* Proceedings of the National Academy of Sciences, 2001. **98**(18): p. 10398-10403.

244. Dash, A. and D.G. Gilliland, *Molecular genetics of acute myeloid leukaemia.* Best practice & research Clinical haematology, 2001. **14**(1): p. 49-64.

245. Gilliland, D.G. and J.D. Griffin, *Role of FLT3 in leukemia.* Current opinion in hematology, 2002. **9**(4): p. 274-281.

246. Meshinchi, S., et al., *Prevalence and prognostic significance of Flt3 internal tandem duplication in pediatric acute myeloid leukemia.* Blood, 2001. **97**(1): p. 89-94.

247. Li, P., et al., *Inhibition of Mnk enhances apoptotic activity of cytarabine in acute myeloid leukemia cells.* Oncotarget, 2016.

248. Bennett, J.M., et al., *Proposed revised criteria for the classification of acute myeloid leukemia: a report of the French-American-British Cooperative Group.* Annals of Internal Medicine, 1985. **103**(4): p. 620-625.

249. Quentmeier, H., et al., *FLT3 mutations in acute myeloid leukemia cell lines.* Leukemia, 2003. **17**(1): p. 120-124.

250. Matsuo, Y., et al., *Two acute monocytic leukemia (AML-M5a) cell lines (MOLM-13 and MOLM-14) with interclonal phenotypic heterogeneity showing MLL-AF9 fusion resulting from an occult chromosome insertion, ins (11; 9)(q23; p22p23).* Leukemia, 1997. **11**(9): p. 1469-1477.

251. Andersson, A., et al., *Gene expression profiling of leukemic cell lines reveals conserved molecular signatures among subtypes with specific genetic aberrations.* Leukemia, 2005. **19**(6): p. 1042-1050.

252. Topisirovic, I., et al., *Aberrant eukaryotic translation initiation factor 4E-dependent mRNA transport impedes hematopoietic differentiation and contributes to leukemogenesis.* Molecular and Cellular Biology, 2003. **23**(24): p. 8992-9002.

253. Traut, T.W., *Physiological concentrations of purines and pyrimidines.* Molecular and Cellular Biochemistry, 1994. **140**(1): p. 1-22.

254. Gribble, F.M., et al., *A novel method for measurement of submembrane ATP concentration.* Journal of Biological Chemistry, 2000. **275**(39): p. 30046-30049.

255. Drexler, H.G. and Y. Matsuo, *Malignant hematopoietic cell lines: in vitro models for the study of multiple myeloma and plasma cell leukemia.* Leukemia Research, 2000. **24**(8): p. 681-703.

256. Diab, S., et al., *Dual Inhibition of Mnk2 and FLT3 for potential treatment of acute myeloid leukaemia.* European Journal of Medicinal Chemistry, 2017. **139**: p. 762-772.

257. Wander, S.A., M.J. Levis, and A.T. Fathi, *The evolving role of FLT3 inhibitors in acute myeloid leukemia: quizartinib and beyond.* Therapeutic Advances in Hematology, 2014. **5**(3): p. 65-77.

258. Kindler, T., D.B. Lipka, and T. Fischer, *FLT3 as a therapeutic target in AML: still challenging after all these years.* Blood, 2010. **116**(24): p. 5089-5102.

259. Knapper, S., et al., *A phase 2 trial of the FLT3 inhibitor lestaurtinib (CEP701) as first-line treatment for older patients with acute myeloid leukemia not considered fit for intensive chemotherapy.* Blood, 2006. **108**(10): p. 3262-3270.

260. Kiyoi, H., *Flt3 inhibitors: recent advances and problems for clinical application.* Nagoya Journal of Medical Science, 2015. **77**(1-2): p. 7.

261. Hayakawa, F., et al., *Tandem-duplicated Flt3 constitutively activates STAT5 and MAP kinase and introduces autonomous cell growth in IL-3-dependent cell lines.* Oncogene, 2000. **19**(5).

262. Levis, M., et al., *A FLT3-targeted tyrosine kinase inhibitor is cytotoxic to leukemia cells in vitro and in vivo.* Blood, 2002. **99**(11): p. 3885-3891.

263. Biosciences, B., *Detection of Apoptosis Using the BD Annexin V FITC Assay on the BD FACSVerse™ System*. 2011.

264. Lakhani, S.A., et al., *Caspases 3 and 7: key mediators of mitochondrial events of apoptosis.* Science, 2006. **311**(5762): p. 847-851.

265. Huijun, Z., et al., *Benzyloxycarbonyl-Val-Ala-Asp (OMe) fluoromethylketone (Z-VAD. FMK) inhibits apoptosis by blocking the processing of CPP32.* Biochemical Journal, 1996. **315**(1): p. 21-24.

266. Shimizu, T. and Y. Pommier, *Camptothecin-induced apoptosis in p53-null human leukemia HL60 cells and their isolated nuclei: effects of the protease inhibitors Z-VAD-fmk and dichloroisocoumarin suggest an involvement of both caspases and serine proteases.* Leukemia (08876924), 1997. **11**(8).

267. Shaw, R.J. and L.C. Cantley, *Ras, PI (3) K and mTOR signalling controls tumour cell growth.* Nature, 2006. **441**(7092): p. 424-430.

268. Fraser, M., et al., *PTEN deletion in prostate cancer cells does not associate with loss of RAD51 function: implications for radiotherapy and chemotherapy.* Clinical Cancer Research, 2012. **18**(4): p. 1015-1027.

269. Skjoth, I. and O.-G. Issinger, *Profiling of signaling molecules in four different human prostate carcinoma cell lines before and after induction of apoptosis.* International Journal of Oncology, 2006. **28**(1): p. 217-230.

270. Lonergan, P.E. and D.J. Tindall, *Androgen receptor signaling in prostate cancer development and progression.* Journal of Carcinogenesis, 2011. **10**(1): p. 20.

271. Thiery, J.P., *Epithelial–mesenchymal transitions in tumour progression.* Nature Reviews Cancer, 2002. **2**(6): p. 442-454.

272. Robichaud, N., et al., *Phosphorylation of eIF4E promotes EMT and metastasis via translational control of SNAIL and MMP-3.* Oncogene, 2015. **34**(16): p. 2032-2042.

273. Rowlett, R.M., et al., *MNK kinases regulate multiple TLR pathways and innate proinflammatory cytokines in macrophages.* American Journal of Physiology-Gastrointestinal and Liver Physiology, 2008. **294**(2): p. G452-G459.

274. Kjellerup, R.B., et al., *Pro-inflammatory cytokine release in keratinocytes is mediated through the MAPK signal-integrating kinases.* Experimental Dermatology, 2008. **17**(6): p. 498-504.

275. Hou, J., et al., *Insights into the importance of DFD-motif and insertion I1 in stabilizing the DFD-out conformation of Mnk2 kinase.* ACS Medicinal Chemistry Letters, 2013. **4**(8): p. 736-741.

276. Schindler, T., et al., *Structural mechanism for STI-571 inhibition of abelson tyrosine kinase.* Science, 2000. **289**(5486): p. 1938-1942.

277. Okram, B., et al., *A general strategy for creating "inactive-conformation" abl inhibitors.* Chemistry & Biology, 2006. **13**(7): p. 779-786.

278. Robinson, P.J., *Differential stimulation of protein kinase C activity by phorbol ester or calcium/phosphatidylserine in vitro and in intact synaptosomes.* Journal of Biological Chemistry, 1992. **267**(30): p. 21637-21644.

279. Hocevar, B.A., et al., *Protein kinase C isotypes in human erythroleukemia cell proliferation and differentiation.* Journal of Cell Science, 1992. **101**(3): p. 671-679.

280. Wilkinson, G.W. and A. Akrigg, *Constitutive and enhanced expression from the CMV major IE promoter in a defective adenovirus vector.* Nucleic Acids Research, 1992. **20**(9): p. 2233-2239.

281. Froger, A. and J.E. Hall, *Transformation of plasmid DNA into E. coli using the heat shock method.* Journal of Vsualized Experiments: JoVE, 2007(6).

282. Hanahan, D., *Studies on transformation of Escherichia coli with plasmids.* Journal of Molecular Biology, 1983. **166**(4): p. 557-580.

283. Sambrook, J., E.F. Fritsch, and T. Maniatis, *Molecular cloning*. Vol. 2. 1989: Cold Spring Harbor Laboratory Press New York.

284. Wiederschain, G.Y., *Handbook of affinity chromatography.* Biochemistry (Moscow), 2007. **72**(7): p. 793-793.

285. Hage, D.S. and J. Cazes, *Handbook of affinity chromatography*. 2005: CRC Press.

286. Sahdev, S., S.K. Khattar, and K.S. Saini, *Production of active eukaryotic proteins through bacterial expression systems: a review of the existing biotechnology strategies.* Molecular and Cellular Biochemistry, 2008. **307**(1-2): p. 249-264.

287. Scheper, G.C., et al., *The N and C termini of the splice variants of the human mitogen-activated protein kinase-interacting kinase Mnk2 determine activity and localization.* Molecular and Cellular Biology, 2003. **23**(16): p. 5692-5705.

288. O'Loghlen, A., et al., *Characterization of the activity of human MAP kinase-interacting kinase Mnk1b.* Biochimica et Biophysica Acta (BBA)-Molecular Cell Research, 2007. **1773**(9): p. 1416-1427.

289. Bergfors, T., *Protein crystallization: techniques, strategies, and tips. A laboratory manual. International University Line.* Biotechnology Series, La Jolla, 1999.

290. McPherson, A., *Crystallization of biological macromolecules*. 1999: Cold Spring Harbor Laboratory Press.

291. McPherson, A., *Introduction to protein crystallization.* Methods, 2004. **34**(3): p. 254-265.

292. Coussens, L.M. and Z. Werb, *Inflammation and cancer.* Nature, 2002. **420**(6917): p. 860-867.

293. Bromberg, J. and T.C. Wang, *Inflammation and cancer: IL-6 and STAT3 complete the link.* Cancer Cell, 2009. **15**(2): p. 79-80.

294. Waugh, D.J. and C. Wilson, *The interleukin-8 pathway in cancer.* Clinical Cancer Research, 2008. **14**(21): p. 6735-6741.

295. Kaler, P., L. Augenlicht, and L. Klampfer, *Macrophage-derived IL-1β stimulates Wnt signaling and growth of colon cancer cells: a crosstalk interrupted by vitamin D3.* Oncogene, 2009. **28**(44): p. 3892-3902.

296. Zhu, X., et al., *IL-17 expression by breast-cancer-associated macrophages: IL-17 promotes invasiveness of breast cancer cell lines.* Breast Cancer Research, 2008. **10**(6): p. 1.

297. Suganuma, M., et al., *Essential role of tumor necrosis factor α (TNF-α) in tumor promotion as revealed by TNF-α-deficient mice.* Cancer Research, 1999. **59**(18): p. 4516-4518.

298. Kessenbrock, K., V. Plaks, and Z. Werb, *Matrix metalloproteinases: regulators of the tumor microenvironment.* Cell, 2010. **141**(1): p. 52-67.

299. Bissell, M.J. and W.C. Hines, *Why don't we get more cancer? A proposed role of the microenvironment in restraining cancer progression.* Nature Medicine, 2011. **17**(3): p. 320-329.

300. Cer, R.Z., et al., *IC50-to-Ki: a web-based tool for converting IC50 to Ki values for inhibitors of enzyme activity and ligand binding.* Nucleic Acids Research, 2009. **37**(2): p. W441-W445.

301. In, I.S., *Enzyme kinetics. Behaviour and Analysis of Rapid Equilibrium and Steady-State Enzyme Systems, ; A Wiley-Interscience Publication, Ed*. 1975, John Wiley and Sons, Inc.: New York Chichester Brisbane Toronto Singapore.

# 8. Appendices

## 8.1 Appendix 1 - GST-Mnk2 and His-Mnk2 kinetics

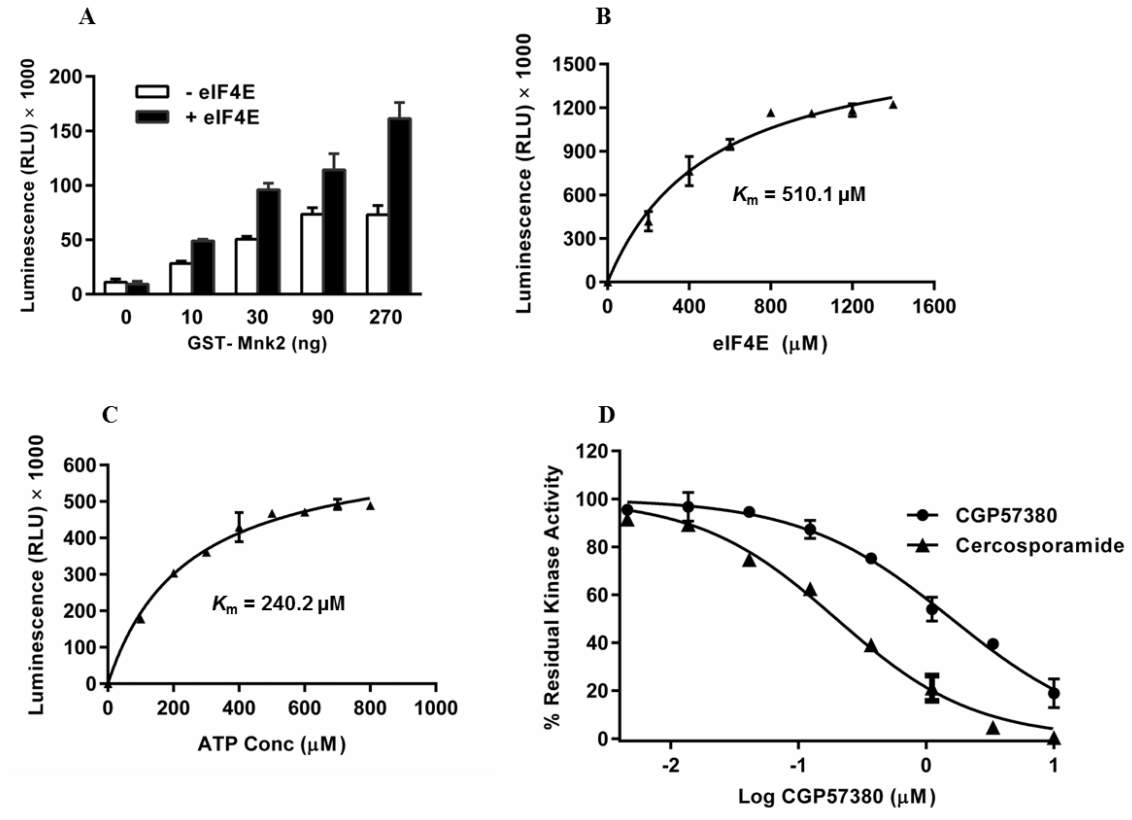



**Figure 8.1: ADP Glo assay validation with GST-Mnk2.** (A) Different amounts of GST- Mnk2 were used in kinase reactions with fixed substrate concentrations of 100 µM ATP and 100 µM of eIF4E$_{202-214}$ peptide substrate. The obtained luminescence signals were compared to control reactions without the peptide substrate. 30 ng of GST- Mnk2 gave sufficient S/B ratio. For all further experiments 30 ng GST-Mnk2 were used. (B) The $V_{max}$ and $K_m$ values were determined for the eIF4E$_{202-214}$ peptide substrate. The ATP concentration was adjusted to 2 mM and 30 ng Mnk2 was used in all reactions which were tested at

different eIF4E$_{202-214}$ peptide substrate concentrations. All data were baseline corrected with signals obtained from kinase control reactions (without peptide substrate) prior to curve fitting using the Michaelis-Menten model. (C) The determination of $V_{max}$ and $K_m$ values for ATP was carried out under identical conditions as described for panel C, with the difference that the eIF4E$_{202-214}$ peptide substrate concentration was fixed at 1.2 mM while different ATP concentrations were used. Control reactions without kinase were performed at the same time and used for background correction prior to fitting with the Michaelis-Menten model. (D) The control inhibitors CGP57380 and cercosporamide were used for final validation of the ADP-Glo™ assays using above parameters in a final assay volume of 15 µL. Concentration-response curves were calculated by iterative fitting to a 4-parameter logistic non-linear regression model.

**Table 8.1: GST and His tagged Mnk2 showed similar kinetic parameters**

| **Kinase** | **GST-Mnk2** | | **His-Mnk2** | |
|---|---|---|---|---|
| Substrate | ATP | eIF4E$_{202-214}$ | ATP | eIF4E$_{202-214}$ |
| $K_m$ (µM) | 240.2 | 510.1 | 215.8 | 608.5 |
| | | | | |
| Compound | CGP57380 | Cercosporamide | CGP57380 | Cercosporamide |
| $K_i$ value (µM) | 0.792 | 0.099 | 0.877 | 0.079 |

## 8.2 Appendix 2 - Interference of inhibitors with ADP-Glo™ system.

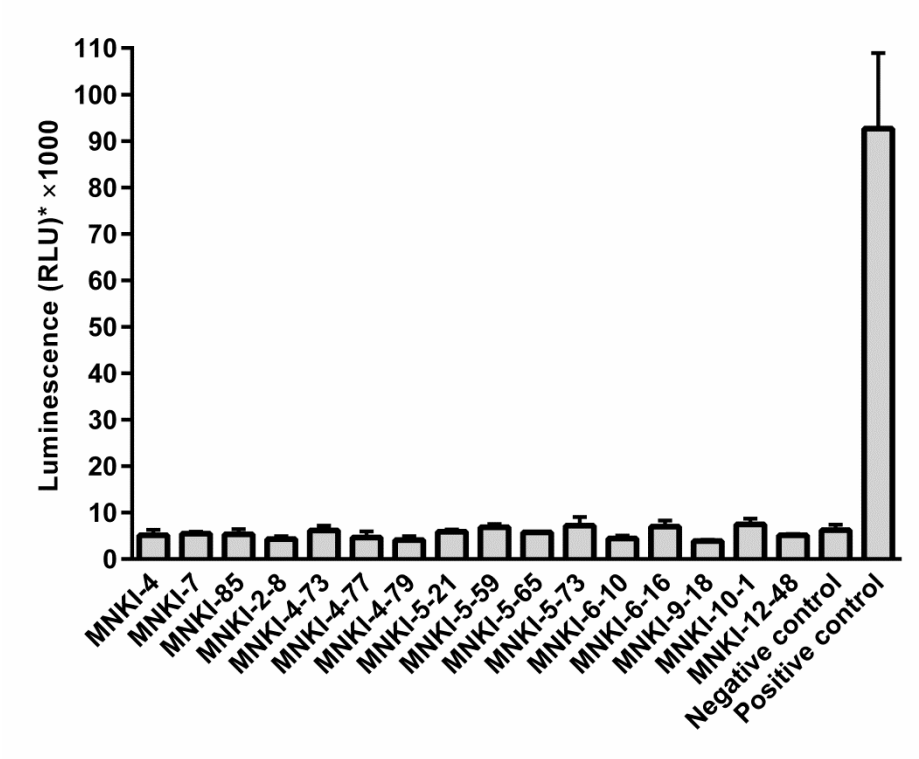



**Figure 8.2: Determination of interference of compounds to assay components.** 16 compunds were choosen randomly including all chemical series and incubated in the negative control (i.e. without Mnk2) and assay run to see if they interfere with the assay system. The result is presented below which showed that the compounds do not interfere with our assay components. Compounds were incubated without Mnk2, negative controls without compounds and Mnk2 and positive control with 30 ng Mnk2. Data ± SEM, n = 2.

## 8.3 Appendix 3 - CDK kinase assays

In order to cross screen against CDKs, ADP-Glo™ kinase assays were validated for CDK4/cyclin D1, CDK6/cylin D1 and CDK9/Cyclin T1 (**Figure 8.3** and **Figure 8.4**). The CDK kinase assays were optimised in a similar way to Mnks except for using different substrates: RB-CTF, Human retinoblastoma (RB), C-terminal fragment, was used for CDK4/6 and RBER-IRStide for CDK9 (Error! Reference source not found.) in section 4.1. For CDK4 and CDK6, PD0332991 ($IC_{50}$ CDK4 = 5.7 nM, CDK6 = 3.9 nM)

and for CDK9, CDKI-73 and Flavopiridol ($IC_{50}$ CDKI-73 = 13 nM, Flavopiridol = 0.012 nM) were used as reference compounds and the obtained $IC_{50}$ values were comparable to literature values.

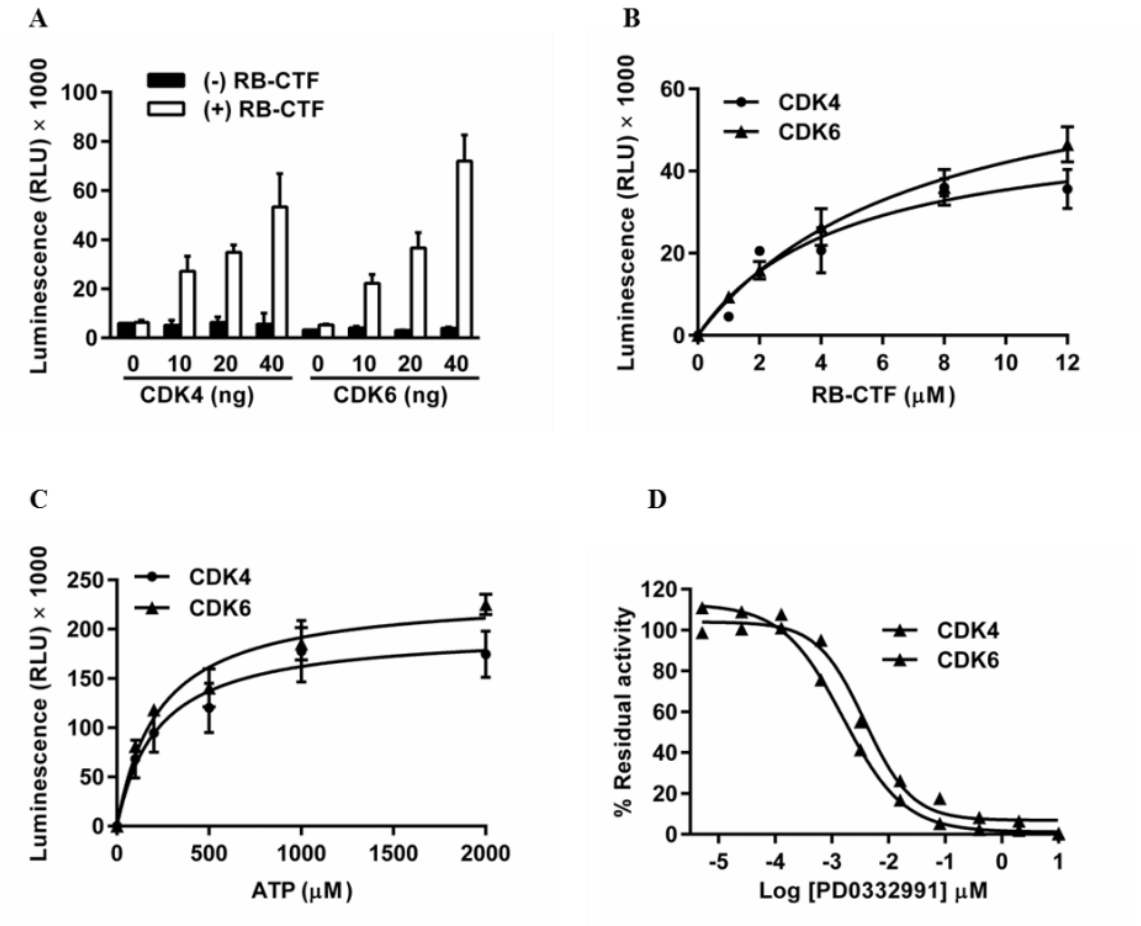



**Figure 8.3: ADP-Glo™ assay validation with CDK4/cyclin D1and CDK6/cyclin D1.** (A) Different amounts of CDK4 or CDK6 were used in kinase reactions with fixed substrate concentrations of 100 µM ATP and 100 µM of RB-CTF. The obtained luminescence signals were compared to control reactions without the RB-CTF substrate. The S/B ratios with 10 ng CDK4 and CDK6 were 5.3 and 5.5, respectively. For all further experiments 10 ng CDK4 and CDK6 were used. (B) The $V_{max}$ and $K_m$ values were determined for RB-CTF substrate. The ATP concentration was adjusted to 2 mM and 10 ng CDK4 and CDK6 were used in all reactions which were tested at different RB-CTF substrate concentrations. All data were baseline corrected with signals obtained from kinase control reactions (without RB-CTF substrate) prior to curve fitting using the Michaelis-Menten model. (C) The determination of $V_{max}$ and $K_m$ values for ATP was carried out under identical conditions as described for RB-CTF, with the difference that the RB-CTF substrate concentration was fixed at 7 µM while different ATP concentrations were used. Control reactions without kinase were performed at the same time and used for background correction prior to fitting with the Michaelis-Menten model. (D) The control inhibitor PD0332991 was used for final validation of the ADP-Glo™ assays using above parameters in a final assay volume of 10 µL. Concentration-response curves were calculated by iterative fitting to a 4-parameter logistic non-linear regression model.

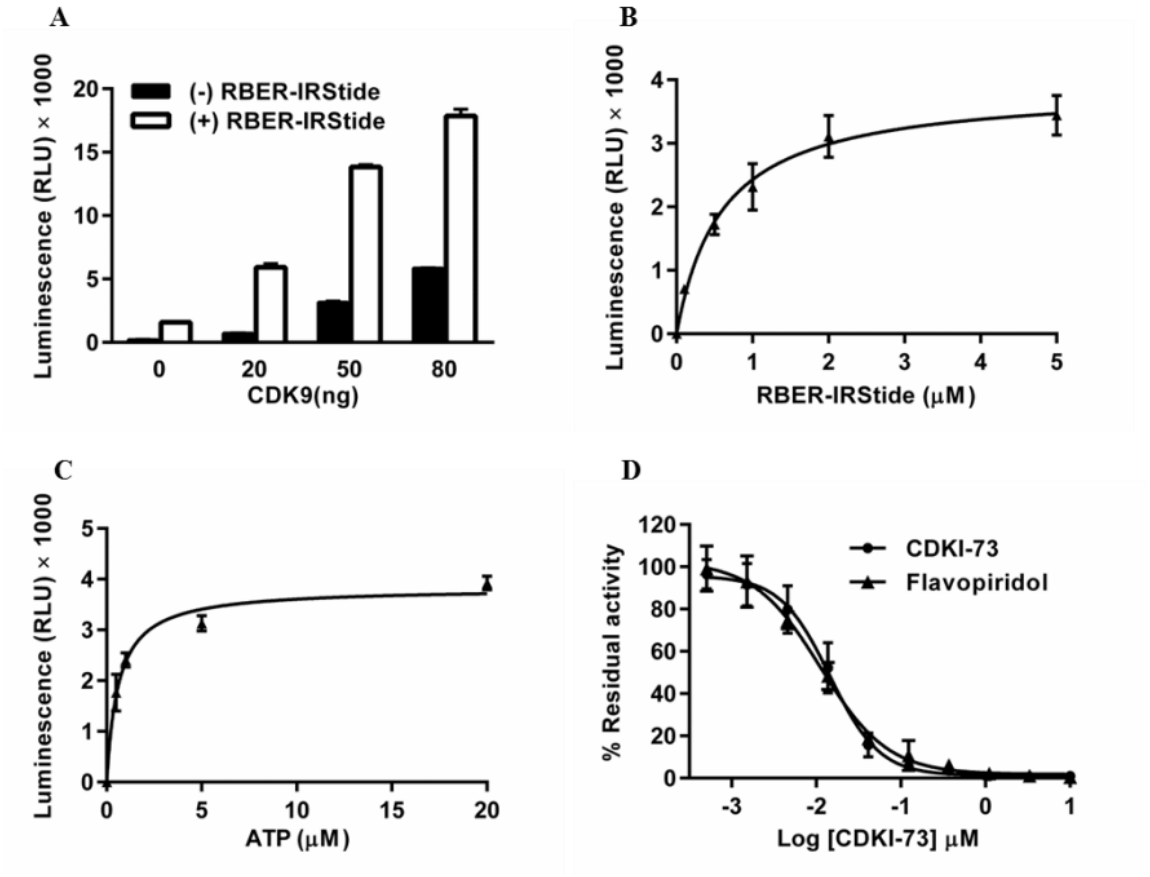



**Figure 8.4: ADP-Glo™ assay validation with CDK9/Cyclin T1.** (A) Different amounts of CDK9 were used in kinase reactions with fixed substrate concentrations of 2 µM ATP and 2 µM of RBER-IRStide. The obtained luminescence signals were compared to control reactions without the RBER-IRStide substrate. The S/B ratio with 50 ng CDK9 was 4.8. For all further experiments 50 ng CDK9 was used. (B) The $V_{max}$ and $K_m$ values were determined for the RBER-IRStide substrate. The ATP concentration was adjusted to 2 µM and 50 ng CDK9 was used in all reactions which were tested at different RBER-IRStide substrate concentrations. All data were baseline corrected with signals obtained from kinase control reactions (without RBER-IRStide substrate) prior to curve fitting using the Michaelis-Menten model. (C) The determination of $V_{max}$ and $K_m$ values for ATP was carried out under identical conditions as described for RBER-IRStide, with the difference that the RBER-IRStide substrate concentration was fixed at 2 µM while different ATP concentrations were used. Control reactions without kinase were performed at the same time and used for background correction prior to fitting with the Michaelis-Menten model. (D) The control inhibitor CDKI-73 was used for final validation of the ADP-Glo™ assays using above parameters in a final assay volume of 10 µL. Concentration-response curves were calculated by iterative fitting to a 4-parameter logistic non-linear regression model.

# 8.4 Appendix 4 - Profiling data from IMAP® and ADP-Glo™ assays.

**Table 8.2: Compound profiling data from IMAP® and ADP-Glo™ assay for 160 compounds plus CGP57380 and cercosporamide are used as standards.**

| | IMAP® assay (% residual activity) | | | | ADP Glo assay | |
|---|---|---|---|---|---|---|
| | Mnk1 | | Mnk2 | | Mnk1 | Mnk2 |
| Compound code | 1 µM | 10 µM | 1 µM | 10 µM | $K_i$ (µM) | $K_i$ (µM) |
| CGP57380 | 57.9 | 8.5 | 49.3 | 4.9 | 1.01 | 0.877 |
| Cercosporamide | 20.4 | 0.4 | 1.8 | -3.9 | 0.507 | 0.079 |
| MNKI-2-2 | 89.6 | 49.3 | 98.3 | 45.2 | NT | NT |
| MNKI-2-4 | 102.5 | 70 | 101.6 | 64.4 | NT | NT |
| MNKI-2-8 | 96.4 | 59.3 | 98.7 | 63.9 | NT | NT |
| MNKI-2-11 | 103.2 | 102.5 | 96.3 | 97.7 | NT | NT |
| MNKI-2-16 | 101.2 | 84.3 | 102.3 | 47.1 | NT | NT |
| MNKI-2-22 | 61.1 | 32.1 | 3.1 | 0.4 | 2.06 | 0.24 |
| MNKI-2-25 | 71.3 | 28.1 | 6.2 | 0.3 | 2.33 | 0.339 |
| MNKI-2-30 | 77.9 | 24.7 | 31.1 | 0.5 | 2.15 | 0.905 |
| MNKI-2-32 | 82.3 | 36.1 | 63.1 | 4.9 | 4.51 | 1.6 |
| MNKI-2-83 | 103.5 | 82.2 | 97.5 | 57.6 | NT | NT |
| MNKI-2-85 | 101.2 | 69.4 | 98.5 | 60.2 | NT | NT |
| MNKI-4 | 99.4 | 60.5 | 41.7 | -1.8 | NT | 0.226 |
| MNKI-4-6 | 94.1 | 50.2 | 79.1 | 12.1 | NT | 2.081 |
| MNKI-4-61 | 82.7 | 87.9 | 53.1 | 5.8 | > 10 | 0.615 |
| MNKI-4-63 | 106.1 | 109.4 | 92.3 | 94.3 | NT | NT |
| MNKI-4-73 | 105.1 | 102.8 | 91.9 | 30.6 | NT | 5.405 |
| MNKI-4-77 | 100.8 | 88.9 | 63.3 | 40.1 | NT | 1.385 |
| MNKI-4-79 | 103.8 | 84.9 | 73.7 | 13.4 | NT | 1.45 |
| MNKI-4-81 | 103.8 | 83.8 | 71.7 | 16.5 | NT | 3.206 |
| MNKI-4-89 | 101.5 | 102.5 | 91.1 | 66.1 | NT | NT |
| MNKI-4-91 | 103.5 | 96.3 | 94.7 | 92.4 | NT | NT |
| MNKI-5 | 64.8 | 1.2 | 2.4 | -0.7 | 0.098 | 0.025 |
| MNKI-5-1 | 86.4 | 81.1 | 77.2 | 35.1 | NT | > 10 |
| MNKI-5-13 | 91.9 | 82.8 | 97.9 | 72.5 | NT | NT |
| MNKI-5-17 | 101.8 | 84.5 | 57.9 | 13.1 | > 10 | 0.309 |
| MNKI-5-21 | 88.4 | 76.5 | 87.1 | 45.7 | NT | 2.574 |
| MNKI-5-59 | 105.8 | 86.7 | 77.3 | 23.4 | NT | 3.45 |
| MNKI-5-61 | 96.5 | 76.9 | 91.8 | 37.8 | NT | 1.472 |
| MNKI-5-65 | 88.9 | 81.1 | 84.9 | 42.8 | NT | 2.45 |
| MNKI-5-71 | 107.7 | 100.5 | 98.9 | 79.4 | NT | > 10 |
| MNKI-5-73 | 102.9 | 87.1 | 94.5 | 30.4 | NT | 2.806 |
| MNKI-6 | 19.2 | 3.5 | 0.2 | -0.8 | 0.031 | 0.01 |

| | | | | | | |
|---|---|---|---|---|---|---|
| MNKI-6-10 | 100.3 | 95.8 | 72.9 | 37.4 | NT | 1.606 |
| MNKI-6-16 | 112.3 | 86.5 | 52.7 | 10.3 | NT | 4.55 |
| MNKI-6-44 | 108.2 | 93.5 | 85.6 | 36.1 | NT | 5.04 |
| MNKI-6-77 | 72.2 | 67.3 | 104.5 | 54.2 | >10 | 4.6 |
| MNKI-6-78 | 93.2 | 85.3 | 113.9 | 82.4 | NT | NT |
| MNKI-6-82 | 91.1 | 81.3 | 108.7 | 77.2 | NT | NT |
| MNKI-6-86 | 80.4 | 72.2 | 117.1 | 101.9 | >10 | NT |
| MNKI-6-87 | 72.9 | 65.1 | 104.9 | 80.2 | >10 | NT |
| MNKI-7 | 4.5 | 0.5 | 0.8 | 0.1 | 0.055 | 0.022 |
| MNKI-7-7-1 | 97.3 | 35.6 | 38.6 | 12.3 | NT | 0.372 |
| MNKI-7-7-2 | 58.5 | 18.6 | 25.7 | 6.4 | 0.859 | 0.195 |
| MNKI-7-50 | 74.1 | 25.8 | 70.6 | 12.9 | 3.2 | 0.77 |
| MNKI-7-52 | 101.7 | 96.7 | 91.5 | 75.1 | NT | NT |
| MNKI-7-54 | 86.1 | 44.2 | 88.5 | 43.6 | 6.06 | 6.25 |
| MNKI-7-56 | 89.1 | 72.5 | 86.2 | 37.3 | NT | 4.576 |
| MNKI-7-76 | 101.4 | 99.8 | 99.7 | 74.9 | NT | NT |
| MNKI-7-77 | 98.1 | 92.9 | 95.7 | 33.8 | NT | 4.33 |
| MNKI-7-83 | 99.3 | 99.1 | 87.5 | 69.2 | NT | > 10 |
| MNKI-7-115 | 101.3 | 94.3 | 79.1 | 46.3 | NT | >10 |
| MNKI-7-117 | 101.7 | 99.6 | 100.4 | 101.4 | NT | NT |
| MNKI-7-118 | 100.3 | 56.9 | 94.1 | 79.1 | NT | NT |
| MNKI-8 | 20.9 | 5.9 | 0.2 | -0.5 | 0.109 | 0.026 |
| MNKI-8-10 | 98.8 | 29.8 | 22.6 | 7.5 | 1.471 | 0.106 |
| MNKI-8-17 | 100.2 | 94.7 | 102.1 | 82.1 | NT | NT |
| MNKI-8-18 | 97.9 | 86.4 | 98.6 | 23.6 | >10 | 1.703 |
| MNKI-8-25 | 99.9 | 91.8 | 106.5 | 93.2 | NT | NT |
| MNKI-8-29 | 102.5 | 48.5 | 105.4 | 50.3 | NT | NT |
| MNKI-8-30 | 109.6 | 50.8 | 108.5 | 59.3 | NT | NT |
| MNKI-8-35 | 99.9 | 54.6 | 99.7 | 29.1 | NT | 1.3 |
| MNKI-8-36 | 101.7 | 86.5 | 96.4 | 22.3 | NT | 2.5 |
| MNKI-8-55 | 98.5 | 48.2 | 101.5 | 43.3 | NT | NT |
| MNKI-8-56 | 102.5 | 77.2 | 104.5 | 50.1 | NT | NT |
| MNKI-8-66 | 101.2 | 54.2 | 99.8 | 67.9 | NT | NT |
| MNKI-8-67 | 99.7 | 24.6 | 103.5 | 67.8 | 3.755 | >10 |
| MNKI-8-77 | 107.5 | 59.9 | 88.5 | 16.1 | >10 | 1.15 |
| MNKI-8-78 | 98.8 | 67.9 | 105.2 | 72.2 | NT | NT |
| MNKI-8-79 | 100.8 | 91.2 | 101.4 | 86.8 | NT | NT |
| MNKI-8-81 | 97.9 | 67.3 | 39.7 | 9.3 | >10 | 0.219 |
| MNKI-8-88 | 99.9 | 34.8 | 43.8 | 6.8 | 5.918 | 0.232 |
| MNKI-8-91 | 101.6 | 69.3 | 79.4 | 25.3 | >10 | 1.331 |
| MNKI-8-115 | 109.6 | 62.1 | 67.3 | 14.4 | >10 | 0.398 |
| MNKI-9 | 100.6 | 99.3 | 30.1 | 5.4 | > 10 | 4.05 |
| MNKI-9-7 | 99.9 | 94.3 | 103.6 | 60.4 | NT | NT |
| MNKI-9-9 | 106.7 | 92.9 | 101.3 | 79.9 | NT | NT |

| | | | | | | |
|---|---|---|---|---|---|---|
| MNKI-9-10 | 98.5 | 96.2 | 99.5 | 93.7 | NT | NT |
| MNKI-9-13 | 101.2 | 102.1 | 103.5 | 73.9 | NT | NT |
| MNKI-9-15 | 99.6 | 43.6 | 109.6 | 52.6 | NT | NT |
| MNKI-9-18 | 82.2 | 8.1 | 18.8 | 2.7 | 0.942 | 0.15 |
| MNKI-9-21 | 100 | 73.1 | 99.4 | 65.7 | NT | NT |
| MNKI-9-23 | 101.2 | 57.1 | 102.6 | 73.4 | NT | NT |
| MNKI-9-25 | 102.7 | 64.1 | 104.8 | 47.8 | NT | NT |
| MNKI-9-27 | 102.7 | 96.9 | 106.3 | 87.6 | NT | NT |
| MNKI-9-36 | 67.8 | 10.4 | 10.6 | 8.1 | 0.152 | 0.044 |
| MNKI-9-38 | 56.9 | 12.7 | 105.7 | 20.7 | 0.907 | 1.323 |
| MNKI-9-41 | 75.8 | 35.5 | 45.8 | 7.8 | 1.773 | 0.206 |
| MNKI-9-42 | 99.5 | 54.3 | 27.5 | 2.5 | >10 | 0.233 |
| MNKI-9-45 | 101.7 | 91.5 | 102.8 | 86.4 | NT | NT |
| MNKI-9-50 | 92.9 | 44.3 | 28.7 | 4.2 | >10 | 0.154 |
| MNKI-9-52 | 100.3 | 109.6 | 98.4 | 86.8 | NT | NT |
| MNKI-9-59 | 89.9 | 32.9 | 27.3 | 20.2 | 4.766 | 0.105 |
| MNKI-9-60 | 101.5 | 104.1 | 101.9 | 90.9 | NT | NT |
| MNKI-9-62 | 102.7 | 85.5 | 68.4 | 19.2 | NT | 1.35 |
| MNKI-9-66 | 88.8 | 24.7 | 31.6 | 17.2 | 1.083 | 0.432 |
| MNKI-9-67 | 99.4 | 88.1 | 96.8 | 83.9 | NT | NT |
| MNKI-9-68 | 98.5 | 63.2 | 98.2 | 47.7 | NT | NT |
| MNKI-9-81 | 99.5 | 68.9 | 88.3 | 15.1 | >10 | 1.667 |
| MNKI-10-1 | 101.9 | 7.3 | 33.6 | 1.5 | 0.71 | 0.219 |
| MNKI-10-2 | 86.3 | 20.5 | 26.9 | 3.8 | 1.305 | 0.175 |
| MNKI-10-5 | 105.2 | 79.9 | 55.6 | 10.4 | >10 | 0.631 |
| MNKI-10-6 | 94.7 | 43.6 | 45.9 | 5.2 | >10 | 0.304 |
| MNKI-10-9 | 101.6 | 85.1 | 56.8 | 19.1 | NT | 0.519 |
| MNKI-10-10 | 69.9 | 23.2 | 98.6 | 18.5 | >10 | 4.135 |
| MNKI-10-22 | 103.6 | 47.8 | 62.6 | 5.9 | >10 | 0.393 |
| MNKI-10-25 | 102.8 | 97.7 | 100.3 | 59.4 | NT | NT |
| MNKI-10-26 | 98.4 | 54.1 | 92.6 | 58.6 | NT | NT |
| MNKI-10-27 | 92.9 | 39.7 | 101.4 | 77.4 | NT | NT |
| MNKI-10-30 | 103.9 | 61.8 | 99.4 | 45.3 | >10 | 7.6 |
| MNKI-10-31 | 99.9 | 59.8 | 86.3 | 31.2 | >10 | 1.565 |
| MNKI-10-34 | 105.6 | 102.3 | 101.6 | 98.6 | >10 | >10 |
| MNKI-10-40 | 56.2 | 5.4 | 16.3 | 0.8 | 0.668 | 0.118 |
| MNKI-11 | 99.9 | 83.9 | 98.1 | 87.5 | NT | NT |
| MNKI-11-62 | 102.3 | 79.6 | 92.9 | 56.2 | NT | NT |
| MNKI-11-67 | 97.3 | 95.4 | 98.2 | 47.4 | NT | NT |
| MNKI-11-86 | 58.5 | 28.2 | 23.7 | 3.2 | 1.227 | 0.28 |
| MNKI-11-90 | 98.8 | 46.7 | 83.8 | 23.6 | >10 | 0.864 |
| MNKI- 12 | 90.4 | 58.1 | 40.5 | 0.59 | NT | 0.5 |
| MNKI-12-13 | 102.2 | 108.5 | 101.5 | 63.1 | NT | NT |
| MNKI-12-18 | 97.9 | 102.1 | 99.2 | 65.7 | NT | NT |

| | | | | | | |
|---|---|---|---|---|---|---|
| MNKI-12-27 | 99.9 | 84.4 | 103.8 | 89.7 | NT | NT |
| MNKI-12-48 | 102.5 | 91.7 | 46.3 | 5.8 | >10 | 0.562 |
| MNKI-12-56 | 89.6 | 19.4 | 18.5 | 2.2 | 1.331 | 0.132 |
| MNKI-12-62 | 89.9 | 37.2 | 39.3 | 9.4 | 4.876 | 0.408 |
| MNKI-12-69 | 101.7 | 85.4 | 101.8 | 94.3 | NT | NT |
| MNKI-12-70 | 98.5 | 82.2 | 94.6 | 82.8 | NT | NT |
| MNKI-12-72 | 102.5 | 68.6 | 68.3 | 21.4 | >10 | 1.706 |
| MNKI-12-78 | 101.2 | 75.6 | 79.2 | 18.4 | >10 | 2.432 |
| MNKI-12-81 | 99.7 | 86.1 | 103.5 | 41.8 | NT | NT |
| MNKI-12-86 | 107.5 | 83.7 | 91.8 | 48.4 | NT | NT |
| MNKI-12-90 | 103.6 | 58.4 | 46.2 | 2.3 | >10 | 0.414 |
| MNKI-12-93 | 102.8 | 96.8 | 99.4 | 101.4 | NT | NT |
| MNKI-12-94 | 98.4 | 91.1 | 41.9 | 9.1 | NT | 0.429 |
| MNKI-12-95 | 92.6 | 33.7 | 55.1 | 19.1 | 1.772 | 0.429 |
| MNKI-13-9 | 93.8 | 22.3 | 39.8 | 1.2 | 2.11 | 0.282 |
| MNKI-13-22 | 99.7 | 54.4 | 99.8 | 45.8 | 5.63 | 6.04 |
| MNKI-13-26 | 102.6 | 78.8 | 101.6 | 18.9 | 6.71 | 0.919 |
| MNKI-13-28 | 107.5 | 48.6 | 31.7 | 5.9 | 3.03 | 0.299 |
| MNKI-13-35 | 101.4 | 68 | 47.9 | 11 | 6.53 | 0.561 |
| MNKI-13-40 | 106.5 | 71.8 | 28.8 | 7.1 | 8.45 | 0.282 |
| MNKI-13-43 | 99.9 | 92.9 | 102.6 | 72.5 | > 10 | > 10 |
| MNKI-14 | 100.1 | 98.3 | 96.1 | 79.5 | NT | NT |
| MNKI-15 | 80.3 | 29.9 | 5.1 | -2.2 | 1.9 | 0.164 |
| MNKI-19 | 2.7 | -1.2 | -1.7 | -0.4 | 0.186 | 0.068 |
| MNKI-28 | 84.5 | 38.6 | 20.3 | 5.4 | 4.82 | 0.352 |
| MNKI-32 | 99.6 | 101.4 | 106.2 | 103.2 | NT | NT |
| MNKI-37 | 73.1 | 47.8 | 6.2 | -1.8 | 1.02 | 0.048 |
| MNKI-40 | 91.3 | 59.5 | 85.7 | 35.3 | > 10 | 5.99 |
| MNKI-41 | 94.7 | 80.9 | 50.1 | 56.1 | > 10 | 9.05 |
| MNKI-42 | 96.6 | 85.7 | 99.1 | 84.3 | NT | NT |
| MNKI-44 | 93.2 | 55.1 | 75.4 | 23.6 | 5.4 | 3.17 |
| MNKI-45 | 89.9 | 48.9 | 74.7 | 19.3 | 5 | 2.63 |
| MNKI-57 | 52.5 | 32.3 | 23.6 | 2.1 | 0.106 | 0.018 |
| MNKI-58 | 101.7 | 54.5 | 108.3 | 57.3 | NT | NT |
| MNKI-64 | 102.9 | 82.9 | 101.9 | 74.9 | NT | NT |
| MNKI-67 | 56.7 | 47.9 | 27.6 | 20.7 | 0.933 | 0.018 |
| MNKI-68 | 99.9 | 85.5 | 101.5 | 51.6 | NT | NT |
| MNKI-83 | 81.9 | 51.3 | 74.6 | 7.6 | 0.32 | 0.164 |
| MNKI-85 | 76.3 | 74.9 | 29.6 | 2.7 | > 10 | 0.031 |
| MNKI-92 | 100.4 | 90.3 | 99.4 | 66.7 | NT | NT |

NT; not tested.

# 8.5 Appendix 5 - Anti-proliferative and kinase inhibitory activities of Mnk inhibitors

**Table 8.3: Summary of anti-proliferative effect, inhibition of cellular phosphorylation of eIF4E and kinase (Mnk1/2, CDK2A/9T1 and FLT3) inhibitory activity of compounds in MV4-11 cells.**

| Code | Series | $GI_{50}$ ± SD | $IC_{50}$ | $K_i$ | | | |
|---|---|---|---|---|---|---|---|
| | | | p-eIF4E | Mnk1/2 | CDK2A | CDK9T1 | FLT3 |
| **Group A: $GI_{50}$ < 10 µM; CDK2/9 and FLT3 > 10 µM (or not tested)** | | | | | | | |
| CGP57380 | | 4.52 ± 0.90 | 3.47 | 1.01/0.877 | > 10 | > 10 | NT |
| MNKI-4 | 1 | 8.30 ± 1.49 | 0.521 | > 10/0.226 | > 10 | > 10 | NT |
| MNKI-5-17 | 2 | 5.36 ± 0.29 | NT | > 10/0.309 | 5.36 | 0.13 | NT |
| MNKI-6 | 1 | 0.58 ± 0.02 | 0.023 | 0.031/0.010 | > 10 | > 10 | NT |
| MNKI-7-7-1 | 2 | 0.37 ± 0.07 | NT | ND/0.372 | NT | NT | NT |
| MNKI-7-50 | 3 | 8.52 ± 0.41 | NT | 3.20/0.770 | > 10 | > 10 | NT |
| MNKI-7-54 | 3 | 0.63 ± 0.15 | NT | 6.06/6.25 | NT | NT | NT |
| MNKI-7-56 | 3 | 0.22 ± 0.08 | NT | ND/4.58 | NT | NT | NT |
| MNKI-8 | 1 | 1.15 ± 0.57 | 0.098 | 0.109/0.026 | > 10 | > 10 | NT |
| MNKI-8-35 | 2 | 5.67 ± 1.37 | NT | ND/1.30 | NT | NT | NT |
| MNKI-8-67 | 3 | 9.68 ± 1.73 | NT | 3.76/> 10 | NT | NT | NT |
| MNKI-8-81 | 2 | 0.57 ± 0.06 | NT | > 10/0.219 | NT | 0.345 | NT |
| MNKI-9-18 | 2 | 3.41 ± 0.69 | NT | 0.942/0.150 | NT | NT | NT |
| MNKI-9-36 | 3 | 2.06 ± 0.45 | NT | 0.152/0.044 | NT | NT | NT |
| MNKI-9-41 | 2 | 1.29 ± 0.26 | NT | 1.77/0.206 | NT | NT | NT |
| MNKI-9-42 | 2 | 0.0007 ± 0.0001 | NT | > 10/0.233 | NT | 0.003 | NT |
| MNKI-9-50 | 2 | 0.07 ± 0.02 | NT | > 10/0.154 | NT | NT | NT |
| MNKI-9-66 | 3 | 8.19 ± 0.30 | NT | 1.08/0.432 | NT | NT | NT |
| MNKI-10-1 | 2 | 3.25 ± 0.03 | NT | 0.710/0.219 | 0.8 | > 10 | NT |
| MNKI-10-6 | 2 | 6.65 ± 1.68 | NT | > 10/0.304 | > 10 | > 10 | NT |
| MNKI-10-22 | 2 | 1.74 ± 0.02 | NT | > 10/0.393 | NT | > 10 | NT |
| MNKI-10-30 | 2 | 4.89 ± 0.25 | NT | >10/7.6 | NT | NT | NT |
| MNKI-10-31 | 2 | 3.42 ± 0.25 | NT | > 10/1.56 | NT | NT | NT |
| MNKI-11-86 | 2 | 8.69 ± 1.90 | NT | 1.23/0.280 | NT | > 10 | NT |
| MNKI-11-90 | 2 | 8.69 ± 1.90 | NT | > 10/0.864 | NT | NT | NT |
| MNKI-12-48 | 3 | 7.86 ± 0.35 | NT | > 10/0.562 | NT | NT | NT |
| MNKI-12-56 | 3 | 4.13 ± 0.53 | NT | 1.33/0.132 | NT | NT | NT |
| MNKI-12-62 | 3 | 0.72 ± 0.14 | NT | 4.88/0.408 | NT | NT | NT |
| MNKI-12-72 | 3 | 3.27 ± 0.11 | NT | > 10/1.71 | NT | NT | NT |
| MNKI-12-78 | 3 | 2.09 ± 0.74 | NT | > 10/2.43 | NT | NT | NT |
| MNKI-12-90 | 3 | 9.33 ± 0.37 | NT | > 10/0.414 | NT | NT | NT |
| MNKI-12-94 | 3 | 3.59 ± 0.61 | NT | ND/0.429 | NT | NT | NT |

| | | | | | | | |
|---|---|---|---|---|---|---|---|
| MNKI-12-95 | 3 | 3.62 ± 0.57 | NT | 1.77/0.429 | NT | NT | NT |
| MNKI-13-9 | 3 | 0.34 ± 0.03 | NT | 2.11/0.282 | NT | NT | NT |
| MNKI-13-22 | 3 | 1.99 ± 0.13 | NT | 5.63/6.04 | NT | NT | NT |
| MNKI-13-26 | 3 | 2.54 ± 0.32 | NT | 6.71/0.919 | NT | NT | NT |
| MNKI-13-28 | 3 | 0.16 ± 0.06 | NT | 3.03/0.299 | NT | NT | NT |
| MNKI-13-35 | 3 | 3.26 ± 0.97 | NT | 6.53/0.561 | NT | NT | NT |
| MNKI-40 | 1 | 9.66 ± 0.72 | NT | > 10/5.99 | NT | NT | NT |
| MNKI-45 | 1 | 5.73 ± 0.38 | NT | 5.00/2.63 | NT | NT | NT |
| MNKI-57 | 1 | 6.10 ± 0.79 | 0.196 | 0.106/0.018 | > 10 | > 10 | NT |
| MNKI-67 | 1 | 8.84 ± 1.58 | 0.087 | 0.933/0.018 | > 10 | > 10 | NT |
| **Group B: $GI_{50}$ < 10 µM ; Mnk < 10 µM; CDK2/9 or FLT3 < 10 µM** | | | | | | | |
| MNKI-4-61 | 2 | 0.78 ± 0.07 | NT | > 10/0.615 | > 10 | 1.66 | 0.13 |
| MNKI-7 | 1 | 0.81 ± 0.03 | 0.064 | 0.055/0.022 | > 10 | > 10 | 0.022 |
| MNKI-7-7-2 | 2 | 0.17 ± 0.07 | NT | 0.859/0.195 | NT | NT | 0.005 |
| MNKI-8-10 | 2 | 0.30 ± 0.06 | NT | 1.47/0.106 | NT | NT | 0.032 |
| MNKI-8-18 | 2 | 0.81 ± 0.23 | NT | > 10/1.70 | NT | NT | 0.064 |
| MNKI-8-36 | 2 | 0.59 ± 0.27 | NT | ND/2.50 | NT | NT | 0.093 |
| MNKI-8-77 | 2 | 0.37 ± 0.05 | NT | > 10/1.15 | NT | NT | 0.03 |
| MNKI-8-88 | 2 | 0.09 ± 0.01 | NT | 5.92/0.232 | 0.93 | > 10 | 0.007 |
| MNKI-8-91 | 2 | 0.50 ± 0.10 | NT | > 10/1.33 | NT | NT | 0.1 |
| MNKI-8-115 | 2 | 0.27 ± 0.02 | NT | > 10/0.398 | NT | NT | 0.06 |
| MNKI-9-59 | 2 | 0.60 ± 0.10 | NT | 4.77/0.105 | 3.5 | > 10 | 0.34 |
| MNKI-10-40 | 2 | 0.57 ± 0.04 | NT | 0.668/0.118 | NT | NT | 0.063 |
| MNKI-19 | 1 | 7.30 ± 0.75 | 1.2 | 0.186/0.068 | > 10 | > 10 | 0.098 |
| MNKI-37 | 1 | 6.08 ± 1.99 | 0.125 | 1.02/0.048 | > 10 | > 10 | 0.207 |
| MNKI-85 | 1 | 7.44 ± 0.77 | 0.115 | > 10/0.031 | > 10 | > 10 | 0.166 |
| **Group C: Mnk < 10 µM ; $GI_{50}$ > 10 µM** | | | | | | | |
| MNKI-83 | 1 | > 10 | 1.42 | 0.320/0.164 | > 10 | > 10 | NT |
| MNKI-5 | 1 | > 10 | 1.523 | 0.098/0.025 | > 10 | > 10 | NT |
| MNKI-15 | 1 | > 10 | 0.53 | 1.90/0.164 | > 10 | > 10 | NT |
| MNKI-10-2 | 2 | > 10 | NT | 1.30/0.175 | NT | NT | NT |
| MNKI-2-22 | 1 | > 10 | 0.631 | 2.06/0.240 | > 10 | > 10 | NT |
| MNKI-2-25 | 1 | > 10 | 2.82 | 2.33/0.339 | > 10 | > 10 | NT |
| MNKI-28 | 1 | > 10 | 2.91 | 4.82/0.352 | > 10 | > 10 | NT |
| MNKI-12 | 1 | > 10 | 3.45 | ND/0.500 | > 10 | > 10 | NT |
| MNKI-2-30 | 1 | > 10 | 1.73 | 2.15/0.905 | > 10 | > 10 | NT |
| MNKI-2-32 | 1 | > 10 | NT | 4.51/1.60 | NT | NT | NT |
| MNKI-44 | 1 | > 10 | NT | 5.40/3.17 | NT | NT | NT |
| MNKI-9 | 1 | > 10 | NT | > 10/4.05 | NT | NT | NT |
| MNKI-41 | 1 | > 10 | NT | > 10/9.05 | NT | NT | NT |
| **Group D: Mnk > 10 µM ; $GI_{50}$ < 10 µM** | | | | | | | |

| | | | | | | | |
|---|---|---|---|---|---|---|---|
| MNKI-7-115 | 2 | 0.53 ± 0.12 | NT | ND/ND | NT | NT | NT |
| MNKI-7-117 | 3 | 9.03 ± 1.12 | NT | ND/ND | NT | NT | NT |
| MNKI-8-25 | 2 | 2.24 ± 1.08 | NT | ND/ND | NT | NT | NT |
| MNKI-8-78 | 3 | 6.86 ± 0.21 | NT | ND/ND | NT | NT | NT |
| MNKI-8-79 | 3 | 3.55 ± 0.06 | NT | ND/ND | NT | NT | NT |
| MNKI-9-15 | 3 | 2.06 ± 0.45 | NT | ND/ND | NT | NT | NT |
| MNKI-9-23 | 3 | 4.64 ± 0.88 | NT | ND/ND | NT | NT | NT |
| MNKI-9-25 | 3 | 7.56 ± 0.57 | NT | ND/ND | NT | NT | NT |
| MNKI-9-68 | 3 | 9.20 ± 0.64 | NT | ND/ND | NT | NT | NT |
| MNKI-10-26 | 2 | 3.72 ± 0.31 | NT | ND/ND | NT | NT | NT |
| MNKI-10-27 | 2 | 3.89 ± 0.39 | NT | ND/ND | NT | NT | NT |
| MNKI-10-34 | 2 | 2.00 ± 0.37 | NT | > 10/> 10 | NT | NT | NT |
| MNKI-11-62 | 2 | 1.40 ± 0.66 | NT | ND/ND | NT | NT | NT |
| MNKI-11-67 | 2 | 3.89 ± 0.40 | NT | ND/ND | NT | NT | NT |
| MNKI-12-13 | 3 | 6.55 ± 0.95 | NT | ND/ND | NT | NT | NT |
| MNKI-12-18 | 3 | 7.41 ± 0.47 | NT | ND/ND | NT | NT | NT |
| MNKI-12-27 | 3 | 3.99 ± 0.40 | NT | ND/ND | NT | NT | NT |
| MNKI-12-70 | 2 | 8.00 ± 0.30 | NT | ND/ND | NT | NT | NT |
| MNKI-12-81 | 2 | 5.50 ± 0.18 | NT | ND/ND | NT | NT | NT |
| MNKI-12-86 | 2 | 6.26 ± 0.86 | NT | ND/ND | NT | NT | NT |
| MNKI-12-93 | 2 | 1.90 ± 0.15 | NT | ND/ND | NT | NT | NT |
| **Group E: Mnk > 10 µM ; $GI_{50}$ > 10 µM** | | | | | | | |
| MNKI-7-52 | 3 | > 10 | NT | ND/ND | NT | NT | NT |
| MNKI-7-118 | 3 | > 10 | NT | ND/ND | NT | NT | NT |
| MNKI-8-17 | 2 | > 10 | NT | ND/ND | NT | NT | NT |
| MNKI-8-29 | 3 | > 10 | NT | ND/ND | NT | NT | NT |
| MNKI-8-56 | 3 | > 10 | NT | ND/ND | NT | NT | NT |
| MNKI-9-13 | 3 | > 10 | NT | ND/ND | NT | NT | NT |
| MNKI-9-67 | 3 | > 10 | NT | ND/ND | NT | NT | NT |
| MNKI-11 | 1 | > 10 | NT | ND/ND | NT | NT | NT |
| MNKI-12-69 | 2 | > 10 | NT | ND/ND | NT | NT | NT |
| MNKI-32 | 1 | > 10 | NT | ND/ND | NT | NT | NT |
| MNKI-42 | 1 | > 10 | NT | ND/ND | NT | NT | NT |
| MNKI-58 | 1 | > 10 | NT | ND/ND | NT | NT | NT |

| | | | | | | | |
|---|---|---|---|---|---|---|---|
| MNKI-64 | 1 | > 10 | NT | ND/ND | NT | NT | NT |
| MNKI-2-11 | 1 | > 10 | NT | ND/ND | NT | NT | NT |

$GI_{50}$ values shown are the mean values from at least two independent experiments with three replicates each. All values represented are in µM. ND; not determined as found inactive from IMAP® assay, refer to **Table 8.2** for detail values determined using IMAP® assay. NT; not tested.